

THE UNIVERSITY OF CHICAGO

EFFECTS AND DESIGN OF CENTRAL BANK CORPORATE CREDIT FACILITIES

A DISSERTATION SUBMITTED TO
THE FACULTY OF THE UNIVERSITY OF CHICAGO
BOOTH SCHOOL OF BUSINESS
IN CANDIDACY FOR THE DEGREE OF
DOCTOR OF PHILOSOPHY

BY

RAYHAN MOMIN

CHICAGO, ILLINOIS

JUNE 2025

Copyright © 2025 by Rayhan Momin
All Rights Reserved

To Tehreem

CONTENTS

LIST OF FIGURES	vii
LIST OF TABLES	ix
ACKNOWLEDGMENTS	xi
ABSTRACT	xiii
1 THE CAUSAL EFFECT OF THE FED'S CORPORATE CREDIT FACILITIES ON ELIGIBLE ISSUER BONDS	1
1.1 Introduction	1
1.1.1 Contribution to Literature	7
1.2 Related Literature	9
1.3 Data and Institutional Background	11
1.3.1 Term Sheets	11
1.3.2 Sample Construction	12
1.3.3 Descriptive Statistics	16
1.4 Treatment Effects for Eligible Issuers	17
1.4.1 Baseline Results	17
1.4.2 Measurement Error from Using Issue Ratings	21
1.4.3 Quasi-Natural Experiment	24
1.5 Counterfactual Treatment Effects for Ineligible Issuers	34
1.5.1 Causal Machine Learning Approach with High-Dimensional Controls	34
1.6 Conclusion	39
1.7 Appendix	41
1.7.1 Robustness	41
1.7.2 Features	46
1.7.3 Deep Net Architectures	48
1.7.4 Causal ML Treatment Effect Estimates Across Models	49
2 HETEROGENEOUS TREATMENT EFFECTS AND COUNTERFACTUAL POLICY TARGETING USING DEEP NEURAL NETWORKS: AN APPLICATION TO CEN- TRAL BANK CORPORATE CREDIT FACILITIES	50
2.1 Introduction	50
2.2 Institutional Background	58
2.3 Data	59
2.3.1 Sample Construction	59
2.3.2 Descriptive Statistics	60
2.4 Static Homogeneous Average Treatment Effects: Difference-in-Differences Regressions	64
2.4.1 Potential Selection Bias and Parallel Trends	64
2.4.2 Results	65

2.5	Dynamic Homogeneous Average Treatment Effects: Event Study Regressions with Two-Way Fixed Effects	67
2.5.1	Discussion	72
2.6	Dynamic Heterogeneous Average Treatment Effects: Two-Step Semi-Parametric DiD Estimators	73
2.6.1	Overview of Empirical Design	73
2.6.2	Modelling Framework	75
2.6.3	Discussion on Identification	78
2.6.4	Estimation Procedure	81
2.6.5	Base Effects	83
2.6.6	ATE with Heterogeneity	88
2.7	Counterfactual Treatment Effects and Targeting	97
2.8	Conclusion	103
2.9	Appendix	105
2.9.1	Event Study Regressions with Two-Way Fixed Effects	105
2.9.2	Features	106
2.9.3	Base Effect Estimator Derivation	108
2.9.4	ATE Estimator Derivation	109
2.9.5	ATET Estimator Derivation	110
2.9.6	Deep Net Architectures	112
2.9.7	Base Effects	113
2.9.8	Average Treatment Effects	116
2.9.9	ATE and ATET Comparison	120
2.9.10	Counterfactual Treatment Effects	123
2.9.11	Alternative Investment Proxy: Change in Gross Property, Plant, and Equipment	127
3	CENTRAL BANK CORPORATE BOND PURCHASE PROGRAMS: COMMITMENT MATTERS	132
3.1	Introduction	132
3.2	Model with Short-Term Secured Debt	139
3.2.1	Setup	139
3.2.2	Equity's Problem	142
3.2.3	Discussion on Collateral Constraint and Financial Slack	146
3.2.4	Unsecured Creditors' Problem	148
3.2.5	Optimal Policies	149
3.3	Crisis Dynamics with Short-Term Debt	151
3.3.1	Secured Debt Intervention	153
3.3.2	Unsecured Debt Intervention	154
3.3.3	Dividend Restriction	156
3.4	Numerical Results	159
3.4.1	Model Calibration and Fit	159
3.4.2	Numerically Solved Model and Dynamics	162

3.4.3	Dividend and Debt Repurchase Restrictions with Unsecured Debt Intervention	172
3.5	Conclusion	172
3.6	Appendix	174
3.6.1	Strict Convexity of the Joint Value Function	174
3.6.2	Collateral Constraint with Short-Term Secured Debt	175
3.6.3	Collateral Constraint with Long-Term Secured Debt	178
3.6.4	Deriving Equity HJB By Assuming Collateral Constraint Always Binds	183
3.6.5	Binding Collateral Constraints in Rampini and Viswanathan (2010)	185
3.6.6	Crisis Collateral Constraint in Model with Short-Term Secured Debt	188
3.6.7	Secured Debt Intervention Strictly Increases Value Function	191
3.6.8	Secured Debt Intervention Boosts Investment Via Direct and Indirect Channels	193
3.6.9	Segmented Markets in Model with Short-Term Secured Debt	194
3.6.10	Unsecured Debt Intervention and Joint Equity and Short-Term Debt Value Function	195
3.6.11	Dividend Restriction in Model with Short-Term Secured Debt	197
3.6.12	Dividend Restriction and Unsecured Debt Repurchase Restriction in Model with Short-Term Secured Debt	202
3.6.13	Numerical Solution for Model with Short-Term Debt	206
3.6.14	Numerical Results for Model with Short-Term Debt	219
3.6.15	Dividend and Debt Repurchase Restrictions with Unsecured Debt Intervention	221
	REFERENCES	233

LIST OF FIGURES

1.1	Distribution of Corporate Bond Ratings by Fed CCF Eligibility	2
1.2	CDS Spreads of Control (IG Ineligible) and Treatment (Fallen Angel) Share Common Support	28
1.3	Capital Structure of Control (IG Ineligible) and Treatment (Fallen Angel) Overlap	29
1.4	Treatment Effect Estimates for March 23, 2020	37
2.1	Eligible Issuers are Larger, with More Substantial Cash Flows	61
2.2	Eligible Issuers are also More Liquid with Lower Leverage	62
2.3	CDS Spreads Consistent with Higher Default Risk of Ineligible Firms	63
2.4	Eligible Firm Cash Holdings Show Relative Decline, Before Reverting	68
2.5	Relative Leverage of Ineligible Firms Rise	69
2.6	Relative Payouts by Eligible Firms Rise	70
2.7	Eligible Firms Display Relative Decline in Investment in 2020 Before Reversion .	71
2.8	Deep Net Architecture for the Potential Outcomes Model	81
2.9	Deep Net Architecture for Propensity Scores	81
2.10	Large Base Effect with Increase in Cash Holdings	84
2.11	Large Base Effect with Increase in Total Debt	85
2.12	Payout Base Effect Initially Negative Then Increases	86
2.13	Investment Base Effect Null then Increasing	87
2.14	Cash ATE With Heterogeneity Shows Large Negative Effect	89
2.15	Debt ATE With Heterogeneity Negative After 2020	91
2.16	Payout ATE Generally Positive	93
2.17	Investment ATE With Heterogeneity Consistent With Previous Estimates . . .	94
2.18	Positive Counterfactual Treatment Effect for Investment Not Robust to Alternative Proxy	99
2.19	Null Counterfactual Treatment Effects for Cash	100
2.20	Positive Counterfactual Treatment Effect for Debt	101
2.21	Positive Counterfactual Treatment Effect for Payouts	102
2.22	Base Effect for PPE Investment Proxy Negative Before Reverting to Null . . .	127
2.23	ATE for PPE Investment Proxy Null	129
2.24	Null Estimates for Ineligible Firms' Investment Counterfactual Treatment Effects	130
3.1	Secured Debt Intervention Boosts Equity Prices After Shock	162
3.2	Expected Equity Value Evolution Higher with Secured Debt Intervention . . .	163
3.3	Investment Rate Higher with Secured Debt Intervention	164
3.4	Evolution of of Expected Investment Rates Higher with Secured Debt Intervention	165
3.5	Unsecured Debt Prices Higher With Secured Debt Intervention for More Leveraged Firms	166
3.6	Unsecured Debt Issuance Rate Higher with Intervention	166

3.7	Secured Debt Intervention Boosts Unsecured Debt Price More Than Unsecured Debt Intervention	167
3.8	Secured Debt Intervention Increases Unsecured Debt Issuance and Payouts	168
3.9	Secured Debt Intervention Pushes Back Default Threshold	169
3.10	Secured Debt Intervention Reduces Expected Cumulative Default Rates	170
3.11	Secured Debt Intervention Supports Higher Leverage Ratios	171
3.12	Secured Debt Intervention Distribution Features First Order Stochastic Dominance Over Unsecured Debt Intervention	171
3.13	Initial Distribution of Firms	220
3.14	Dividend Restriction Binds for Large Portion of State Space	222
3.15	Debt Repurchase Motive With Dividend Restriction	223
3.16	Dividend Restriction Decreases Equity Value	224
3.17	Dividend Restriction Sharply Increases Investment Rates	225
3.18	Expected Evolution of Investment Rates Also Far Higher	226
3.19	Dividend Restriction Increases Unsecured Debt Price	227
3.20	Dividend Restriction has No Impact on Default Threshold	227
3.21	Dividend Restriction Sharply Reduces Long-Run Defaults	228
3.22	Surviving Firms Have Far Lower Leverage With Dividend Restriction; Even Less Without Debt Repurchase Restriction	229
3.23	Surviving Firms Have Far Lower Leverage With Dividend Restriction; Even Less Without Debt Repurchase Restriction	230
3.24	Expected Average Equity Values Increase Over Time With Restrictions	231

LIST OF TABLES

1.1	Comparison of Fed CCF Term Sheets on March 23, 2020, and April 9, 2020	11
1.2	Ratings Scales	13
1.3	Change in G-Spreads (Issuer Ratings as Proxy)	19
1.4	Change in G-Spreads (Issue Ratings as Proxy)	23
1.5	Change in G-Spreads (with Fallen Angel Interaction)	26
1.6	Change in G-Spreads (Quasi-Natural Experiment)	32
1.7	Treatment Effects of CCF Announcements on Bond Support	33
1.8	Change in Log Prices	42
1.9	Ratings Distribution of SMCCF Holdings and Index	43
1.10	Change in G-Spreads (SMCCF Index Proxy for Eligibility)	45
1.11	Features with Less than One Percent Missing Observations	46
1.12	Additional Features with Less than Ten Percent Missing Observations	47
1.13	Architecture for Deep Nets with 1% Tolerance for Missing Observations	48
1.14	Architecture for Deep Nets with 10% Tolerance for Missing Observations	48
1.15	Treatment Effects Estimates for March 23, 2020	49
2.1	Descriptive Statistics - Eligible	60
2.2	Descriptive Statistics - Ineligible	60
2.3	Debt Levels and Cash Holdings Broadly Increased, With Negative Treatment Effect for Eligible Firms	65
2.4	Eligible Firms' Payout Shows Positive Effect; No Effect Seen for Investment	66
2.5	Cash Treatment Effect Comparison	90
2.6	Debt Treatment Effect Comparison	92
2.7	Payout Treatment Effect Comparison	95
2.8	Investment Treatment Effect Comparison	96
2.9	Dynamic (Homogeneous) Treatment Effects	105
2.10	Features with Less than One Percent Missing Observations	106
2.11	Additional Features with Less than Ten Percent Missing Observations	107
2.12	Architecture for Deep Nets with 1% Tolerance for Missing Observations	112
2.13	Architecture for Deep Nets with 10% Tolerance for Missing Observations	112
2.14	Cash Base Effect	113
2.15	Debt Base Effect	114
2.16	Payout Base Effect	114
2.17	Investment Base Effect	115
2.18	Cash ATE	116
2.19	Debt ATE	117
2.20	Payout ATE	118
2.21	Investment ATE	119
2.22	Cash Treatment Effect Comparison	120
2.23	Debt Treatment Effect Comparison	121
2.24	Payout Treatment Effect Comparison	121
2.25	Investment Treatment Effect Comparison	122

2.26	Ineligible Firms' Cash Counterfactual Treatment Effect	123
2.27	Ineligible Firms' Debt Counterfactual Treatment Effect	124
2.28	Ineligible Firms' Payout Counterfactual Treatment Effect	125
2.29	Ineligible Firms' Investment Counterfactual Treatment Effect	126
2.30	Base Effect for PPE Investment Proxy	128
2.31	ATE for PPE Investment	128
2.32	Ineligible Firms Counterfactual Treatment Effect	131
3.1	Calibrated Parameters	159
3.2	Model Fit	161
3.3	Parameters for Numerical Estimation	221

ACKNOWLEDGMENTS

I am deeply grateful to my co-chairs, Raghuram Rajan and Zhiguo He, for their steadfast guidance, insightful discussions, and constructive feedback throughout the development of this dissertation. Their mentorship has profoundly shaped my academic journey. I am also indebted to Stefan Nagel, Fabrice Tourre, and Quentin Vandeweyer, the other members of my committee, whose valuable suggestions significantly improved the quality and rigor of my research.

I am grateful for helpful comments from (among many others) Amir Sufi, Ben Marrow, Eric Budish, Eric Zwick, Falk Bräuning, Fulin Li, Jessica S. Li, Jin Park, Jon Pogach, José L. Fillat, Lars Hansen, Mark Kutzbach, Max Farrell, Nishant Vats, Pietro Veronesi, Ralph Kojen, Sanjog Misra, Shohini Kundu, Yang Su, and Yusheng Fei, which greatly enhanced my understanding and the presentation of my findings. Separately, I want to thank Malaina Brown and Cynthia Hillman for cheering me on and providing significant administrative support (and emotional labor) as I persevered through the dissertation.

My heartfelt appreciation goes to the many other peers and colleagues at the University of Chicago Booth School of Business who I have not named for their support, encouragement, and contribution to a stimulating intellectual environment. In particular, I want to emphasize the enormous impact my PhD cohort-mate Yiran Fan had in helping me navigate and survive the challenging early stages of my PhD (2017 to 2020). Yiran's kindness, intelligence, and patience were critical to my progress and well-being. He was taken from us far too soon, robbing the world of a promising researcher, and I deeply mourn his absence.

Above all, I dedicate this dissertation to my wife, Tehreem, who not only completed an emergency medicine residency in Chicago during the challenges of the COVID-19 pandemic but also demonstrated immense patience and understanding during my frequent absences as I traveled between Chicago and Denver (2021 to 2023) and subsequently be-

tween Chicago and New York (2023 to 2025). Her boundless support, resilience, and love have been my greatest sources of strength and inspiration.

Finally, my appreciation extends to my family (AKM, Taslima, Anika, Jasia, Rubab, among many others) and friends (Will, Peter, Santosh, Gabe, Rich, among many others) whose unconditional support has been invaluable throughout this journey. I would also be remiss if I did not thank my cats, Angie and Marcel.

ABSTRACT

This dissertation investigates the price effects, real effects, and design of the Federal Reserve’s Corporate Credit Facilities (CCFs), launched in 2020 to stabilize U.S. corporate bond markets during the COVID-19 pandemic.

Chapter 1, based on work with Jessica S. Li, estimates impact of the CCFs on corporate bond spreads. The CCFs included both direct support via cash bond purchases and indirect support via exchange-traded fund (ETF) purchases. We exploit bond-level ratings heterogeneity across firms to identify treatment effects from direct bond support. The March 23, 2020 announcement of the CCFs reduced spreads by 96 basis points (bps) for eligible issuers. To estimate the impact of the April 9 expansion, we leverage a quasi-natural experiment involving “Fallen Angel” firms—those initially eligible, then briefly ineligible, but reinstated during the expansion. Relative to a control group, we find a -126 bps treatment effect. Using a causal machine learning approach detailed in Chapter 2, we estimate that ineligible firms would have seen a -500 bps spread reduction had they received direct bond support on March 23.

Chapter 2 develops a novel two-step semi-parametric difference-in-differences (DiD) estimator for dynamic and heterogeneous treatment effects, allowing for flexible policy counterfactuals. Applying the method to firm-level outcomes, I analyze the real effects of the CCFs on cash holdings, leverage, payouts, and investment. The estimator produces results consistent with conventional panel and event study regressions but highlights important heterogeneity. Firms generally increased cash and leverage, while payout and investment initially declined. However, CCF-eligible firms began deleveraging by 2021 and accumulated less cash compared to ineligible peers. Despite increased shareholder payouts, eligible firms did not raise investment levels, suggesting that the CCFs failed to achieve their stated real economy goals. Counterfactual treatment effects suggest that broadening eligibility for direct bond support might have increased leverage and payouts, but evidence on

investment gains is weak or inconclusive.

Chapter 3 provides a theoretical framework to explain these findings. I construct a dynamic capital structure model with investment in which firms cannot commit to a debt issuance policy. In the model, unsecured debt interventions accelerate borrowing but undermine the benefit of lower bond yields due to increased leverage. The proceeds are primarily distributed to shareholders rather than invested. In contrast, secured debt interventions support better investment outcomes because the collateral constraint on secured debt issuance induces commitment. Even for financially unconstrained firms, secured debt interventions yield more favorable dynamics, aligning firm incentives with the policy's intended real effects.

Together, these chapters demonstrate that while the CCFs were highly effective in reducing borrowing costs, their real effects were muted or misdirected, in part due to firms' inability to commit to future financial policies. The findings underscore the importance of policy design—particularly the role of collateral and commitment—in determining the effectiveness of credit market interventions.

CHAPTER 1

THE CAUSAL EFFECT OF THE FED'S CORPORATE CREDIT FACILITIES ON ELIGIBLE ISSUER BONDS

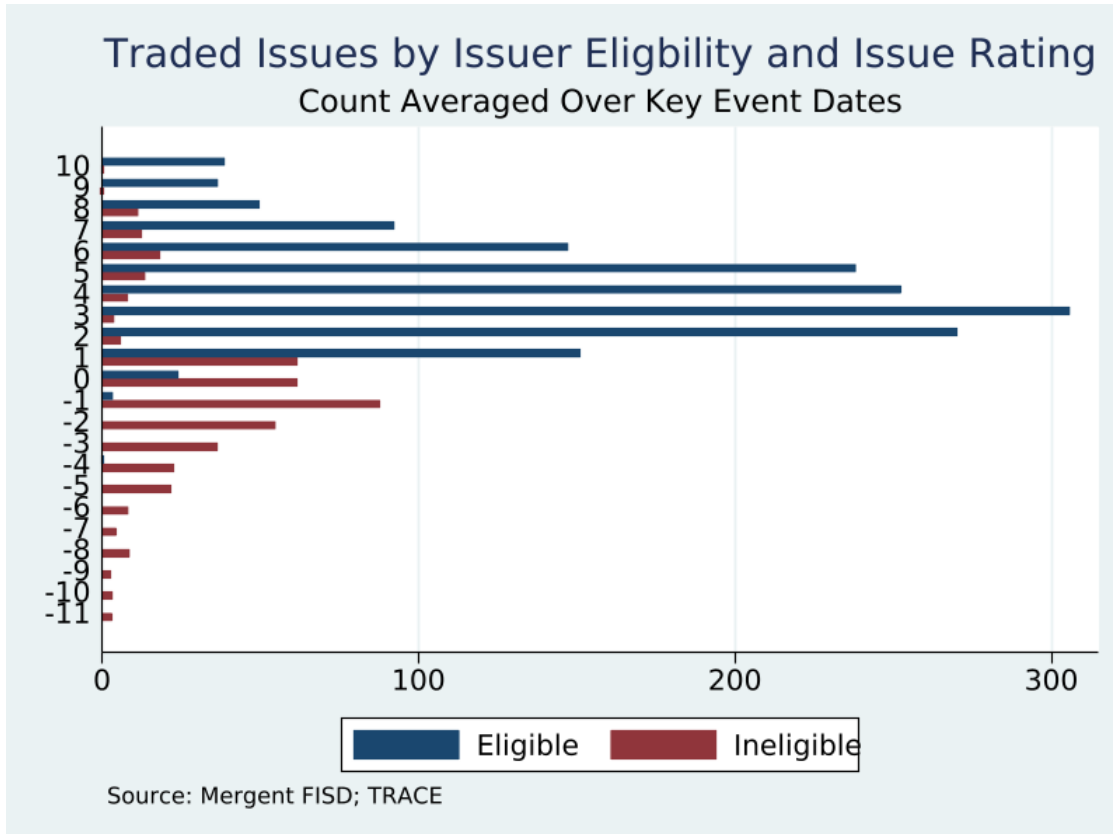
1.1 Introduction

In response to market and economic stress caused by the COVID-19 pandemic, the Federal Reserve expanded its monetary policy toolkit to include corporate bond purchases for the first time in its history. In this paper, we estimate the treatment effect of direct cash bond support from the Fed's Corporate Credit Facilities (CCFs). Complicating the estimation of these treatment effects is that the Fed staggered the announcements of the CCFs and also provided indirect support to issuers via potential exchange-traded fund (ETF) purchases. While eligibility for direct cash bond support was determined by issuer credit ratings, we note that existing studies identify eligibility by using issue-level credit ratings.¹

To address this, we introduce a novel identification strategy that exploits the capital structure heterogeneity of corporate bonds, as illustrated in Figure 1.1. Our strategy identifies the treatment effect of direct cash bond support by comparing similarly rated bonds with similar maturity but issued by differentially eligible firms in panel DiD regressions with fixed effects. This approach controls for the indirect support directed to bonds via potential ETF purchases. In contrast, papers using issue ratings to determine eligibility for direct cash bond support effectively compare the investment-grade (IG) bonds of both eligible and ineligible issuers with the high-yield (HY) bonds of mostly ineligible issuers,

1. These include papers studying prices/spread reactions, as well as liquidity impacts: Boyarchenko, Kovner, and Shachar [2020], D'Amico, Kurakula, and Lee [2020], Haddad, Moreira, and Muir [2021], Kargar et al. [2021], O'Hara and Zhou [2021], and Nozawa and Qiu [2021]. Notable exceptions are Flanagan and Purnanandam [2020] and Gilchrist et al. [2021], both of which limit their analyses to investment-grade (IG) issuers.

Figure 1.1: Distribution of Corporate Bond Ratings by Fed CCF Eligibility



The figure shows the relative count of issues by eligible and ineligible issuers over their numerical issue ratings (see Table 1.2 for the mapping between the letter and numerical ratings). We numerate issue ratings for corporate bonds which traded on March 23, 2020 and April 9, 2020. See Section 1.3 for additional elaboration on the eligibility criteria.

generating potential measurement error.

Using our identification strategy, we find that the initial announcement on March 23, 2020 of the Fed CCFs, with a potential size of up to \$300 bn, led to 96.0 bps of additional tightening for eligible issuers' spreads versus those of ineligible issuers. When the sample of bonds is restricted to those with less than five years maturity, which further aligns with the CCFs' eligibility criteria for direct support, the effect increases in magnitude to -135.5 bps.

These results are robust to using the change in log bond prices, instead of spreads, as the outcome variable and to proxying eligibility with the constituents of the SMCCF Broad

Market Index, which was announced prior to the start of direct cash bond purchases in mid-June. Interestingly, the SMCCF Broad Market Index proxy for eligibility suggests a far smaller magnitude for the treatment effect (-47.0 bps and -68.6 bps for all bonds and for bonds with less than five years maturity, respectively). This suggests that broader population of eligible bonds was more sensitive to the CCFs than those targeted by the Fed for purchase, which is consistent with the findings of Flanagan and Purnanandam [2020].

In the follow-up announcement on April 9, 2020, the Fed both increased the potential size of the CCFs to \$750 bn and also announced the purchases of HY ETFs. Despite emphasizing that HY ETF purchases would be much more limited in scope,² ineligible issuers' spreads reacted strongly to the announcement. On balance, while all bond spreads tightened on April 9, 2020, ineligible issuers' bonds were more sensitive to the inclusion of HY ETFs than eligible issuers' bonds were to the expansion of the facilities. The coefficient estimates are 65.1 bps and 87.0 bps for all bonds and for bonds with less than five years maturity, respectively, suggesting that eligible issuers' spreads widened relative to those of ineligible issuers.

We find that the measurement error induced by using issue ratings, rather than issuer ratings, to determine eligibility for direct cash bond support further underestimates the impact of the facility expansion on eligible issuers' spreads. The coefficient estimates become 91.0 bps and 107.0 bps for all bonds and for bonds with less than five years maturity, respectively, suggesting an even greater widening of eligible issuers' spreads relative to those of ineligible issuers. Hence, using issue ratings to proxy eligibility for direct cash bond support leads to a bias of around 20 bps to 26 bps, which is driven by classifying the IG bonds of HY issuers as eligible when they were not, thus underestimating the effect of the April 9, 2020 on eligible issuers' spreads.

To better isolate the effects of the April 9, 2020 facility announcement on direct cash

2. Realized purchases of HY ETFs totaled less than 8% of all CCF purchases.

bond support, we exploit a quasi-natural experiment around the eligibility of Fallen Angel issuers. Fallen Angel issuers were initially eligible for direct cash bond support but fell out of eligibility after experiencing downgrades between March 23, 2020 and April 9, 2020. The April 9, 2020 facility announcement restored the eligibility of these issuers. We compare the relative movement of the spreads of Fallen Angel issuers to a control group of similarly rated but never eligible issuers: those rated as IG by one rating agency but who were not eligible for the CCFs due to being rated HY by at least one other rating agency. We show that the distribution of their CDS spreads and the ratings of their bonds are similar, suggesting that they have similar risk characteristics and were similarly exposed to indirect support from ETF purchases.

Using the panel difference-in-differences (DiD) regressions with fixed effects and appropriately differencing coefficients, we compare the relative changes in spreads across these two groups and estimate treatment effects of -125.6 bps and -85.6 bps for all bonds and for bonds with less than five years maturity, respectively. The finding that the magnitude of the estimated treatment is smaller for bonds with less than five years maturity is surprising and contrary to previous estimates. It is driven by a greater tightening of the control groups' spreads versus those of Fallen Angel issuers within the subsample of bonds with less than five years maturity.

Nonetheless, as Fallen Angel issuers lost eligibility for direct cash bond support heading into April 9, 2020, the treatment effect of -125.6 bps roughly reflects the impact of the implied support when facilities were sized up to \$750 bn. While greater than the -96.0 bps effect estimated from the initial announcement of the facilities on March 23, 2020 at a size of up to \$300 bn, it is not proportionally higher in magnitude as the increase in the size of the facilities would suggest. This is consistent with the findings of Haddad, Moreira, and Muir [2025] that most of the effects of the CCFs were realized at their announcement, when markets priced in reduced tail-risk, reflecting a 'Fed put.'

To estimate the counterfactual treatment effect of direct cash bond support for ineligible issuers,³ we use the two-step semi-parametric DiD estimator introduced in Momin [2025b], which is based on Farrell, Liang, and Misra [2021a] and Farrell, Liang, and Misra [2021b]. The estimator is derived to adjust for any bias arising from the use of machine learning (ML) in estimating parameters which are inputs into the estimator. We refer to this as the causal ML approach. Identification is facilitated by the Fed’s use of credit ratings to determine eligibility for direct cash bond support, since credit ratings often lag fundamentals and market-based measures of risk, such as credit default swap (CDS) spreads [Altman and Rijken, 2004, Altman, 2020, Lee, Naranjo, and Velioglu, 2018, Lee, Naranjo, and Sirmans, 2021]. Momin [2025b] shows that eligible and ineligible issuers have significant overlaps in their distributions of CDS spreads and firm characteristics. The empirical strategy uses a high-dimensional set of features that allows for the ‘prediction’ of ineligible issuers’ counterfactual response to receiving the treatment (direct cash bond support), as well as allowing heterogeneity to be assessed. Under the assumptions of overlap and unconfoundedness, i.e. treatment assignment and potential outcomes are independent given the high-dimensional set of features, the average treatment effect (ATE), average treatment effect on the treated (ATET),⁴ group average treatment effects (GATEs), and counterfactual treatment effects are identified.

We focus on the response in bond spreads on March 23, 2020, since the impact of the Fed announcing direct cash bond support can be measured most accurately on this date. However, the causal ML approach also incorporates in any additional impact of potential ETF support, since the two are not separately identified. As such, the estimates of ATET obtained from comparing the difference in the change in spreads between eligible and in-

3. As well as any additional indirect support via promised ETF purchases on March 23, 2020.

4. ATET remains identified even if the assumption of unconfoundedness is relaxed to conditional no anticipation and parallel trends.

eligible issuers for the causal ML approach is analogous to the results from the panel DiD regressions without fixed effects. The range of ATET estimates from the causal ML approach is comparable to the estimate from the panel DiD regression without fixed effects.

To study heterogeneity, we compute the GATEs across the IG rating buckets (i.e. BBB, A, AA, AAA). This corresponds to the average treatment effect among eligible issuers with the same rating. We find a generally monotonic pattern where the magnitude of the treatment effect increases as the credit rating worsens, in line with a simple theoretical framework on the sensitivity of bond spreads to intervention, as a function of default risk [Brunnermeier and Krishnamurthy, 2020]. The exception to this pattern is the higher GATE for AAA-rated issuers versus AA-rated issuers. This may reflect the well-documented sell-off pressures faced by the safest securities at the onset of the pandemic, due to investors' heightened liquidity demand [Haddad, Moreira, and Muir, 2021, He, Nagel, and Song, 2022, Ma, Xiao, and Zeng, 2022].

The counterfactual treatment effect for ineligible issuers had they received direct cash bond support (as well as any additional indirect support from ETF purchases) is given by the GATE estimate for B- and BB-rated issuers. This is estimated to be around -500 bps and is statistically significant despite extremely large standard errors. Notably, the causal ML approach estimates such a large effect despite ineligible issuers' spreads generally widening on March 23, 2020. For comparison, the spreads of Fallen Angel issuers narrowed by around 300 bps on April 9, 2020. To the extent that ineligible issuers are of worse credit quality than Fallen Angel issuers, and if the estimate reflects additional indirect support from ETF purchases, the magnitude of the counterfactual treatment effect for ineligible issuers appears plausible.

1.1.1 *Contribution to Literature*

This paper primarily contributes to the large literature studying the effects of the Fed CCFs on corporate bond pricing, spreads, and liquidity, that were written contemporaneously with ours. First, it points out a potential identification concern that affects most of these papers, which determine eligibility by issue rather than issuer ratings [Boyarchenko, Kovner, and Shachar, 2020, D’Amico, Kurakula, and Lee, 2020, Haddad, Moreira, and Muir, 2021, Kargar et al., 2021, O’Hara and Zhou, 2021, Nozawa and Qiu, 2021].⁵ The novel identification strategy used here exploits the heterogeneity of the corporate bond capital structure, and the fact that differentially rated issuers have similarly rated bonds to measure the differential impact of the CCFs for bonds with similar ratings and maturity. Second, armed with this, we study the potential measurement bias that may have arisen from using issue rather than issuer ratings to determine eligibility. We find that this measurement bias arises particularly when determining the effect of the April 9, 2020 announcement on eligible issuer spreads, relative to ineligible issuer spreads, and understates its impact by 20 to 26 bps. It is driven by classifying the IG bonds of HY issuers as eligible for direct cash bond support.

Third, noting that the expansion of the CCFs on April 9, 2020 also brought into inclusion HY ETFs for purchases, we observe the difficulty of measuring the effect of the April 9, 2020 facility expansion on eligible issuers. To better identify this effect, we exploit quasi-experimental variation between the March 23, 2020 and April 9, 2020 announcement dates. There were several firms that were initially eligible for the CCFs but were subsequently downgraded out of eligibility before having their eligibility reinstated (the so-called Fallen Angels). We track the relative movements of the spreads of this group of firms with a control group of firms that just missed the ratings cutoff for eligibility to determine the

5. Notable exceptions are Flanagan and Purnanandam [2020] and Gilchrist et al. [2021], both of which limit their analyses to IG issuers.

treatment effect of the April 9, 2020 announcement. While the treatment effect estimate for expanded facility size is larger than the estimate from the initial announcement, it is not proportionally as large as the expansion in the facility size. This corroborates the finding in Haddad, Moreira, and Muir [2025] that markets priced in most of the conditional policy support promised by the Fed at the initial announcement.

Fourth, we utilize another novel identification strategy to estimate counterfactual treatment effects: the two-step semi-parametric DiD estimator of Momin [2025b], which is based on Farrell, Liang, and Misra [2021a] and Farrell, Liang, and Misra [2021b]. The causal ML approach allows for correct inference while using high-dimensional controls and ML-driven model selection. Other papers using double-debiased ML (DML) methods⁶ in the empirical asset pricing literature include Borri et al. [2024], Feng, Giglio, and Xiu [2020], Gomez-Gonzalez, Uribe, and Valencia [2024], Hansen and Siggaard [2024], and Maasoumi et al. [2024]. To the best of our knowledge, this paper is the first to use DML and related methods to assess counterfactual treatment effects in the finance literature.

The remainder of the paper is organized as follows. Section 1.2 discusses the related literature. Section 1.3 provides a general description of the data and sample construction, alongside relevant institutional details. Section 1.4 discusses the treatment effects for eligible issuers using panel DiD regressions and from exploiting the quasi-natural experiment around the eligibility of Fallen Angel issuers. Section 1.5 presents the counterfactual treatment effect estimates for ineligible issuers using the causal ML approach. Section 1.6 concludes.

6. See the canonical references of Belloni, Chernozhukov, and Hansen [2014] and Chernozhukov et al. [2018].

1.2 Related Literature

There are several papers that study the effect of the CCFs on prices/spreads, as well as liquidity. Haddad, Moreira, and Muir [2021] argue that the safest securities, including IG corporate bonds, experienced relatively greater selling pressure at the start of the COVID-19 financial crisis due to investor liquidity demands. O’Hara and Zhou [2021] and Kargar et al. [2021] corroborate this narrative by showing that liquidity deteriorated as corporate bond dealers shed inventory. O’Hara and Zhou [2021] further show that customer trades migrated to centralized client-to-client exchanges, though at higher costs. Kargar et al. [2021] show that costs of principal trades rose markedly, leading to an increase of lower-quality, slower agency trades. These papers all find that the Fed’s interventions worked to drastically improve liquidity in corporate bond markets. However, Nozawa and Qiu [2021] use a variance decomposition approach to identify a greater reduction in bond spreads due to the reduction of default risk, rather than improvements in liquidity, due to the announcement of the Fed CCFs.

Among all papers, there is tentative consensus that the March 23, 2020 event was more beneficial for eligible issuer bonds, but Boyarchenko, Kovner, and Shachar [2020] and Haddad, Moreira, and Muir [2021] present some evidence that April 9, 2020 may have been more beneficial for eligible issuer bonds. In contrast, this paper, D’Amico, Kurakula, and Lee [2020] and Nozawa and Qiu [2021] find that April 9, 2020 may have benefited ineligible issuer bonds to a greater extent. Using option prices to infer conditional policy support, Haddad, Moreira, and Muir [2025] finds that the initial March 23 announcement of the facilities had the largest effect in reducing tail risk for IG bonds, while the subsequent announcement on April 9 expanding the size of the facilities had more modest effects. Additionally, D’Amico, Kurakula, and Lee [2020] and Boyarchenko, Kovner, and Shachar [2020] find that issuance, particularly for IG issuers, quickly picked up pace following the introduction of the CCFs.

Similar to our focus on Fallen Angel issuers to estimate a counterfactual treatment, Nozawa and Qiu [2021] perform a similar, albeit descriptive, exercise and compare the change in spreads averaged across bonds for both the treated Fallen Angels and a matched control group. They compute an average two-day change in spreads of 340 bps for Fallen Angels versus 120 bps for the control group around the facility announcement dates. The implied treatment effect of 220 bps far exceeds our estimate of 126 bps.⁷

Unlike this paper and those above, Flanagan and Purnanandam [2020] and Gilchrist et al. [2021] restrict their samples to only IG issuers. Consequently, they do not bias their results by identifying eligible issuers by the use of issuer rather than issue ratings. Flanagan and Purnanandam [2020] find that the bonds that the Fed ultimately ended up purchasing were those that had become more ‘informationally sensitive,’ in the sense that these bonds were used as collateral in repo transactions and were sold by mutual funds meeting redemption demand. In contrast, the extent of bond price depreciation and the issuer’s payroll size seems to have matter less for SMCCF Index inclusion. Among eligible issuers, Gilchrist et al. [2021] find that issues below the five year maturity cutoff experienced a greater decrease in spreads than those issues above the cutoff. The authors find that the impact of the facilities on spreads seem to come from a reduction in credit risk premia, though this effect disappears when controlling for a correction in the credit term structure induced by the facility announcements. Consistent with our results and those of other papers, they find that the facility announcements induced a greater reduction in spreads than actual purchases of bonds.

This paper also relates to the literature on the ECB’s corporate bond purchase facility, the Corporate Sector Purchase Programme (CSPP), which predates the Fed CCFs. A

7. Nozawa and Qiu [2021] do not report standard errors, so it is unclear if the difference they find is statistically significant. In contrast, our results, reported in Table 1.6 are statistically significant at the 1% level with standard errors double-clustered by date and issuer.

key difference between the Fed CCFs and the CSPP relates to eligibility criteria, as the CCFs' ratings eligibility is determined at the issuer level whereas the CSPP is determined at the issue level. Several papers study the impact of the CSPP on European corporate bonds. Using pooled regression, Zaghini [2019] focus on the primary market issuances and find that the CSPP improved yield spreads for both eligible and ineligible bonds, upholding the re-balance channel. Abidi and Miquel-Flores [2018] exploit a slight difference between the CSPP and market IG/HY cutoff and propose a regression discontinuity design. They document both an improvement in bond spreads and an increase in primary market issuance and find that the announcement impact was most noticeable in the sample of CSPP-eligible bonds that were perceived as HY by the market, highlighting both the portfolio re-balance channel and the liquidity channel. Similarly, Todorov [2020] finds a sizable impact on the spreads of eligible bonds from the introduction of the CSPP.

1.3 Data and Institutional Background

1.3.1 Term Sheets

Table 1.1: Comparison of Fed CCF Term Sheets on March 23, 2020, and April 9, 2020

	March 23, 2020	April 9, 2020
Size of Facilities	Up to \$300 bn	Up to \$750 bn
IG Issuers (Direct Cash Bond Support)	Introduced	Expanded
HY Issuers (Direct Cash Bond Support)	Not Included	Only Fallen Angels Included
IG ETFs (Indirect Support)	Introduced	Expanded
HY ETFs (Indirect Support)	Not Included	Introduced

The table shows the high-level details of the Federal Reserve's announcements of the Primary Market Corporate Credit Facility (PMCCF) and the Secondary Market Corporate Credit Facility (SMCCF). The facilities were initially announced on March 23, 2020 and subsequently expanded on April 9, 2020. At inception, the CCFs provided direct cash bond support for IG issuers through potential primary and secondary market purchases. It also included support for IG ETFs. The facilities were expanded in April 9, 2020. In addition, Fallen Angel (FA) issuers, those who were eligible as of March 22, 2020 but were subsequently downgraded out of eligibility, had their eligibility reinstated. The Fed also amended the term sheet of the SMCCF to include purchases HY ETFs but stressed that the “preponderance” of ETF purchases would be IG ETFs.

On March 23, 2020, with equity capital provided by the U.S. Treasury, the Fed established two emergency lending facilities: the Primary Market Corporate Credit Facility (PMCCF) and the Secondary Market Corporate Credit Facility (SMCCF) to purchase primary market debt of up to four years in maturity and secondary market bonds of up to five years in maturity for non-financial IG issuers with significant U.S. operations. Additionally, the facilities gave the Fed the ability to purchase corporate bond ETFs with broad exposure to IG issuers. On April 9, 2020, the Fed expanded the size of the PMCCF and the SMCCF, as well as its scope to include HY corporate bond ETFs and extended eligibility to issuers who were rated as IG as of March 22, 2020, as long as on the day of purchase they are rated BB- or above (i.e. Fallen Angels). These announcements are summarized in Table 1.1.

1.3.2 Sample Construction

Corporate bond transaction data are obtained from the Enhanced TRACE database. The enhanced version of TRACE is made available on Wharton Research Data Services (WRDS) and updated quarterly. The Enhanced TRACE contains trade-level information on U.S. corporate bond transactions, including bond CUSIP, trade-level price, uncapped trade volume, execution time-stamp, buy/sell indicator, counterparty code, and other related metrics. We follow the literature and apply a standard filtering procedure (e.g., Dick-Nielsen [2014]) to clean the Enhanced TRACE. We remove all primary transactions from the data.

We obtain bond characteristics from Mergent FISD Bond Issues dataset via WRDS. These characteristics include issuer CUSIP, coupon, coupon type, maturity, offering date, maturity date, total par amount outstanding, industry, currency, country domicile, etc. The dataset also includes indicators for whether the bonds are perpetual, convertible, pay-in-kind, etc. Bond characteristics are merged with the TRACE dataset, and thus only TRACE-reportable bonds that have traded between January 1, 2020 and June 30, 2020

Table 1.2: Ratings Scales

Moody's	<i>S&P</i>	<i>Fitch</i>	<i>Value</i>
Aaa	<i>AAA</i>	<i>AAA</i>	10
Aa1	<i>AA+</i>	<i>AA+</i>	9
Aa2	<i>AA</i>	<i>AA</i>	8
Aa3	<i>AA-</i>	<i>AA-</i>	7
A1	<i>A+</i>	<i>A+</i>	6
A2	<i>A</i>	<i>A</i>	5
A3	<i>A-</i>	<i>A-</i>	4
Baa1	<i>BBB+</i>	<i>BBB+</i>	3
Baa2	<i>BBB</i>	<i>BBB</i>	2
Baa3	<i>BBB-</i>	<i>BBB-</i>	1
Ba1	<i>BB+</i>	<i>BB+</i>	0
Ba2	<i>BB</i>	<i>BB</i>	-1
Ba3	<i>BB-</i>	<i>BB-</i>	-2
B1	<i>B+</i>	<i>B+</i>	-3
B2	<i>B</i>	<i>B</i>	-4
B3	<i>B-</i>	<i>B-</i>	-5
Caa1	<i>CCC+</i>		-6
Caa2	<i>CCC</i>	<i>CCC</i>	-7
Caa3	<i>CCC-</i>		-8
Ca	<i>CC</i>	<i>CC</i>	-9
C	<i>C</i>	<i>C</i>	-10
	<i>D</i>	<i>D</i>	-11

Credit ratings scales and corresponding numeric values for Moody's, S&P, and Fitch.

are included in our sample. We also filter out any variable-coupon, convertible, perpetual or pay-in-kind securities as well as any security that appears in TRACE but is not included in the Mergent FISD dataset. We further only keep issuers domiciled in the U.S. since CCF eligibility was restricted to issuers with material U.S. operations.

We obtain bond ratings from Mergent FISD Bond Ratings dataset. This dataset contains issue ratings from Moody's, S&P, and Fitch, which are mapped by us to their corresponding numeric values according to Table 1.2. We compute issuer ratings from issue ratings by selecting the minimal issue rating on senior unsecured debt per issuer.⁸⁹ After obtaining issuer ratings, we determine eligibility for direct cash bond support from the Fed CCFs by using ratings as of March 22, 2020, and classify issuers as eligible if they were rated as IG or had at least two IG ratings if the issuer had more than one issuer rating.¹⁰ To compute issue fixed effects, we aggregate issue ratings by using its maximal issue rating and assign it to its respective rating bucket (eg. AAA, AA, A, BBB, BB, B).¹¹ The results are robust to other definitions aggregating issue ratings.

Thus, our sample is constructed using corporate bond transaction data from cleaned Enhanced TRACE for the period between January 1, 2020 and June 30, 2020 merged with

8. Issue ratings take into consideration bond seniority in the capital structure and any collateral security. See: <https://www.spglobal.com/ratings/en/products-benefits/products/issue-credit-ratings>.

9. Moody's explicitly equates the two in its ratings definition, issuer ratings corresponding to the ratings on senior unsecured bonds: "Long-Term Issuer Ratings are opinions of the ability of entities to honor long-term senior unsecured financial obligations and contracts." See: <https://www.moodysanalytics.com/-/media/products/Moodys-Rating-Symbols-and-Definitions.pdf>.

10. In addition to using issuer ratings to determine eligibility, the Fed also restricted direct cash bond support to securities with less than five years maturity. We explore this in our analysis by computing effects over a full sample and a sub-sample of bonds with less than five years maturity.

11. This is consistent with the fact that ETFs generally tend to use a less restrictive inclusion criteria than the Fed CCFs, often considering a bond's highest rating.

the Mergent FISD Bond Issues and Bond Ratings information and filters. Daily volume-weighted price and yield data is computed using trades of institutional size (i.e., greater than or equal to \$100,000). While this is a standard cleaning procedure, our results are robust to using the entire sample of trades.

We compute G-spreads for bonds by differencing the yields on corporate bonds and the corresponding zero-coupon bond spread of the same duration. The zero-coupon bond spreads are generated using the Nelson-Siegel-Svensson yield curve parametrization of Gurkaynak, Sack, and Wright [2006]. Data is available through the Federal Reserve.¹² Since TRACE reports ‘clean’ bond prices without accrued interest, we compute the accrued interest between a bond’s last coupon date and the settlement date and add this to the ‘clean’ price to get the final ‘dirty’ bond price faced by an investor at settlement. Spreads and bond prices are trimmed at the 1 percent and 99 percent levels to limit the influence of outliers. Results are robust to using untrimmed data. Spread changes and change in log bond prices are computed as one-day changes and, hence, are conditional on the availability of trade-weighted data in the current and previous trading days.

As a robustness check, we proxy eligibility for direct cash bond support from the CCFs by using the constituents of the Fed’s SMCCF Broad Market Index at inception.¹³ While the creation of the SMCCF Broad Market Index was announced on June 15, 2020, the initial index constituent list dates from June 5, 2020. If this list of eligible issuers was both the same set of eligible issuers as of the facility launch date on March 23, 2020 and could have also been inferred by the markets using issuer ratings information, then it would be a perfect proxy for eligible issuers. However, Flanagan and Purnanandam [2020] and Gilchrist et al. [2021] show that the SMCCF Broad Market Index constituents are a subset

12. <https://www.federalreserve.gov/data/nominal-yield-curve.htm>

13. <https://www.newyorkfed.org/markets/secondary-market-corporate-credit-facility/secondary-market-corporate-credit-facility-broad-market-index>

of all eligible issuers and that certain characteristics can predict index inclusion. Consequently, this proxy is a subset of the set of eligible issuers constructed using issuer ratings, as we do in our main results. See Section 1.7.1 for further discussion.

Additionally, the paper uses CDS spread data obtained from Markit through WRDS to compare market-based risk measures across issuers. The causal ML approach used in Section 1.5.1 uses firm fundamental characteristics obtained from the Financial Ratios Suites on WRDS.

1.3.3 *Descriptive Statistics*

Issuer Characteristics

Momin [2025b] examines the differences in firm fundamentals and CDS spreads across publicly traded eligible and ineligible firms. Although there is substantial overlap and in real and financial variables, eligible firms are larger, more liquid, and more solvent than ineligible firms. Likewise, while the distribution of CDS spreads across eligible and ineligible firms show considerable overlap, ineligible issuers have larger CDS spreads, consistent with ineligible issuers have lower credit ratings.

Issuer Capital Structure

Despite ineligible issuers having worse risk characteristics on average, this does not imply that ineligible issuers' bonds are strictly worse rated than eligible issuers' bonds. Figure 1.1 shows the ratings distribution across eligible and ineligible traded issuers for issuer-bond observations averaged over key event dates. While the vast majority of eligible issuers have IG-rated bonds, ineligible issuers have bonds spanning the HY and IG spectrum. The reason is principally due to some HY issuers issuing IG-rated debt. HY issuers can issue bonds which are rated higher than their issuer rating if the bonds are sufficiently

senior and are secured by collateral.

Figure 1.1 reinforces our concern about potential measurement issues when identifying bonds eligible for direct cash bond support by the CCFs by issue rather than issuer ratings. This would inadvertently classify the IG bonds of HY-rated issuers as eligible, which is inconsistent with the CCF's eligibility criteria. Similar concerns arise when using IG or HY ETFs to track the relatively changes in eligible issuer bonds since ETFs typically use bond ratings, not issuer ratings, for inclusion. On the other hand, the overlap in HY- and IG-rated bonds across eligible and ineligible issuers suggests a natural identification strategy: fix the bond rating (and other characteristics, such as maturity) and compare the relative changes in eligible versus ineligible issuer securities. This is the strategy we pursue in the next section.

1.4 Treatment Effects for Eligible Issuers

1.4.1 Baseline Results

As a baseline, we compute estimates of the impact of the CCF announcements on eligible issuer bond G-spreads versus ineligible issuer bond G-spreads, using issuer ratings to determine eligibility. We use a difference-in-differences panel regression with fixed effects to compare the relative change in spreads across eligible and ineligible issuers' bonds. The corresponding regression equation is:

$$\Delta S_{ijt} = \alpha + \beta_1 \text{Eligible}_i + \beta_2 \text{Events}_t + \beta_3 \text{Events}_t \times \text{Eligible}_i + \theta_{jt}^{\text{Rating}} + \theta_{jt}^{\text{Maturity}} + \epsilon_{jt} \quad (1.1)$$

where ΔS_{ijt} is the change in the G-spread of bond j at time t and Eligible_i is an indicator variable equal to one if issuer i is eligible for the Fed CCFs based on its issuer ratings as of March 22, 2020. Events_t is an indicator variable equal to one if day t is an event day

(e.g. March 23, 2020 or April 9, 2020), θ_{jt}^{Rating} are fixed effects for bond j rating (i.e. Aaa, Aa1, etc.) by week, and $\theta_{jt}^{Maturity}$ are fixed effects for bond remaining time-to-maturity (i.e. < 1 year, 1-2 years, 2-3 years, 3-4 years, 4-5 years, and 5+ years) by week. We use bond rating and time-to-maturity by date fixed effects due to the stationarity of our outcome variables, which tend toward zero as we increase the time horizon of its average to the full time-series. We compute fixed effects at the weekly instead of daily frequency to avoid issues of multicollinearity arising between the fixed effects and indicator variables. The inclusion of fixed effects approximates the comparison of spreads across differentially eligible issuers, while holding bond-level rating and maturity fixed. Additionally, we note that the parallel trends assumptions for our DiD regressions are satisfied as a result of using first-differenced, and hence, stationary, outcome variables.¹⁴

The results corresponding to the panel regression given by Equation (1.1) are reported in Table 1.3. Columns (1) and (2) correspond to specifications where fixed effects are omitted, while columns (3) and (4) report the coefficient estimates with fixed effects included. Columns (1) and (3) are estimates over the full sample of bonds, while columns (2) and (4) are estimates for the sample bonds with less than five years maturity. We note that the coefficient estimates decrease with the inclusion of fixed effects, consistent with our expectations that these fixed effects absorb variation common across issue ratings or bond maturities.

Our main estimates of interest correspond to the interacted variables, “March 23 X Eligible” and “April 9 X Eligible,” which map to β_3 in Equation (1.1). We focus on our full specification with fixed effects: columns (3) and (4). We find that the coefficient estimates for “March 23 X Eligible” are negative for the full sample and restricted sample with bonds with less than five years maturity and significant at the one percent level. These values

14. We perform panel data unit root tests of our key outcome variables (e.g. change in G-spreads) and find evidence consistent with this data being stationary (unreported).

Table 1.3: Change in G-Spreads (Issuer Ratings as Proxy)

	(1)	(2)	(3)	(4)
	<5yrs Maturity		<5yrs Maturity	
Eligible	-2.0307 (2.3932)	-2.2468 (3.1463)	-0.6726 (0.6668)	-0.8641 (1.2100)
March 23	62.3515*** (3.3844)	90.6787*** (7.0570)	16.2943 (36.3108)	37.0732 (47.9197)
April 9	-138.4193*** (3.5355)	-172.0778*** (7.5417)	-104.2630*** (9.8927)	-130.8509*** (12.9011)
March 23 X Eligible	-106.4632*** (3.0282)	-145.9185*** (6.6175)	-95.9738*** (17.8893)	-135.5091*** (28.4905)
April 9 X Eligible	90.2442*** (3.1742)	116.6548*** (7.0753)	65.0596*** (12.4963)	87.0349*** (16.3173)
Constant	2.4722 (2.9531)	2.4600 (3.7777)	1.5160 (0.9777)	1.5448 (1.3948)
Issue Ratings by Week F.E.	N	N	Y	Y
Remaining Maturity by Week F.E.	N	N	Y	Y
Observations	4.304e+05	2.100e+05	4.303e+05	2.100e+05
R2	0.0030	0.0030	0.1206	0.1242

Standard errors in parentheses

* $p < 0.1$, ** $p < 0.05$, *** $p < 0.01$

The table reports the regression coefficients and standard errors (double-clustered by issuer and time) for $\Delta S_{ijt} = \alpha + \beta_1 \text{Eligible}_i + \beta_2 \text{Events}_t + \beta_3 \text{Events}_t \times \text{Eligible}_i + \theta_{jt}^{\text{Rating}} + \theta_{jt}^{\text{Maturity}} + \epsilon_{jt}$. ΔS_{ijt} is the change in G-spread of bond j at time t for issuer i , Eligible_i is an indicator variable equal to one if issuer i is eligible for the Fed CCFs based on its issuer ratings as of March 22, 2020, Events_t is an indicator variable equal to one if day t is an event day, $\theta_{jt}^{\text{Rating}}$ are fixed effects for bond j rating (i.e. Aaa, Aa1, etc.) by week, and $\theta_{jt}^{\text{Maturity}}$ are fixed effects for bond remaining time-to-maturity (i.e. < 1 year, 1-2 years, 2-3 years, 3-4 years, 4-5 years, and 5+ years) by week. Columns (1) and (2) report the regression estimates without fixed effects. Columns (3) and (4) report the estimates with fixed effects. Columns (1) and (3) show the results for the regression run over the full sample of bonds, while columns (2) and (4) show the results for the sample of bonds with less than five years maturity (the CCFs targeted bonds with less than five years maturity for eligible issuers). From the table, we see that eligible issuer bonds tightened more than ineligible issuer bonds on March 23, 2020, as indicated by the coefficient estimate for “March 23 X Eligible.” On April 9, 2020, we uncover the opposite relationship, as indicated by the positive coefficient estimate for “April 9 X Eligible.” Since the Fed also announced purchases of HY ETFs on April 9, 2020, comparing bonds across issuer eligibility cannot uncover the effect of the CCFs expansion on bond spreads for issuer eligible direct cash bond support.

result indicate that eligible issuer bonds decreased -96 bps and -135 bps, respectively, for the full sample and restricted sample, which is consistent with the CCFs targeting bonds with less than five years maturity for eligible issuers. Note that on this date the Fed only indicated that it would support eligible issuer bonds, either directly through primary or secondary market purchases, or through purchases of IG ETFs. Hence, the estimates for March 23, 2020 provide a clearer estimate of the treatment effect on bond spreads for issuers eligible for direct cash bond support under the Fed CCFs.¹⁵ These estimates are also consistent with the finding in Haddad, Moreira, and Muir [2025] that the March 23, 2020 introduced a ‘Fed put’ on eligible issuers’ bonds, protecting against downside risk.

In contrast, the Fed’s announcement on April 9, 2020, while expanding the size of the facilities (from \$300 billion to \$750 billion), featured two other innovations: 1. the intention to purchase HY ETFs and 2. reinstating the eligibility of ‘Fallen Angels,’ issuers eligible as of March 22, 2020, but who were downgraded out of eligibility between March 22, 2020 and April 9, 2020. These are summarized in Table 1.1.

The coefficient estimates on “April 9 X Eligible” in Table 1.3 measure the relative impact of the program expansion. The positive coefficients indicate that ineligible issuers’ bonds tightened relatively more than those of eligible issuers. In the full specification, columns (3) and (4), on April 9, 2020, we find that ineligible issuer spreads experienced 65 bps and 87 bps additional tightening, compared to eligible issuer spreads, in the full sample and restricted sample, respectively. Given that the Fed indicated that it would purchase HY ETFs in much smaller quantities than other securities, a fact validated by ex post purchases,¹⁶ these results imply that ineligible issuer securities were far more responsive to announced monetary stimulus.

15. Implicitly, we assume that IG-rated bonds across differentially eligible issuers would experience the same effect from IG ETF purchases, holding fixed bond rating and maturity.

16. Realized purchases of HY ETFs totaled less than 8% of all CCF purchases.

Consequently, simply comparing the relative movements in eligible versus ineligible issuer spreads does not adequately identify the treatment effect of the expansion of direct cash bond support on the spreads of eligible issuers' bonds. To this end, we exploit a quasi-natural experiment around the reinstated eligibility of Fallen Angel issuers to better measure the effect of the facilities' expansion, which is reported in Table 1.6.

Robustness

Robustness checks are provided in Section 1.7.1 in the Appendix. First, change in log bond prices, instead of change in bond spreads, is used as the outcome variable when re-estimating Equation (1.1). Unsurprisingly, the qualitative results are similar in return space, with eligible issuer bond prices showing a relatively higher increase on March 23 and ineligible issuer bond prices showing a relatively higher increase on April 9.

Additionally, Equation (1.1) is re-estimated in spread space while proxying eligible issuers using the SMCCF Broad Market Index constituents. The Fed announced the SMCCF Broad Market Index on June 15, 2020 ahead of purchases of secondary market cash bonds on June 16, 2020. The index constituents are a subset of all eligible issuers. While the qualitative patterns of the estimated coefficients is similar to Table 1.3, magnitudes are strikingly smaller. This appears consistent with the findings of Flanagan and Purnanandam [2020] that the Fed did not select the bonds that experienced the greatest decline in prices (increase in spreads) for inclusion into the index and hence, for purchase by the SMCCF.

1.4.2 Measurement Error from Using Issue Ratings

In Table 1.4, we re-run the specification given by Equation (1.1), but instead proxy issue eligibility by issue-level ratings, as of March 22, 2020, instead of using issuer-level ratings as the Fed criteria stipulates. We do this to quantify the bias that results from using an

improper proxy for issue eligibility. This is an important question since we find that the literature uses such proxies when analyzing the effects of the facilities across IG and HY issuers.¹⁷ Consequently, our specification becomes:

$$\Delta S_{ijt} = \alpha + \beta_1 \text{IG Issue}_{ij} + \beta_2 \text{Events}_t + \beta_3 \text{Events}_t \times \text{IG Issue}_{ij} + \theta_{jt}^{\text{Rating}} + \theta_{jt}^{\text{Maturity}} + \epsilon_{jt} \quad (1.2)$$

where the subscript on the variable IG Issue_{ij} suggests that its possible for issuers i to have some issues j classified as eligible for the CCFs and others ineligible, depending on the issue rating. Figure 1.1 shows that a nontrivial of HY issuers have both IG and HY bonds, which give rise to the preceding dynamic.

Comparing columns (3) and (4) of Table 1.4 with columns (3) and (4) of Table 1.3, we find that the coefficient estimates for the interacted event and eligibility proxy variable for March 23, 2020 are roughly the same, suggesting that using issue ratings does not significantly bias the results. The values are -96 bps and -136 bps for “March 23 X Eligible” in Table 1.3 versus -100 bps and -135 bps for “March 23 X IG Issue” in Table 1.4 for all bonds and bonds with less than five years maturity, respectively. In contrast, we find that there is notable distortion of the coefficient estimates for April 9, 2020. We compute coefficient estimates of 65 bps and 87 bps for “April 9 X Eligible” in Table 1.3 versus 91 bps and 107 bps for “April 9 X IG Issue” in Table 1.4 for all bonds and bonds with less than five years maturity, respectively. Moreover, the common effect on all bonds on April 9, 2020 is denoted by the “April 9” variable in Tables 1.3 and 1.4 and is estimated to be roughly the same.

17. These include papers studying prices/spread reactions, as well as liquidity impacts: Boyarchenko, Kovner, and Shachar [2020], D’Amico, Kurakula, and Lee [2020], Haddad, Moreira, and Muir [2021], Kargar et al. [2021], O’Hara and Zhou [2021], and Nozawa and Qiu [2021]. Notable exceptions are Flanagan and Purnanandam [2020] and Gilchrist et al. [2021], both of which limit their analyses to IG issuers.

Table 1.4: Change in G-Spreads (Issue Ratings as Proxy)

	(1)	(2)	(3)	(4)
	<5yrs Maturity		<5yrs Maturity	
IG Issue	-1.8840 (3.2672)	-1.8512 (3.8830)		
March 23	71.7128*** (5.2138)	94.5870*** (9.8448)	25.6632 (42.9512)	43.0376 (54.3325)
April 9	-158.6382*** (5.5242)	-186.6985*** (10.6646)	-129.0811*** (4.4110)	-150.5372*** (10.1600)
March 23 X IG Issue	-109.9258*** (5.5746)	-142.3483*** (10.1711)	-100.2265*** (26.2299)	-135.0450*** (38.2180)
April 9 X IG Issue	109.5167*** (5.2386)	129.2813*** (10.5055)	91.0465*** (7.5892)	107.0200*** (13.8572)
Constant	2.4427 (3.7445)	2.2147 (4.3929)	0.9900 (0.7378)	0.8904 (0.9631)
Issue Ratings by Week F.E.	N	N	Y	Y
Remaining Maturity by Week F.E.	N	N	Y	Y
Observations	4.304e+05	2.100e+05	4.303e+05	2.100e+05
R2	0.0029	0.0028	0.1206	0.1241

Standard errors in parentheses

* $p < 0.1$, ** $p < 0.05$, *** $p < 0.01$

The table reports the regression coefficients and standard errors (double-clustered by issuer and time) for $\Delta S_{ijt} = \alpha + \beta_1 \text{IG Issue}_{ij} + \beta_2 \text{Events}_t + \beta_3 \text{Events}_t \times \text{IG Issue}_{ij} + \theta_{jt}^{\text{Rating}} + \theta_{jt}^{\text{Maturity}} + \epsilon_{jt}$. ΔS_{ijt} is the change in G-spread of bond j at time t for issuer i , IG Issue_{ij} is an indicator variable equal to one if issue j is eligible for the Fed CCFs based on its issue ratings as of March 22, 2020, Events_t is an indicator variable equal to one if day t is an event day, $\theta_{jt}^{\text{Rating}}$ are fixed effects for bond j rating (i.e. Aaa, Aa1, etc.) by week, and $\theta_{jt}^{\text{Maturity}}$ are fixed effects for bond remaining time-to-maturity (i.e. < 1 year, 1-2 years, 2-3 years, 3-4 years, 4-5 years, and 5+ years) by week. In contrast to Table 1.3, treated bonds are determined by issue ratings, as opposed to issuer ratings. Columns (1) and (2) report the regression estimates without fixed effects. Columns (3) and (4) report the estimates with fixed effects. Columns (1) and (3) show the results for the regression run over the full sample of bonds, while columns (2) and (4) show the results for the sample of bonds with less than five years maturity. Similar to Table 1.3, we see that eligible issuer bonds tightened more than ineligible issuer bonds on March 23, 2020, as indicated by the coefficient estimate for “March 23 X Eligible.” Similarly, on April 9, 2020, we find the opposite relationship, as indicated by the positive coefficient estimate for “April 9 X Eligible.” However, in contrast to Table 1.3, we find a larger estimate for “April 9 X Eligible,” which we attribute to the bias induced by incorrectly using issue ratings, as opposed to issuer ratings, to identify treated bonds.

Consequently, the issue ratings identification leads one to conclude that eligible issuer bonds widened 26 bps and 20 bps more on April 9, for all bonds and bond with less than five years maturity, respectively, than the more accurate specification proxying issuer eligibility using issuer ratings. Stated otherwise, the relative effect on bonds eligible for direct cash bond support is underestimated when using issue ratings to determine eligibility. This result is driven by the IG bonds of HY issuers being classified as eligible for direct cash bond support, contrary to the stated eligibility criteria. As shown in Table 1.1, the IG bonds of eligible issuers stood to benefit both from expanded IG ETF purchases and greater direct support. In contrast, the IG bonds of HY issuers only benefited from potential greater IG ETFs. Hence, classifying IG bonds of HY issuers as eligible for direct bond support dilutes the estimated relative effect of the facility expansion on April 9, 2020.

1.4.3 Quasi-Natural Experiment

The focus of this paper has been on determining the treatment effect on issuer spreads from receiving direct cash bond support from the CCFs. The coefficient on the variable "March 23 X Eligible" in Table 1.3 in columns (3) and (4) may provide one estimate of this effect, since on March 23, 2020 the Fed's announcements primarily targeted eligible issuers, at least for the initial level of support the Fed pledged (up to \$300 bn). To obtain an estimate of this effect, issue rating and maturity fixed effects are used to approximate the comparison of bonds with similar ratings and maturity but with differently eligible issuers, exploiting the capital structure heterogeneity for identification, as shown in Figure 1.1. Assuming that the effects from announcing purchases of IG ETFs net out across similarly rated bonds with similar durations, the 'March 23 X Eligible" coefficient estimates the effect of direct cash bond support on eligible issuers' spreads.

However, the coefficient estimates for the effect on April 9, 2020 do not provide a meaningful estimate of the effects of expanded direct cash bond support, since the Fed also an-

nounced purchases of HY ETFs. This is reinforced by the negative coefficient estimates for the “April 9” indicator variable in Table 1.3, which suggests that spreads significantly tightened for all issuers, while the positive coefficient estimates for the interacted term “April 9 X Eligible” suggests eligible issuers’ spreads widened relative to ineligible issuers’ spreads. Stated otherwise, ineligible issuers’ spreads were more sensitive to the announcement of HY ETF purchases than eligible issuers’ spreads were to expanded direct cash bond support.

To identify the impact of the total promised direct cash bond support, we exploit the quasi-natural experiment around the reinstated eligibility of Fallen Angel issuers on April 9, 2020. These issuers were eligible at initial program announcement date on March 23, 2020, but then fell out of eligibility as they were downgraded between March 23, 2020 and April 9, 2020. To get a baseline sense of the movement in Fallen Angel issuers, we modify Equation (1.1) to add an additional interaction term:

$$\begin{aligned}\Delta S_{ijt} = & \alpha + \beta_1 \text{Eligible}_i + \beta_2 \text{Fallen Angel}_i + \beta_3 \text{Events}_t \\ & + \beta_4 \text{Events}_t \times \text{Eligible}_i + \beta_5 \text{Events}_t \times \text{Eligible}_i \times \text{Fallen Angel}_i + \theta_{jt}^{\text{Rating}} \quad (1.3) \\ & + \theta_{jt}^{\text{Maturity}} + \epsilon_{jt}\end{aligned}$$

where Fallen Angel_i indicates if issuer i is a Fallen Angel as defined above. Since Fallen Angel issuers are a subset of eligible issuers, we drop the term $\text{Eligible}_i \times \text{Fallen Angel}_i$ term from the saturated regression.

The results of the regression of Equation (1.3) is shown in Table 1.5. We first check to see how the coefficients on “March 23 X Eligible” and “April 9 X Eligible” change with the effect from the Fallen Angel issuers separated out. Compared to Table 1.3, in columns (3) and (4), we find that the coefficient estimates are roughly unchanged for the “March 23 X Eligible” estimate. However, we find that the coefficient on “April 9 X Eligible” now increases to 78 bps from 65 bps for all bonds and to 104 bps from 87 bps for bonds with less

Table 1.5: Change in G-Spreads (with Fallen Angel Interaction)

	(1)	(2)	(3)	(4)
	<5yrs Maturity		<5yrs Maturity	
Eligible	-2.0283 (2.4711)	-2.2572 (3.2700)	-0.7865 (0.6733)	-1.1253 (1.3835)
Fallen Angel	-0.0828 (2.8414)	0.2670 (3.5955)	1.1462 (1.8098)	1.3553 (2.4170)
March 23	62.3515*** (3.3819)	90.6787*** (6.9953)	16.5548 (36.3555)	37.6210 (48.0478)
April 9	-138.4193*** (3.5358)	-172.0778*** (7.4739)	-108.1523*** (6.1970)	-134.8096*** (9.9283)
March 23 X Eligible	-108.0201*** (2.9902)	-148.7916*** (6.7883)	-97.4222*** (17.9364)	-138.4093*** (28.7550)
April 9 X Eligible	99.0936*** (3.1483)	129.9784*** (7.2762)	78.1181*** (8.1861)	104.4044*** (12.8580)
March 23 X Eligible X Fallen Angel	76.4135*** (21.6537)	108.7288*** (27.9802)	55.3663** (22.1747)	84.0850*** (28.3553)
April 9 X Eligible X Fallen Angel	-244.7509*** (14.3982)	-289.0271*** (7.1994)	-229.2277*** (14.7137)	-271.9726*** (16.9799)
Constant	2.4722 (2.9533)	2.4600 (3.7782)	1.5791 (1.0371)	1.7033 (1.5822)
Issue Ratings by Week F.E.	N	N	Y	Y
Maturity Bucket by Week F.E.	N	N	Y	Y
Observations	4.304e+05	2.100e+05	4.303e+05	2.100e+05
R2	0.0036	0.0037	0.1211	0.1247

Standard errors in parentheses

* $p < 0.1$, ** $p < 0.05$, *** $p < 0.01$

The table reports the regression coefficients and standard errors (double-clustered by issuer and time) for $\Delta S_{ijt} = \alpha + \beta_1 \text{Eligible}_i + \beta_2 \text{Fallen Angel}_i + \beta_3 \text{Events}_t + \beta_4 \text{Events}_t \times \text{Eligible}_i + \beta_5 \text{Events}_t \times \text{Eligible}_i \times \text{Fallen Angel}_i + \theta_{jt}^{\text{Rating}} + \theta_{jt}^{\text{Maturity}} + \epsilon_{jt}$. As in Table 1.3, ΔS_{ijt} is the change in G-spread of bond j at time t for issuer i , Eligible_i is an indicator variable equal to one if issuer i is eligible for the Fed CCFs based on its issuer ratings as of March 22, 2020, Events_t is an indicator variable equal to one if day t is an event day, $\theta_{jt}^{\text{Rating}}$ are fixed effects for bond j rating (i.e. Aaa, Aa1, etc.) by week, and $\theta_{jt}^{\text{Maturity}}$ are fixed effects for bond remaining time-to-maturity (i.e. < 1 year, 1-2 years, 2-3 years, 3-4 years, 4-5 years, and 5+ years) by week. The new variable, Fallen Angel_i , indicates if issuer i was eligible for the Fed CCFs on March 23, 2020 but lost eligibility between March 23, 2020 and April 9, 2020 due to being downgraded. On April 9, 2020, the Fed restored the eligibility of these issuers. Columns (1) and (2) report the regression estimates without fixed effects. Columns (3) and (4) report the estimates with fixed effects. Columns (1) and (3) show the results for the regression run over the full sample of bonds, while columns (2) and (4) show the results for the sample of bonds with less than five years maturity. We find that Fallen Angel issuer bonds tighten less than eligible issuer bonds on March 23, 2020 and tighten significantly more than eligible issuer bonds on April 9, 2020.

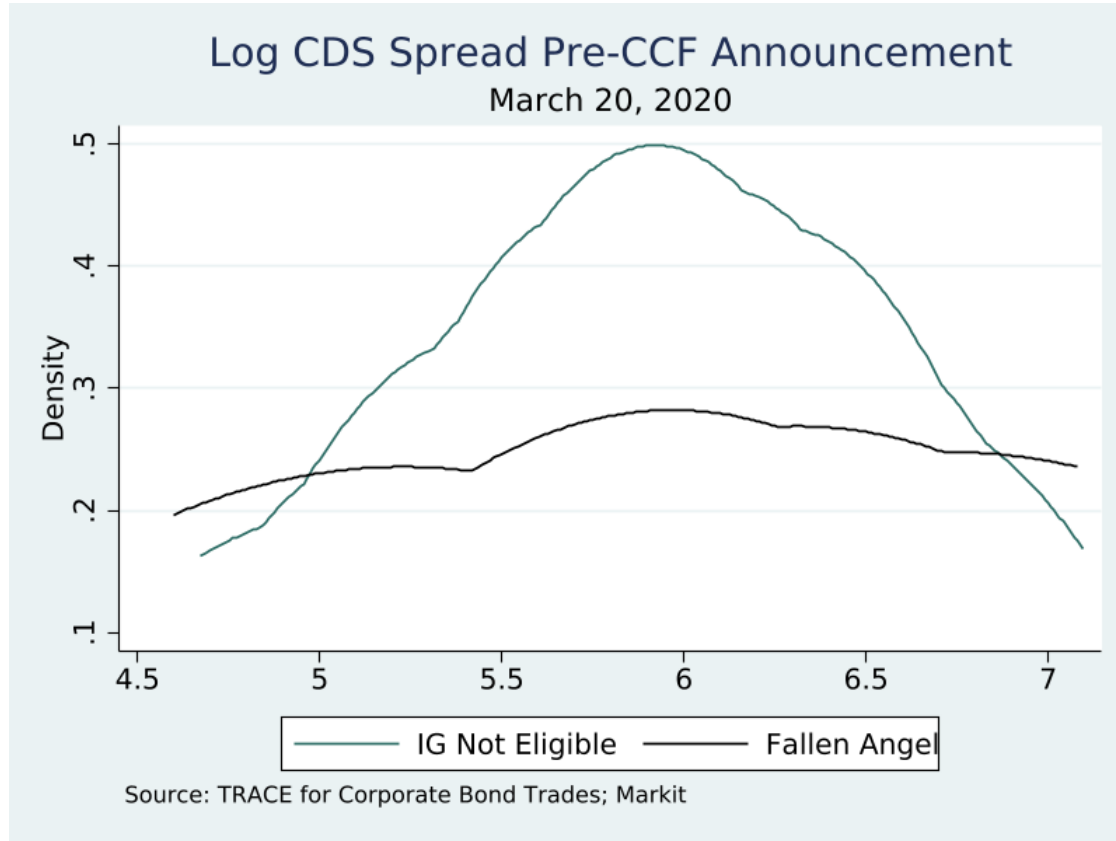
than five years maturity. There are two forces at play: 1. the number of Fallen Angel issues is orders of magnitudes lower than the overall number of eligible issues, 2. Fallen Angel issues can be more sensitive to the facility announcements. On balance, the latter force dominated the former in increasing the coefficient estimate for “April 9 X Eligible.” That is, the sharp narrowing of Fallen Angel issuer spreads decreased the overall average effect estimated for eligible issuer spreads in Table 1.3. With this effect partialled out, we find instead that non-Fallen Angel eligible issuer bonds widened more compared to ineligible issuer bonds than previously estimated.

The additional spread narrowing or widening of Fallen Angel issuer spreads are given by the coefficients ‘March 23 X Eligible X Fallen Angel’ and ‘April 9 X Eligible X Fallen Angel’ in Table 1.5. Interestingly, we estimate a positive effect on March 23, 2020 but a negative effect on April 9, 2020. The former suggests that Fallen Angel issuers spreads did not narrow as much as other eligible issuer spreads. However, by summing the coefficients on ‘Eligible’, ‘Fallen Angel’, ‘March 23’, ‘March 23 X Eligible’, and ‘March 23 X Eligible X Fallen Angel’, we do see that Fallen Angel issuers spreads did decline on average on this date. This suggests that the markets factored in the possibility that Fallen Angel issuers would, in fact, be downgraded out of eligibility, thus losing CCF support.

In contrast, when Fallen Angel issuer eligibility was restored on April 9, 2020, we find that their spreads narrowed 229 bps and 272 bps more compared to eligible issuer spreads for all bonds and bonds with less than five years maturity, respectively. This may be one potential estimate of the counterfactual treatment effect on ineligible issuer spreads we are after, since Fallen Angel issuers were technically ineligible for CCF support entering April 9, 2020. However, other eligible issuers may not be the most appropriate control group for the Fallen Angel issuers. First, these issuers have a better risk profile than the Fallen Angel issuers, and second, the effect of additional stimulus on spreads may generally not be as strong as initial announcement effects pledging stimulus for the bonds of certain issuers.

Consequently, both of these reasons may lead to an overstatement of the counterfactual treatment effect we see to estimate. Instead, we will seek to refine this estimate by choosing a more suitable control group that may better share the risk profile of the Fallen Angel issuers than other eligible issuers do.

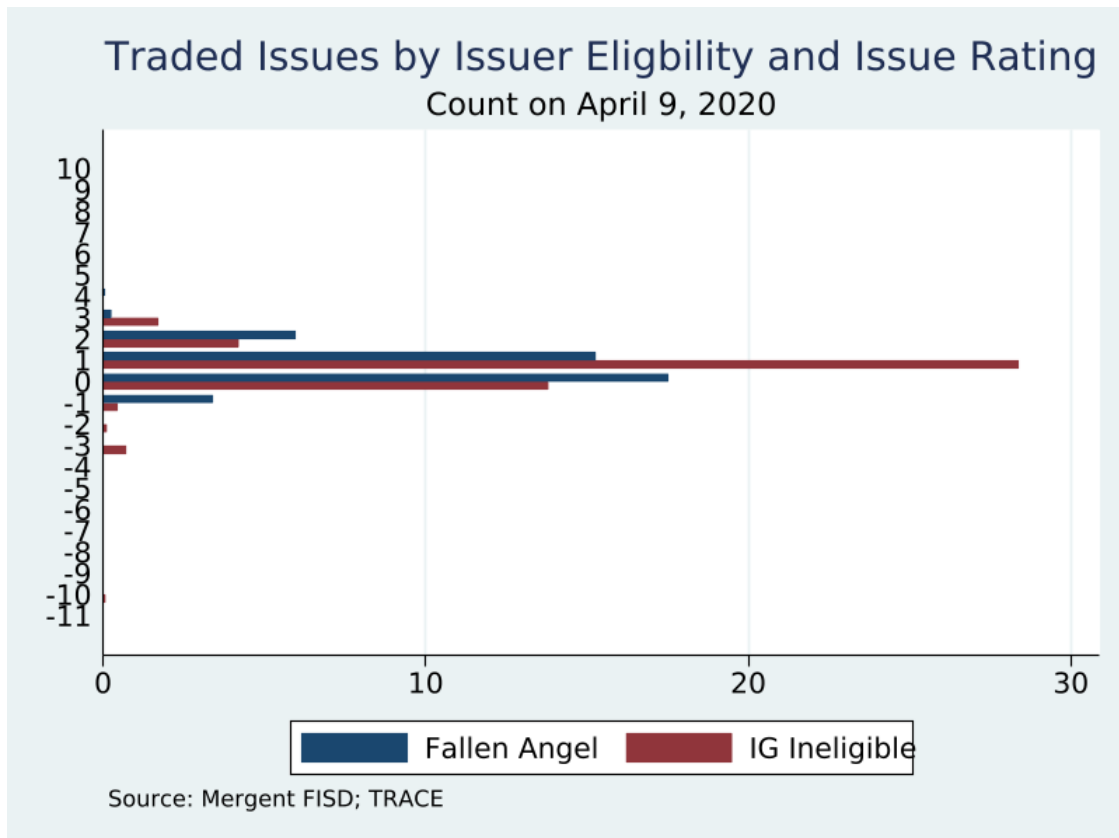
Figure 1.2: CDS Spreads of Control (IG Ineligible) and Treatment (Fallen Angel) Share Common Support



The figure plots the log CDS spread distributions of IG ineligible (i.e. those issuers with multiple ratings where exactly one is IG so are not eligible for the Fed CCFs) and Fallen Angel issuers on March 20, 2020. We find that IG ineligible and Fallen Angel issuers share a common support.

Specifically, we compare Fallen Angel issuers to issuers ‘just below’ the Fed’s eligibility cutoff: issuers with multiple ratings and exactly one IG rating. By the CCF criteria, these issuers are ineligible since they lack at least two IG ratings when they have more than one rating. Figure 1.2 compares the distribution of log CDS spreads for IG but never eligible issuers with Fallen Angel issuers. We see that the support of the two groups coincides,

Figure 1.3: Capital Structure of Control (IG Ineligible) and Treatment (Fallen Angel) Overlap



The figure shows the count of issue ratings for IG ineligible and Fallen Angel bonds which traded on April 9, 2020. We find considerably less heterogeneity between IG ineligible and Fallen Angel issuer capital structures along the bond risk dimension than we see for the broader sample of eligible and ineligible issuer capital structures, as seen in Figure 1.1. On this note, we find relatively similar proportions of IG and HY debt by IG ineligible and Fallen Angel issuers. While our identification strategy compares same-rated, same-maturity but differentially eligible bonds, the similar exposure to IG and HY ETFs across IG ineligible and Fallen Angel issuers is an advantage compared to comparing the broader sample of eligible and ineligible issuer bonds with each other, since the broader samples are differentially exposed to IG and HY ETFs.

suggesting that the market-based risk assessment of the two groups are similar. Figure 1.3 shows the capital structure of Fallen Angel and IG ineligible issuers.¹⁸ While there is a higher count of IG ineligible issues, we see that the number of issues is roughly comparable across the two groups and that the relative risk distribution of their capital structures, as of April 9, 2020, is aligned around the IG/HY cutoff. Besides reinforcing the argument that the relative risk in Fallen Angel and IG ineligible bonds is similar, it also suggests that both groups are similarly exposed to the Fed's ETF purchases, either through IG or HY ETFs.

To recover the treatment effect of the full promise of direct cash bond support implied by the final size of the CCFs, we specify a saturated regression comparing these two groups:

$$\begin{aligned}
\Delta S_{ijt} = & \beta_0 + \beta_1 \text{IG (Max Rating)}_i + \beta_2 \text{Eligible}_i + \beta_3 \text{Fallen Angel}_i \\
& + \beta_4 \text{Events}_t + \beta_5 \text{Events} \times \text{IG (Max Rating)}_{it} \\
& + \beta_6 \text{Events}_t \times \text{IG (Max Rating)} \times \text{Eligible}_{it} \\
& + \beta_7 \text{Events}_t \times \text{IG (Max Rating)} \times \text{FA}_{it} \\
& + \theta_{jt}^{\text{Rating}} + \theta_{jt}^{\text{Maturity}} + \epsilon_{jt}
\end{aligned} \tag{1.4}$$

where IG (Max Rating)_i is the sample of issuers which have a maximum issuer rating that is IG, as of March 22, 2020. Since $\text{Fallen Angel} \subset \text{Eligible} \subset \text{IG (Max Rating)}$, the above is a saturated regression with collinear terms omitted. To obtain our estimate for the counterfactual treatment effect, we subtract the effect on IG but ineligible issuers from the effect on Fallen Angel issuers:

- Effect on IG but ineligible issuers given by: $\beta_0 + \beta_1 + \beta_4 + \beta_5$

18. The approach to aggregate bond-level ratings is discussed in Section 1.3. It reflects that the inclusion criteria for IG ETFs is generally less restrictive than the eligibility criteria for the CCFs. The panel regression estimates are robust to using alternative rating aggregations.

- Effect on Fallen Angel issuers given by: $\beta_0 + \beta_1 + \beta_2 + \beta_3 + \beta_4 + \beta_5 + \beta_6 + \beta_7$
- Estimate of additional effect of Fed CCF eligibility given by difference: $\beta_2 + \beta_3 + \beta_6 + \beta_7$.

After estimating Equation (1.4), we compute the effects on the control (IG ineligible) and treatment (Fallen Angel) groups by summing coefficients as detailed above. We also compute the variance-covariance matrix for the coefficients by double-clustering on issuer and time. The difference between the treatment and control group gives our estimate of the treatment effect of the full promise of direct cash bond support implied by the final size of the CCFs. Standard errors for the summed estimates are obtained using the delta method. These results are reported in Table 1.6.

We can interpret the March 23, 2020 treatment effect as an alternative estimate of the effect the facilities had on eligible issuers, with the caveat that Table 1.5 suggests that the market seems to have priced in the possibility that Fallen Angels would fall out of eligibility. This may explain why the resulting treatment effect estimate is smaller than what we compute on the ‘March 23 X Eligible’ coefficients in Table 1.3. In fact, Table 1.6 presents evidence supporting a null effect for both issuers, as well as their difference, on March 23, 2020.

The treatment effect estimates for April 9, 2020 are more precisely estimated as indicated by the standard errors and are significant at the one percent level. We estimate that Fallen Angel spreads declined 126 bps points more than the control group for all bonds and 86 bps more for bonds with less than five years maturity. Contrary to expectations and other estimates, the treatment effect is larger when computed over all bonds than for bonds with less than five years maturity. This reversal seems to be driven by a proportionally greater decline from the control group’s spreads versus that of Fallen Angels for bonds with less than five years maturity, though both groups show greater declines for shorter maturity bonds, as expected.

Table 1.6: Change in G-Spreads (Quasi-Natural Experiment)

March 23, 2020		
	All	5yrs Maturity
Effect on IG Ineligible Issuers:	43.1 bps (35.8 bps)	81.9 bps (54.2 bps)
Effect on Fallen Angels:	-22.8 bps (33.3 bps)	-13.5 bps (43.6 bps)
Treatment Effect:	-65.9 bps (46.0 bps)	-95.4 bps (61.3 bps)
April 9, 2020		
	All	5yrs Maturity
Effect on IG Ineligible Issuers:	-132.8 bps*** (18.1 bps)	-217.4 bps*** (30.4 bps)
Effect on Fallen Angels:	-258.4 bps*** (18.5 bps)	-303.0 bps*** (19.4 bps)
Treatment Effect:	-125.6 bps*** (24.5 bps)	-85.6 bps*** (35.1 bps)

Standard errors in parentheses. Standard errors are double-clustered by issuer and time.

* $p < 0.1$, ** $p < 0.05$, *** $p < 0.01$

The table shows particular linear combinations of coefficient estimates corresponding to the regression $\Delta S_{ijt} = \beta_0 + \beta_1 \text{IG}(\text{Max Rating})_i + \beta_2 \text{Eligible}_i + \beta_3 \text{Fallen Angel}_i + \beta_4 \text{Events}_t + \beta_5 \text{Events} \times \text{IG}(\text{Max Rating})_{it} + \beta_6 \text{Events}_t \times \text{IG}(\text{Max Rating}) \times \text{Eligible}_{it} + \beta_7 \text{Events}_t \times \text{IG}(\text{Max Rating}) \times \text{FA}_{it} + \theta_{jt}^{\text{Rating}} + \theta_{jt}^{\text{Maturity}} + \epsilon_{jt}$. ΔS_{ijt} is the change in G-spread of bond j at time t for issuer i , $\text{IG}(\text{Max Rating})_i$ indicates if the maximum issuer rating of issuer i is IG on March 22, 2020, Fallen Angel_i indicates if issuer i is a Fallen Angel (see text for definition), Eligible_i is an indicator variable equal to one if issuer i is eligible for the Fed CCFs based on its issuer ratings as of March 22, 2020, Events_t is an indicator variable equal to one if day t is an event day, $\theta_{jt}^{\text{Rating}}$ are fixed effects for bond j rating (i.e. Aaa, Aa1, etc.) by week, and $\theta_{jt}^{\text{Maturity}}$ are fixed effects for bond remaining time-to-maturity (i.e. < 1 year, 1-2 years, 2-3 years, 3-4 years, 4-5 years, and 5+ years) by week. The effect of the CCF announcements on IG ineligible issuers (see text for definition) are given by $\beta_0 + \beta_1 + \beta_4 + \beta_5$. The effect on Fallen Angel issuers are given by $\beta_0 + \beta_1 + \beta_2 + \beta_3 + \beta_4 + \beta_5 + \beta_6 + \beta_7$. Hence, our estimates of the effect of the full promise of direct cash bond support implied by the final size of the CCFs are given by the difference, specifically for April 9, 2020 (see text for explanation). This is given by $\beta_2 + \beta_3 + \beta_6 + \beta_7$. Standard errors are computed using the delta method on the variance-covariance matrix for the coefficients, which are double-clustered by issuer and time.

Table 1.7: Treatment Effects of CCF Announcements on Bond Support

Treatment Effect	Announcement Date	Identification Strategy	Estimate
Direct Cash Bond Support on Eligible Issuers	Introduction of CCFs on March 23, 2020	Panel DiD with Fixed Effects	-96 bps (17.9 bps)
Direct Cash Bond and ETF Support on Ineligible Issuers	Introduction of CCFs on March 23, 2020	Causal ML using Characteristics	-553 bps (144.1 bps)
Direct Cash Bond Support on Eligible Issuers	Expansion of CCFs on April 9, 2020	Quasi-Natural Experiment (DiD)	-126 bps (24.5 bps)

Standard errors in parentheses

The table summarizes the treatment effect estimates presented in this paper. Eligible issuers are those issuers who were eligible for direct cash bond support from the Fed CCFs, as per the eligibility criteria presented in Section 1.3. The effect shown in the first row is taken from column (3) in Table 1.3 and corresponds to the parameter estimate for β_3 in Equation (1.1). This is the effect on eligible issuers' spreads from the implied direct cash bond support when the facilities were initially sized to be up to \$300 bn. The effect shown in the third row is estimated from the quasi-natural experiment reinstating the eligibility of Fallen Angel issuers on April 9, 2020, when the size of the facilities were also increased to up to \$750 bn. The estimate is taken the second column in Table 1.6 and corresponds to the treatment effect estimate computed from the saturated regression presented in Equation (1.4). The effect shown in the second row is the counterfactual treatment effect for ineligible issuers had they also received direct cash bond support and any additional indirect support from ETFs when the facilities were initially announced. The effect estimate is taken from Figure 1.4 and corresponds to the model specification with 10 years of feature history and 1% missingness tolerance for features. Table 1.15 reports the estimates across all model specifications.

Recall that implied treatment effects for direct cash bond support on eligible issuers' spreads for the initial size of the facilities are presented in Table 1.3 as the coefficient estimates for the 'March 23 X Eligible' interacted variable. These are -96 bps for all bonds and -136 bps for bonds with less than five years maturity. While the potential size of the facilities were increased by 150% from \$300 bn to \$750 bn, the implied treatment effect is not proportionally larger, even for the sample of all bonds (-96 bps versus -126 bps). This is consistent with the findings of Haddad, Moreira, and Muir [2025] that markets mostly priced in downside protection for IG bonds on March 23, 2020 when support was initially announced (extensive margin) and did not price in proportionally more downside protection on April 9, 2020 when the potential extent of support was significantly increased (intensive margin).

1.5 Counterfactual Treatment Effects for Ineligible Issuers

1.5.1 *Causal Machine Learning Approach with High-Dimensional Controls*

Section 1.4.1 presented an empirical strategy to estimate the effects of the initial announcement of the CCFs on March 23, 2020 on eligible issuers' bond spreads. The effect of the initially announced direct cash bond support is isolated by comparing bonds with similar ratings and maturity but with issuers that were differentially eligible for direct cash bond support from the CCFs, using panel DiD regressions with fixed effects. Section 1.4.3 exploits a quasi-natural experiment around the eligibility of Fallen Angels, as well as plausibly exogenous variation around the eligibility criteria, to measure the effects of the implied expansion of direct cash bond support via the CCFs on April 9, 2020 on eligible issuers' bond spreads. The treatment group, Fallen Angels, is compared with a control group, similarly rated but never eligible issuers, to isolate the effects of the final, expanded promise of direct cash bond support implied by the potential size of the facilities. These two groups are shown to have similar risk characteristics, as implied by CDS spreads, as well as similar distributions of IG and HY bonds. These effects are summarized in Table 1.7.

This section estimates the counterfactual treatment effect for ineligible issuers had they received direct cash bond support, as well as any additional implied ETF support,¹⁹ at the initial introduction of the CCFs on March 23, 2020, which is also summarized in Table 1.7. To do so, we use the identification method based on the two-step semi-parametric DiD estimator presented in Momin [2025b], which is based on Farrell, Liang, and Misra [2021a]

19. Recall that ineligible issuers have IG bonds, as shown in Figure 1.1, so would have benefited from the announced purchases of IG ETFs on March 23, 2020. However, indirect support for HY bonds through HY ETFs is not observed on March 23, 2020. Nonetheless, because eligible issuers' bonds reflect both direct cash bond support and indirect support for IG ETFs, the causal ML methodology used in this section invariably captures both effects since direct cash bond support is not separately identified.

and Farrell, Liang, and Misra [2021b]. The identification strategy exploits the use of high-dimensional features, and the estimator accounts for possible heterogeneous treatment effects, which could be important as several papers identified the heterogeneous dynamics of firms during the pandemic.²⁰

The structural equation representing the potential outcomes model is given by:

$$\Delta S_{ijt} = \alpha(X_i) + \beta(X_i)\text{Eligible}_i + \epsilon_{ijt} \quad (1.5)$$

where ΔS_{ijt} is the change in the G-spread for bond j for issuer i at time t from the previous market close, X_i are a collection of pre-treatment covariates (data realized on or before 2019Q4, see list in Section 1.7.2), and Eligible_i is an indicator if issuer i is eligible for cash bond purchases under the CCFs. The $\alpha(X_i)$ and $\beta(X_i)$ terms are non-parametric functions of the pre-treatment covariates and are computed using deep neural networks. In addition, the estimators for $\alpha(X_i)$ and $\beta(X_i)$ require the estimation of a non-parametric propensity score, $p(X_i)$, which takes values between 0 and 1 and represents the probability of a firm being treated, given its pre-treatment covariates. This is also done using deep nets.

The distribution of the conditional average treatment effects (CATEs) is given by the vector $\beta(X_i)$. Note that $\beta(X_i)$ reflects both the effects of direct cash bond support as well as indirect support from ETF purchases, unlike the panel DiD regressions with issue rating and maturity fixed effects presented in Section 1.4.1. The average treatment effect (ATE) is given by $\mathbb{E}[\beta(X_i)]$ and so, incorporates potential heterogeneous responses. The ATE is identified if the assumptions of unconfoundedness and the overlap condition holds. Unconfoundedness is justified on the basis of a high-dimensional feature set and estimation using deep nets which permit rich, nonlinear interactions between features. Overlap is argued to

20. See Darmouni and Siani [2024], Greenwald, Krainer, and Paul [2023], Haque and Varghese [2021], Hassan et al. [2023], Pagano and Zechner [2022].

hold because ratings are slow-moving and far more stable than firm characteristics, allowing for significant overlap in these distributions.²¹

In addition, if the unconfoundedness and overlap conditions are satisfied, we can compute group average treatment effects, given by $\mathbb{E}[g\beta(X_i)]$, where g is a vector of indicator variables denoting group membership, i.e. for ineligible issuers, BBB-rated issuers, etc. We can relax the condition of unconfoundedness to conditional no anticipation and parallel trends to identify the average treatment effect on the treated (ATET). This is given by the analogous DiD estimator for Equation (1.5).

The comparable estimates in Section 1.4 are given by the panel DiD regressions without issue rating and maturity fixed effects in Equation (1.1). Hence, these capture both the effects of direct cash bond support as well as indirect support from ETF purchases. Additionally, since the causal ML approach requires exploiting variation in characteristics, the empirical strategy in this section only considers the volume-weighted change in bond spreads from public firms on March 23, 2020.²² Nonetheless, as discussed below, the estimate for the ATET from both approaches are comparable.

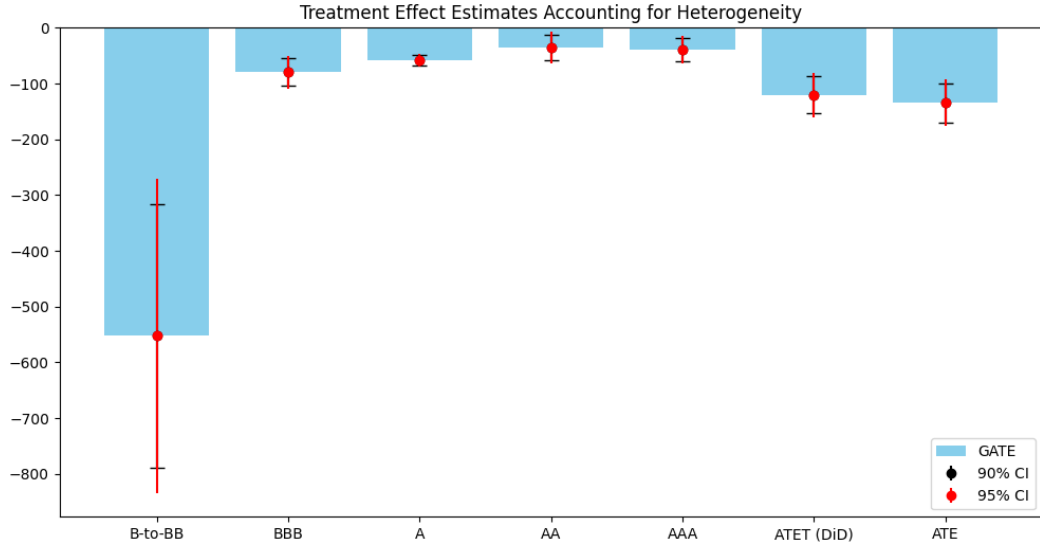
Figure 1.4 shows the estimates for the causal ML model using 10 years of feature history with 1% missingness tolerance for the features. The list of features is shown in Table 2.10. Additionally, indicator variables for two-digit NAICS industry classification are included. The deep net architectures for the potential outcomes and propensity score models are given in Table 2.12. The estimates across all model specifications are reported in Table 1.15.

The estimator for the ATET is obtained by differencing the change in spreads of eligible and ineligible issuers, as in the DiD panel regressions. For specifications with at least 5

21. See Momin [2025b] for further discussion on these assumptions, as well as explicit expressions for the estimators.

22. There are 1,085 such observations.

Figure 1.4: Treatment Effect Estimates for March 23, 2020



The figure shows the estimates for the causal ML model using 10 years of feature history with 1% missingness tolerance for the features. The list of features is shown in Table 2.10. Additionally, indicator variables for two-digit NAICS industry classification are included. The deep net architectures for the potential outcomes and propensity score models are given in Table 2.12. The estimates across all model specifications are reported in Table 1.15. The estimator for the ATET is obtained by differencing the change in spreads of eligible and ineligible issuers, as in the DiD panel regressions. For specifications with at least 5 years of feature history, the estimate ranges from -99.7 bps to -120.8 bps, comparable to the estimate of -106.5 bps from the panel DiD regression reported in column (1) of Table 1.3. The ATE estimate corresponds to the estimator for $\mathbb{E}[\beta(X_i)]$ and at -134.9 is notably higher than the ATET estimate. This reflects the fact that the counterfactual treatment effect estimates for ineligible firms are large. The GATE estimates are indicated by ratings and correspond to estimates of $\mathbb{E}[g\beta(X_i)]$, where $\beta(X_i)$ is the vector of CATEs and g is a vector of indicator variables denoting group membership. We find a generally monotonic decrease in the GATE estimates (greater decrease in spreads) as the issuer credit rating deteriorates. This is consistent with expectations that the bonds of lower-rated issuers would be more sensitive to intervention, as argued in Brunnermeier and Krishnamurthy [2020]. The notable exception to the monotonic pattern is the GATE for AAA-rated issuers of -40.1 bps versus the GATE for AA-rated issuers of -35.3. This is consistent with the narrative that the highest rated securities faced the steepest sell-offs early in the pandemic due to investor demand for liquidity [Haddad, Moreira, and Muir, 2021, He, Nagel, and Song, 2022, Ma, Xiao, and Zeng, 2022]. The counterfactual treatment effect for direct cash bond and ETF support for ineligible issuers is given by the GATE for B-to-BB rated issuers. The estimate is sizable and statistically significant, ranging from -464.2 bps to -562.6 bps for specifications with at least 5 years of feature history, albeit with large standard errors. Given that the spreads of Fallen Angel issuers tightened by around 300 bps on April 9, 2020, as reported in column (1) of Table 1.5, this appears plausible.

years of feature history, the estimate ranges from -99.7 bps to -120.8 bps, comparable to the estimate of -106.5 bps from the panel DiD regression reported in column (1) of Table 1.3. The ATE estimate corresponds to the estimator for $\mathbb{E}[\beta(X_i)]$ and at -134.9 is notably higher than the ATET estimate. This reflects the fact that the counterfactual treatment effect estimates for ineligible firms are large.

The GATE estimates are indicated by ratings and correspond to estimates of $\mathbb{E}[g\beta(X_i)]$, where $\beta(X_i)$ is the vector of CATEs and g is a vector of indicator variables denoting group membership. We find that GATE estimates generally decrease (implying a greater impact on spreads) as issuer credit rating deteriorates. This monotonic pattern is consistent with expectations that the bonds of lower-rated issuers would be more sensitive to intervention, as argued in Brunnermeier and Krishnamurthy [2020]. The notable exception to the monotonic pattern is the GATE for AAA-rated issuers of -40.1 bps versus the GATE for AA-rated issuers of -35.3. This is consistent with the finding that the highest rated securities faced the steepest sell-offs early in the pandemic due to investor demand for liquidity [Haddad, Moreira, and Muir, 2021, He, Nagel, and Song, 2022, Ma, Xiao, and Zeng, 2022].

The counterfactual treatment effect for direct cash bond and ETF support for ineligible issuers is given by the GATE for B-to-BB rated issuers. The estimate is sizable and statistically significant, ranging from -464.2 bps to -562.6 bps for specifications with at least 5 years of feature history, albeit with large standard errors. Interestingly, the causal ML estimator picks up this sizable negative treatment effect despite spreads of ineligible issuers actually widening on March 23, 2020, as seen in the coefficient estimate of 62.4 bps for “March 23” in column (1) of Table 1.3. Nonetheless, this sizable negative treatment effect appears plausible, given that the spreads of Fallen Angel issuers tightened by around 300 bps on April 9, 2020, as reported in column (1) of Table 1.5. Recall that Fallen Angel issuers were eligible for direct cash bond support through the CCFs based on their issuer ratings as of March 22, 2020. As such, these were generally the highest rated ineligible is-

suers heading into April 9, 2020 when their eligibility was reinstated. Moreover, as seen in Figure 1.3, Fallen Angel issuers held significant IG rated bonds through this period, which should have benefited from continued indirect support through potential IG ETF purchases by the CCFs. To the extent that ineligible issuers are lower-rated and more sensitive to ETF purchases, the treatment effect of around -500 bps can be rationalized.

1.6 Conclusion

We estimate the treatment effects of implied direct cash bond support from the Fed’s CCFs on corporate bond spreads. The measurement of treatment effects is complicated by the staggered nature of the Fed CCF announcements that changed both the level of implied support via the potential size of the facilities, as well as the breadth of securities targeted. Particularly, corporate bonds experienced indirect support through the planned purchases of ETFs.

To estimate the treatment effect from the initial policy announcement, we utilize panel DiD regressions with issue ratings and maturity fixed effects. This approximates the experiment where we hold fixed the rating and maturity of bonds and compare across differentially eligible issuers. We note that several papers in the literature determine eligibility for direct cash support using issue rather than issuer ratings. We find that this results in a measurement bias when assessing the change in the spreads of eligible issuers’ bonds relative those of ineligible issuers, particularly for April 9, 2020. Using issue ratings to determine eligibility underestimates the effect of the April 9, 2020 announcement on eligible issuer bonds because it classifies the IG bonds of ineligible issuers as eligible.

We use a quasi-natural experiment to determine the effect of the expanded size of the facilities on April 9, 2020 on issuers eligible for direct cash bond support. This involves comparing Fallen Angel issuers, who were initially eligible for the facilities, fell out of eligibility, and then had their eligibility reinstated, with a control group of issuers with simi-

lar ratings but who were never eligible direct cash bond support. We show that these two groups have similar distributions of CDS spreads and capital structures. While our estimate of the treatment effect is larger in magnitude for April 9, 2020, the increase is not proportional to the increase in the size of the facilities. This echoes findings that markets priced in significant conditional policy support from the Fed at the initial announcement date.

Identifying the counterfactual treatment effect for ineligible issuers had they received direct cash bond support requires stronger assumptions. We use a causal ML approach that uses a high-dimensional set of features to estimate the counterfactual treatment effect, as well as average treatment effects by group. We confirm that the causal ML approach delivers estimates for the treatment effect for eligible issuers similar to the panel DiD regressions without fixed effects. Averaged treatment effects across ratings buckets reveal a generally monotonic pattern with magnitudes increasing as credit quality deteriorates. The exception to this is the effect for AAA-rated issuers, which is larger in magnitude than the effect for AA-rated issuers. This heightened sensitivity for AAA-rated issuers is consistent with the sell-off experienced in the safest securities at the onset of the pandemic, due to heightened investor demand for liquidity. We estimate a sizable counterfactual treatment effect for ineligible issuers and argue that it is plausible given the significant tightening of Fallen Angel issuers' spreads on April 9, 2020 when their eligibility for direct cash bond support was reinstated.

While several papers have studied the financial effects of the Fed CCFs, including ours, far fewer papers have studied the potential real effects of the Fed CCFs and its design. Momin [2025b] and Momin [2025a] aim to fill these gaps.

1.7 Appendix

1.7.1 Robustness

Return Space

As a check on results, we update the outcome variable in our regression specifications in Section 1.4.1 to change in log bond prices, from change in bond spreads. The appeal of using the change in log bond prices as the regressand is that transaction prices are directly reported by TRACE.

Table 1.8 reports the relative changes in log bond prices for eligible issuer bonds and ineligible issuer bonds on the two main event dates including March 23, 2020 and April 9, 2020. Columns (1) and (2) of Table 1.8 present the regression results for the full sample and the sub-sample of bonds maturing in less five years, without fixed effects. Columns (3) and (4) repeat the regressions in columns (1) and (2) respectively, but including rating-week and maturity-week fixed effects. The coefficients of interest are the interaction terms between the event date and the eligibility dummy. As before, we find that eligible issuer bonds experienced relatively greater increase in log bond prices on March 23, 2020, in both the full sample and the sample containing bonds with maturities less than five years. Using issue ratings and maturity fixed effects, eligible issuer bonds experienced a higher return of 3.72 percent on March 23, 2020, relative to ineligible issuer bonds. For bonds with less than five years maturity, eligible issuer bonds experienced 2.71 percent higher returns compared to ineligible issuer bonds on the same day. In fact, while eligible issuer bonds increase in log prices on March 23, 2020 ineligible issuer bonds continued to decrease in prices and reached their trough on March 23. In contrast, ineligible issuer bonds enjoyed relatively greater increase in log bond prices on April 9. Using issue ratings and maturity fixed effects, ineligible issuer bonds experienced a higher return of 1.47 percent, relative to ineligible issuer bonds. For bonds with less than five years maturity, ineligible issuer bonds

Table 1.8: Change in Log Prices

	(1)	(2) <5yrs Maturity	(3)	(4) <5yrs Maturity
Eligible	0.0561 (0.0784)	0.0396 (0.0891)	0.0227 (0.0302)	0.0107 (0.0275)
March 23	-2.0193*** (0.1605)	-2.1996*** (0.1040)	-0.5026 (1.1060)	-0.9625 (0.8812)
April 9	4.3257*** (0.1755)	3.7855*** (0.1106)	3.2744*** (0.2142)	2.8066*** (0.2135)
March 23 X Eligible	3.9629*** (0.1492)	3.2772*** (0.0981)	3.7199*** (0.2551)	2.7132*** (0.5640)
April 9 X Eligible	-2.1414*** (0.1655)	-2.6724*** (0.1039)	-1.4698*** (0.3053)	-1.9348*** (0.2897)
Constant	-0.0565 (0.1019)	-0.0421 (0.0942)	-0.0340 (0.0359)	-0.0221 (0.0308)
Issue Ratings by Week F.E.	N	N	Y	Y
Remaining Maturity by Week F.E.	N	N	Y	Y
Observations	4.317e+05	2.163e+05	4.317e+05	2.163e+05
R2	0.0039	0.0024	0.1732	0.1864

Standard errors in parentheses

* $p < 0.1$, ** $p < 0.05$, *** $p < 0.01$

Similar to Table 1.3, this table reports the regression coefficients and standard errors (double-clustered by issuer and time) for $R_{ijt} = \alpha + \beta_1 \text{Eligible}_i + \beta_2 \text{Events}_t + \beta_3 \text{Events}_t \times \text{Eligible}_i + \theta_{jt}^{\text{Rating}} + \theta_{jt}^{\text{Maturity}} + \epsilon_{jt}$. R_{ijt} is the change in log bond prices of bond j at time t for issuer i , Eligible_i is an indicator variable equal to one if issuer i is eligible for the Fed CCFs based on its issuer ratings as of March 22, 2020, Events_t is an indicator variable equal to one if day t is an event day, $\theta_{jt}^{\text{Rating}}$ are fixed effects for bond j rating (i.e. Aaa, Aa1, etc.) by week, and $\theta_{jt}^{\text{Maturity}}$ are fixed effects for bond remaining time-to-maturity (i.e. < 1 year, 1-2 years, 2-3 years, 3-4 years, 4-5 years, and 5+ years) by week. Columns (1) and (2) report the regression estimates without fixed effects. Columns (3) and (4) report the estimates with fixed effects. Columns (1) and (3) show the results for the regression run over the full sample of bonds, while columns (2) and (4) show the results for the sample of bonds with less than five years maturity. The results here in ‘return-space’ corroborate our core results in ‘spread-space’ (Table 1.3): eligible issuer bonds experience higher returns on the initial facility announcement date on March 23, 2020, and ineligible issuer bonds experience higher returns on the facility expansion announcement date on April 9, 2020.

experienced 1.93 percent higher returns compared to eligible issuer bonds on that day. All estimated coefficients of interest are statistically significant at the one percent level.

SMCCF Index Constituents as Proxy

For additional robustness, we carry out our previous analyses while using the published SMCCF Broad Market Index constituents to define the population of eligible and ineligible issuers. While the creation of the SMCCF Broad Market Index was announced on June 15, 2020, the initial index constituent list dates from June 5, 2020. This method to identify issuer eligibility relies on the assumptions that this list of eligible issuers was the same set of eligible issuers as of the facility launch date on March 23, 2020 and that these eligible issuers could have been correctly inferred by the market using publicly-available information. As discussed in Section 1.3, proxying eligible issuers this way likely identifies a subset of the true set of eligible issuers on the event dates. Nonetheless, the SMCCF Broad Market Index constituents published by the Fed bypasses the many issues involved in attempting to accurately identify the set of eligible issuers. Thus, it is important to see if our previous results are robust to this alternative method of identifying eligible issuers.

Table 1.9: Ratings Distribution of SMCCF Holdings and Index

Rating	SMCCF Holding	SMCCF Broad Market Index
AAA/AA/A	48.07%	42.43%
BBB	48.31%	54.77%
BB	3.62%	2.80%
Weighted Average Maturity	3.3	2.8

Source: <https://www.federalreserve.gov/publications/files/smccf-transition-specific-disclosures-6-28-20.xlsx>

Table 1.9 presents the rating distributions of the SMCCF Broad Market Index published on June 15, 2020, as well as the actual holdings of the SMCCF at the end of June 2020. Overall, the actual holdings of the SMCCF match the published index quite well. The actual bonds holdings of the SMCCF tend to be slightly higher in credit quality and longer

in maturity, compared to the index.

In Table 1.10, we repeat our regressions in Table 1.3 but instead identify eligible issuers using the published SMCCF Broad Market Index constituents. Again, we compare the relative spread changes for eligible and ineligible issuer bonds on the key event dates of March 23, 2020 and April 9, 2020. The results are similar as before, albeit smaller in magnitude. Using issue ratings and remaining maturity fixed effects, the credit spreads of eligible issuer bonds decreased 47 bps more than the credit spreads of ineligible issuer bonds, on March 23, 2020. For bonds with less than five years maturity, on the other hand, the credit spreads of eligible issuer bonds decreased 69 bps more than the credit spreads of ineligible issuer bonds on the same day. In contrast, on April 9, 2020, the credit spreads of ineligible issuer bonds decreased 32 bps more than those of eligible issuer bonds for the full sample, and 35 bps for bonds maturing in less than five years. All estimated coefficients of interest are statistically significant at the one percent level. The lower magnitudes are consistent with the findings by Flanagan and Purnanandam [2020] that the Fed did not select bonds that experienced the greatest decline in prices (increase in spreads), leading up to the facility announcements, for inclusion in the SMCCF Broad Market Index. Additionally, this proxy results in comparing SMCCF constituents, which are a subset of eligible issuers, to a broader set of both eligible and ineligible issuers. Hence, using the SMCCF Broad Market Index constituents to identify eligible issuers likely yields a conservative estimate of the program effect.

Table 1.10: Change in G-Spreads (SMCCF Index Proxy for Eligibility)

	(1)	(2)	(3)	(4)
	<5yrs Maturity		<5yrs Maturity	
Eligible (SMCCF Index)	-1.22 (1.50)	-1.38 (1.81)	-0.47 (0.29)	-0.52 (0.46)
March 23	12.85*** (4.41)	18.66*** (5.00)	-30.55 (29.90)	-30.34 (36.07)
April 9	-97.06*** (4.89)	-111.39*** (5.60)	-71.95*** (7.03)	-82.43*** (8.08)
March 23 X Eligible (SMCCF Index)	-56.25*** (4.21)	-75.05*** (4.76)	-47.01*** (10.35)	-68.61*** (15.02)
April 9 X Eligible (SMCCF Index)	49.17*** (4.67)	54.03*** (5.30)	31.57*** (9.64)	35.03*** (11.94)
Constant	1.64 (2.05)	1.53 (2.44)	1.28 (0.79)	1.18 (1.00)
Issue Ratings by Week F.E.	N	N	Y	Y
Remaining Maturity by Week F.E.	N	N	Y	Y
Observations	4.3e+05	2.1e+05	4.3e+05	2.1e+05
R2	0.00	0.00	0.12	0.12

Standard errors in parentheses

* $p < 0.1$, ** $p < 0.05$, *** $p < 0.01$

Similar to Table 1.3, this table reports the regression coefficients and standard errors (double-clustered by issuer and time) for $\Delta S_{ijt} = \alpha + \beta_1 \text{Eligible}_i + \beta_2 \text{Events}_t + \beta_3 \text{Events}_t \times \text{Eligible (SMCCF Index)}_i + \theta_{jt}^{\text{Rating}} + \theta_{jt}^{\text{Maturity}} + \epsilon_{jt}$. ΔS_{ijt} is the change in G-spread of bond j at time t for issuer i , $\text{Eligible (SMCCF Index)}_i$ is an indicator variable equal to one if issuer i was a member of the initial constituent list for the SMCCF Broad Market Index, published on June 15, 2020, Events_t is an indicator variable equal to one if day t is an event day, $\theta_{jt}^{\text{Rating}}$ are fixed effects for bond j rating (i.e. Aaa, Aa1, etc.) by week, and $\theta_{jt}^{\text{Maturity}}$ are fixed effects for bond remaining time-to-maturity (i.e. < 1 year, 1-2 years, 2-3 years, 3-4 years, 4-5 years, and 5+ years) by week. Columns (1) and (2) report the regression estimates without fixed effects. Columns (3) and (4) report the estimates with fixed effects. Columns (1) and (3) show the results for the regression run over the full sample of bonds, while columns (2) and (4) show the results for the sample of bonds with less than five years maturity. The coefficient results broadly align with those reported in Table 1.3. However, we do find that the magnitude of the coefficient estimates here are smaller than those in Table 1.3. This is consistent with Flanagan and Purnanandam [2020], who find that the Fed did not select eligible issuer bonds which experienced the greatest decline (leading up to the facility announcements) for the SMCCF Broad Market Index.

1.7.2 Features

Variable	Description
accrual	Accruals/Average Assets
adv_sale	Advertising Expenses/Sales
aftret_eq	After-tax Return on Average Common Equity
aftret_equity	After-tax Return on Total Stockholders Equity
aftret_invcapx	After-tax Return on Invested Capital
at_turn	Asset Turnover
capital_ratio	Capitalization Ratio
cash_debt	Cash Flow/Total Debt
cash_lt	Cash Balance/Total Liabilities
cfm	Cash Flow Margin
de_ratio	Total Debt/Equity
debt_assets	Total Debt (ltq)/Total Assets
debt_at	Total Debt (dlcq+dlttq)/Total Assets
debt_capital	Total Debt/Capital
debt_ebitda	Total Debt/EBITDA
debt_invcap	Long-term Debt/Invested Capital
equity_invcap	Common Equity/Invested Capital
evm	Enterprise Value Multiple
gpm	Gross Profit Margin
gprof	Gross Profit/Total Assets
lt_debt	Long-term Debt/Total Liabilities
lt_ppent	Total Liabilities/Total Tangible Assets
npm	Net Profit Margin
opmad	Operating Profit Margin After Depreciation
opmbd	Operating Profit Margin Before Depreciation
pcf	Price/Cash flow
pe_exi	P/E (Diluted, Excl. EI)
pe_inc	P/E (Diluted, Incl. EI)
pe_op_basic	Price/Operating Earnings (Basic, Excl. EI)
pe_op_dil	Price/Operating Earnings (Diluted, Excl. EI)
ps	Price/Sales
ptpm	Pre-tax Profit Margin
rd_sale	Research and Development/Sales
roa	Return on Assets
roce	Return on Capital Employed
staff_sale	Labor Expenses/Sales
totdebt_invcap	Total Debt/Invested Capital

Table 1.11: Features with Less than One Percent Missing Observations

Variable	Description
bm	Book/Market
capei	Shillers Cyclically Adjusted P/E Ratio
cash_ratio	Cash Ratio
curr_debt	Current Liabilities/Total Liabilities
curr_ratio	Current Ratio
dltt_be	Long-term Debt/Book Equity
int_debt	Interest/Average Long-term Debt
intcov	After-tax Interest Coverage
intcov_ratio	Interest Coverage Ratio
ocf_lct	Operating CF/Current Liabilities
pay_turn	Payables Turnover
peg_1yrforward	Forward P/E to 1-year Growth (PEG) ratio
pretret_earnat	Pre-tax Return on Total Earning Assets
pretret_noa	Pre-tax return on Net Operating Assets
profit_lct	Profit Before Depreciation/Current Liabilities
ptb	Price/Book
quick_ratio	Quick Ratio (Acid Test)
rect_act	Receivables/Current Assets
rect_turn	Receivables Turnover
roe	Return on Equity
sale_equity	Sales/Stockholders Equity
sale_invcap	Sales/Invested Capital
short_debt	Short-Term Debt/Total Debt

Table 1.12: Additional Features with Less than Ten Percent Missing Observations

1.7.3 Deep Net Architectures

Feature History (Years)			
	1	5	10
Number of Features	333	1342	3204
Hidden Layer Architecture	[300, 150, 75, 35, 15]	[1500, 750, 375, 150, 75, 35, 15]	[2700, 1350, 675, 300, 150, 75, 35, 15]
Dropout Rate	20%		

Table 1.13: Architecture for Deep Nets with 1% Tolerance for Missing Observations

Feature History (Years)			
	1	5	10
Number of Features	517	2502	5314
Hidden Layer Architecture	[500, 300, 150, 75, 35, 15]	[3000, 1500, 750, 375, 150, 75, 35, 15]	[5000, 2700, 1350, 675, 300, 150, 75, 35, 15]
Dropout Rate	20%		

Table 1.14: Architecture for Deep Nets with 10% Tolerance for Missing Observations

1.7.4 Causal ML Treatment Effect Estimates Across Models

Table 1.15: Treatment Effects Estimates for March 23, 2020

		Change in G-Spreads					
		Treatment Effect Estimates Accounting for Heterogeneity					
		Model					
		(Feature History, Missingness Tolerance)					
Rating		(1,1)	(1,10)	(5,1)	(5,10)	(10,1)	(10,10)
B-to-BB		-858.71 (800.61)	-493.19 (370.08)	-498.99*** (148.55)	-562.61*** (136.17)	-552.89*** (144.14)	-464.24*** (128.15)
BBB		-122.03 (109.11)	-131.65** (59.73)	-80.08*** (15.99)	-64.82*** (15.32)	-79.80*** (15.05)	-79.39*** (14.40)
A		-53.78 (39.43)	-81.73*** (10.68)	-73.13*** (5.55)	-49.51*** (5.34)	-58.30*** (5.44)	-57.55*** (5.79)
AA		-61.12*** (13.26)	-59.86*** (13.40)	-45.51*** (14.15)	-23.93* (14.05)	-35.33** (14.17)	-36.80*** (14.22)
AAA		-64.61*** (11.28)	-56.35*** (11.54)	-46.26*** (12.36)	-31.07** (12.23)	-40.06*** (12.60)	-39.14*** (13.13)
ATET (DiD)		-139.93 (117.15)	-157.32*** (60.95)	-99.66*** (23.40)	-115.33*** (20.92)	-120.81*** (20.20)	-107.68*** (19.68)
ATE		-199.05 (130.17)	-160.15** (71.19)	-126.67*** (24.34)	-123.58*** (21.57)	-134.88*** (21.27)	-130.75*** (19.40)

Standard-errors in parentheses

Signif. Codes: ***: 0.01, **: 0.05, *: 0.1

The table reports the treatment effects for the change in spreads for different model specifications, with the results corresponding to the benchmark specification of 10 years of features history with 1% missingness tolerance plotted in Figure 1.4. The deep net architectures for the potential outcomes and propensity score models are reported in Tables 2.12 and 2.13. The list of features with 1% and 10% missingness tolerance are reported in Tables 2.12 and 2.13, respectively. Additionally, indicator variables for two-digit NAICS industry classification are included. The coefficient estimates for the analogous DiD estimator for ATET are broadly in-line with those obtained from the DiD panel regressions without fixed effects, reported in column (1) in Table 1.3. The estimates for the ATE are greater than the ATET estimates, reflecting the higher counterfactual treatment effects for ineligible issuers. We generally find a monotonic relationship between the GATE and credit rating, with the GATE decreasing, implying a greater effect on spreads, as credit ratings deteriorates, in-line with expectations [Brunnermeier and Krishnamurthy, 2020]. The exception to this pattern may be the higher magnitude of the GATE for AAA-rated issuers versus AA-rated issuers. This is consistent with the finding that investors' demand for liquidity led to a sell-off in the highest rated securities at the onset of the pandemic [Haddad, Moreira, and Muir, 2021, He, Nagel, and Song, 2022, Ma, Xiao, and Zeng, 2022].

CHAPTER 2

HETEROGENEOUS TREATMENT EFFECTS AND COUNTERFACTUAL POLICY TARGETING USING DEEP NEURAL NETWORKS: AN APPLICATION TO CENTRAL BANK CORPORATE CREDIT FACILITIES

2.1 Introduction

In announcing, and later expanding, the Corporate Credit Facilities (CCFs) in early 2020, the Federal Reserve references its dual-mandate to promote maximum employment and stable prices.¹ Through purchases of corporate bonds in the primary and secondary market, as well as exchange-traded funds (ETFs), the CCFs were intended to support credit to firms and business activity, despite the shock created by the COVID-19 pandemic.

While the CCFs could provide up to \$750 billion in financing, actual purchases totaled just \$14.1 billion at 2020 year-end. However, markets priced in significant contingent support by the Fed, especially if conditions were to deteriorate and tail risks materialized [Haddad, Moreira, and Muir, 2025]. Consequently, the bulk of the financial market effect of the CCFs were realized around its announcement, with a significant decline in bond spreads.² Record bond issuance followed,³ as did equity issuance, particularly for more

1. https://www.federalreserve.gov/news_events/pressreleases/monetary200323b.htm, https://www.federalreserve.gov/news_events/pressreleases/monetary200409a.htm

2. See Boyarchenko, Kovner, and Shachar [2022], D'Amico, Kurakula, and Lee [2020], Flanagan and Purnanandam [2020], Gilchrist et al. [2021], Haddad, Moreira, and Muir [2021], Kargar et al. [2021], Momin and Li [2025], O'Hara and Zhou [2021].

3. See Becker and Benmelech [2021], Boyarchenko, Kovner, and Shachar [2022], Darmouni and Siani [2024], Dutordoir et al. [2024], Halling, Yu, and Zechner [2020], Hotchkiss, Nini, and Smith [2022]

financially constrained firms.⁴ Firms used the proceeds to satisfy their demand for cash,⁵ paying back heavily utilized credit lines drawn on prior to the intervention.⁶ Research on the implementation of corporate bond purchase program in Europe by the European Central Bank (ECB), operational since 2016, found decreases in financing costs for firms eligible for the program which translated into higher bond issuance and payouts to shareholders but not investment.⁷ Was this also the case for the Fed CCF intervention during the pandemic?

There is very good reason to believe the CCFs should have supported investment by reducing financial constraints. Surveys of Chief Financial Officers (CFOs) by Barry et al. [2022] during the pandemic suggest that improving financial flexibility would improve hiring and capital spending. This echoes the CFO survey results of Campello, Graham, and Harvey [2010] during the Great Financial Crisis (GFC), where the vast majority of CFOs stated that financial constraints restricted investments in attractive projects. Firms do seem to have prioritized financial flexibility at the onset of the pandemic by initially cutting payouts.⁸ Were these actions taken to both preserve cash and support operations? Becker and Benmelech [2021] and Darmouni and Siani [2024] find firms do not increase investment, but does this hold on a relative basis for firms targeted by the CCFs versus those that are not? How about after accounting for the heterogeneous reactions of firms?⁹

4. See Dutordoir et al. [2024], Halling, Yu, and Zechner [2020], Hotchkiss, Nini, and Smith [2022].

5. See Acharya and Steffen [2020], Darmouni and Siani [2024], Pettenuzzo, Sabbatucci, and Timmermann [2023]

6. See: Acharya and Steffen [2020], Darmouni and Siani [2024], Greenwald, Krainer, and Paul [2023].

7. See Abidi and Miquel-Flores [2018], Grosse-Rueschkamp, Steffen, and Streitz [2019], Todorov [2020].

8. See Ali [2022], Cejnek, Randl, and Zechner [2021], Gormsen and Koijen [2020], Krieger, Mauck, and Pruitt [2021], Pettenuzzo, Sabbatucci, and Timmermann [2023].

9. See Darmouni and Siani [2024], Greenwald, Krainer, and Paul [2023], Haque and Varghese [2021], Hassan et al. [2023], Pagano and Zechner [2022].

And is this still true in the years following the pandemic, as the shock fades, and investment opportunities improve?

To answer these questions, I introduce a novel two-step semi-parametric difference-in-differences (DiD) estimator to compute dynamic (heterogeneous) treatment effects from the onset of the pandemic in 2020 through 2023. To achieve identification, I use an extremely high-dimensional set of controls, allowing for rich, potentially, non-linear interactions. The number of controls far exceeds the number of observations used in estimation, thus requiring tools from the double/debiased machine learning (DML) and causal machine learning literature to perform proper inference. This is accomplished by using an influence function (IF) estimator, alternatively called a Neyman orthogonal score function.

The first step requires estimating the non-parametric terms in the structural equation for the potential outcomes model which specifies the treatment effect. The structural equation for potential outcomes is the linear combination of a non-parametric intercept term and the interaction of a treatment indicator (eligibility for the CCFs) and a non-parametric slope term. The slope term captures individual level heterogeneity, that is, conditional average treatment effects (CATEs). Another ingredient for the estimator is an estimation of propensity scores, the probability of a firm being classified as eligible for the CCFs, which is also modeled as a non-parametric function of a high-dimensional set of characteristics. The non-parametric terms are estimated using deep feed-forward neural networks. Deep nets are used because ability to approximate continuous functions of real variables arbitrarily well, showing exceptional performance in this regard [Chronopoulos et al., 2023]. Farrell, Liang, and Misra [2021b] provides the theoretical justification for using deep nets to estimate non-parametric terms in the first step of two-step semi-parametric estimation and inference. The expression for the two-step semi-parametric DiD estimator is derived from the general expressions for IF estimators given in Farrell, Liang, and Misra [2021a]. Identification of average treatment effects (ATEs) requires that the assumptions of un-

confoundedness and overlap are satisfied. I defend the assumption of unconfoundedness by appealing to the extremely large set of covariates used in the estimation of the non-parametric terms, along with the usage of deep nets allows for the estimation of rich interactions and potential non-linearities. The covariate set consists of the quarterly histories of 37 to 60 pre-treatment variables going back up to 10 years, along with indicator variables for industry classification. However, I note that at the cost of identifying the average treatment effect on the treated (ATET), instead of the ATE, given the DiD nature of the estimator, I can use the weaker assumptions of conditional no anticipation and parallel trends, instead of unconfoundedness. This requires that, conditional on the pre-treatment variables, firms did not anticipate the CCFs in 2019 and that comparable firms would have exhibited similar dynamics, absent intervention. A general lack of pre-trends in event study regressions suggests that conditional parallel trends is a justifiable assumption, and estimates of the ATE and ATET are not statistically different from zero. Overlap is justified by the slow-moving nature of credit ratings, which determined firm eligibility for the CCFs, and the significant overlap in the distributions of fundamental characteristics and market-based measures of risk (CDS spreads) across eligible and ineligible firms.

I compare the dynamic (heterogeneous) treatment effects from the novel estimator to static (homogeneous) treatment effects from a DiD panel regression and dynamic (homogeneous) treatment effects from an event study design with two-way fixed effects. The magnitudes of the point estimates and standard errors are similar. The results show that while all firms increased leverage and cash holdings as a proportion of 2019 year-end assets, firms eligible for the CCFs increased leverage and cash to a relatively lower extent than ineligible firms. Both the static (homogeneous) treatment effects and the dynamic (heterogeneous) treatment effects indicate that eligible firms do not show an increased investment response over the treatment horizon, thus suggesting that the CCFs may not have met its objective for producing real effects. These results are robust to alternative proxies

for investment. I argue in preference for the result from the two-step semi-parametric estimator, since the high-dimensional set of controls can better control for potential selection bias and account for heterogeneity. In contrast, all models general indicate that eligible firms did increase payouts to shareholders, at least on a relative basis, with the two-step semi-parametric estimator showing that this was apparent even in 2020.

Since an intermediary step to computing ATEs using the two-step semi-parametric estimator is to compute the distribution of CATEs, I can study the effects of counterfactual policy targeting schemes, particularly to see if investment can be improve. This is also identified if the unconfoundedness assumption and overlap condition holds. Although, without the unconfoundedness assumption, the estimator is still valid and recovers the predictive effects of alternative policy targeting schemes, which is still important for policy diagnostics. The CFO survey evidence of Campello, Graham, and Harvey [2010] and Barry et al. [2022] suggests that targeting weaker, more financially constrained credits may produce stronger real effects. This is also echoed in the simple theoretical setup of Brunnermeier and Krishnamurthy [2020]. Momin and Li [2025] finds that extending direct cash bond support from the CCFs to ineligible firms would have led to around 500 bps of spread tightening. However, in this paper, I find that extending eligibility suggests weak to inconclusive evidence of improving investment outcomes in 2020, while showing no evidence of improved outcomes for later years. In contrast, the counterfactual treatment effect estimates suggest that ineligible firms, had they received direct cash bond support from the CCFs, would have increased leverage in 2020 and payouts in 2020 and 2022.

This paper contributes to several literatures. First, it contributes to the extensive literature on the financial and real dynamics of firms during the COVID-19 pandemic that was earlier cited. Among these, the paper closest to this one is that of Darmouni and Siani [2024]. They also show that firms drastically increased bond issuance following the announcement of the Fed CCFs and that the proceeds from these were used to pay down

previously drawn credit lines and build cash buffers. They find that firms maintained equity payouts but did not increase investment. While I echo most of their findings, I utilize a different identification strategy that involves inferring treatment effects from comparing the relative dynamics of eligible firms versus ineligible firms using high-dimensional controls in a non-linear setting, rather than an instrumental variable (IV) approach as was used in their approach. One

Additionally, to the best of my knowledge, I am the first to study the counterfactual effects of the Fed CCFs from counterfactual policy targeting.

Second, this paper contributes to the DML and CML literature. The canonical references to using DML for estimation and inference are Belloni, Chernozhukov, and Hansen [2014] and Chernozhukov et al. [2018].¹⁰ The DML literature commonly uses a partially linear model for specifying the structural potential outcomes model where the intercept term is referred to as an infinite-dimensional nuisance parameter and the slope term is the product of a constant, homogeneous treatment effect and a treatment indicator. Farrell, Liang, and Misra [2021a] provides the general expression for the IF estimator for smooth structural models. From this I derive a two-step semi-parametric DiD estimator with non-parametric, heterogeneous CATEs and show that the dynamic (heterogeneous) treatment effects estimated from this estimator is similar to the static (homogeneous) treatment effect estimated from a panel DiD regression and to the dynamic (homogeneous) treatment effects estimated from event study regressions with two-way fixed effects. This estimator has a similar functional form and is analogous to the doubly-robust DiD estimator of Sant'Anna and Zhao [2020] in the non-ML context and the DML DiD estimator of Chang [2020]. While the derivation of the estimator that I utilize in this paper is straightforward, to the best of my knowledge, I am the first to present this, at least in the context of an application in finance.

10. See also the textbook Chernozhukov et al. [2024].

Third, this paper contributions to the finance and accounting literatures featuring applications of DML and two-step semi-parameteric estimators, more generally. The majority of these papers utilize DML for model selection and inference in high-dimensional settings. Among empirical asset pricing papers, specifically, on factor models for explaining the cross-section of stock returns, Feng, Giglio, and Xiu [2020] is the first to use DML to assess new factors given control factors from the factor zoo. Maasoumi et al. [2024] proposes a DML-based method to identify factors with the most significant explanatory power for explaining the cross-section of stock returns, rather than just evaluating new factors as in Feng, Giglio, and Xiu [2020]. Borri et al. [2024] uses DML to compare their proposed novel, nonlinear asset pricing factor for explaining the cross-section of equity returns against the factor zoo, finding that their proposed factor significant while the majority of factor zoo is not. Other empirical asset pricing applications include Hansen and Siggaard [2024], who uses DML to revisit explanations of the post-earnings announcement drift (PEAD), and Gomez-Gonzalez, Uribe, and Valencia [2024], who employs DML to study the effect of economic complexity index on sovereign yield spreads, considering a large number of explanatory variables.

There are also numerous accounting and corporate finance applications of DML. Bilgin [2023] studies the significance of cash holdings, current ratio, and non-debt tax shield in determining firms' capital structure in the face of high-dimensional controls. De Marco and Limodio [2022] uses DML to understand which characteristics among a high dimensional set contributes the most to bank climate resilience. Movaghari, Tsoukas, and Vagenas-Nanos [2024] studies the determinants of cash holdings. Wasserbacher and Spindler [2024] studies the heterogeneous effects causal effect of ratings on the leverage ratio, also taking into consideration high dimensional controls. Finally, Yang, Chuang, and Kuan [2020] studies the 'Big N' audit quality effect.

Papers specifically using the two-step semi-parameteric estimation/inference methodol-

ogy of Farrell, Liang, and Misra [2021b] and Farrell, Liang, and Misra [2021a], along with deep nets to estimate non-parameteric terms, include Kim and Nikolaev [2024a] and Kim and Nikolaev [2024b]. Kim and Nikolaev [2024a] uses the approach of Farrell, Liang, and Misra [2021a] to specify a semi-parameteric function that allows for interactions between numerical and narrative data to forecast operating profitability. Similarly, Kim and Nikolaev [2024b] studies the narrative context provided by disclosures around the release of numeric information to understand the effect of contextual information on earnings persistence, combining textual and numeric data via deep nets to uncover heterogeneous effects. In a spirit similar to Farrell, Liang, and Misra [2021a], Simon, Weibels, and Zimmermann [2022] embeds a structural model of portfolio allocation in a deep net via the loss function used to train the deep net and learn the parameters for portfolio weights.

While my application also utilizes the methods from this literature for model selection and inference in high-dimensional settings, and to infer heterogeneous effects, in the context of estimating non-parameteric terms using deep nets, I also compute counterfactual treatment effects for policy evaluation. To the best of my knowledge, this is the first such application of its kind in the finance and accounting literatures.

The rest of the paper is organized as follows. Section 2.2 provides the institutional background of the Fed CCFs. Section 2.3 describes the data and presents the descriptive statistics for eligible and ineligible firm variables. Section 2.4 presents the static (homogeneous) treatment effects obtained from a panel DiD regression. Section 2.5 presents the dynamic (homogeneous) treatment effects obtained from event study regressions with two-way fixed effects. Section 2.6 presents the dynamic (heterogeneous) treatment effects obtained from the two-step semi-parameteric DiD estimators. Section 2.7 presents the results from counterfactual policy targeting experiments. Section 2.8 concludes.

2.2 Institutional Background

The Federal Reserve initially announced the Primary Market Corporate Credit Facility (PMCCF) and the Secondary Market Corporate Facility (SMCCF) on March 23, 2020.¹¹ Both facilities were established with a liquidity backstop provided by the Treasury. Initially, the CCFs, along with the Term Asset-Backed Securities Loan Facility (TALF), had the potential to provide up to \$300 billion in financing.¹²

Eligibility for the CCFs was determined at the issuer level with eligible issuers needing to be American companies with headquarters and material operations domestically. Additionally, eligible issuers needed to be rated investment-grade (IG). In the case issuers had multiple ratings, the plurality of these ratings were required to be IG. Depository institutions and depository holding companies were excluded from eligibility. Moreover, the SMCCF also targeted IG ETFs.

On April 9, 2020, the Federal Reserve increased the size of the facilities, such that the CCFs could provide up to \$750 billion in financing.¹³ Additionally, the eligibility criteria of the facilities were amended such that issuers meeting the rating criteria as of March 22, 2020 were deemed eligible for the facilities. Effectively, this meant that issuers ('Fallen Angels') downgraded out of eligibility between the initial and subsequent announcement dates had their eligibility restored. The term sheet of the SMCCF was also amended to expand eligible ETFs to include high-yield (HY) ETFs.

The Federal Reserve began the purchases of ETFs on May 12, 2020¹⁴ and of secondary market cash bonds according to a "broad, diversified market index" on June 15, 2020.¹⁵

11. https://www.federalreserve.gov/news_events/press_releases/monetary20200323b.htm

12. <https://home.treasury.gov/news/press-releases/sm951>

13. https://www.federalreserve.gov/news_events/press_releases/monetary20200409a.htm

14. https://www.newyorkfed.org/news_events/news/markets/2020/20200511

15. https://www.federalreserve.gov/news_events/press_releases/monetary20200615a.htm

Participation in the SMCCF initially required corporate issuers certify compliance with the eligibility criteria.¹⁶ The SMCCF continued purchases until December 31, 2020, finishing with a total portfolio of \$14.1 billion, while the PMCCF was not utilized.¹⁷ The SMCCF began winding down its ETF holdings on June 7, 2021 and corporate bond holdings on July 12, 2021, completing the divestitures by August 31, 2021.¹⁸ Equity capital was returned to the Treasury and the facilities were terminated by the end of 2021. For information on the full range of public sector interventions undertaken in the United States during the pandemic, see Clarida, Duygan-Bump, and Scotti [2021].

2.3 Data

2.3.1 Sample Construction

Firm fundamental characteristics are obtained from Compustat North America via Wharton WRDS and the Financial Ratios Suite by WRDS. Firms incorporated outside of the United States are dropped, as are firms with two-digit NAICS code 52, which corresponds to the Finance and Insurance industry. This drops firms outside the eligibility criteria for CCF cash bond purchases. Additionally, CDS spread data for five-year senior unsecured debt is obtained from IHS Markit through WRDS. Eligibility criteria is determined using issue ratings corresponding to senior unsecured debt (which correspond to issuer ratings), obtained from Mergent Fixed Income Securities Database (FISD) via Wharton WRDs.

16. <https://www.newyorkfed.org/markets/primary-and-secondary-market-faq/archive/corporate-credit-facility-faq-201204>

17. <https://newbagehot.yale.edu/docs/united-states-primary-market-corporate-credit-facility-and-secondary-market-corporate-credit>

18. <https://www.newyorkfed.org/markets/secondary-market-corporate-credit-facility>

2.3.2 Descriptive Statistics

Table 2.1: Descriptive Statistics - Eligible

	Median	Mean	Standard Deviation	Observations
Common Equity at Market Value (Millions)	22,421.93	58,526.71	122,246.57	321
Total Debt (Millions)	5,718.30	13,352.45	22,580.30	358
Total Assets (Millions)	17,642.35	39,488.83	73,815.12	358
Employees (Thousands)	16.30	56.42	146.44	345
Book Leverage (Percent)	49.03	49.86	17.21	345
Market Leverage (Percent)	21.84	24.00	13.64	321
Sales (Millions)	8,980.15	25,430.24	51,988.78	358
EBITDA (Millions)	2,211.30	5,106.62	10,418.35	340
EBITDA Interest Coverage	9.44	13.77	17.03	338
Debt-to-EBITDA	2.87	3.17	1.82	340

The table shows accounting and financial information for publicly traded firms who are identified to be eligible for direct cash bond purchases under the Fed CCFs based on their ratings. The data corresponds to fiscal year 2019. Compared to ineligible firms, eligible firms are far larger as measured by market equity, total assets, employee headcount, and sales. Moreover, they have stronger liquidity and solvency indicators.

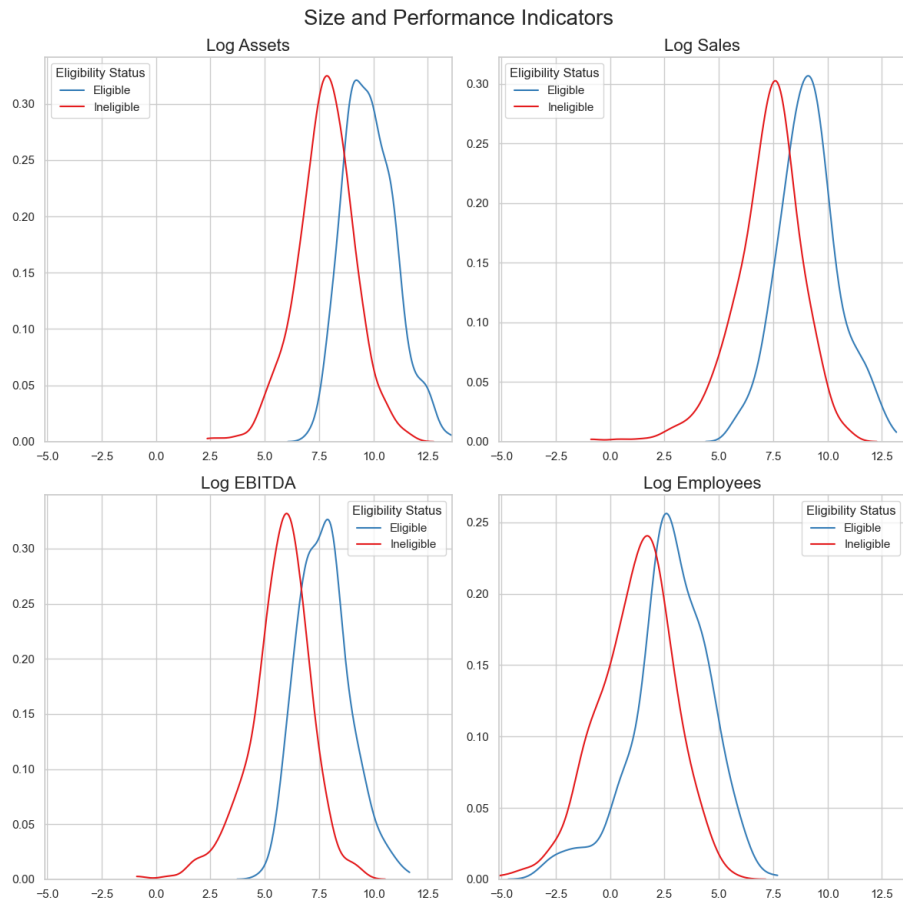
Table 2.2: Descriptive Statistics - Ineligible

	Median	Mean	Standard Deviation	Observations
Common Equity at Market Value (Millions)	2,075.07	5,054.11	10,387.18	460
Total Debt (Millions)	1,043.55	2,532.42	4,979.49	464
Total Assets (Millions)	2,502.09	5,584.92	10,617.85	465
Employees (Thousands)	3.63	10.82	22.73	458
Book Leverage (Percent)	52.47	53.71	20.14	412
Market Leverage (Percent)	33.16	37.43	23.93	459
Sales (Millions)	1,667.11	3,556.65	6,182.18	462
EBITDA (Millions)	228.18	488.68	1,182.23	461
EBITDA Interest Coverage	3.86	3.89	16.70	452
Debt-to-EBITDA	3.65	3.92	25.65	460

The table shows accounting and financial information for publicly traded firms who are identified to be ineligible for direct cash bond purchases under the Fed CCFs based on their ratings. The data corresponds to fiscal year 2019. Compared to eligible firms, ineligible firms are far smaller as measured by market equity, total assets, employee headcount, and sales. Moreover, they have weaker liquidity and solvency indicators.

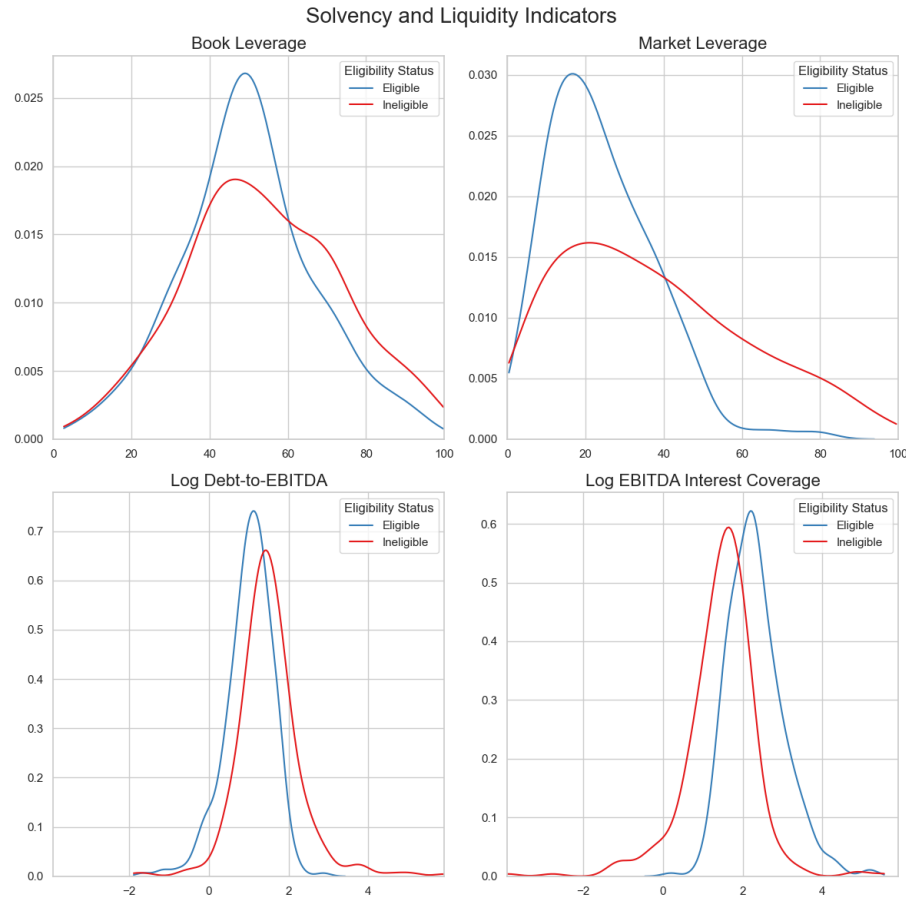
Tables 2.1 and 2.2 report key fundamental characteristics and financial indicators for public eligible and ineligible traded firms, respectively, for the 2019 fiscal year. There are more eligible firms than ineligible firms, but the counts for each are sizeable. In general, eligible issuers are larger, more solvent, and more liquid. The larger size of eligible firms are reflected in far larger equity valuations, higher debt levels, greater asset holdings, more sales, and higher EBITDA. While eligible firms have more employees, the gap here is much

Figure 2.1: Eligible Issuers are Larger, with More Substantial Cash Flows



The figure shows the distributions of the logged values of several size and performance indicators across eligible and ineligible issuers of the Fed CCFs. Eligible issuers have more assets and higher employee headcounts. Additionally, they generate higher revenue and register higher EBITDA.

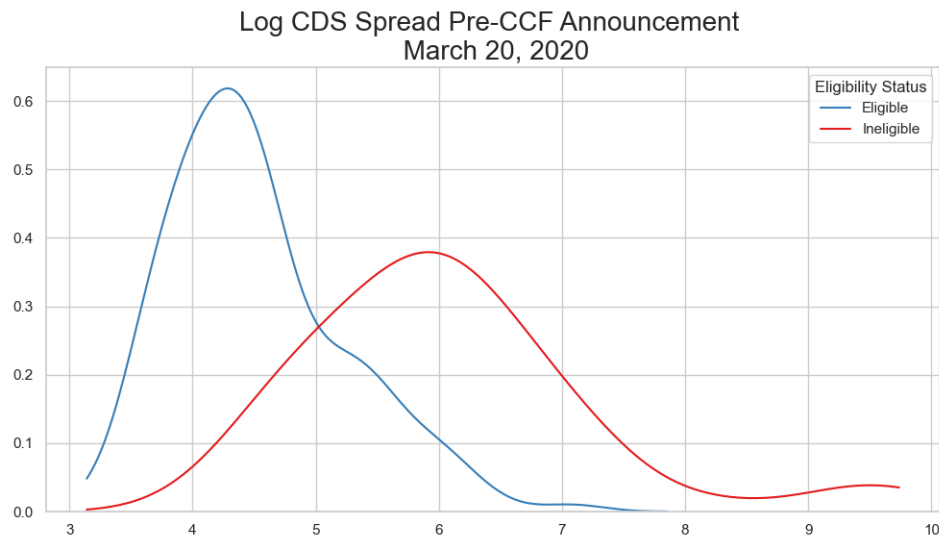
Figure 2.2: Eligible Issuers are also More Liquid with Lower Leverage



The figure shows the distributions of the logged values of several solvency and liquidity indicators across eligible and ineligible issuers of the Fed CCFs. While both sets of issuers have comparable distributions of book leverage, eligible issuers have far lower levels of market leverage (as measured with respect to firm market value). Additionally, eligible issuers have greater cash flow coverage of debt and debt servicing costs.

smaller compared to ineligible firms. Ineligible firms are less solvent as reflected in higher book and market leverage and larger five-year senior unsecured CDS spreads. The lower liquidity of ineligible firms are reflected in lower EBITDA interest coverage, debt-to-EBITDA, and profit margin. These trends are reinforced in the distributions of size and performance indicators in Figure 2.1, and of solvency and liquidity indicators in Figure 2.2.

Figure 2.3: CDS Spreads Consistent with Higher Default Risk of Ineligible Firms



The figure shows the distributions of logged CDS spreads on March 20, 2020 prior to the Fed CCF announcement date on March 23, 2020, across eligible and ineligible firms. Consistent with the fundamental characteristics shown in Figures 2.1 and 2.2 and Tables 2.1 and 2.2, the market assessed ineligible firms to be riskier than eligible firms. However, there is a significant area of overlap between the two sets of firms.

Figure 2.3 graphs the distribution of log CDS spreads on March 20, 2020, the last business day before the CCF announcement on March 23, 2020, for both eligible and ineligible firms. Firms with CDS spreads are a subset of all firms with public financials. The figure reinforces the information presented in the tables, but also reveals that eligible firms are not uniformly perceived to have lower default risk than ineligible firms. Notably, there is a significant overlap in the supports of the two distributions, with the support of eligible firms' CDS spread distribution almost entirely lying within the corresponding support for ineligible firms.

2.4 Static Homogeneous Average Treatment Effects: Difference-in-Differences Regressions

Static (homogeneous) treatment effects are estimated using a difference-in-differences (DiD) regression. The specification is:

$$y_{i,t} = \beta_0 + \beta_1 \text{Eligible}_i + \beta_2 \text{Post}_t + \beta_3 (\text{Eligible}_i \times \text{Post}_t) + \gamma_i + \epsilon_{i,t} \quad (2.1)$$

where $y_{i,t}$ is the outcome variable of interest, Eligible_i is an indicator variable with value 1 if firm i was eligible for cash bond purchases under the CCFs, Post_t is an indicator variable equal to 1 if date t is 2020 or later, and γ are two-digit NAICS industry fixed effects. The static treatment effect is given by β_3 . The DiD regressions are computed over 2017 to 2023. Standard errors are clustered by issuer and date.

2.4.1 Potential Selection Bias and Parallel Trends

For both the DiD panel regression in this section, and the event study design in Section 2.5, a key concern may be potential selection bias contaminating the estimated treatment effect, in addition to any biases attributable to ignoring heterogeneity. An obvious source of this selection bias may arise from the fact that eligibility for the CCFs is essentially a proxy for IG status.

Consequently, the treatment variable may simply be capturing the differing dynamics between IG and HY firms. Section 2.6 tackles this issue more seriously by using a large set of controls as well as permitting arbitrary interactions between these controls, motivated by Section 2.3.2 showing considerable overlap in the distributions of eligible and ineligible firms along fundamentals and market-based measures of risk. Nonetheless, the general lack of pre-trends observed in the event study regressions in Section 2.5 suggests that the parallel trends assumption can be justified and hence, the DiD regressions in this section

identify the ATET. Section 2.6.6 includes further discussion about selection bias.

2.4.2 Results

Table 2.3: Debt Levels and Cash Holdings Broadly Increased, With Negative Treatment Effect for Eligible Firms

Dependent Variables:	Cash (% 2019Q4 Assets)		Total Debt (% 2019Q4 Assets)	
Model:	(1)	(2)	(3)	(4)
<i>Variables</i>				
Constant	10.01*** (0.9476)		36.37*** (2.943)	
Eligible (Fed CCFs)	-4.477*** (0.9565)	-3.120*** (1.009)	-10.54*** (1.969)	-12.49*** (2.010)
Post 2020	9.866*** (2.015)	9.903*** (2.005)	23.16*** (4.075)	23.17*** (4.082)
Eligible (Fed CCFs) \times Post 2020	-7.295*** (2.042)	-7.464*** (2.046)	-6.141** (2.733)	-6.212** (2.729)
<i>Fixed-effects</i>				
NAICS (2-Digit)		Yes		Yes
<i>Fit statistics</i>				
Observations	9,912	9,912	9,502	9,502
R ²	0.03349	0.07229	0.07234	0.10256
Within R ²		0.02740		0.07712

Clustered (Issuer & Date) standard-errors in parentheses

Signif. Codes: ***: 0.01, **: 0.05, *: 0.1

The table reports the regression results from Equation 2.1 for cash holdings (% 2019Q4 assets) and total debt (% 2019Q4 assets). The results suggest that firms broadly increased leverage while increasing cash holdings in the treatment period (2020 onward). Additionally, the regressions pick up negative treatment effects for eligible firms for both variables, suggesting that these firms increased cash holdings and debt to a lesser extent than ineligible firms.

Table 2.3 reports the DiD regression results for cash holdings (% 2019Q4 assets) and total debt (% 2019Q4 assets). Columns (1) and (3) show results without industry fixed-effects, while Columns (2) and (4) include industry fixed effects, but the results are broadly consistent across the different specifications. The DiD regressions suggest that eligible firms generally hold less cash and have less debt than ineligible firms. Furthermore, the

regressions suggest that firms broadly increased cash holdings and leverage in the treatment period (2020 onward). This result can be seen by the positive coefficient on the ‘Post 2020’ variable for ineligible firms and the sum of the coefficients for ‘Post 2020’ and ‘Eligible (Fed CCFs) \times Post 2020’ for eligible firms. Interestingly, negative treatment effects are picked up on eligible firms’ relative cash holdings and total debt. Hence, while eligible firms increased cash holdings and leverage in the treatment period, they appear to have done so proportionally less than ineligible firms.

Table 2.4: Eligible Firms’ Payout Shows Positive Effect; No Effect Seen for Investment

Dependent Variables: Model:	Dividends and Buybacks (% 2019Q4 Assets) (1)	Capital Expenditures and R&D (% 2019Q4 Assets) (2)	Capital Expenditures and R&D (% 2019Q4 Assets) (3)	Capital Expenditures and R&D (% 2019Q4 Assets) (4)
<i>Variables</i>				
Constant	1.062*** (0.2192)		2.456*** (0.2956)	
Eligible (Fed CCFs)	0.9875*** (0.2433)	0.8328*** (0.2519)	-1.217*** (0.3103)	-1.150*** (0.3168)
Post 2020	-0.1769 (0.2470)	-0.1554 (0.2473)	1.240* (0.6771)	1.305* (0.6843)
Eligible (Fed CCFs) \times Post 2020	1.180*** (0.2377)	1.158*** (0.2345)	-0.8407 (0.6597)	-0.9016 (0.6642)
<i>Fixed-effects</i>				
NAICS (2-Digit)		Yes		Yes
<i>Fit statistics</i>				
Observations	9,641	9,641	9,798	9,798
R ²	0.00907	0.01695	0.00988	0.03614
Within R ²		0.00657		0.00882

Clustered (Issuer & Date) standard-errors in parentheses

Signif. Codes: ***: 0.01, **: 0.05, *: 0.1

The table reports the DiD regression results for payouts (% 2019Q4 assets), investment (% 2019Q4 assets), and capital expenditure (% 2019Q4 assets). Payouts are computed as the annual sum of dividends and share buybacks. Investment is proxied as the annual change in the gross value of Property, Plant, and Equipment. The results show a positive effect for firm payouts over the treatment period, while both investment and capital expenditure exhibit null effects, despite the general increases in cash holdings and leverage shown in Table 2.3.

Table 2.4 reports the DiD regression results for for payouts (% 2019Q4 assets) and investment (% 2019Q4 assets). Payouts are computed as the annual sum of dividends and share buybacks. Investment is proxied as the annual change in the gross value of property, plant, and equipment.¹⁹ The results show a positive effect for firm payouts over the treat-

19. In contrast, when investment is proxied by the annual change in the gross value of property, plant,

ment period, while investment exhibit nulls effects. Together, Tables 2.3 and 2.4 suggest that while firms generally increased leverage and cash in the treatment period, this translated into higher payouts by eligible firms but not investment.

2.5 Dynamic Homogeneous Average Treatment Effects: Event Study Regressions with Two-Way Fixed Effects

To study the dynamic impact of the CCF intervention, I employ event study regressions with two-way fixed effects. These have the functional form:

$$y_{i,t} = \sum_{\tau=-3}^{-2} \beta_{\tau} D_t^{\tau} \text{Eligible}_i + \sum_{\tau=0}^3 \beta_{\tau} D_t^{\tau} \text{Eligible}_i + \gamma_i + \zeta_t + \epsilon_{i,t} \quad (2.2)$$

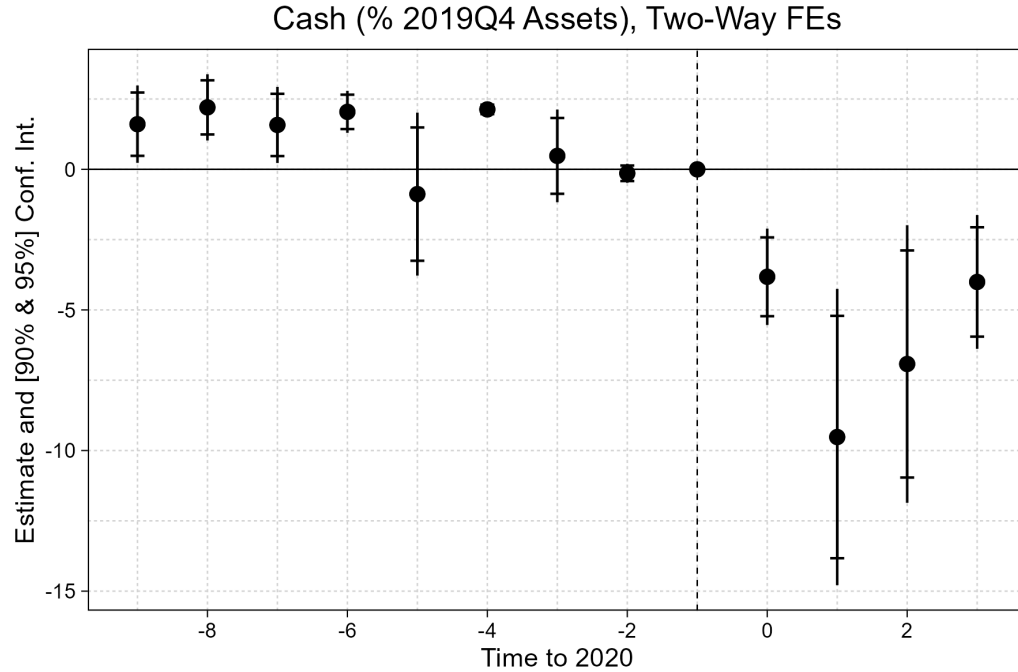
where $y_{i,t}$ is the outcome variable of interest, $D^{\tau} = \mathbf{1}\{t - 2020 = \tau\}$ is an indicator variable equal to 1 if the difference between the year t and 2020 is equal to τ , Eligible is an indicator variable with value 1 if the firm was eligible for direct cash bond purchases under the CCFs, 0 otherwise, and finally, β_{τ} are the coefficients being estimated. Two-way unit and time fixed effects are given by γ_i for issuer and ζ_t for year, respectively. The event study regressions are computed over the window 2017 to 2023. Standard errors are clustered by issuer and year.

Consequently, β_{τ} for $\tau \geq 0$ are dynamic treatment effects, while for $\tau < 0$, β_{τ} corresponds to a placebo or falsification test. However, notice that $\tau = -1, t = 2019$ is omitted from the regression specification; this is the baseline comparison group, which will also be the case for the two-step semi-parametric DiD estimator introduced in Section 2.6. Additionally, as discussed in Section 2.4, the estimation of treatment effects may suffer from

and equipment, a positive coefficient is estimated for the eligible indicator, while the coefficient on the interaction term is negative. The causal ML results for the property, plant, and equipment investment proxy is discussed further in Section 2.6 and reported in Appendix 2.9.11.

potential selection bias and neglect of heterogeneity, which further motivates the method used in Section 2.6. Nonetheless, there generally appears to be a lack of pre-trends, which suggests that the parallel trends assumption holds for the treatment period.

Figure 2.4: Eligible Firm Cash Holdings Show Relative Decline, Before Reverting

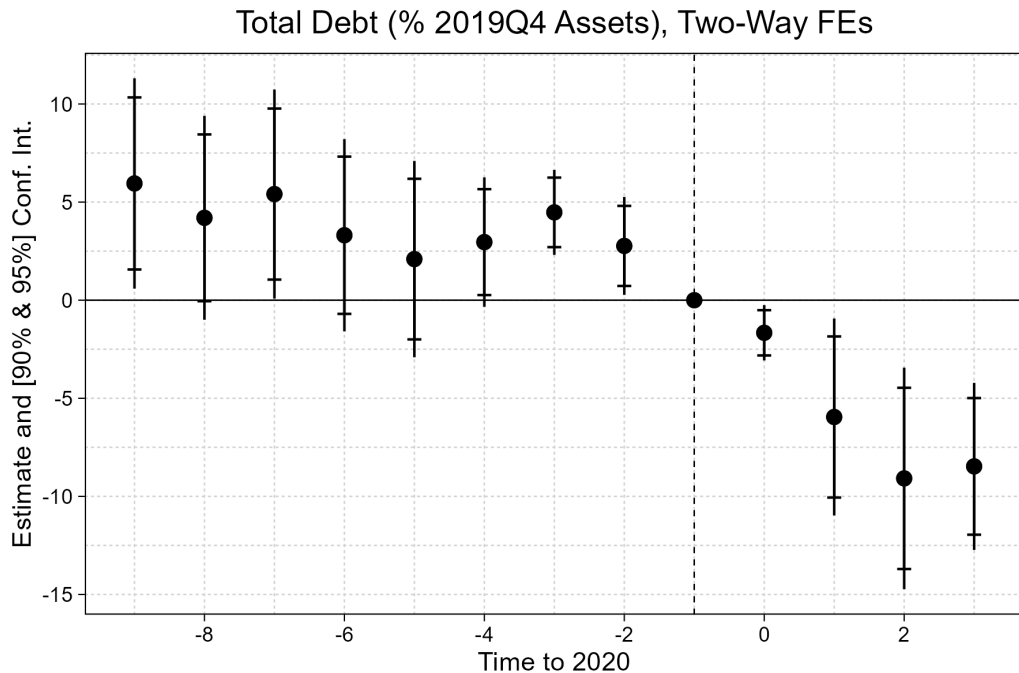


The figure plots the dynamic treatment effects from the regression given by Equation 2.2 for cash as proportion of 2019Q4 assets. The coefficient estimates prior to 2020 are null or positive, suggesting that either there are not meaningful differences in relative cash holdings between eligible and ineligible firms or that eligible firms hold more cash. However, after the onset of the pandemic, the dynamic treatment effects are negative, reaching a bottom in 2021 before reverting. This suggests that ineligible firms increased cash balances to a greater extent than eligible firms.

Figure 2.4 shows the dynamic effects of the CCF intervention on firm cash balances as a proportion of total assets as of 2019Q4. The coefficient estimates prior to 2020 are null or positive, suggesting that either there are not meaningful differences in relative cash holdings between eligible and ineligible firms or that eligible firms hold more cash. However, after the onset of the pandemic, the dynamic treatment effects are negative, reaching a bottom in 2021 before reverting. This suggests that ineligible firms increased cash balances to a greater extent than eligible firms.

Figure 2.5 shows the dynamic effects on firm gross debt as a proportion of total assets

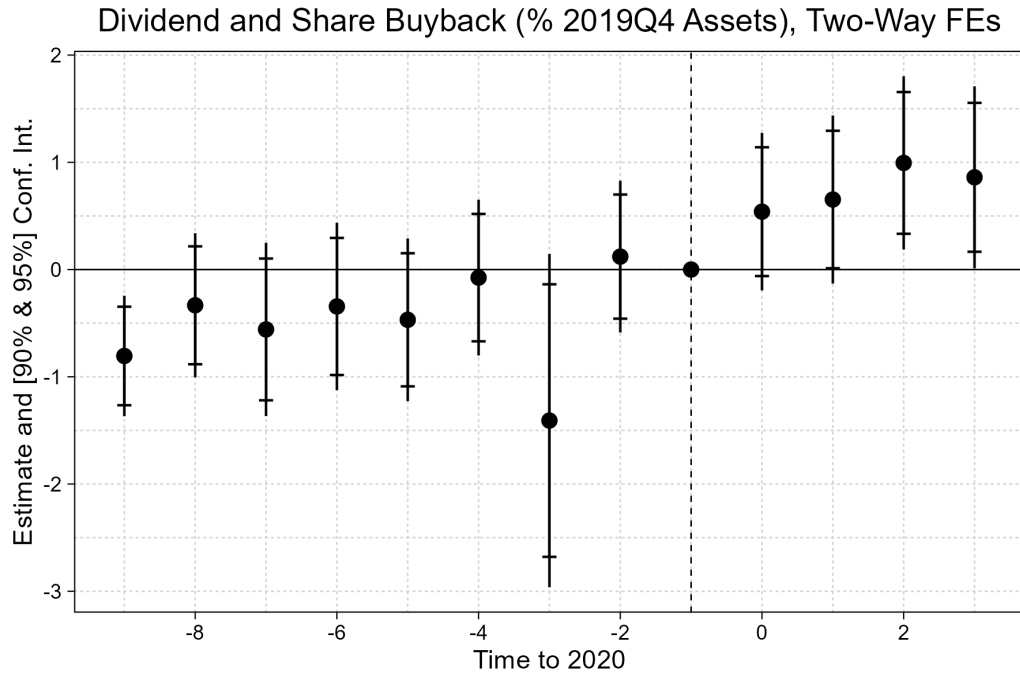
Figure 2.5: Relative Leverage of Ineligible Firms Rise



The figure plots the dynamic treatment effects from the regression given by Equation 2.2 for total debt as a proportion of 2019Q4 assets. The coefficient estimates in the pre-treatment period are null or positive. Particularly, the recent coefficient estimates for 2017 and 2018 are positive, indicating that eligible firms are more leveraged than ineligible firms prior to the pandemic, with a possible declining trend. In the treatment horizon, the coefficients become negative and continue to decrease, indicating greater relative increases in leverage for ineligible firms.

as of 2019Q4. The coefficient estimates in the pre-treatment period are null or positive. Particularly, the recent coefficient estimates for 2017 and 2018 are positive, indicating that eligible firms are more leveraged than ineligible firms prior to the pandemic, with a possible declining trend. In the treatment horizon, the coefficients become negative and continue to decrease, indicating greater relative increases in leverage for ineligible firms.

Figure 2.6: Relative Payouts by Eligible Firms Rise

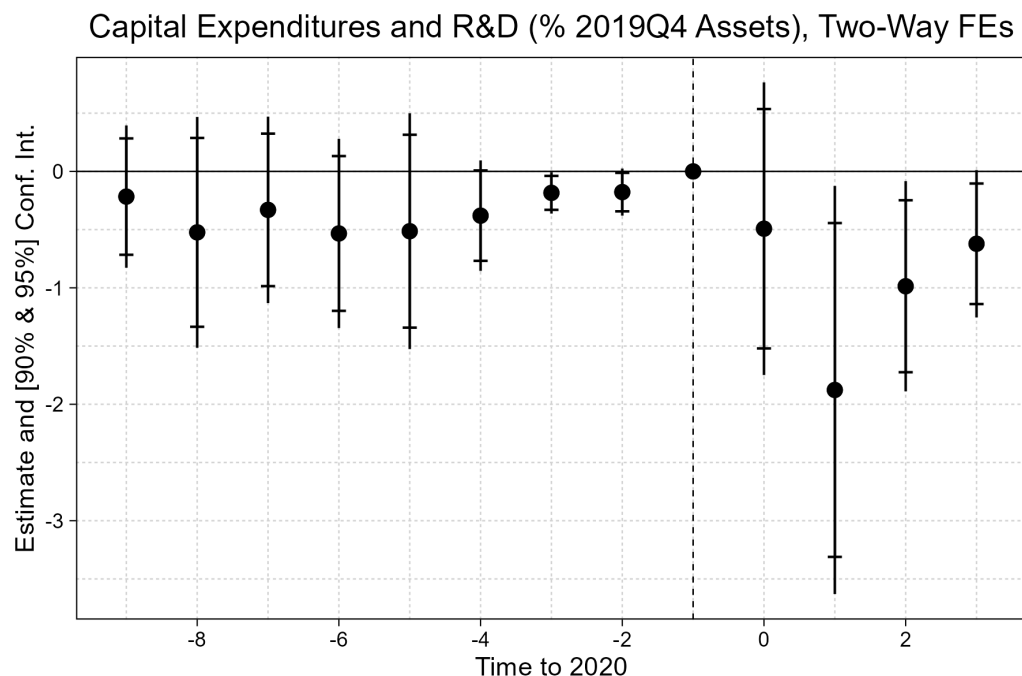


The figure plots the dynamic treatment effects from the regression given by Equation 2.2 for payouts as a portion of 2019Q4 total assets. The relative level of payouts between eligible and ineligible firms are generally null for the pre-treatment period. In the treatment horizon, the point estimates for the dynamic treatment effects are positive and increasing in the treatment horizon.

Figure 2.6 plots the dynamic treatment effects for payouts as a portion of 2019Q4 total assets. The relative level of payouts between eligible and ineligible firms are generally null for the pre-treatment period. In the treatment horizon, the point estimates for the dynamic treatment effects are positive and increasing in the treatment horizon.

Figure 2.7 plots the dynamic treatment effects for investment as a proportion of 2019Q4 total assets. In the pre-treatment period, the relative levels of investment between eligible and ineligible firms were generally null in the pre-treatment period, although it was pos-

Figure 2.7: Eligible Firms Display Relative Decline in Investment in 2020 Before Reversion



The figure plots the dynamic treatment effects for investment as a proportion of 2019Q4 total assets. In the pre-treatment period, the relative levels of investment between eligible and ineligible firms were generally null in the pre-treatment period, although it was possibly negative and statistically significant more recently. While the point estimate falls in 2020, there is significant variation. It falls further in 2021 before starting to revert.

sibly negative and statistically significant more recently. While the point estimate falls in 2020, there is significant variation. It falls further in 2021 before starting to revert.

2.5.1 Discussion

Coefficients from the event study regressions are reported in Tables 2.9 in Appendix 2.9.1. The dynamic (homogeneous) treatment effects for cash and debt presented in this section broadly align with the static (homogeneous) treatment effects shown in Table 2.3. That is, the dynamic (homogeneous) treatment effects are consistently negative. Likewise, the dynamic (homogeneous) treatment effects from payouts are consistent with the positive effect found in Table 2.4. Interestingly, while the static (homogeneous) treatment effect was null over the entire treatment horizon, as seen in Table 2.4, the dynamic (homogeneous) treatment effects for investment were negative for 2021, 2022, and 2022. Moreover, the standard errors are particularly wide for investment, suggesting the presence of heterogeneous effects.

Overall, while the general absence of pre-trends may suggest that parallel trends may hold in the treatment period, there may still be concerns about potential selection bias or heterogeneous effects. Eligible issuers may have better navigated the pandemic by taking on relatively lower leverage and increasing cash buffers to a lesser extant, while being more cautious about investment and supporting payouts more as the crisis faded. The next section attempts to better address potential threats to identification from regression designs by using a deep nets in a setting with high-dimensional controls and flexible functional forms, in addition to accounting for heterogeneous effects.

2.6 Dynamic Heterogeneous Average Treatment Effects: Two-Step Semi-Parametric DiD Estimators

2.6.1 Overview of Empirical Design

As mentioned, a key concern of the regression frameworks in Sections 2.4 and 2.5 is the potential selection bias that is associated with the treatment variable being a proxy for IG status. IG firms may naturally have been more resilient than HY firms, taking on less leverage and increasing cash to a lesser extent, while maintaining firm payouts. The ideal experiment would compare two virtually identical firms that only differ based on treatment assignment (e.g. eligibility for the CCFs).

The causal ML approach used in this section attempts to take this idea to furthest extent possible by using a high-dimensional set of covariates that far exceeds the number of observations without imposing variable selection or functional form restrictions on the interactions across variables beforehand. The novel two-step semi-parametric DiD estimator for computing dynamic (heterogeneous) treatment effects presented here is comparable to an event study design with two-way fixed effects, which computes dynamic (homogeneous) treatment effects. The structural equation for potential outcomes consists of a linear combination of a non-parametric intercept term and the interaction between a treatment indicator and non-parametric slope term. The intercept term corresponds to the outcome of ineligible firms, or potential outcome of eligible firms had they not received treatment. The slope term corresponds to the unit-level heterogeneous treatment effect, otherwise called the CATE for eligible firms or the counterfactual, potential CATE for ineligible firms.

In the first step, the non-parametric intercept and slope terms are estimated using deep nets, as is the propensity score, which is a key ingredient in the estimators for the coefficients. The propensity score is the probability of a firm being classified as eligible given

the high-dimensional set of characteristics. Deep nets are used because ability to approximate continuous functions of real variables arbitrarily well, showing exceptional performance in this regard [Chronopoulos et al., 2023]. Farrell, Liang, and Misra [2021b] provides the theoretical justification for using deep nets to estimate non-parametric terms in the first step of two-step semi-parametric estimation and inference. Nonetheless, the results should be similar if using other high-quality ML algorithms, such as random forests [Belloni, Chernozhukov, and Hansen, 2014, Chernozhukov et al., 2018].

However, because of the bias induced by regularization in a high-dimensional setting, an IF estimator, or Neyman orthogonal score function, is required. The expression for the DiD estimator used in this section is derived from the general formulation of IF estimators given in Farrell, Liang, and Misra [2021a]. In addition, cross-fitting, the estimation and evaluation of models across different samples, is used to prevent overfitting and produce unbiased estimates [Chernozhukov et al., 2018]. Section 2.6.3 goes into the requirements for identification of parameter estimates in greater detail, the key requirements are that the unconfoundedness (or selection on observables) assumption and the overlap condition holds [Farrell, Liang, and Misra, 2021b]. Given the DiD setup, unconfoundedness can be relaxed to the conditional versions of the no anticipation and parallel trends to identify the average treatment effect on the treated (ATET), instead of the average treatment effect (ATE) [Chernozhukov et al., 2024]. Indeed, the general lack of pre-trends in the event study regressions in Section 2.5 suggests that conditional parallel trends is a reasonable assumption. Moreover, estimates of the ATE and ATET are not statistically different from zero, as shown in Appendix 2.9.9.

The empirical design is used not only to address potential concerns around selection bias but also to account for the effects of heterogeneity. As mentioned, CATEs for all firms are recovered. The IF estimator appropriately weights the individual heterogeneous effects when constructing the estimate of the ATE. In addition, the knowledge of CATEs allows

for the study the effects of counterfactual policy targeting, which is undertaken in Section 2.7. Counterfactual effects are also identified, so long as unconfoundedness and overlap holds [Farrell, Liang, and Misra, 2021b]. If unconfoundedness does not hold, the estimator is still valid and recovers the predictive effects from alternative policy schemes. This is still useful for policy analysis and diagnostics.

2.6.2 Modelling Framework

Let \mathcal{F} denote the realized information for firms by the end of 2019. Let $h = t - 2020$, where t is the year. Define $\Delta y_i^h = y_i^h - y_i^{-1}$, which is the difference in the outcome variable for some year 2020 or later and its value in 2019. I restrict attention to all covariates realized by the end of 2019, with less than 1% of observations missing: $x_i \subset \mathcal{F}$. I further consider an expanded list of covariates by relaxing the tolerance for missing observations to 10%. Binary treatment, z_i , is defined to equal 1 if a firm's cash bonds were eligible for direct purchase by the Fed CCFs at the announcement date. All together this gives the following potential outcomes model:

$$\Delta y_i^h = \alpha(x_i) + \beta(x_i)z_i + e_i \quad (2.3)$$

Note that this is a linear combination of a non-parameteric intercept term, $\alpha(x_i)$, and the interaction between a non-parameteric slope term, $\beta(x_i)$, and a binary variable, z_i .

Let $Y^h(z)$ be the potential outcome at time h where Z denotes the treatment status:

$$\mathbb{E}[\Delta Y^h|X = x, Z = z] = \mathbb{E}[\Delta Y^h(z)|X = x, Z = z] = \mathbb{E}[\Delta Y^h(z)|X = x] = \alpha(x) + \beta(x)z$$

where the first equality follows from the consistency assumption (the potential outcome is consistent with the treatment assignment) and the second equality follows from the unconfoundedness and overlap assumptions (these are discussed further in Section 2.6.3).

Taking the difference in the differences in the outcome variables yields:

$$\mathbb{E}[\Delta Y^h(1) - \Delta Y^h(0)|X = x] = \beta(x)$$

Hence, the CATE is given by $\beta(x)$ and ATE, incorporating in heterogeneity, is given by:

$$\mu = \mathbb{E}[\beta(x)] \quad (2.4)$$

Given the DiD setting, the assumption of unconfoundedness can be relaxed to the weaker assumptions of no anticipation and parallel trends, conditional on pre-treatment covariates.²⁰ This would identify the ATET, as is the case in Sections 2.4 and 2.5 [Chernozhukov et al., 2024].²¹ ²² The general lack of pre-trends observed in the event study regressions in

20. In effect, these assumptions require that, conditional on pre-treatment covariates, firms do not anticipate the treatment (CCFs) in 2019 and absent the treatment, comparable firms' dynamics would have evolved similarly.

21. The ATET is given by the difference between the difference in the outcome variables for treated and untreated firms, averaging over the entire sample. This is expressed as:

$$\begin{aligned} \text{ATET} &= \mathbb{E}[\mathbb{E}[\Delta Y^h(1)|Z = 1, X] - \mathbb{E}[\Delta Y^h(0)|Z = 0, X]] \\ &= \mathbb{E}[\mathbb{E}[\alpha(x) + \beta(x)|Z = 1, X] - \mathbb{E}[\alpha(x)|Z = 0, X]] \\ &= \mathbb{E}[\alpha(x) + \beta(x)|Z = 1] - \mathbb{E}[\alpha(x)|Z = 0] \end{aligned}$$

Hence, the ATET is equal to the average of the CATEs among treated firms if the average of the potential outcome absent treatment is the same between treated and untreated firms. Section 2.9.9 derives the IF estimator for the ATET. Section 2.9.9 compares the ATE and ATET estimates for the benchmark model across all outcome variables, showing that the two are similar with no statistically significant difference in any instance.

22. Another motivation of using a two-step semi-parametric DiD estimator is that adding controls to the linear models in Sections 2.4 and 2.5 may not recover causal effects without strong restrictions functional form and heterogeneity [Caetano et al., 2024].

Section 2.5 suggests that the parallel trends assumption can be justified.

I also estimate the quantity, $\mathbb{E}[\alpha(x)]$, and refer to it as the base effect. Plotting the evolution of the base effect gives insight into the dynamics for outcome variables for ineligible firms, as well as the potential outcome for eligible firms absent treatment.

Let the parameter vector be given by $\theta = (\alpha, \beta)$, then the general expression for the influence function estimator follows from Farrell, Liang, and Misra [2021a]:

$$\psi(\Delta y_i^h, z_i, x_i, \theta(x_i)) = H(x_i, \theta(x_i)) - (\nabla_\theta H)(\mathbb{E}[l_{\theta\theta}|X = x]^{-1}l_\theta) \quad (2.5)$$

where l the loss function, $l_\theta = \frac{\partial}{\partial \theta} l$ is the score function, and $l_{\theta\theta} = \frac{\partial^2}{\partial \theta \partial \theta'} l$ is the Hessian.

Given a mean squared error loss function, we can express l as:

$$l(\Delta y^h, z, \theta(x)) = l(\Delta y^h, z, \alpha(x), \beta(x)) = \frac{1}{2}(\Delta y^h - \alpha(x) - \beta(x)z)^2$$

Consequently, the expression for the score is:

$$l_\theta = - \begin{pmatrix} 1 \\ z \end{pmatrix} (\Delta y^h - \alpha(x) - \beta(x)z)$$

And likewise, for the Hessian:

$$l_{\theta\theta} = \begin{pmatrix} 1 & z \\ z & z^2 \end{pmatrix}$$

Let $\Lambda(x) = \mathbb{E}[l_{\theta\theta}|X = x]$. Hence,

$$\Lambda(x) = \begin{pmatrix} 1 & p(x) \\ p(x) & p(x) \end{pmatrix} \quad (2.6)$$

where,

$$p(x) \equiv \Pr(z|X = x) \quad (2.7)$$

is the propensity score, or the probability of a firm being treated given its features.

The derivation for the ATE involves setting $H(x, \theta(x)) = \beta(x)$ and is shown in Appendix 2.9.4. The resultant estimator is analogous to the doubly-robust DiD estimator of Sant'Anna and Zhao [2020] in a non-ML setting and the DML DiD estimator of Chang [2020] for partially linear models.²³ The setup for all three models is the basic 2×2 , or $N \times 2$, difference in differences model with 2 units, which are either treated or control, or N units split into these groups, and 2 time periods, pre- and post- treatment. All three estimators have the doubly-robust property: they are consistent estimators of the average treatment effect if either the potential outcome model given by Equation 2.3 or the propensity scores, Equation 2.7, are correctly estimated, but not necessarily both.

Consequently, in the results presented here, the dynamic (heterogeneous) base and treatment effects are computed by re-running the two-step semi-parameteric model period by period over the treatment horizon. Alternatively, this can be extended to estimating the dynamic effects simultaneously in a panel version of two-step semi-parametric estimators, as in Chronopoulos et al. [2023]. Identification is similar in both cases [Miller, 2023].

2.6.3 Discussion on Identification

As mentioned, Farrell, Liang, and Misra [2021b] provide the theoretical justification for using deep nets in the first step of two step estimation when inference is conducted on the second step using an influence function estimator, as in Equation 2.5. In addition, they mention two requirements the estimation of a potential outcomes model, as in Equation 2.3, need to satisfy in order to identify causal parameters of interest. These are uncon-

23. This corresponds to case where $\beta(x) = \beta$ is homogeneous in Equation 2.3.

foundedness (i.e. selection on observables) and overlap.²⁴

Unconfoundedness

An advantage of using deep nets is that it allows for the consideration of a high-dimensional feature space along with arbitrary interactions and transformations among potential covariates. The list of firm characteristics used in estimation is given by Tables 2.10 and 2.11. In addition, indicator variables for industry classification are used. The histories of data used range from 1 year to 10 years. To accommodate such a high-dimensional feature space, deep architectures are used for the neural networks, as shown in Tables 2.12 and 2.13. Consequently, the claim is that any unobserved variable correlated with the treatment, and potentially biasing the results, is likely to be spanned by the high-dimensional feature space, the transformation of features, and their interactions. As such, the selection on observables assumption is likely satisfied.

As previously noted, given the DiD setup, the assumption of unconfoundedness can be relaxed to the weaker assumptions of conditional no anticipation and parallel trends. This requires that, conditional on pre-treatment covariates, comparable firms did not anticipate the CCF interventions in 2019, which is reasonable given the unprecedented nature of the pandemic, and that treated firms would have had similar dynamics to their untreated counterparts, absent intervention. The general lack of pre-trends observed in the event study regressions in Section 2.5 suggests that the parallel trends assumption can be justified. The cost of moving to these weaker assumptions is that the model identifies the ATET rather than the ATE [Chernozhukov et al., 2024]. Section 2.5 suggests that the parallel trends assumption can be justified. Section 2.9.9 compares the ATE and ATET estimates, finding statistically negligible differences.

24. The assumption of consistency is also required to ensure that observed outcomes correspond to the assigned treatment, which is also assumed here.

Overlap

The overlap condition is satisfied if propensity scores, given by Equation 2.7 are bounded away from zero and one. Figures 2.1, 2.2, and 2.3 help support the argument that the overlap condition is satisfied. Graphically, both the data on firm characteristics and CDS spreads shows a significant overlap in distributions between eligible and ineligible firms.

Indeed, the CCF's reliance on ratings to determine eligibility is critical to the identification strategy. As argued by several papers, ratings lag and can be predicted by fundamental data [Altman and Rijken, 2004], given ratings agencies' desire for ratings stability. In addition, there is some evidence of a loosening of ratings standards heading into the pandemic. Celik, Demirtaş, and Isaksson [2020] document that within-rating leverage ratios increased by 2019, as the number of BBB-rated firms increased. Additionally, downgrade frequency declined relative to upgrades, with BB+ rated issuers having the highest probability of a 1-notch upgrade within a year and BBB- rated issuers having the lowest probability of a 1-notch downgrade. Consistent with this, Altman [2020] finds that based on 2019 data, 34% of BBB-rated firms can be classified as HY based largely on fundamental characteristics based on the Altman Z-score.

In the same vein, CDS spreads lead and predict future ratings changes CDS spreads [Lee, Naranjo, and Velioglu, 2018, Lee, Naranjo, and Sirmans, 2021]. Not only does Figure 2.3 show a significant overlap between eligible and ineligible firms' CDS spread distribution, the support of the former lies almost entirely within the support of the latter. This suggests had the eligibility criteria been determined by CDS spreads rather than credit ratings, many eligible firms would have been deemed ineligible, and vice-versa.

In summary, there is rich overlap in the feature space across eligible and ineligible firms. This suggests that the overlap condition is satisfied and allows for the IF estimator given by Equation 2.5 to be well-defined.

2.6.4 Estimation Procedure

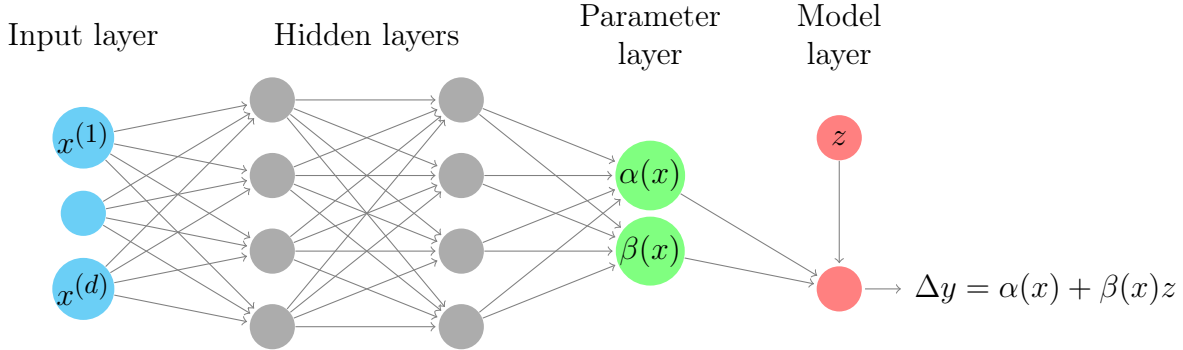


Figure 2.8: Deep Net Architecture for the Potential Outcomes Model

The figure represents the deep net architecture for estimating the parameters in the potential outcomes model given by Equation 2.3. Specific values for the number of inputs and hidden layer architecture are reported in Table 2.12 for models with features with less than 1% missing observations and Table 2.13 for models with features with less than 10% missing observations.

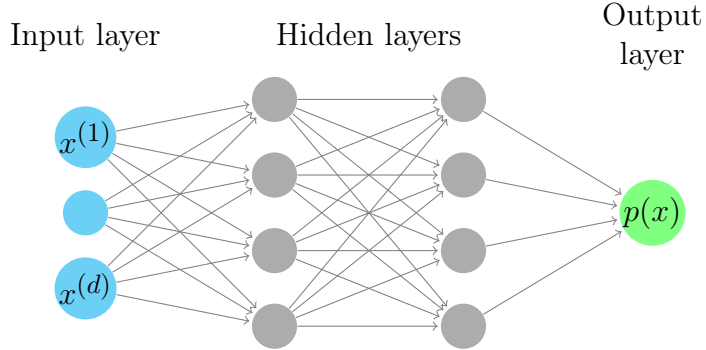


Figure 2.9: Deep Net Architecture for Propensity Scores

The figure represents the deep net architecture for estimating the propensity scores given by Equation 2.7. Specific values for the number of inputs and hidden layer architecture are reported in Table 2.12 for models with features with less than 1% missing observations and Table 2.13 for models with features with less than 10% missing observations.

I obtain features for the deep nets from the Financial Ratios Suite by WRDS. Quarterly variables with less than 1% missing observations are used with histories going back 1, 5, and 10 years. Table 2.10 in the Appendix reports the list of 37 features where less than 1% of observations are missing over a 10 year history from 2010Q1 to 2019Q4. As a robustness check, 23 additional features are added by increasing the tolerance of missing observations to 10%; these are reported in Table 2.11. Missing information is replaced with

the quarter-industry median and dummy variables are added to track missing data. Additionally, dummy variables for two-digit NAICS industry codes are used.

Figure 2.8 illustrates the architecture used to estimate the parameters for Equation 2.3. Table 2.12 reports specific values for the number of inputs and the hidden layer architectures associated with the models with covariate histories of 1, 5, and 10 years, respectively. Propensity scores are estimated in a similar fashion and with the same architecture, as seen in Figure 2.9. The deep net models for the parameters for Equation 2.3 use rectified linear (ReLU) activation functions within the hidden layers. A linear output layer combines the parameter estimates and treatment indicator to get an estimated outcome. Then, a mean-squared error loss function is applied to the estimated and actual outcomes. The deep net models for propensity scores use hyperbolic tangent (tanh) activation functions within the hidden layers with a sigmoid output layer and a binary cross-entropy loss function. This is done to have propensity scores bounded within zero and one so that the IF estimator is well-defined.

The procedure to estimate any parameter of interest requires three folds of cross-fitting. Cross-fitting involves estimating deep nets on one set of data and evaluating it on another. This is done to prevent over-fitting and to produce unbiased estimators [Chernozhukov et al., 2018]. The dataset is split into three random samples of equal size. A deep net is trained on each sample to produce models for the parameters in Equation 2.3. Separately, deep nets are trained to produce propensity scores. Finally, the influence function is computed by evaluating data from a third sample on models for the CATEs and propensity scores each trained on different samples.²⁵ Given the cross-fit procedure, dropout regularization is used in training the deep nets to reduce overfitting and so, increase efficiency.²⁶

25. Sample code demonstrating the ability of the estimator to recover parameters in simulated data can be found here: <https://github.com/rmmomin/causal-ml-auto-inference>.

26. The reported results are from models trained with a dropout rate of 20% but similar results are obtained by using a dropout rate equal to 30%, 40%, or 50%.

To further improve efficiency, I run multiple cross-fit iterations. I take the median of estimators computed across M cross-fit partitions and its associated variance:²⁷

$$\begin{aligned}\tilde{\mu}_0 &= \text{Median} \left((\mu_{0,m})_{m \in [M]} \right) \\ \hat{\sigma}^2 &= \sqrt{\text{Median} \left(\hat{\sigma}_m^2 + (\tilde{\mu}_{0,m} - \tilde{\mu}_0)^2 \right)_{m \in [M]}}\end{aligned}$$

where $\tilde{\mu}_0$ is the parameter of interest, $\tilde{\mu}_{0,m}$ is the parameter estimate corresponding to partition m of cross-fitting, and $\hat{\sigma}^2$ is the variance. The asymptotic standard error is given by $\hat{\sigma}^2/\sqrt{N}$, where N is the number of observations. In the reported results, 10 cross-fit partitions are generated for each deep net estimation.²⁸

Additionally, as mentioned in Section 2.6.2, the model is estimated period by period over the treatment horizon. An extension to the framework would be to estimate these effects simultaneously in a panel setting of the two-step semi-parametric model, as in Chronopoulos et al. [2023].

2.6.5 Base Effects

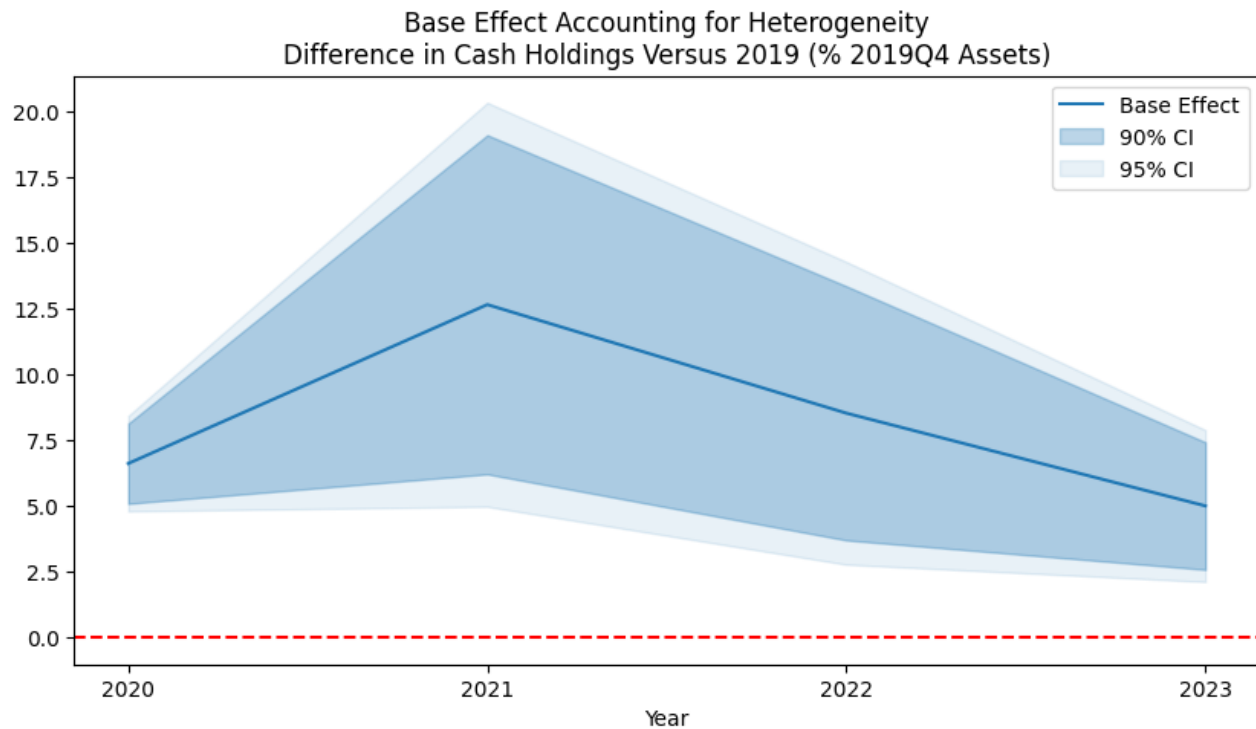
To estimate the base effect, set $H(x, \theta(x)) = \alpha(x)$ in Equation 2.5. Appendix 2.9.3 provides details on the derivation of the estimator.

Figure 2.10 plots the base effects for the change in cash holdings, as a percent of 2019Q4 assets, using a model with 10 years of feature history and 1% tolerance for missing observations. Details on its architecture are reported in Table 2.12 in the Appendix. Consistent with the DiD regressions reported in Table 2.3, a large base effect is identified for 2020 onwards. However, the dynamics of cash holdings suggests that these peaked for all firms in

27. See <https://docs.doubleml.org/stable/guide/resampling.html>.

28. The results are similar when the models are run using 5 cross-fit partitions for each deep net estimation. Nonetheless, the cross-fitting approach inherently introduces stochasticity to the results which motivates the use of multiple partitions for robustness.

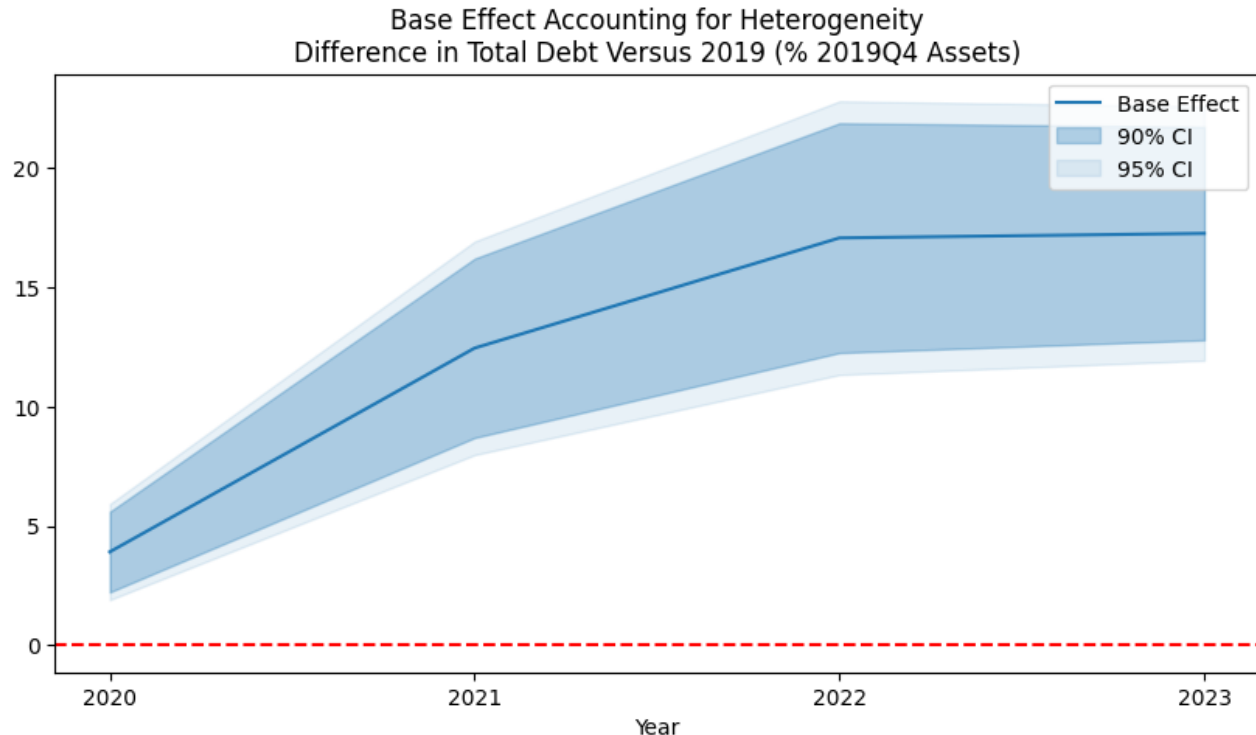
Figure 2.10: Large Base Effect with Increase in Cash Holdings



The figure plots the base effects for the change in cash holdings, as a percent of 2019Q4 assets. The model above uses 10 years of feature history and 1% tolerance for missing observations. Details on its architecture are reported in Table 2.12 in the Appendix. Table 2.14 reports results across all model specifications. Consistent with the DiD regressions reported in Table 2.3, a large base effect is identified for 2020 onwards.

2021 and then began to fall, perhaps as uncertainty from the pandemic and so, demand for precautionary liquidity began to fade. The finding of large, positive base effects, as well as its dynamics, are largely consistent across different model specifications, as shown in Table 2.14.

Figure 2.11: Large Base Effect with Increase in Total Debt

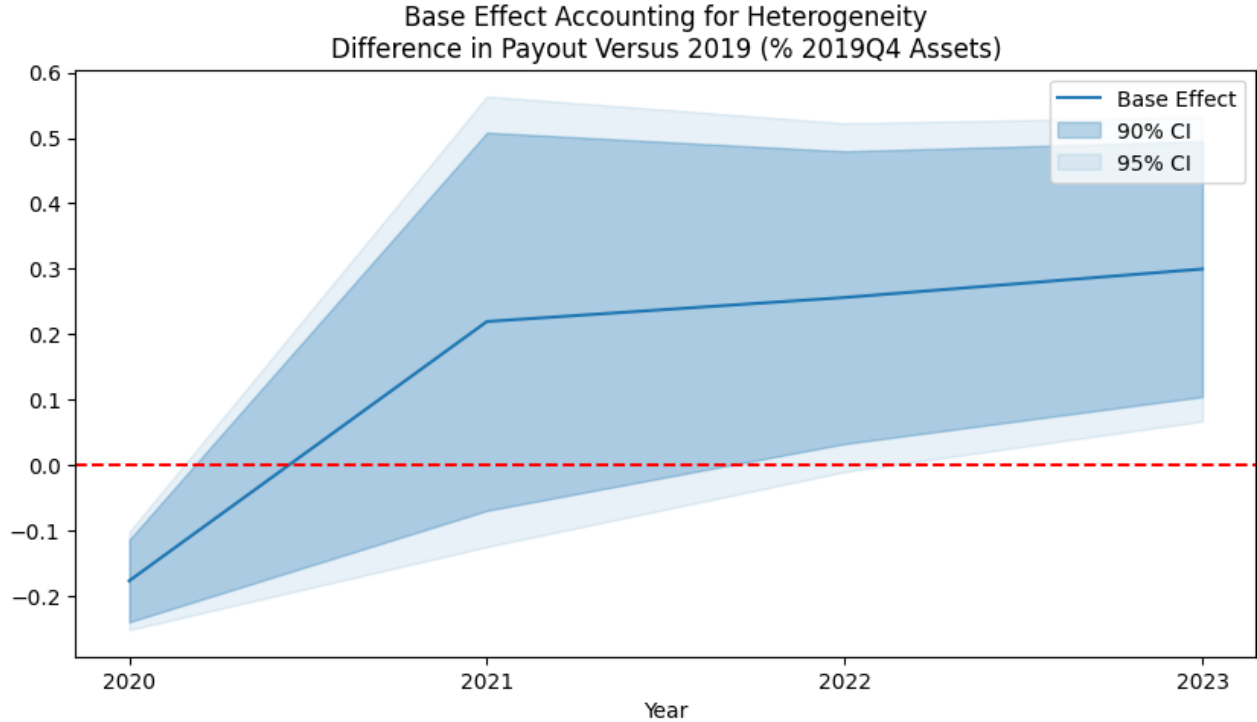


The figure plots the base effects for the change in debt, as a percent of 2019Q4 assets. The model above uses 10 years of feature history and 1% tolerance for missing observations. Details on its architecture are reported in Table 2.12 in the Appendix. Table 2.15 reports results across all model specifications. Consistent with the DiD regressions reported in Table 2.3, a large base effect is identified for 2020 onwards.

Figure 2.11 plots the base effects for the change in debt, as a percent of 2019Q4 assets, using a model with 10 years of feature history and 1% tolerance for missing observations. Details on its architecture are reported in Table 2.12 in the Appendix. Consistent with the DiD regressions reported in Table 2.3, a large base effect is identified for 2020 onwards. In contrast to cash holdings, the base effects for leverage has remain elevated. This suggests that ineligible firms did not deleverage as their cash reserves fell. The finding of large, positive base effects, as well as an increasing trend, are largely consistent across different

model specifications, as shown in Table 2.15.

Figure 2.12: Payout Base Effect Initially Negative Then Increases

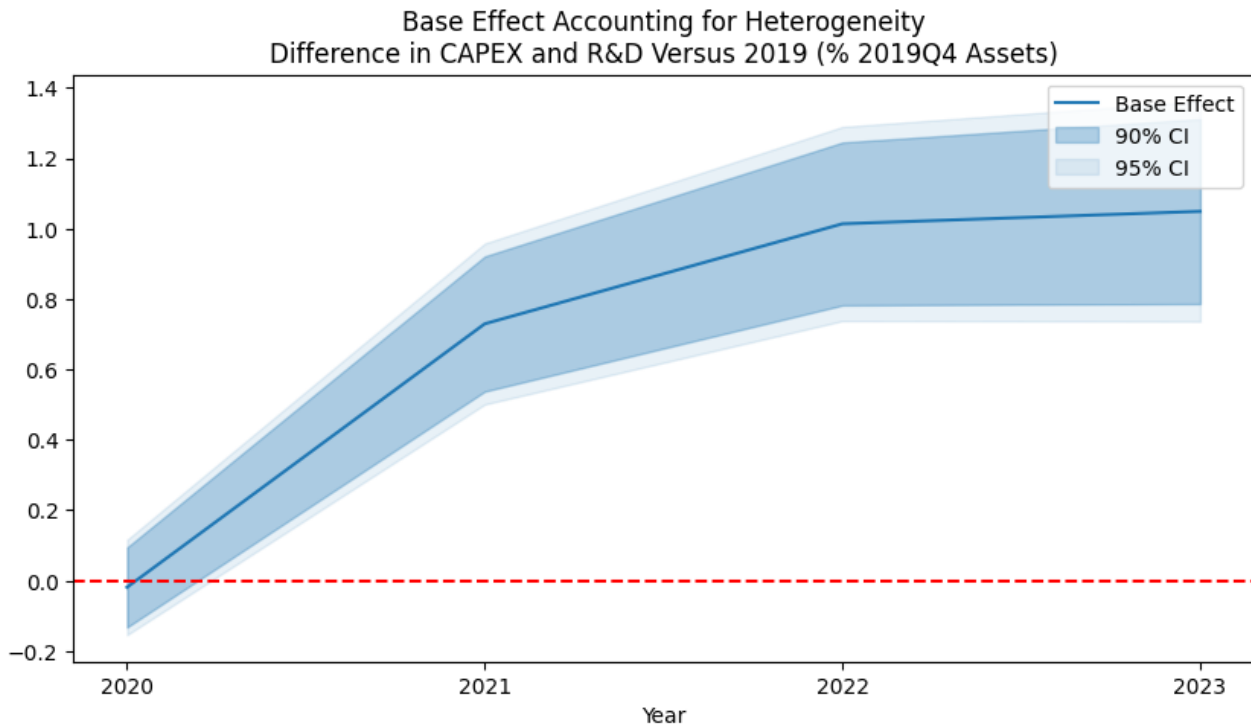


The figure plots the base effects for the difference in annual payouts versus 2019, scaled by 2019Q4 assets. The model above uses 10 years of feature history and 1% tolerance for missing observations. Details on its architecture are reported in Table 2.12 in the Appendix. Table 2.16 reports results across all model specifications. In contrast to the null results picked up by the DiD regressions reported in Table 2.4, the base effect here changes over the observation period, initially negative in 2020 and then increasing.

Figure 2.12 plots the base effects for the difference in annual payouts versus 2019, scaled by 2019Q4 assets, using a model with 10 years of feature history and 1% tolerance for missing observations. Details on its architecture are reported in Table 2.12 in the Appendix. In contrast to the null results picked up by the DiD regressions reported in Table 2.4, the base effect here changes over the observation period, initially negative in 2020 and then increasing. This is consistent with firms initially reducing payouts to preserve liquidity and then resuming them as conditions improved. These results are largely consistent across different model specifications, as shown in Table 2.16.

Figure 2.13 plots the base effects for the difference in annual investment versus 2019, scaled by 2019Q4 assets, using a model with 10 years of feature history and 1% tolerance

Figure 2.13: Investment Base Effect Null then Increasing



The figure plots the base effects for the difference in annual investment versus 2019, scaled by 2019Q4 assets. The model above uses 10 years of feature history and 1% tolerance for missing observations. Details on its architecture are reported in Table 2.12 in the Appendix. Table 2.17 reports results across all model specifications. Consistent with the positive effect found for the post period in the DiD regressions reported in Table 2.4, positive effects are generally found over the treatment period. Figure 2.22 plots the base effects corresponding to proxying investment with the annual change in gross property, plant, and equipment. In contrast to here, negative base effects are estimated for 2020 and 2021, which then become null for 2022 and 2023.

for missing observations. Details on its architecture are reported in Table 2.12 in the Appendix. Consistent with the positive effect found for the post period in the DiD regressions reported in Table 2.4, positive effects are generally found over the treatment period. However, these results are not robust to an alternative proxy for investment. Figure 2.22 plots the base effects corresponding to proxying investment with the annual change in gross property, plant, and equipment. In contrast to here, negative base effects are estimated for 2020 and 2021, which then become null for 2022 and 2023. These results are largely consistent across different model specification, as shown in Table 2.30.

2.6.6 ATE with Heterogeneity

To estimate the ATE, set $H(x, \theta(x)) = \beta(x)$ in Equation 2.5. For each cross-fit fold, the estimator becomes:

$$\hat{\mu}_s = \frac{1}{N} \sum \psi(\Delta y^h, z, x, \theta) = \frac{1}{N} \sum \left[\beta(x) + \frac{z(\Delta y^h - \alpha(x) - \beta(x)z)}{p(x)} - \frac{(1-z)(\Delta y^h - \alpha(x))}{1-p(x)} \right] \quad (2.8)$$

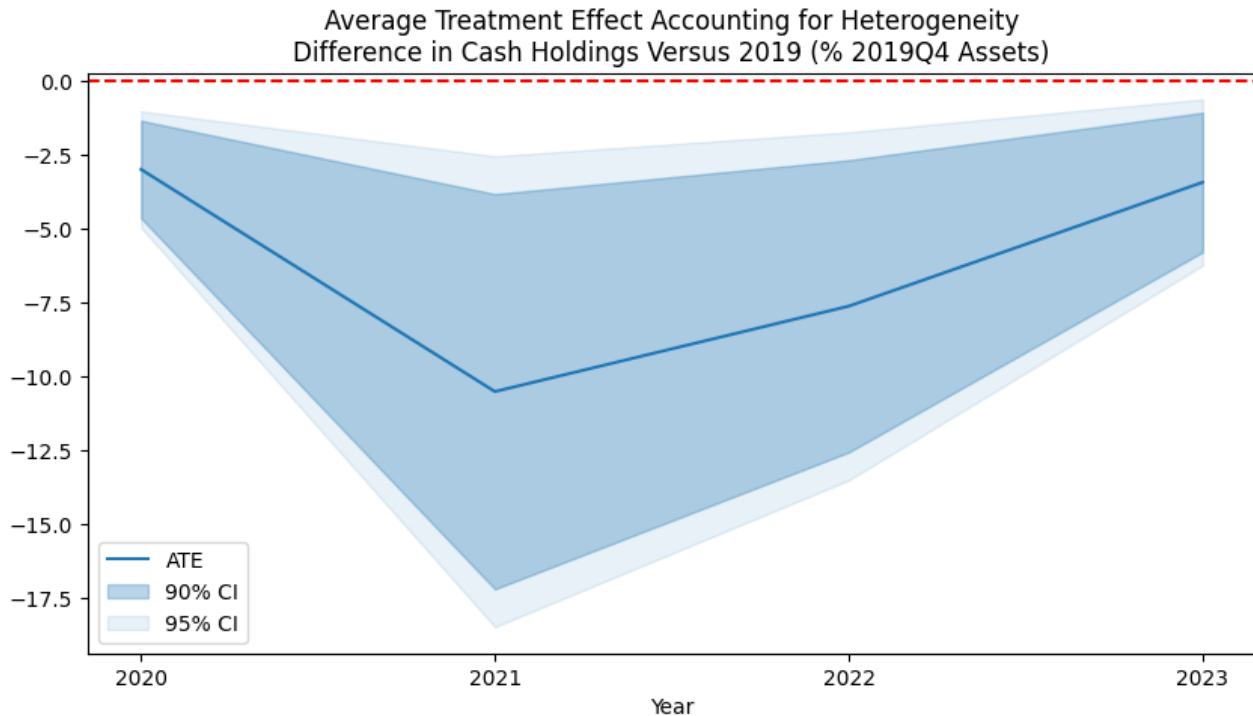
Appendix 2.9.4 provides details on the derivation. The final estimate of Equation 2.4 is then obtained by averaging the estimates from each fold:

$$\hat{\mu} = \frac{1}{3} \sum \hat{\mu}_s \quad (2.9)$$

While the ATE is identified under the assumption of unconfoundedness, this assumption can be relaxed to conditional no anticipation and parallel trends to identify the ATET instead. The general lack of pre-trends observed in the event study regressions in Section 2.5 suggests that the parallel trends assumption can be justified. Section 2.9.9 compares the ATE and ATET estimates, finding statistically negligible differences.

Figure 2.14 plots the average treatment effects for the change in cash holdings over different horizons, accounting for heterogeneity, using a model with 10 years of feature his-

Figure 2.14: Cash ATE With Heterogeneity Shows Large Negative Effect



The figure plots the average treatment effects for the change in cash holdings, as a percent of 2019Q4 assets. This corresponds to the estimator reported in Equation 2.9. The model above uses 10 years of feature history and 1% tolerance for missing observations. Details on its architecture are reported in Table 2.12 in the Appendix. Table 2.18 reports results across all model specifications. Large negative treatment effects are estimated over the entire horizon. Table 2.5 compares the treatment effect estimates across different models and suggests that results are broadly in line.

tory and 1% tolerance for missing observations. Details on its architecture are reported in Table 2.12 in the Appendix. Large negative treatment effects are estimated over the entire horizon, consistent with static (homogeneous) treatment effects estimated by the DiD regressions and the dynamic (homogeneous) treatment effects estimated by the event study regressions. These are summarized in Table 2.5. Table 2.18 reports the results across different model specifications, showing that the estimates are robust.

Table 2.5: Cash Treatment Effect Comparison

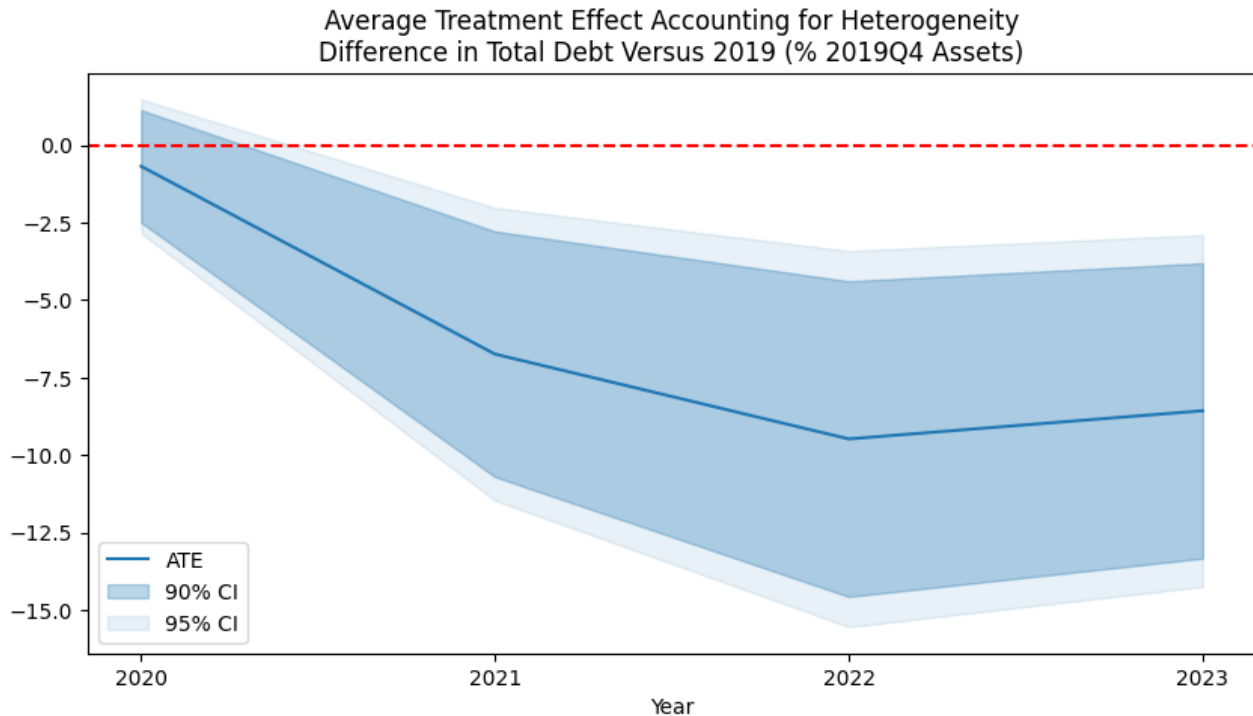
Year	Treatment Effect Estimates			
	Static (Homogeneous)	Dynamic (Heterogeneous) (1)	Dynamic (Homogeneous) (2)	Difference (1)-(2)
2020		-2.98 (1.00)	-3.82 (0.79)	0.84
2021		-10.50 (4.06)	-9.52 (2.42)	-0.98
2022		-7.61 (3.00)	-6.92 (2.27)	-0.68
2023		-3.42 (1.43)	-4.01 (1.09)	0.59
Eligible × Post 2020	-7.46 (2.05)			

Standard-errors in parentheses

The table reports the treatment effect estimates for cash, as a percent of 2019Q4, across the three models examined in this paper. The static (homogeneous) treatment effect comes from the DiD regressions reported in Table 2.3, while the dynamic (homogeneous) treatment effects correspond to the event study regressions with two-way fixed effects, reported in Table 2.9 and shown in Figure 2.4. The different treatment effect estimates are broadly in line.

Figure 2.15 plots the average treatment effects for change in total debt over different horizons, accounting for heterogeneity, using a model with 10 years of feature history and 1% tolerance for missing observations. Details on its architecture are reported in Table 2.12 in the Appendix. While an initial null effect is picked up for 2020, this becomes negative and large for the remainder of the horizon. This suggests that both eligible and ineligible firms initially increased leverage in 2020, but subsequently, eligible firms began deleveraging, while ineligible firms did not. Table 2.6 compares the treatment effect estimates across different models and suggests that the results are broadly in line. These

Figure 2.15: Debt ATE With Heterogeneity Negative After 2020



The figure plots the average treatment effects for change in total debt, as a percent of 2019Q4 assets. This corresponds to the estimator reported in Equation 2.9. The model above uses 10 years of feature history and 1% tolerance for missing observations. Details on its architecture are reported in Table 2.12 in the Appendix. Table 2.19 reports results across all model specifications. While an initial null effect is picked up for 2020, this becomes negative and large for the remainder of the horizon. Table 2.6 compares the treatment effect estimates across different models and suggests that the results are broadly in line.

results are robust to other model specifications, as shown in Table 2.19.

Table 2.6: Debt Treatment Effect Comparison

Year	Treatment Effect Estimates			
	Total Debt (% 2019Q4 Assets)			
	Static (Homogeneous)	Dynamic (Heterogeneous) (1)	Dynamic (Homogeneous) (2)	Difference (1)-(2)
2020		-0.69 (1.10)	-1.66 (0.65)	0.98
2021		-6.75 (2.41)	-5.95 (2.30)	-0.79
2022		-9.48 (3.09)	-9.08 (2.59)	-0.40
2023		-8.58 (2.90)	-8.47 (1.95)	-0.10
Eligible \times Post 2020	-6.21 (2.73)			

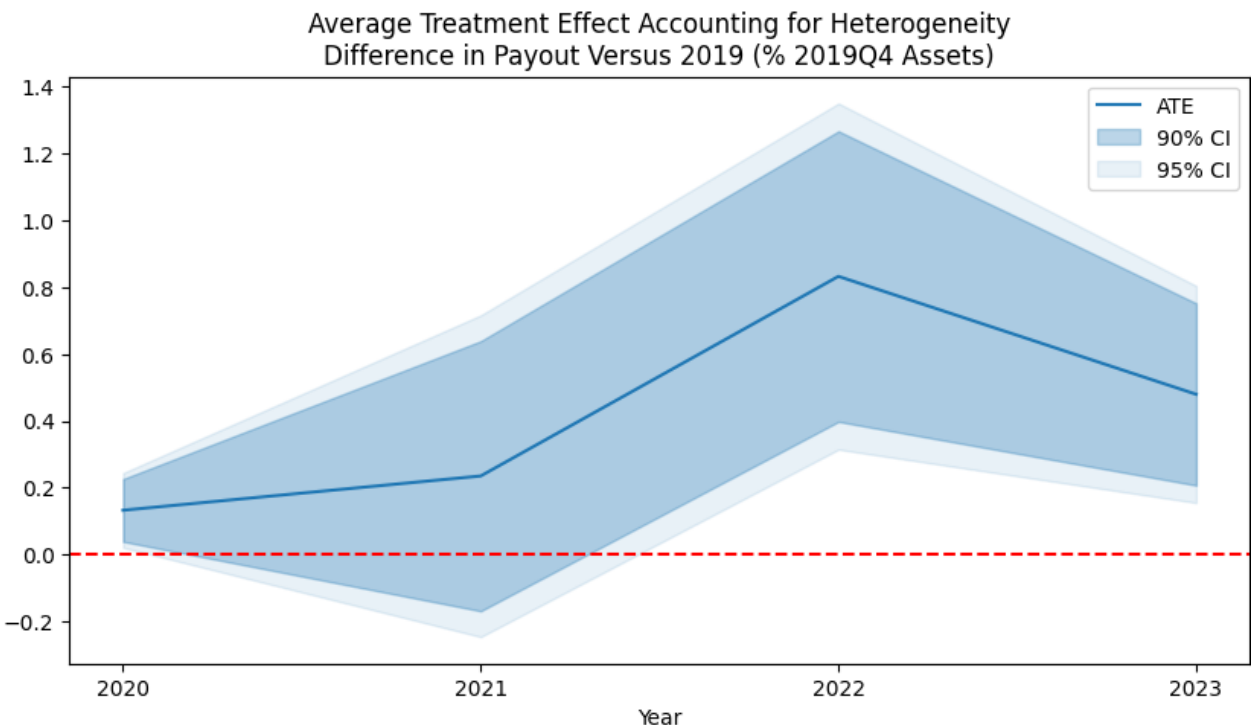
Standard-errors in parentheses

The table reports the treatment effect estimates for debt, as a percent of 2019Q4, across the three models examined in this paper. The static (homogeneous) treatment effect comes from the DiD regressions reported in Table 2.3, while the dynamic (homogeneous) treatment effects correspond to the event study regressions with two-way fixed effects, reported in Table 2.9 and shown in Figure 2.5. The different treatment effect estimates are broadly in line.

Figure 2.16 plots the average treatment effects for the difference in annual payouts versus 2019, as a percent of 2019Q4 assets. The estimates are from the model using 10 years of feature history and 1% tolerance for missing observations; complete Details on its architecture are reported in Table 2.12 in the Appendix. The payout treatment effect is initially positive in 2020, then null for 2021, and again positive for 2022 and 2023. Table 2.7 compares the treatment effect estimates across different models. Interestingly, the point estimates for the dynamic (heterogeneous) treatment effects are smaller than both the static (homogeneous) treatment effects and the dynamic (heterogeneous) treatment effects, but as are the standard errors. In general, this could suggest that the selection bias for the regression models results in an upward bias to treatment effects, consistent with IG firms being more resilient and maintaining payouts. These results are consistent across models using 5 and 10 years of feature history, as seen in Table 2.20.

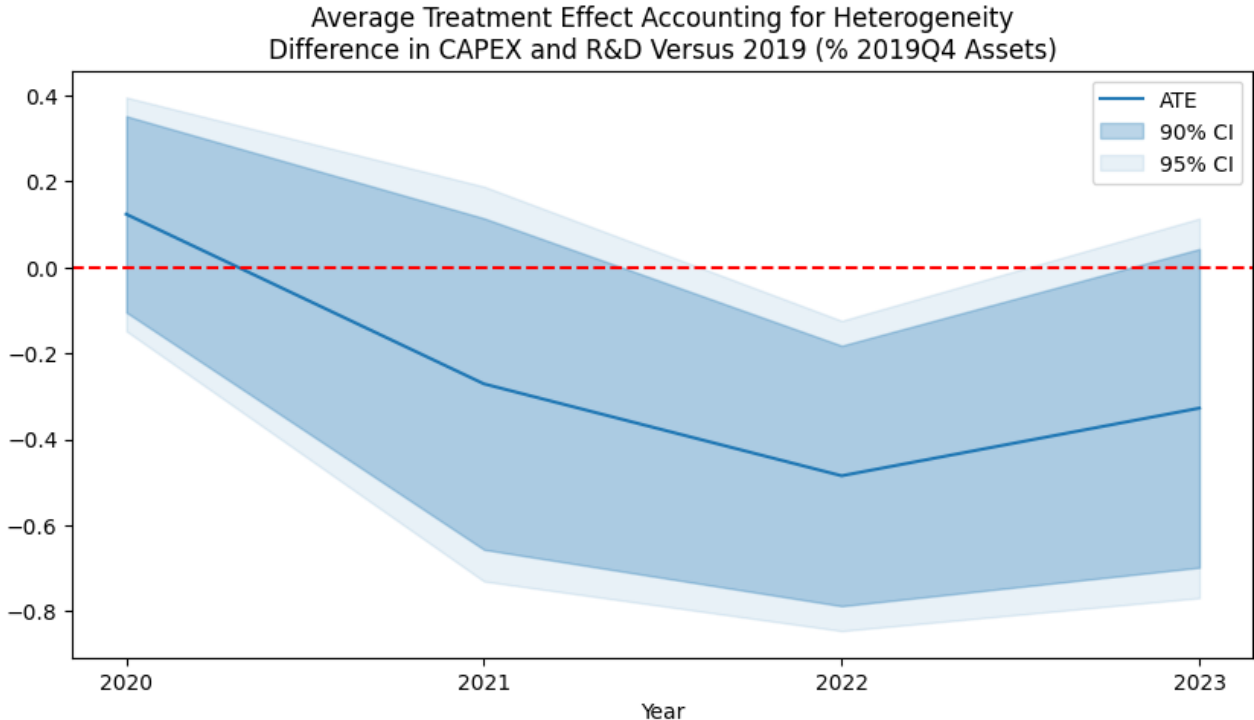
Figure 2.17 plots the average treatment effects for the difference in annual investment

Figure 2.16: Payout ATE Generally Positive



The figure plots the average treatment effects for the difference in annual payouts versus 2019, as a percent of 2019Q4 assets. This corresponds to the estimator reported in Equation 2.9. The model above uses 10 years of feature history and 1% tolerance for missing observations. Details on its architecture are reported in Table 2.12 in the Appendix. Table 2.20 reports results across all model specifications. The payout treatment effect is initially positive in 2020, then null for 2021, and again positive for 2022 and 2023. Table 2.7 compares the treatment effect estimates across different models. While the treatment effects are comparable, the standard errors for the dynamic (heterogeneous) treatment effects are smaller.

Figure 2.17: Investment ATE With Heterogeneity Consistent With Previous Estimates



The figure plots the average treatment effects for the difference in annual investment versus 2019, scaled by 2019Q4 assets. This corresponds to the estimator reported in Equation 2.9. The model above uses 10 years of feature history and 1% tolerance for missing observations. Details on its architecture are reported in Table 2.12 in the Appendix. Table 2.21 reports results across all model specifications, null-to-negative treatment effects are estimated, particularly for the models with longer covariate histories. Table 2.8 compares the different treatment effects estimated by each model, showing that incorporating high-dimensional controls and heterogeneity increases the point estimates for the dynamic effects. Figure 2.23 and Table 2.31 show the treatment effect dynamics when proxying investment by the annual change in gross property, plant, and equipment. For this proxy, null effects are estimated for every specification.

Table 2.7: Payout Treatment Effect Comparison

Year	Treatment Effect Estimates			
	Payout (% 2019Q4 Assets)			
	Static (Homogeneous)	Dynamic (Heterogeneous) (1)	Dynamic (Homogeneous) (2)	Difference (1)-(2)
2020		0.13 (0.06)	0.54 (0.34)	-0.41
2021		0.23 (0.25)	0.65 (0.36)	-0.42
2022		0.83 (0.26)	0.99 (0.37)	-0.16
2023		0.48 (0.17)	0.86 (0.39)	-0.38
Eligible \times Post 2020	1.16 (0.23)			

Standard-errors in parentheses

The table reports the treatment effect estimates for payout, as a percent of 2019Q4 assets, across the three models examined in this paper. The static (homogeneous) treatment effect comes from the DiD regressions reported in Table 2.4, while the dynamic (homogeneous) treatment effects correspond to the event study regressions with two-way fixed effects, reported in Table 2.9 and shown in Figure 2.6. The point estimates for the dynamic (heterogeneous) treatment effects are smaller than both the static (homogeneous) treatment effects and the dynamic (heterogeneous) treatment effects, but as are the standard errors. The systematic negative difference in the point estimates can be attributed to either selection bias in the regression models which is better controlled for by covariates or heterogeneous effects.

versus 2019, scaled by 2019Q4 assets, using a model with 10 years of feature history and 1% tolerance for missing observations. Details on its architecture are reported in Table 2.12 in the Appendix. Table 2.21 reports results across all model specifications, showing that null-to-negative effects are estimated in every instance. Table 2.8 compares the different treatment effects estimated by each model, showing that incorporating high-dimensional controls and heterogeneity actually increases point estimates for the dynamic effects. Figure 2.23 and Table 2.31 show the treatment effect dynamics when proxying investment by the annual change in gross property, plant, and equipment. For this proxy, null effects are estimated for every specification.

The dynamic (heterogeneous) treatment effects estimated in this section suggest that eligible firms increased cash holdings to a lesser extent than ineligible firms and also took on less leverage, as well. These are consistent with both the static (homogeneous) treatment effects estimated by the DiD panel regression in Section 2.4 and the dynamic (ho-

Table 2.8: Investment Treatment Effect Comparison

Treatment Effect Estimates				
CAPEX and R&D (% 2019Q4 Assets)				
Year	Static (Homogeneous)	Dynamic (Heterogeneous) (1)	Dynamic (Homogeneous) (2)	Difference (1)-(2)
2020		0.12 (0.14)	-0.49 (0.58)	0.62
2021		-0.27 (0.23)	-1.88 (0.80)	1.61
2022		-0.49 (0.18)	-0.99 (0.41)	0.50
2023		-0.33 (0.23)	-0.62 (0.29)	0.29
Eligible × Post 2020	-0.90 (0.66)			

Standard-errors in parentheses

The table reports the treatment effect estimates for investment, as a percent of 2019Q4, across the three models examined in this paper. The static (homogeneous) treatment effect comes from the DiD regressions reported in Table 2.4, while the dynamic (homogeneous) treatment effects correspond to the event study regressions with two-way fixed effects, reported in Table 2.9 and shown in Figure 2.7. The point estimates for the dynamic (heterogeneous) treatment effects are larger than the dynamic (homogeneous) treatment effects. The systematic positive difference in the point estimates can be attributed to either selection bias in the regression models which is better controlled for by covariates or heterogeneous effects.

mogeneous) treatment effects estimated by the event study regressions with two-way fixed effects in Section 2.5. A comparison of the dynamic treatment effects across the two designs reveals relatively similar point estimates with no uniform direction in the difference (positive or negative).

In contrast, the dynamic (heterogeneous) treatment effects estimated in this section are generally smaller than those estimated in Section 2.5, with the exception of investment. This could be due to the effects of either selection bias, which is accounted for by high-dimensional controls, or the effects of heterogeneity. For payouts, the lower point estimates are also accompanied by smaller standard errors and reinforce the result that eligible firms had relatively higher levels of payouts. Even though the dynamic (heterogeneous) treatment effects for investment are larger, these are still null or negative, similar to the dynamic (homogeneous) treatment effect found in 2020 in Section 2.5. An alternative proxy for investment reinforces this conclusion.

Discussion on Selection Bias for Investment

Selection bias for investment may be positive or negative. Given that the treatment was assigned on the basis of IG status, positive selection bias may arise if IG rated firms have more investment opportunities, while negative selection bias may arise if managers of IG firms are more cautious/disciplined about investment, as examples. The lack of pre-trends in the event study regressions in Section 2.5 suggests that there is no systematic difference in relative investment in the pre-treatment period. The causal ML estimator with a high-dimensional control structure presented in this section should provide additional safeguards against this by spanning any potential omitted variable. To the extent that the effect of such omitted variables are not controlled, then a positive selection bias due to investment opportunities would suggest that the estimated treatment effect is biased upwards. Given that negative or null effects are found for both investment proxies, this should strengthen the argument that the Fed CCFs did not meet its objectives of improving real outcomes.

However, if negative selection bias is present, then the results shown here underestimate the true effect and do not necessarily provide evidence that Fed CCF eligibility failed to spur investment. This would require that differencing out the trend in the outcome variable for ineligible firms as well as controlling for a high dimensional set of variables fails to properly address (negative) selection effects. More precise identification strategies exploiting plausibly exogenous variation may better assuage fears around selection bias but would come at the cost of external validity. Uniquely, the causal ML approach presented here allows for the estimation of heterogeneous effects and permits counterfactual analysis.

2.7 Counterfactual Treatment Effects and Targeting

This section explores the impact of extending direct cash bond support to ineligible firms. The counterfactual treatment effect is given by the group average treatment effect (GATE)

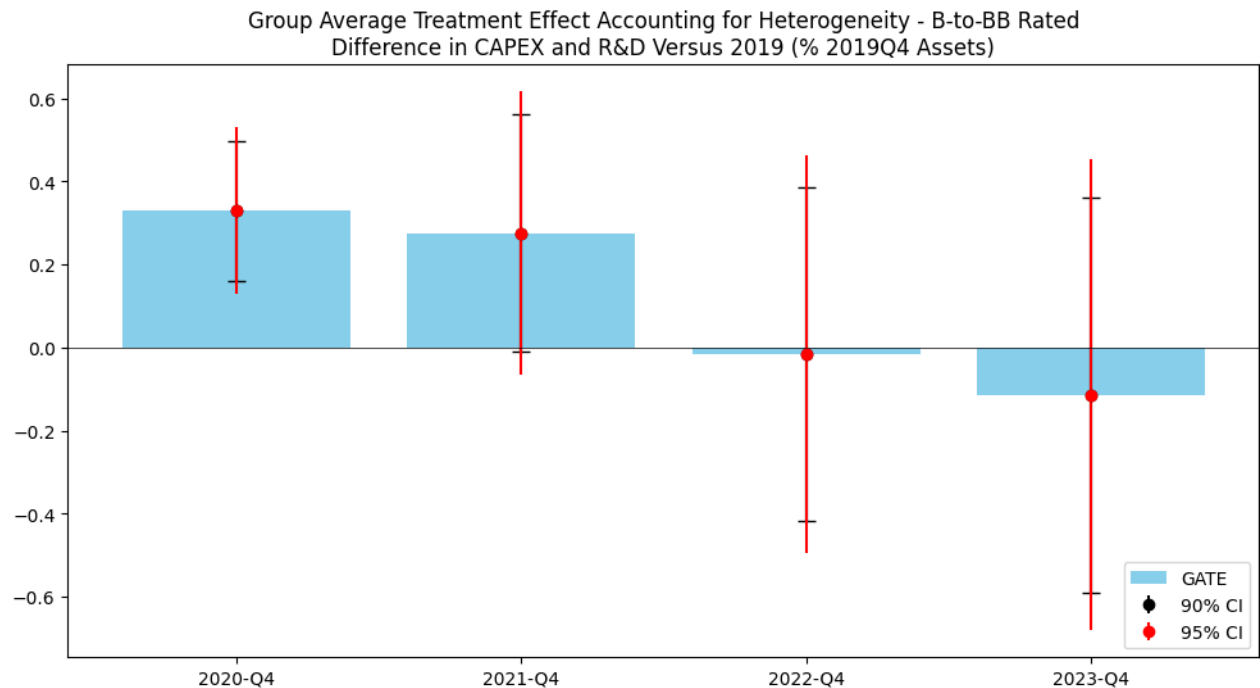
for ineligible firms: $\mathbb{E}[g\beta(x)]$, where g is a vector of indicator variables denoting if a firm is rated B or BB. Hence, set $H(x, \theta(x)) = g\beta(x)$ in Equation 2.5, and the derivation of the estimator proceeds similarly to Appendix 2.9.4. The assumption of unconfoundedness is needed here to have a causal interpretation. If this fails to hold, the estimator is still valid but instead identifies a predictive effect, which would still be useful for policy analysis.

A simple framework, such as in Brunnermeier and Krishnamurthy [2020], would suggest that targeting lower-rated firms should result in a stronger decrease in borrowing costs, and so, should stimulate more real activity. This argument is further strengthened by the CFO survey evidence of Campello, Graham, and Harvey [2010] and Barry et al. [2022] which suggests that financial constraints hamper investment during crisis periods. Momin and Li [2025] apply the counterfactual treatment effect estimator presented in this section to ineligible issuers' bond spreads and find that extending direct cash bond support to ineligible issuers would have resulted in around 500 bps of spread tightening.

Figure 2.18 plots the counterfactual treatment effect for ineligible firms' annual investment versus 2019, as a percent of 2019Q4 assets, for the model using 10 years of feature history and 1% tolerance for missing observations. A statistically significant positive effect is estimated for 2020 while null effects are estimated for subsequent years. This suggests that had ineligible firms' received direct cash bond support from the CCFs, their investment in 2020 would have been higher. However, this estimate is not robust to using an alternative proxy for investment based on the annual change in gross property, plant, and equipment, as shown in Figure 2.24.

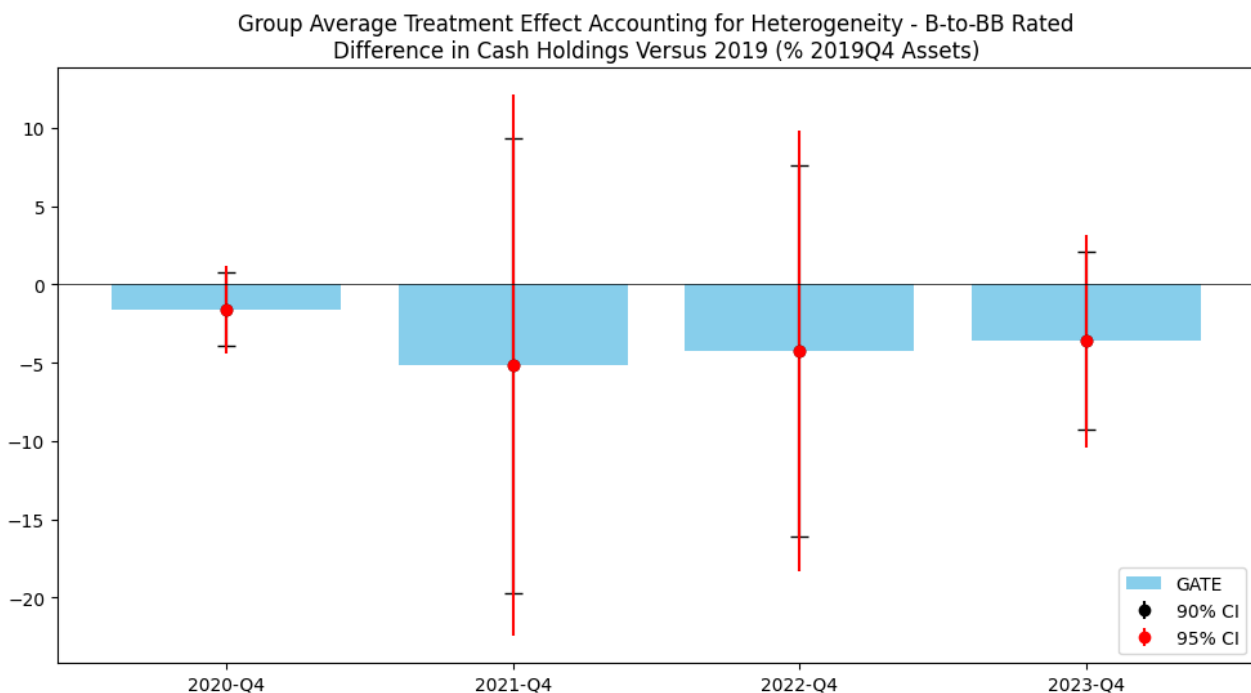
While the counterfactual treatment effect estimates provide inconclusive evidence on the investment effects from extending direct cash bond support from the CCFs to ineligible firms, the estimates for debt, Figure 2.20, and payouts, Figure 2.21, suggest that ineligible firms would have increased leverage in 2020 and distributed larger payouts in 2020 and 2022. In contrast, the estimate of the effect of the counterfactual treatment on cash is null

Figure 2.18: Positive Counterfactual Treatment Effect for Investment Not Robust to Alternative Proxy



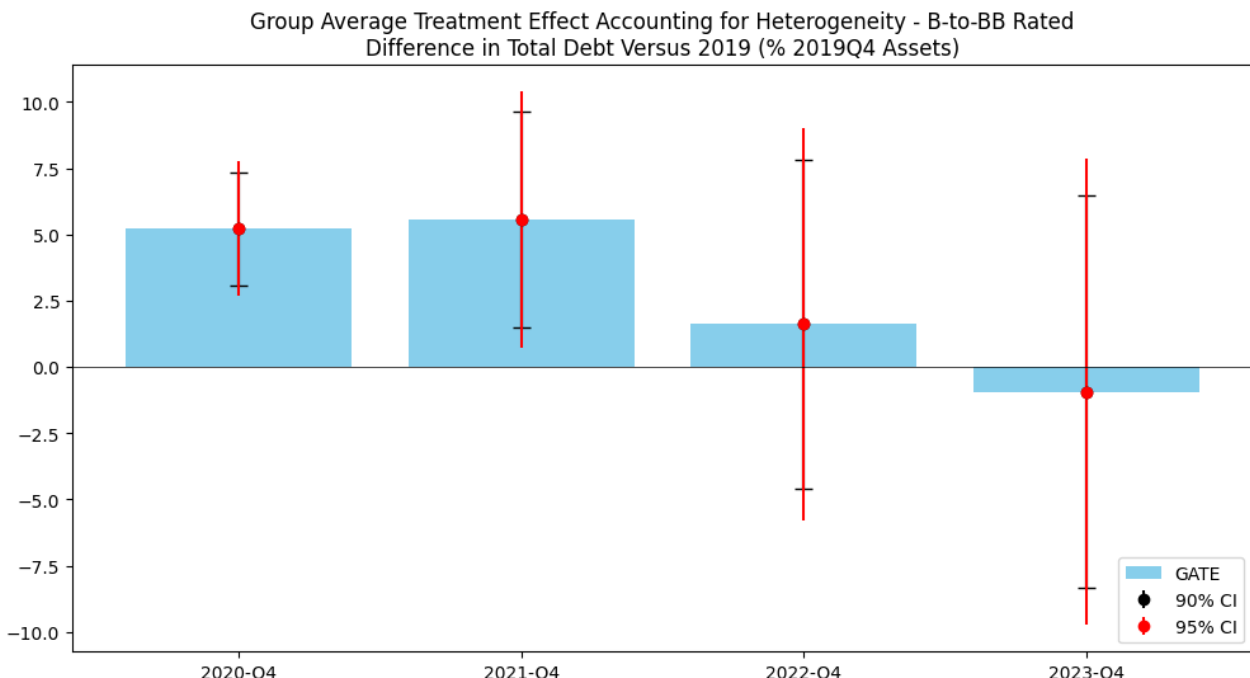
The figure plots the counterfactual treatment effect for ineligible firms' annual investment versus 2019, as a percent of 2019Q4 assets, for the model using 10 years of feature history and 1% tolerance for missing observations. Details on its architecture are reported in Table 2.12 in the Appendix. The positive estimate for 2020 suggests that ineligible firms' investment may have received a boost in case of direct cash bond support from the CCFs. This estimate is generally robust across specifications, as shown in Table 2.29. However, the result is not robust to using an alternative proxy for investment, computed as the annual change in gross property, plant, and equipment, as shown in Figure 2.24. Both proxies suggest a lack of statistically significant positive effects for 2021 onward.

Figure 2.19: Null Counterfactual Treatment Effects for Cash



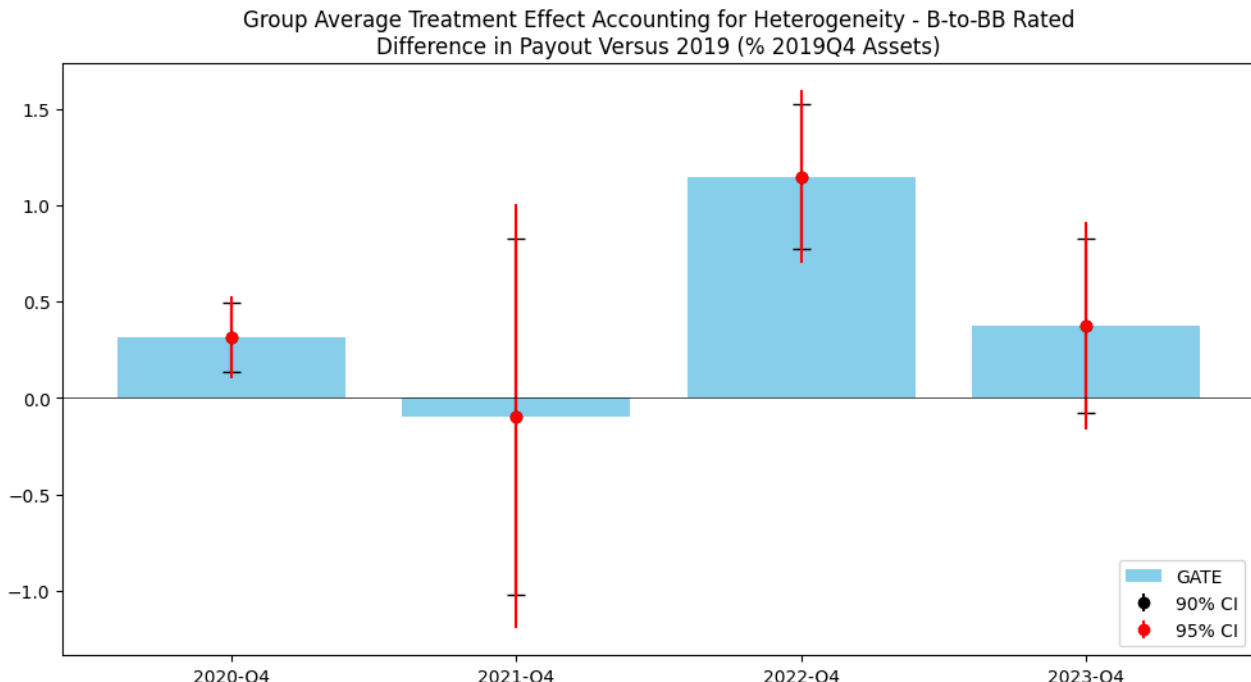
The figure plots the counterfactual treatment effect for ineligible firms' change in cash holdings, as a percent of 2019Q4 assets, for the model using 10 years of feature history and 1% tolerance for missing observations. Details on its architecture are reported in Table 2.12 in the Appendix. Null results are estimated across different model specifications and horizons, as reported in Table 2.26.

Figure 2.20: Positive Counterfactual Treatment Effect for Debt



The figure plots the counterfactual treatment effect for ineligible firms' change in total debt, as a percent of 2019Q4 assets, for the model using 10 years of feature history and 1% tolerance for missing observations. Details on its architecture are reported in Table 2.12 in the Appendix. positive and statistically significant effects are generally estimated for 2020 for model specifications with at least 5 years of feature history, as shown in Table 2.27. However, the estimate for 2021 is not robust to different model specifications. Together with the counterfactual treatment effect estimate for payouts, reported in Figure 2.21, the results suggest that had direct cash bond support from the CCFs been extended to ineligible firms, their leverage and payouts would have increased in 2020.

Figure 2.21: Positive Counterfactual Treatment Effect for Payouts



The figure plots the counterfactual treatment effect for ineligible firms' annual payouts versus 2019, as a percent of 2019Q4 assets, for the model using 10 years of feature history and 1% tolerance for missing observations. Details on its architecture are reported in Table 2.12 in the Appendix. Positive and statistically significant effects are generally estimated for 2020 and 2022 for model specifications with at least 5 years of feature history, as shown in Table 2.28. Together with the counterfactual treatment effect estimate for debt, reported in Figure 2.21, the results suggest that had direct cash bond support from the CCFs been extended to ineligible firms, their leverage and payouts would have increased in 2020, while payouts would have increased in 2022.

across horizons, as seen in Figure 2.19. This broad, stylized pattern (a possible lack of investment response, higher leverage, and higher payouts) is rationalized by Momin [2025a] in a dynamic capital structure model with investment where firms lack the ability to commit to a debt issuance policy and where the public sector intervenes in the unsecured debt of financially unconstrained firms.

2.8 Conclusion

I present a novel two-step semi-parametric difference-in-differences estimator for computing dynamic (heterogeneous) treatment effects that is comparable to an event study design with two-way fixed effects. The structural equation for potential outcomes is the linear combination of a non-parametric intercept term and the interaction of a treatment indicator and a non-parametric slope term. The slope term captures individual level heterogeneity, that is, conditional average treatment effects. Another ingredient for the estimator is an estimation of propensity scores, the probability of a firm being classified as eligible for the CCFs, which is also modeled as a non-parametric function of a high-dimensional set of characteristics. The non-parametric terms are estimated using deep neural networks. Given that the assumptions of unconfoundedness and the overlap condition are satisfied, this allows for the identification of average treatment effects that account for heterogeneity and counterfactual treatment effects from alternative policy targeting. Given the difference-in-differences setup, the assumption of unconfoundedness can be relaxed to weaker assumptions of (conditional) no anticipation and parallel trends, thus identifying the average treatment effect on the treated, instead. Given a general lack of pre-trends in the event study regressions, conditional parallel trends is a justifiable assumption, and estimates of the ATE and ATET from the two-step estimator are not statistically different from zero.

The estimator is applied to study the financial and real effects of the Federal Reserve's

Corporate Credit Facilities launched in 2020 amid the COVID-19 pandemic, as well as the effects of counterfactual eligibility criteria. Dynamic (heterogeneous) treatment effects from the novel estimator are comparable to static (homogeneous) treatment effects from a difference-in-differences panel regression and dynamic (homogeneous) treatment effects from an event study design with two-way fixed effects. The results show that while all firms increased leverage and cash holdings as a proportion of 2019 year-end assets, firms eligible for the CCFs increased leverage and cash to a relatively lower extent than ineligible firms. Moreover, eligible firms do not show an increased investment response, which suggests that the CCFs may not have met its objective for producing real effects. This is robust to alternative proxies for investment. In contrast, eligible firms did increase payouts to shareholders. Counterfactual policy targeting loosening the CCFs eligibility criteria to target weaker credits with possibly more binding financially constraints produces weak to inconclusive evidence of improved investment outcomes in 2020, while there is no evidence of improved outcomes found for later periods. However, counterfactual treatment effect estimates suggest that ineligible firms, had they received direct cash bond support from the CCFs, would have increased leverage in 2020 and payouts in 2020 and 2022.

Noting that both in the United States, as well as in Europe, CCFs failed to stimulate investment [De Santis and Zaghini, 2021, Grosse-Rueschkamp, Steffen, and Streitz, 2019, Todorov, 2020], Momin [2025a] rationalizes these stylized empirical facts and explores changes to the design of the CCFs to encourage firm investment.

2.9 Appendix

2.9.1 Event Study Regressions with Two-Way Fixed Effects

Table 2.9: Dynamic (Homogeneous) Treatment Effects

Dependent Variables:	Cash (% 2019Q4 Assets)	Total Debt (% 2019Q4 Assets)	Dividends and Buybacks (% 2019Q4 Assets)	Capital Expenditures and R&D (% 2019Q4 Assets)
Model:	(1)	(2)	(3)	(4)
<i>Variables</i>				
2011	1.605** (0.6316)	5.950** (2.460)	-0.8059*** (0.2578)	-0.2164 (0.2804)
2012	2.202*** (0.5401)	4.198 (2.385)	-0.3333 (0.3084)	-0.5236 (0.4549)
2013	1.577** (0.6211)	5.409** (2.446)	-0.5584 (0.3708)	-0.3305 (0.3674)
2014	2.043*** (0.3430)	3.310 (2.249)	-0.3442 (0.3585)	-0.5331 (0.3729)
2015	-0.8817 (1.330)	2.094 (2.297)	-0.4685 (0.3482)	-0.5136 (0.4647)
2016	2.130*** (0.0944)	2.960* (1.514)	-0.0752 (0.3333)	-0.3801 (0.2178)
2017	0.4773 (0.7562)	4.476*** (0.9942)	-1.408* (0.7130)	-0.1844** (0.0817)
2018	-0.1416 (0.1550)	2.766** (1.145)	0.1208 (0.3248)	-0.1778* (0.0927)
2020	-3.829*** (0.7861)	-1.662** (0.6474)	0.5398 (0.3370)	-0.4923 (0.5767)
2021	-9.520*** (2.418)	-5.954** (2.304)	0.6531* (0.3596)	-1.877** (0.8043)
2022	-6.923*** (2.265)	-9.084*** (2.591)	0.9944** (0.3708)	-0.9863** (0.4143)
2023	-4.005*** (1.091)	-8.471*** (1.954)	0.8602** (0.3895)	-0.6217* (0.2904)
<i>Fixed-effects</i>				
Issuer	Yes	Yes	Yes	Yes
year	Yes	Yes	Yes	Yes
<i>Fit statistics</i>				
Observations	9,912	9,502	9,641	9,798
R ²	0.44205	0.56682	0.17201	0.39251
Within R ²	0.00827	0.00736	0.00212	0.00116

Clustered (Issuer & Date) standard-errors in parentheses

Signif. Codes: ***: 0.01, **: 0.05, *: 0.1

The table reports the coefficients related to the event study regressions presented in Section 2.5 corresponding to Figures 2.4, 2.5, 2.6, and 2.7. Negative, sizeable effects are found for cash and total debt over the treatment period. Positive effects are found for payouts, which are statistically significant for 2021, 2022, and 2023. Similarly, negative effects are found for investment, which are statistically significant for 2021, 2022, and 2023.

2.9.2 Features

Variable	Description
accrual	Accruals/Average Assets
adv_sale	Advertising Expenses/Sales
aftret_eq	After-tax Return on Average Common Equity
aftret_equity	After-tax Return on Total Stockholders Equity
aftret_invcapx	After-tax Return on Invested Capital
at_turn	Asset Turnover
capital_ratio	Capitalization Ratio
cash_debt	Cash Flow/Total Debt
cash_lt	Cash Balance/Total Liabilities
cfm	Cash Flow Margin
de_ratio	Total Debt/Equity
debt_assets	Total Debt (ltq)/Total Assets
debt_at	Total Debt (dlcq+dlttq)/Total Assets
debt_capital	Total Debt/Capital
debt_ebitda	Total Debt/EBITDA
debt_invcap	Long-term Debt/Invested Capital
equity_invcap	Common Equity/Invested Capital
evm	Enterprise Value Multiple
gpm	Gross Profit Margin
gprof	Gross Profit/Total Assets
lt_debt	Long-term Debt/Total Liabilities
lt_ppent	Total Liabilities/Total Tangible Assets
npm	Net Profit Margin
opmad	Operating Profit Margin After Depreciation
opmbd	Operating Profit Margin Before Depreciation
pcf	Price/Cash flow
pe_exi	P/E (Diluted, Excl. EI)
pe_inc	P/E (Diluted, Incl. EI)
pe_op_basic	Price/Operating Earnings (Basic, Excl. EI)
pe_op_dil	Price/Operating Earnings (Diluted, Excl. EI)
ps	Price/Sales
ptpm	Pre-tax Profit Margin
rd_sale	Research and Development/Sales
roa	Return on Assets
roce	Return on Capital Employed
staff_sale	Labor Expenses/Sales
totdebt_invcap	Total Debt/Invested Capital

Table 2.10: Features with Less than One Percent Missing Observations

Variable	Description
bm	Book/Market
capei	Shillers Cyclically Adjusted P/E Ratio
cash_ratio	Cash Ratio
curr_debt	Current Liabilities/Total Liabilities
curr_ratio	Current Ratio
dltt_be	Long-term Debt/Book Equity
int_debt	Interest/Average Long-term Debt
intcov	After-tax Interest Coverage
intcov_ratio	Interest Coverage Ratio
ocf_lct	Operating CF/Current Liabilities
pay_turn	Payables Turnover
peg_1yrforward	Forward P/E to 1-year Growth (PEG) ratio
pretret_earnat	Pre-tax Return on Total Earning Assets
pretret_noa	Pre-tax return on Net Operating Assets
profit_lct	Profit Before Depreciation/Current Liabilities
ptb	Price/Book
quick_ratio	Quick Ratio (Acid Test)
rect_act	Receivables/Current Assets
rect_turn	Receivables Turnover
roe	Return on Equity
sale_equity	Sales/Stockholders Equity
sale_invcap	Sales/Invested Capital
short_debt	Short-Term Debt/Total Debt

Table 2.11: Additional Features with Less than Ten Percent Missing Observations

2.9.3 Base Effect Estimator Derivation

Set $H(x, \theta(x)) = \alpha(x)$. Then, $\nabla_{\theta} H = \begin{bmatrix} 1 & 0 \end{bmatrix}$.

Compute the inverse of Equation 2.6:

$$\begin{aligned} \Lambda(x)^{-1} &= \frac{1}{p(x)(1-p(x))} \begin{bmatrix} p(x) & -p(x) \\ -p(x) & 1 \end{bmatrix} \\ &= \begin{bmatrix} \frac{1}{1-p(x)} & -\frac{1}{1-p(x)} \\ -\frac{1}{1-p(x)} & \frac{1}{p(x)(1-p(x))} \end{bmatrix} \end{aligned}$$

This gives:

$$\begin{aligned} (\nabla_{\theta} H) \Lambda(x)^{-1} &= \begin{bmatrix} 1 & 0 \end{bmatrix} \begin{bmatrix} \frac{1}{1-p(x)} & -\frac{1}{1-p(x)} \\ -\frac{1}{1-p(x)} & \frac{1}{p(x)(1-p(x))} \end{bmatrix} \\ &= \begin{bmatrix} \frac{1}{1-p(x)} & -\frac{1}{1-p(x)} \end{bmatrix} \end{aligned}$$

Plug these in.

$$\begin{aligned} \psi(\Delta y_i^h, z_i, x_i, \theta(x_i)) &= \alpha(x) - (\nabla_{\theta} H) \Lambda(x)^{-1} l_{\theta} \\ &= \alpha(x) - (\nabla_{\theta} H) \Lambda(x)^{-1} \left(- \begin{bmatrix} 1 \\ z \end{bmatrix} (\Delta y^h - \alpha(x) - \beta(x)z) \right) \\ &= \alpha(x) + \begin{bmatrix} \frac{1}{1-p(x)} & -\frac{1}{1-p(x)} \end{bmatrix} \begin{bmatrix} 1 \\ z \end{bmatrix} (\Delta y^h - \alpha(x) - \beta(x)z) \\ &= \alpha(x) + \left(\frac{1}{1-p(x)} - \frac{z}{1-p(x)} \right) (\Delta y^h - \alpha(x) - \beta(x)z) \\ &= \alpha(x) + \frac{(1-z)(\Delta y^h - \alpha(x) - \beta(x)z)}{1-p(x)} \\ &= \alpha(x) + \frac{(1-z)(\Delta y^h - \alpha(x))}{1-p(x)} \end{aligned}$$

where the last line uses the fact that $(1 - z)z = 0$.

2.9.4 ATE Estimator Derivation

Set $H(x, \theta(x)) = \beta(x)$. Then, $\nabla_{\theta}H = \begin{bmatrix} 0 & 1 \end{bmatrix}$. The inverse of Equation 2.6 is the same as in Appendix 2.9.3.

This gives:

$$\begin{aligned} (\nabla_{\theta}H)\Lambda(x)^{-1} &= \begin{bmatrix} 0 & 1 \end{bmatrix} \begin{bmatrix} \frac{1}{1-p(x)} & -\frac{1}{1-p(x)} \\ -\frac{1}{1-p(x)} & \frac{1}{p(x)(1-p(x))} \end{bmatrix} \\ &= \begin{bmatrix} -\frac{1}{1-p(x)} & \frac{1}{p(x)(1-p(x))} \end{bmatrix} \end{aligned}$$

Plug these into Equation 2.5.

$$\begin{aligned} \psi(\Delta y_i^h, z_i, x_i, \theta(x_i)) &= \beta(x) - (\nabla_{\theta}H)\Lambda(x)^{-1}l_{\theta} \\ &= \beta(x) - (\nabla_{\theta}H)\Lambda(x)^{-1} \left(- \begin{bmatrix} 1 \\ z \end{bmatrix} (\Delta y^h - \alpha(x) - \beta(x)z) \right) \\ &= \beta(x) + \begin{bmatrix} -\frac{1}{1-p(x)} & \frac{1}{p(x)(1-p(x))} \end{bmatrix} \begin{bmatrix} 1 \\ z \end{bmatrix} (\Delta y^h - \alpha(x) - \beta(x)z) \\ &= \beta(x) + \left(-\frac{1}{1-p(x)} + \frac{z}{p(x)(1-p(x))} \right) (\Delta y^h - \alpha(x) - \beta(x)z) \\ &= \beta(x) + \frac{(z - p(x))(\Delta y^h - \alpha(x) - \beta(x)z)}{p(x)(1-p(x))} \end{aligned}$$

Add and subtract $p(x)z$ to the numerator of the second term.

$$\begin{aligned}
\psi(\Delta y_i^h, z_i, x_i, \theta(x_i)) &= \beta(x) + \frac{(z - p(x) + p(x)z - p(x)z)(\Delta y^h - \alpha(x) - \beta(x)z)}{p(x)(1 - p(x))} \\
&= \beta(x) + \frac{[(1 - p(x))z - p(x)(1 - z)]\Delta y^h - \alpha(x) - \beta(x)z}{p(x)(1 - p(x))} \\
&= \beta(x) + \frac{(1 - p(x))z(\Delta y^h - \alpha(x) - \beta(x)z)}{p(x)(1 - p(x))} \\
&\quad - \frac{p(x)(1 - z)(\Delta y^h - \alpha(x) - \beta(x)z)}{p(x)(1 - p(x))} \\
&= \beta(x) + \frac{z(\Delta y^h - \alpha(x) - \beta(x)z)}{p(x)} - \frac{(1 - z)(\Delta y^h - \alpha(x) - \beta(x)z)}{1 - p(x)} \\
&= \beta(x) + \frac{z(\Delta y^h - \alpha(x) - \beta(x)z)}{p(x)} - \frac{(1 - z)(\Delta y^h - \alpha(x))}{1 - p(x)}
\end{aligned}$$

where the last line uses the fact that $(1 - z)z = 0$.

2.9.5 ATET Estimator Derivation

Let $c = 1 - z$. Set $H(x, \theta(x)) = (\alpha(x) + \beta(x))z - \alpha(x)c$. Then, $\nabla_{\theta}H = \begin{bmatrix} z - c & z \end{bmatrix}$. The inverse of Equation 2.6 is the same as in Appendix 2.9.3.

This gives:

$$\begin{aligned}
(\nabla_{\theta}H)\Lambda(x)^{-1} &= \begin{bmatrix} z - c & z \end{bmatrix} \begin{bmatrix} \frac{1}{1-p(x)} & -\frac{1}{1-p(x)} \\ -\frac{1}{1-p(x)} & \frac{1}{p(x)(1-p(x))} \end{bmatrix} \\
&= \begin{bmatrix} \frac{z-c}{1-p(x)} - \frac{z}{1-p(x)} & -\frac{z-c}{1-p(x)} + \frac{z}{p(x)(1-p(x))} \end{bmatrix} \\
&= \begin{bmatrix} -\frac{c}{1-p(x)} & -\frac{(z-c)p(x)}{p(x)(1-p(x))} + \frac{z}{p(x)(1-p(x))} \end{bmatrix} \\
&= \begin{bmatrix} -\frac{c}{1-p(x)} & \frac{cp(x)+(1-p(x))z}{p(x)(1-p(x))} \end{bmatrix}
\end{aligned}$$

Plug these into Equation 2.5.

$$\begin{aligned}
\psi(\Delta y_i^h, z_i, x_i, \theta(x_i)) &= (\alpha(x) + \beta(x))z - \alpha(x)c - (\nabla_\theta H)\Lambda(x)^{-1}l_\theta \\
&= (\alpha(x) + \beta(x))z - \alpha(x)c - (\nabla_\theta H)\Lambda(x)^{-1} \times \\
&\quad \left(- \begin{bmatrix} 1 \\ z \end{bmatrix} (\Delta y^h - \alpha(x) - \beta(x)z) \right) \\
&= (\alpha(x) + \beta(x))z - \alpha(x)c \\
&\quad + \begin{bmatrix} 1 \\ z \end{bmatrix} \left[\begin{bmatrix} cp(x) + (1-p(x))z \\ p(x)(1-p(x)) \end{bmatrix} \right] (\Delta y^h - \alpha(x) - \beta(x)z) \\
&= (\alpha(x) + \beta(x))z - \alpha(x)c + \left(-\frac{p(x)}{p(x)(1-p(x))} + \frac{z}{p(x)(1-p(x))} \right) \times \\
&\quad (\Delta y^h - \alpha(x) - \beta(x)z) \\
&= (\alpha(x) + \beta(x))z - \alpha(x)c + \frac{(z - p(x))(\Delta y^h - \alpha(x) - \beta(x)z)}{p(x)(1-p(x))}
\end{aligned}$$

Add and subtract $p(x)z$ to the numerator of the second term, as in Section 2.9.4.

$$\begin{aligned}
\psi(\Delta y_i^h, z_i, x_i, \theta(x_i)) &= (\alpha(x) + \beta(x))z - \alpha(x)c + \frac{z(\Delta y^h - \alpha(x) - \beta(x)z)}{p(x)} \\
&\quad - \frac{(1-z)(\Delta y^h - \alpha(x))}{1-p(x)}
\end{aligned}$$

2.9.6 Deep Net Architectures

Feature History (Years)			
	1	5	10
Number of Features	333	1342	3204
Hidden Layer Architecture	[300, 150, 75, 35, 15]	[1500, 750, 375, 150, 75, 35, 15]	[2700, 1350, 675, 300, 150, 75, 35, 15]
Dropout Rate	20%		

Table 2.12: Architecture for Deep Nets with 1% Tolerance for Missing Observations

Feature History (Years)			
	1	5	10
Number of Features	517	2502	5314
Hidden Layer Architecture	[500, 300, 150, 75, 35, 15]	[3000, 1500, 750, 375, 150, 75, 35, 15]	[5000, 2700, 1350, 675, 300, 150, 75, 35, 15]
Dropout Rate	20%		

Table 2.13: Architecture for Deep Nets with 10% Tolerance for Missing Observations

2.9.7 Base Effects

Table 2.14: Cash Base Effect

Difference in Cash Holdings Versus 2019 (% 2019Q4 Assets)						
	Base Effect Accounting for Heterogeneity					
Year	Model					
	(Feature History, Missingness Tolerance)					
2020	(1,1)	(1,10)	(5,1)	(5,10)	(10,1)	(10,10)
2020	5.36 (6.75)	5.93*** (1.59)	6.17*** (0.87)	6.79*** (0.99)	6.61*** (0.92)	6.69*** (0.94)
2021	8.76 (6.35)	8.16*** (3.11)	11.70*** (3.85)	12.42*** (4.16)	12.65*** (3.92)	13.30*** (4.36)
2022	7.17 (5.53)	7.13*** (2.52)	7.84*** (2.81)	8.57*** (3.06)	8.53*** (2.93)	8.80*** (3.13)
2023	6.30* (3.53)	4.87*** (1.73)	4.88*** (1.43)	5.01*** (1.43)	5.00*** (1.47)	5.05*** (1.37)

Standard-errors in parentheses

Signif. Codes: ***: 0.01, **: 0.05, *: 0.1

The table reports the base effects for the change in cash holdings, as a percent of 2019Q4 assets. Results for all model specifications are reported here; the corresponding architectures are reported in Tables 2.12 and 2.13 in the Appendix. The finding of large, positive base effects are largely consistent across different model specifications, as well as the DiD regressions reported in Table 2.3.

Table 2.15: Debt Base Effect

Difference in Total Debt Versus 2019 (% 2019Q4 Assets)						
Base Effect Accounting for Heterogeneity						
Year	Model					
	(Feature History, Missingness Tolerance)					
2020	7.60 (5.20)	5.38*** (1.81)	3.67*** (0.94)	3.78*** (1.00)	3.91*** (1.03)	4.13*** (1.06)
2021	18.21** (8.18)	13.22*** (3.19)	11.30*** (1.98)	11.61*** (2.17)	12.45*** (2.28)	12.26*** (2.28)
2022	26.91 (16.46)	21.19*** (4.40)	15.74*** (2.49)	17.03*** (3.02)	17.08*** (2.93)	16.94*** (3.00)
2023	25.16** (12.64)	19.45*** (4.40)	16.57*** (2.61)	17.89*** (2.81)	17.27*** (2.72)	17.57*** (2.70)

Standard-errors in parentheses

Signif. Codes: ***: 0.01, **: 0.05, *: 0.1

The table reports the base effects for the change in debt, as a percent of 2019Q4 assets. Results for all model specifications are reported here; the corresponding architectures are reported in Tables 2.12 and 2.13 in the Appendix. The finding of large, positive base effects are largely consistent across different model specifications, as well as the DiD regressions reported in Table 2.3.

Table 2.16: Payout Base Effect

Difference in Payout Versus 2019 (% 2019Q4 Assets)						
Base Effect Accounting for Heterogeneity						
Year	Model					
	(Feature History, Missingness Tolerance)					
2020	-0.17 (0.20)	-0.23** (0.10)	-0.17*** (0.04)	-0.16*** (0.04)	-0.18*** (0.04)	-0.18*** (0.04)
2021	0.28 (0.70)	0.27 (0.33)	0.18 (0.19)	0.18 (0.17)	0.22 (0.18)	0.16 (0.17)
2022	0.38 (0.44)	0.11 (0.19)	0.23** (0.11)	0.29** (0.13)	0.26* (0.14)	0.25* (0.14)
2023	0.37 (0.28)	0.26* (0.15)	0.27** (0.11)	0.32*** (0.12)	0.30** (0.12)	0.29** (0.11)

Standard-errors in parentheses

Signif. Codes: ***: 0.01, **: 0.05, *: 0.1

The table reports the base effects for the change in payouts with respect to 2019, scaled by 2019Q4 assets. Results for all model specifications are reported here; the corresponding architectures are reported in Tables 2.12 and 2.13 in the Appendix. Generally consistent results are found whereby the base effect is initially negative in 2020, null in 2021, and then positive in 2022 and 2023. This is in contrast to the null results picked up by the DiD regressions reported in Table 2.4.

Table 2.17: Investment Base Effect

Difference in CAPEX and R&D Versus 2019 (% 2019Q4 Assets)						
	Base Effect Accounting for Heterogeneity					
Year	Model					
	(Feature History, Missingness Tolerance)					
2020	(1,1)	(1,10)	(5,1)	(5,10)	(10,1)	(10,10)
	0.17 (0.39)	0.14 (0.16)	-0.04 (0.07)	-0.02 (0.07)	-0.02 (0.07)	-0.02 (0.07)
2021	0.95 (0.75)	0.98*** (0.29)	0.66*** (0.11)	0.71*** (0.12)	0.73*** (0.12)	0.71*** (0.12)
2022	0.90 (0.88)	1.13*** (0.36)	0.97*** (0.15)	0.94*** (0.15)	1.01*** (0.14)	1.04*** (0.14)
2023	1.65** (0.81)	1.19*** (0.32)	1.00*** (0.16)	1.04*** (0.17)	1.05*** (0.16)	1.05*** (0.16)

Standard-errors in parentheses

Signif. Codes: ***: 0.01, **: 0.05, *: 0.1

The table reports the base effects for the difference in annual investment versus 2019, scaled by 2019Q4 assets. Results for all model specifications are reported here; the corresponding architectures are reported in Tables 2.12 and 2.13 in the Appendix. Consistent with the positive coefficient found for the post period in Table 2.4 for the DiD regressions, positive base effects are generally found. However, this is not robust to an alternative proxy for investment. As seen in Table 2.30, proxying investment by the annual change in gross property, plant, and equipment suggests a negative effect which reverts to null.

2.9.8 Average Treatment Effects

Table 2.18: Cash ATE

Difference in Cash Holdings Versus 2019 (% 2019Q4 Assets)						
Average Treatment Effect Accounting for Heterogeneity						
Year	Model (Feature History, Missingness Tolerance)					
	(1,1)	(1,10)	(5,1)	(5,10)	(10,1)	(10,10)
2020	-10.77 (16.50)	-4.98 (4.64)	-3.55*** (1.06)	-3.38*** (1.06)	-2.98*** (1.00)	-3.19*** (1.07)
2021	-1.97 (19.83)	-10.45** (4.62)	-10.11** (4.13)	-10.71** (4.24)	-10.50*** (4.06)	-11.03** (4.36)
2022	-14.65 (10.95)	-8.70** (3.51)	-6.57** (2.90)	-7.21** (2.86)	-7.61** (3.00)	-7.48** (3.02)
2023	-9.66 (11.21)	-5.85* (3.08)	-3.57** (1.49)	-3.90*** (1.51)	-3.42** (1.43)	-3.28** (1.36)

Standard-errors in parentheses

Signif. Codes: ***: 0.01, **: 0.05, *: 0.1

The table reports the average treatment effects for the change in cash holdings, as a percent of 2019Q4 assets. This corresponds to the estimator reported in Equation 2.9. Results for all model specifications are reported here; the corresponding architectures are reported in Tables 2.12 and 2.13 in the Appendix. The results are robust across model specifications, showing large, negative treatment effects. These are also consistent with the DiD regressions reported in Table 2.3.

Table 2.19: Debt ATE

Difference in Total Debt Versus 2019 (% 2019Q4 Assets)						
Average Treatment Effect Accounting for Heterogeneity						
Year	Model					
	(Feature History, Missingness Tolerance)					
2020	(1,1)	(1,10)	(5,1)	(5,10)	(10,1)	(10,10)
	-15.73 (15.44)	-3.39 (4.13)	-1.24 (1.35)	-1.06 (1.10)	-0.69 (1.10)	-0.88 (1.14)
2021	-46.26* (26.31)	-15.70** (7.28)	-5.78** (2.25)	-6.52*** (2.23)	-6.75*** (2.41)	-6.73*** (2.35)
2022	-52.73* (27.60)	-21.93*** (7.90)	-9.28*** (2.82)	-9.90*** (3.04)	-9.48*** (3.09)	-9.85*** (3.20)
2023	-40.13* (23.36)	-18.28*** (5.66)	-9.02*** (2.96)	-9.25*** (2.93)	-8.58*** (2.90)	-8.90*** (2.89)

Standard-errors in parentheses

Signif. Codes: ***: 0.01, **: 0.05, *: 0.1

The table reports the average treatment effects for change in total debt, as a percent of 2019Q4 assets. This corresponds to the estimator reported in Equation 2.9. Results for all model specifications are reported here; the corresponding architectures are reported in Tables 2.12 and 2.13 in the Appendix. The finding of an initial null effect and subsequent large, negative effects are generally consistent across specifications. Table 2.6 compares the treatment effect estimates across different models and suggests that the results are broadly in line.

Table 2.20: Payout ATE

Difference in Payout Versus 2019 (% 2019Q4 Assets)						
Average Treatment Effect Accounting for Heterogeneity						
Year	Model					
	(Feature History, Missingness Tolerance)					
Year	(1,1)	(1,10)	(5,1)	(5,10)	(10,1)	(10,10)
2020	-1.02 (0.89)	-0.27 (0.29)	0.15** (0.06)	0.15*** (0.05)	0.13** (0.06)	0.14*** (0.06)
2021	-0.83 (2.19)	-0.16 (0.97)	0.23 (0.25)	0.25 (0.25)	0.23 (0.25)	0.31 (0.23)
2022	-0.69 (3.99)	0.75 (1.48)	1.07*** (0.36)	0.75*** (0.27)	0.83*** (0.26)	0.83*** (0.28)
2023	-0.62 (2.34)	0.24 (0.87)	0.63*** (0.22)	0.56*** (0.22)	0.48*** (0.17)	0.55*** (0.16)

Standard-errors in parentheses

Signif. Codes: ***: 0.01, **: 0.05, *: 0.1

The table reports the average treatment effects for the different in annual payouts versus 2019, as a percent of 2019Q4 assets. This corresponds to the estimator reported in Equation 2.9. Results for all model specifications are reported here; the corresponding architectures are reported in Tables 2.12 and 2.13 in the Appendix. The model results are consistent across models using 5 and 10 years of feature history, showing an initial positive effect in 2020 followed by a null effect in 2021 before returning to positive effects for 2022 and 2023. Table 2.7 compares the treatment effect estimates across different models. While the treatment effects are comparable, the standard errors for the dynamic (heterogeneous) treatment effects are smaller.

Table 2.21: Investment ATE

Difference in CAPEX and R&D Versus 2019 (% 2019Q4 Assets)						
Average Treatment Effect Accounting for Heterogeneity						
Year	Model					
	(Feature History, Missingness Tolerance)					
2020	(1,1)	(1,10)	(5,1)	(5,10)	(10,1)	(10,10)
	-0.35 (2.59)	-0.26 (0.57)	-0.05 (0.28)	0.02 (0.20)	0.12 (0.14)	-0.01 (0.11)
2021	-2.20 (2.26)	-0.86 (0.72)	0.05 (0.48)	0.11 (0.44)	-0.27 (0.23)	-0.40*** (0.15)
2022	-4.05 (3.86)	-1.12 (0.89)	-0.43* (0.23)	-0.51** (0.21)	-0.49*** (0.18)	-0.66*** (0.17)
2023	-1.62 (2.00)	-0.63 (0.78)	-0.26 (0.25)	-0.33 (0.21)	-0.33 (0.23)	-0.44** (0.19)

Standard-errors in parentheses

Signif. Codes: ***: 0.01, **: 0.05, *: 0.1

The table reports the average treatment effects for the difference in annual investment versus 2019, scaled by 2019Q4 assets. This corresponds to the estimator reported in Equation 2.9. Results for all model specifications are reported here; the corresponding architectures are reported in Tables 2.12 and 2.13 in the Appendix. Particularly for the models with longer covariate histories, null-to-negative treatment effects are estimated. Table 2.8 compares the different treatment effects, showing that incorporating high-dimensional controls and heterogeneity increases the point estimates for the dynamic effects. Additionally, when proxying investment using the annual change in gross plants, property, and equipment, Table 2.31, null effects are generally estimated across different models and cumulation horizons.

2.9.9 ATE and ATET Comparison

Table 2.22: Cash Treatment Effect Comparison

Dynamic (Heterogeneous) Treatment Effect Comparison			
Cash (% 2019Q4 Assets)			
Year	Average Treatment Effect (1)	ATE on Treated (2)	Difference (1)-(2)
2020	-2.98 (1.00)	-3.96 (1.03)	0.98 (1.44)
	-10.50 (4.06)	-10.00 (4.18)	-0.50 (5.83)
2021	-7.61 (3.00)	-6.63 (3.07)	-0.98 (4.29)
	-3.42 (1.43)	-2.83 (1.47)	-0.59 (2.05)
<i>Standard-errors in parentheses</i>			

The table compares the dynamic (heterogeneous) ATE and ATET estimates for cash, as a percent of 2019Q4, for the model which uses 10 years of feature history and 1% tolerance for missing observations. The architecture for the model is given by Tables 2.12 and 2.13 in the Appendix. Section 2.9.4 and 2.9.9 derives the IF estimator for the ATE and ATET, respectively. The estimates are comparable with the difference not being statistically significant.

Table 2.23: Debt Treatment Effect Comparison

Dynamic (Heterogeneous) Treatment Effect Comparison			
Total Debt (% 2019Q4 Assets)			
Year	Average Treatment Effect (1)	ATE on Treated (2)	Difference (1)-(2)
2020	-0.69 (1.10)	-1.54 (1.12)	0.86 (1.57)
	-6.75 (2.41)	-7.88 (2.42)	1.13 (3.42)
2022	-9.48 (3.09)	-10.47 (3.03)	0.98 (4.33)
	-8.58 (2.90)	-10.57 (2.92)	1.99 (4.11)

Standard-errors in parentheses

The table compares the dynamic (heterogeneous) ATE and ATET estimates for debt, as a percent of 2019Q4, for the model which uses 10 years of feature history and 1% tolerance for missing observations. The architecture for the model is given by Tables 2.12 and 2.13 in the Appendix. Section 2.9.4 and 2.9.9 derives the IF estimator for the ATE and ATET, respectively. The estimates are comparable with the difference not being statistically significant.

Table 2.24: Payout Treatment Effect Comparison

Dynamic (Heterogeneous) Treatment Effect Comparison			
Payout (% 2019Q4 Assets)			
Year	Average Treatment Effect (1)	ATE on Treated (2)	Difference (1)-(2)
2020	0.13 (0.06)	0.10 (0.05)	0.03 (0.08)
	0.23 (0.25)	0.09 (0.24)	0.15 (0.34)
2022	0.83 (0.26)	0.49 (0.27)	0.35 (0.38)
	0.48 (0.17)	0.30 (0.17)	0.18 (0.24)

Standard-errors in parentheses

The table compares the dynamic (heterogeneous) ATE and ATET estimates for payout, as a percent of 2019Q4, for the model which uses 10 years of feature history and 1% tolerance for missing observations. The architecture for the model is given by Tables 2.12 and 2.13 in the Appendix. Section 2.9.4 and 2.9.9 derives the IF estimator for the ATE and ATET, respectively. The estimates are comparable with the difference not being statistically significant.

Table 2.25: Investment Treatment Effect Comparison

Dynamic (Heterogeneous) Treatment Effect Comparison			
CAPEX and R&D (% 2019Q4 Assets)			
Year	Average Treatment Effect (1)	ATE on Treated (2)	Difference (1)-(2)
2020	0.12 (0.14)	0.11 (0.15)	0.02 (0.20)
	-0.27 (0.23)	-0.21 (0.23)	-0.06 (0.33)
2021	-0.49 (0.18)	-0.51 (0.19)	0.02 (0.26)
	-0.33 (0.23)	-0.33 (0.22)	0.01 (0.31)
<i>Standard-errors in parentheses</i>			

The table compares the dynamic (heterogeneous) ATE and ATET estimates for investment, as a percent of 2019Q4, for the model which uses 10 years of feature history and 1% tolerance for missing observations. The architecture for the model is given by Tables 2.12 and 2.13 in the Appendix. Section 2.9.4 and 2.9.9 derives the IF estimator for the ATE and ATET, respectively. The estimates are comparable with the difference not being statistically significant.

2.9.10 Counterfactual Treatment Effects

Table 2.26: Ineligible Firms' Cash Counterfactual Treatment Effect

Difference in Cash Holdings Versus 2019 (% 2019Q4 Assets)						
Counterfactual Group Average Treatment Effect Accounting for Heterogeneity - B-BB Rated						
Year	Model (Feature History, Missingness Tolerance)					
	(1,1)	(1,10)	(5,1)	(5,10)	(10,1)	(10,10)
2020	-0.47 (7.74)	1.90 (3.49)	0.99 (1.62)	-2.95* (1.76)	-1.60 (1.43)	-4.36*** (1.55)
2021	-2.06 (8.23)	2.95 (6.01)	-4.82 (11.07)	-4.30 (9.69)	-5.17 (8.82)	-9.13 (9.74)
2022	2.17 (11.00)	-0.07 (5.28)	-3.69 (8.48)	-5.21 (7.77)	-4.24 (7.19)	-8.17 (7.03)
2023	-3.95 (6.27)	-1.56 (3.38)	-2.71 (3.75)	-4.26 (3.92)	-3.60 (3.46)	-6.79** (3.26)

Standard-errors in parentheses

*Signif. Codes: ***: 0.01, **: 0.05, *: 0.1*

The table reports the counterfactual treatment effect for ineligible firms' change in cash holdings, as a percent of 2019Q4 assets. Results for all model specifications are reported here; the corresponding architectures are reported in Tables 2.12 and 2.13 in the Appendix. Null effects are generally estimated across model specifications and years.

Table 2.27: Ineligible Firms' Debt Counterfactual Treatment Effect

Difference in Total Debt Versus 2019 (% 2019Q4 Assets)						
Counterfactual Group Average Treatment Effect Accounting for Heterogeneity - B-BB Rated						
Year	Model (Feature History, Missingness Tolerance)					
	(1,1)	(1,10)	(5,1)	(5,10)	(10,1)	(10,10)
2020	0.95 (11.04)	0.65 (3.61)	5.68*** (1.52)	4.16*** (1.36)	5.22*** (1.30)	1.58 (1.28)
2021	-2.74 (12.38)	-5.09 (5.55)	4.50 (3.07)	3.34 (2.72)	5.56** (2.47)	-2.41 (2.53)
2022	-33.74 (38.34)	-8.01 (11.28)	-0.07 (4.45)	-2.29 (4.13)	1.62 (3.78)	-9.01** (3.70)
2023	-33.45 (28.67)	-7.59 (11.11)	-2.30 (5.28)	-2.08 (4.92)	-0.94 (4.49)	-11.80*** (4.50)

Standard-errors in parentheses

*Signif. Codes: ***: 0.01, **: 0.05, *: 0.1*

The table reports the counterfactual treatment effect for ineligible firms' change in total debt, as a percent of 2019Q4 assets. Results for all model specifications are reported here; the corresponding architectures are reported in Tables 2.12 and 2.13 in the Appendix. Positive effects are generally estimated for 2020 across model specifications with at least 5 years of feature history. Combined with Table 2.28, this suggests that had ineligible firms been eligible for direct cash bond support from the CCFs, they would have increased debt, as well as payouts in 2020.

Table 2.28: Ineligible Firms' Payout Counterfactual Treatment Effect

Difference in Payout Versus 2019 (% 2019Q4 Assets)						
Counterfactual Group Average Treatment Effect Accounting for Heterogeneity - B-BB Rated						
Year	Model (Feature History, Missingness Tolerance)					
	(1,1)	(1,10)	(5,1)	(5,10)	(10,1)	(10,10)
2020	0.47 (0.48)	0.44 (0.28)	0.34*** (0.12)	0.30*** (0.11)	0.31*** (0.11)	0.27** (0.12)
2021	0.78 (1.76)	-0.21 (1.45)	0.07 (0.61)	-0.07 (0.59)	-0.09 (0.56)	-0.36 (0.54)
2022	1.22 (0.87)	1.46*** (0.36)	1.30*** (0.22)	0.99*** (0.22)	1.15*** (0.23)	0.23 (0.23)
2023	0.19 (0.76)	0.64 (0.57)	0.81*** (0.28)	0.33 (0.27)	0.38 (0.28)	0.28 (0.27)

Standard-errors in parentheses

Signif. Codes: ***: 0.01, **: 0.05, *: 0.1

The table reports the counterfactual treatment effect for ineligible firms' annual payouts versus 2019, as a percent of 2019Q4 assets. Results for all model specifications are reported here; the corresponding architectures are reported in Tables 2.12 and 2.13 in the Appendix. Positive effects are generally estimated for 2020 and 2022 across model specifications with at least 5 years of feature history. Table 2.27 generally reports a positive and statistically significant estimate for the counterfactual treatment effect for ineligible firms' debt in 2020 for model specifications with at least 5 years of feature history. Taken together, the results suggest that had ineligible firms received direct cash bond support from the CCFs, they would have increased debt and payouts in 2020, as well as increasing payouts in 2022.

Table 2.29: Ineligible Firms' Investment Counterfactual Treatment Effect

Difference in CAPEX and R&D Versus 2019 (% 2019Q4 Assets)						
Counterfactual Group Average Treatment Effect Accounting for Heterogeneity - B-BB Rated						
Year	Model (Feature History, Missingness Tolerance)					
	(1,1)	(1,10)	(5,1)	(5,10)	(10,1)	(10,10)
2020	0.56 (1.10)	0.07 (0.35)	0.35*** (0.12)	0.29*** (0.11)	0.33*** (0.10)	0.17 (0.11)
2021	0.54 (1.08)	-0.05 (0.39)	0.43** (0.20)	0.04 (0.17)	0.28 (0.17)	-0.20 (0.18)
2022	-0.71 (1.32)	-0.61 (0.84)	0.24 (0.29)	-0.26 (0.26)	-0.02 (0.24)	-0.74*** (0.25)
2023	-0.35 (1.35)	-0.14 (0.68)	0.18 (0.34)	-0.58* (0.31)	-0.11 (0.29)	-0.94*** (0.30)

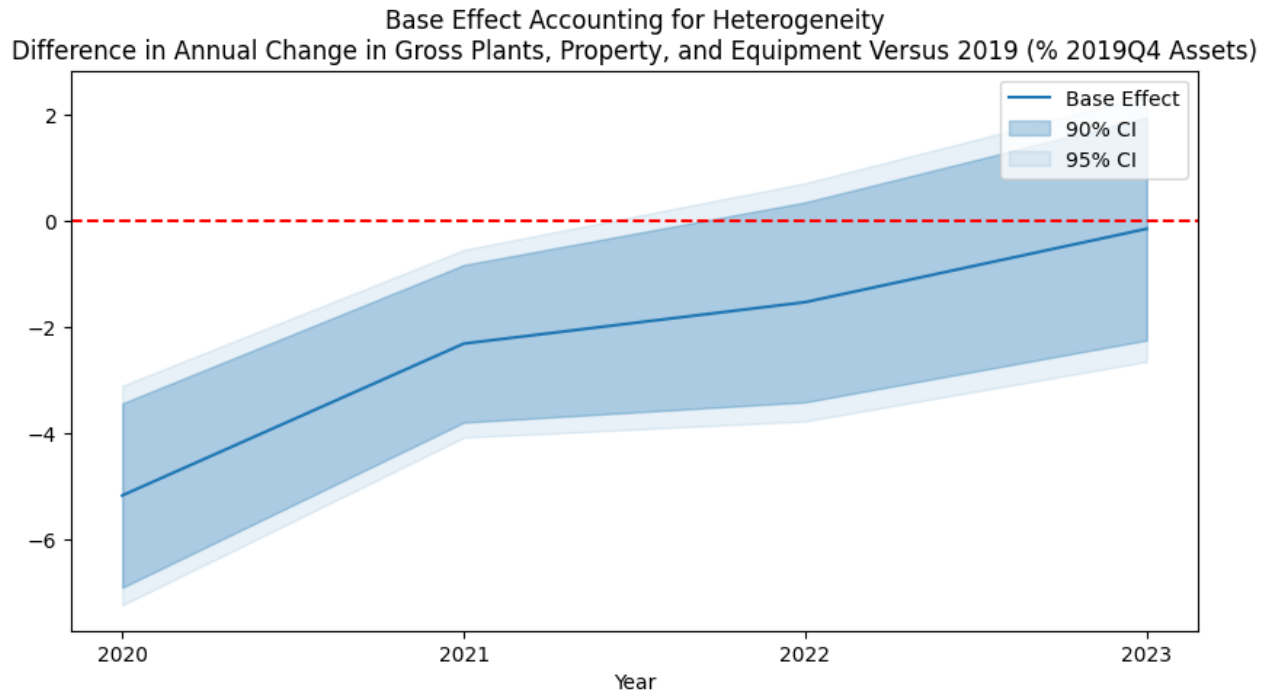
Standard-errors in parentheses

Signif. Codes: ***: 0.01, **: 0.05, *: 0.1

The table reports the counterfactual treatment effect for ineligible firms' annual investment versus 2019, as a percent of 2019Q4 assets. Results for all model specifications are reported here; the corresponding architectures are reported in Tables 2.12 and 2.13 in the Appendix. Positive effects are generally estimated for 2020 across model specifications with at least 5 years of feature history. However, an alternative proxy of investment using the annual change in gross property, plant, and equipment suggests null effects, as reported in Table 2.32.

2.9.11 Alternative Investment Proxy: Change in Gross Property, Plant, and Equipment

Figure 2.22: Base Effect for PPE Investment Proxy Negative Before Reverting to Null



The figure plots the base effects for the difference in annual investment versus 2019, scaled by 2019Q4 assets. Investment here is proxied by the annual change in gross property, plant, and equipment, in contrast to Figure 2.13 where investment is proxied by capital expenditures and R&D. The model above uses 10 years of feature history and 1% tolerance for missing observations. Details on its architecture are reported in Table 2.12 in the Appendix. Table 2.30 reports results across all model specifications. In contrast to the null-to-positive effects found using the CAPEX and R&D proxy for investment, here there are negative base effects estimated for 2020 and 2021, which then become null for 2022 and 2023.

Table 2.30: Base Effect for PPE Investment Proxy

Difference in Annual Change in Gross Plants, Property, and Equipment Versus 2019 (% 2019Q4 Assets)						
Base Effect Accounting for Heterogeneity						
Year	Model					
	(Feature History, Missingness Tolerance)					
2020	(1,1)	(1,10)	(5,1)	(5,10)	(10,1)	(10,10)
	-6.06 (5.56)	-4.96*** (1.90)	-5.07*** (1.06)	-5.24*** (0.98)	-5.17*** (1.06)	-5.08*** (1.09)
2021	-2.96 (4.69)	-1.42 (1.91)	-2.66*** (0.89)	-2.50*** (0.85)	-2.31** (0.90)	-2.13** (0.91)
2022	-1.34 (4.90)	-2.23 (1.87)	-1.82* (0.93)	-1.97** (0.92)	-1.53 (1.15)	-1.36 (1.10)
2023	0.38 (7.86)	-0.15 (2.43)	-0.28 (1.11)	-0.41 (1.05)	-0.14 (1.28)	0.09 (1.29)

Standard-errors in parentheses

Signif. Codes: ***: 0.01, **: 0.05, *: 0.1

The table reports the base effects for the difference in annual investment versus 2019, scaled by 2019Q4 assets. Investment here is proxied by the annual change in gross property, plant, and equipment, in contrast to Table 2.17 where investment is proxied by capital expenditures and R&D. Results for all model specifications are reported here; the corresponding architectures are reported in Tables 2.12 and 2.13 in the Appendix. The models produce relatively consistent results, with an initially negative base effect found for 2020 and 2021, becomes null for 2022 and 2023. This is in contrast to the null-to-positive effects found using the CAPEX and R&D proxy for investment.

Table 2.31: ATE for PPE Investment

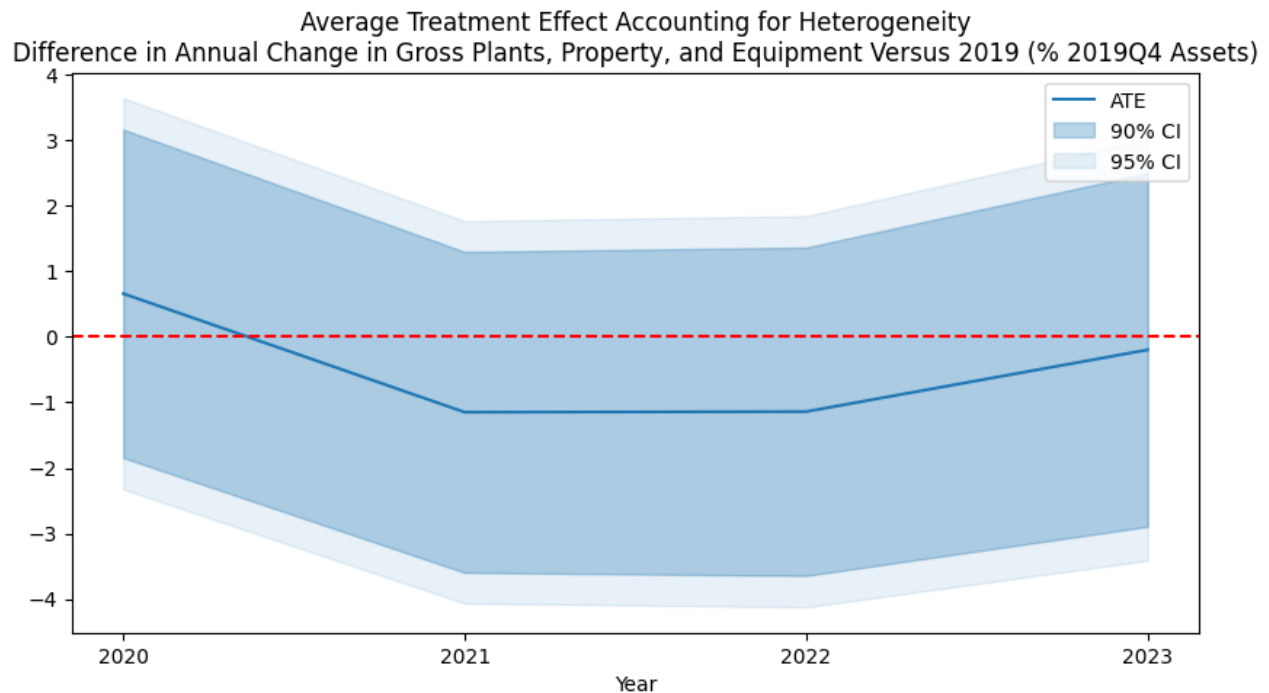
Difference in Annual Change in Gross Plants, Property, and Equipment Versus 2019 (% 2019Q4 Assets)						
Average Treatment Effect Accounting for Heterogeneity						
Year	Model					
	(Feature History, Missingness Tolerance)					
2020	(1,1)	(1,10)	(5,1)	(5,10)	(10,1)	(10,10)
	44.60 (41.28)	14.26 (11.73)	0.05 (3.72)	-1.22 (2.39)	0.66 (1.52)	-0.37 (2.26)
2021	92.38 (74.92)	17.16 (17.00)	0.28 (2.13)	-0.06 (1.66)	-1.15 (1.49)	-0.64 (1.43)
2022	45.07 (52.12)	13.47 (10.41)	-0.36 (2.08)	0.25 (1.82)	-1.14 (1.52)	-1.73 (1.48)
2023	28.49 (41.88)	11.64 (12.27)	0.67 (1.82)	0.38 (1.73)	-0.20 (1.64)	-0.79 (1.62)

Standard-errors in parentheses

Signif. Codes: ***: 0.01, **: 0.05, *: 0.1

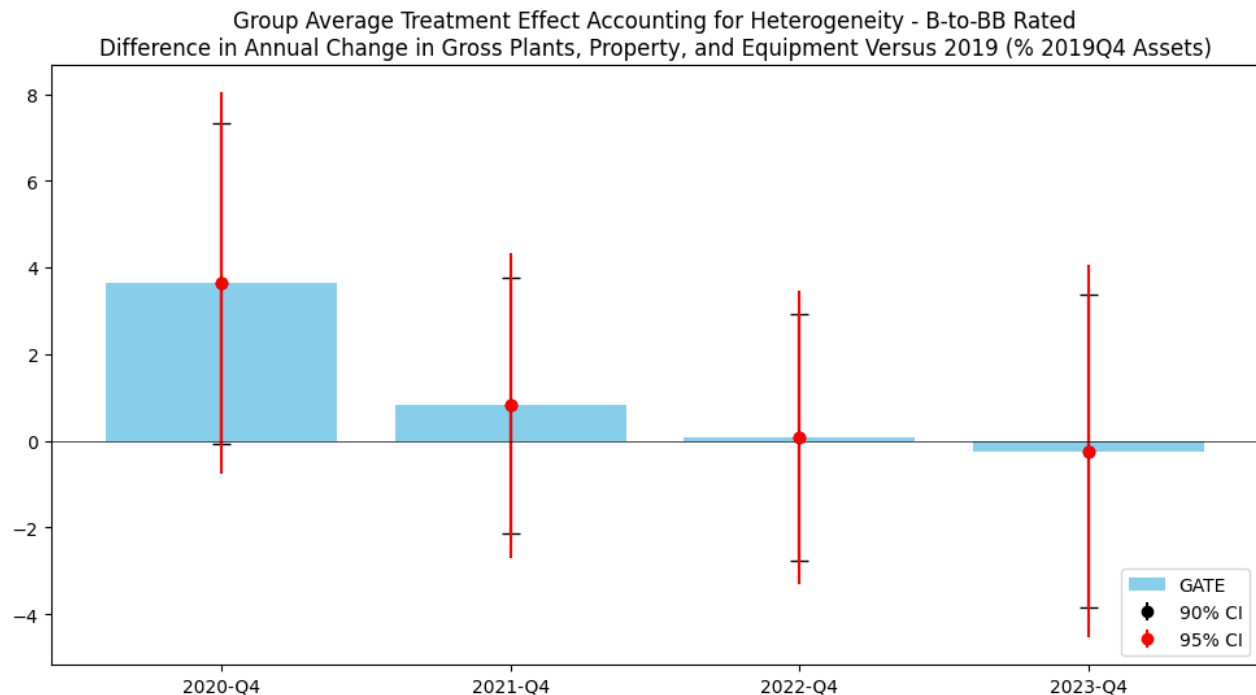
The table reports the average treatment effects for the difference in annual investment versus 2019, scaled by 2019Q4 assets. Investment here is proxied by the annual change in gross property, plant, and equipment, in contrast to Table 2.21 where investment is proxied by capital expenditures and R&D. This corresponds to the estimator reported in Equation 2.9. Results for all model specifications are reported here; the corresponding architectures are reported in Tables 2.12 and 2.13 in the Appendix. Null effects are generally estimated across different models and cumulation horizons. In contrast, the proxy for investment using CAPEX and R&D indicates a negative treatment effect for 2022.

Figure 2.23: ATE for PPE Investment Proxy Null



The figure plots the average treatment effects for the difference in annual investment versus 2019, scaled by 2019Q4 assets. Investment here is proxied by the annual change in gross property, plant, and equipment, in contrast to Figure 2.17 where investment is proxied by capital expenditures and R&D. This corresponds to the estimator reported in Equation 2.9. The model above uses 10 years of feature history and 1% tolerance for missing observations. Details on its architecture are reported in Table 2.12 in the Appendix. Table 2.31 reports results across all model specifications, showing that null effects are estimated in every instance. In contrast, the proxy for investment using CAPEX and R&D indicates a negative treatment effect for 2022.

Figure 2.24: Null Estimates for Ineligible Firms' Investment Counterfactual Treatment Effects



The figure plots the counterfactual treatment effect for ineligible firms' annual investment versus 2019, as a percent of 2019Q4 assets, for the model using 10 years of feature history and 1% tolerance for missing observations. Null effects are estimated for each year through 2023, although the point estimates are initially positive. Table 2.32 shows that null effects are generally estimated across different model specifications. Notably, the estimate for 2020 contrasts with the counterfactual treatment effect estimated when proxying investment using CAPEX and R&D, as shown in Figure 2.18. In that case, a positive and statistically significant effect is estimated for 2020.

Table 2.32: Ineligible Firms Counterfactual Treatment Effect

Difference in Annual Change in Gross Plants, Property, and Equipment Versus 2019 (% 2019Q4 Assets)						
Counterfactual Group Average Treatment Effect Accounting for Heterogeneity - B-BB Rated						
Year	Model					
	(Feature History, Missingness Tolerance)					
Year	(1,1)	(1,10)	(5,1)	(5,10)	(10,1)	(10,10)
2020	-1.19 (8.73)	0.08 (4.00)	0.24 (3.02)	3.47 (2.49)	3.63 (2.25)	6.43*** (2.30)
2021	0.06 (8.44)	-5.51 (4.55)	-1.05 (2.37)	0.69 (1.90)	0.82 (1.80)	2.19 (1.81)
2022	-3.61 (9.69)	-1.09 (3.51)	-0.54 (2.03)	0.57 (1.79)	0.08 (1.73)	1.45 (1.75)
2023	-1.59 (11.92)	-2.30 (4.85)	-0.36 (2.50)	0.31 (2.38)	-0.24 (2.20)	0.21 (2.21)

Standard-errors in parentheses

Signif. Codes: ***: 0.01, **: 0.05, *: 0.1

The table reports the counterfactual treatment effect for ineligible firms' annual investment versus 2019, as a percent of 2019Q4 assets. Results for all model specifications are reported here; the corresponding architectures are reported in Tables 2.12 and 2.13 in the Appendix. The results generally suggest null effects for investment. This contrasts with positive effects detected for the proxy of investment using CAPEX and R&D in Table 2.29.

CHAPTER 3

CENTRAL BANK CORPORATE BOND PURCHASE PROGRAMS: COMMITMENT MATTERS

3.1 Introduction

Over the past decade, central banks have expanded their use of unconventional monetary policy. Notably, they have shown a willingness to directly provide monetary stimulus to risky non-financial corporations through the purchases of corporate bonds. The European Central Bank (ECB) launched the Corporate Sector Purchase Programme (CSPP) in 2016, while the Federal Reserve introduced the Corporate Credit Facilities (CCFs) in 2020. The programs have been immensely successful in reducing the financing costs of targeted firms.¹

However, the substantial reduction in borrowing costs did not translate into relatively greater investment, a key proxy of real activity, for firms directly targeted by these programs. In both Europe and the United States, firms directly benefiting from corporate bond market stimulus increased leverage and increased payouts to shareholders relative to other firms but did not relatively increase investment.² Both the CSPP and CCF directed stimulus to largely financially unconstrained firms rated investment-grade (IG).³

1. Papers documenting the financial effects of the CSPP include Abidi and Miquel-Flores [2018], Pegeraro and Montagna [2025], Todorov [2020], and Zagħini [2019]. For the CCFs, papers include Boyarchenko, Kovner, and Shachar [2022], D'Amico, Kurakula, and Lee [2020], Flanagan and Purnanandam [2020], Gilchrist et al. [2021], Haddad, Moreira, and Muir [2021], Kargar et al. [2021], Momin and Li [2025], O'Hara and Zhou [2021]

2. Papers documenting these dynamics in Europe include De Santis and Zagħini [2021], Grosse-Rueschkamp, Steffen, and Streitz [2019], and Todorov [2020]. For the U.S., papers include Darmouni and Siani [2024] and Momin [2025b].

3. Given that eligibility for either program requires the existence of a credit rating, and that the (lack

Both programs were also de facto unsecured corporate bond interventions.⁴ Indeed, firms in Europe tilted their financing mix toward securities eligible for the CSPP and increased the issuance of unsecured debt [Abidi and Miquel-Flores, 2018, Grosse-Rueschkamp, Steffen, and Streitz, 2019, Pegoraro and Montagna, 2025, Todorov, 2020].

In this context, this paper is the first to explicitly connect the documented stylized facts of firm dynamics following corporate bond intervention (increased leverage, relative increase in payouts, relative lack of investment response) to the facility design itself (unsecured debt intervention in financially unconstrained firms). This paper rationalizes the empirical patterns observed in the data in a dynamic capital structure model with investment, where firms have access to both equity and (unsecured and secured) debt financing but cannot commit to a leverage policy *ex ante*, in the vein of Demarzo and He [2021]. The model is numerically estimated with parameters taken from the literature and is shown to fit key empirical moments. It is further used to show how (counterfactual) secured debt intervention, rather than unsecured debt intervention, can induce a stronger investment response among financially unconstrained firms. To the extent that central banks intervene in corporate debt markets to stimulate real activity, this is an important consideration for policy design.⁵

of) availability of credit ratings is a common proxy for financial constraints (e.g. Whited [1992], Almeida, Campello, and Weisbach [2004], Faulkender and Petersen [2006], Denis and Sibilkov [2010], Harford and Uysal [2014]), an extreme argument would be that any intervention in corporate bonds would necessarily direct stimulus to relatively unconstrained firms. Indeed, Greenwald, Krainer, and Paul [2023] make precisely this modeling assumption.

4. Nearly all of the corporate bonds purchased by both the CSPP and CCF were senior unsecured debt (over 95% for both programs). Detail on security-level CSPP purchases are available here: <https://www.ecb.europa.eu/mopo/implement/app/html/index.en.html#cspp>. Equivalent data for the CCFs are posted here: <https://www.federalreserve.gov/monetarypolicy/smccf.htm>.

5. Both the ECB and Fed emphasize how loosening financial conditions are expected to support real activity in their announcements of corporate bond purchase programs. For the ECB's announcement, see

While the arguments presented in this paper are novel, the dynamics involving unsecured debt intervention are also present in the model of Crouzet and Tourre [2021], which this paper builds on. Crouzet and Tourre [2021] extend the model of Demarzo and He [2021] to feature investment, subject to convex adjustment costs, that follow ‘*q*-theory’ dynamics [Hayashi, 1982]. Hence, the investment rate is proportional to the marginal value of equity with respect to capital. Without commitment, the firm cannot realize the tax shield benefits of debt issuance. Bond investors anticipate the equilibrium leverage policy of equity shareholders and price in higher default costs, exactly offsetting any gains to firm value from the presence of a debt tax shield.

Likewise, unsecured debt intervention results in accelerated debt issuance which is paid out by the firm to shareholders, leaving the firm with higher leverage. Higher leverage, and hence, bankruptcy costs, imply a lower continuation value. These two forces (higher payouts and higher bankruptcy costs) cancel out to leave firm equity value, as well as investment, unchanged.⁶ However, longer-run investment dynamics suffer due to higher firm leverage (as implied by the lower continuation value).⁷ While stark, I emphasize this mechanism as an explanation for the stylized firm dynamics seen in both Europe and the United States following the introduction of corporate bond purchase programs.

I extend the model of Crouzet and Tourre [2021] to feature secured debt that is issued subject to a non-state contingent collateral constraint, similar to Kiyotaki and Moore [1997].

<https://eur-lex.europa.eu/legal-content/EN/TXT/PDF/?uri=CELEX:32016D0016>. For the Fed's, see <https://www.federalreserve.gov/newsevents/pressreleases/monetary20200323b.htm>.

6. DeMarzo, He, and Tourre [2023] document similar dynamics in the context of a risk-neutral sovereign borrower and more patient international creditors.

7. This prediction also has some empirical support. Momin [2025b] finds that while firm leverage rose following the introduction of the CCFs, investment rates have not exceeded their pre-pandemic levels through 2023, in the case when investment is proxied as the change in gross property, plant, and equipment (PP&E).

Secured debt, unlike unsecured debt, induces commitment via this collateral constraint, echoing the finding in Demarzo [2019]. I show that the value of the Lagrange multiplier on the collateral constraint is precisely equal to the marginal value of the debt tax shield. Intuitively, the firm can enjoy the benefits of the debt tax shield because the issuance of fully collateralized secured debt is limited by the collateral constraint, which prevents the firm from diluting creditors through excessive debt issuance, as was the case with unsecured debt issuance, given a lack of firm commitment to an *ex ante* debt policy.

Given that fully collateralized secured debt is risk-free, while firms benefit from the debt tax shield, firms issue up to the collateral constraint, which thus binds. The result that firms exhaust debt capacity is seemingly at odds with Rampini and Viswanathan [2010], who model state-contingent collateral constraints and show that firms engage in risk management by maintaining financial slack for future states. Secured debt is also risk-free in Rampini and Viswanathan [2010], but the key difference is that firms are subject to additional financial constraints in the form of restrictions on equity issuance. In contrast, I maintain the standard Leland [1994] assumptions in my baseline model that firms can access both debt and equity markets, so long as its continuation value is non-negative. When equity issuance constraints are removed from Rampini and Viswanathan [2010], I recover the result that the collateral constraint binds for all states.⁸

Empirically, firms tapped credit lines, issued corporate bonds, and issued equity through the COVID-19 pandemic.⁹ This supports the modeling choice to maintain the standard Leland [1994] assumptions. However, this results in counterfactual dynamics for the col-

8. See Section 3.2.3 for the discussion and Section 3.6.5 in the Appendix for the proof.

9. Papers documenting credit line drawdowns include: Acharya and Steffen [2020], Darmouni and Siani [2024], Greenwald, Krainer, and Paul [2023]. Similarly, for bond issuance: Becker and Benmelech [2021], Boyarchenko, Kovner, and Shachar [2022], Darmouni and Siani [2024], Dutordoir et al. [2024], Halling, Yu, and Zechner [2020], Hotchkiss, Nini, and Smith [2022]. And for equity issuance: Dutordoir et al. [2024], Halling, Yu, and Zechner [2020], Hotchkiss, Nini, and Smith [2022]

lateral constraint and secured debt issuance, where the collateral constraint always binds and secured debt issuance is procyclical, absent intervention. Empirically, secured debt issuance is countercyclical, with firms maintaining slack in the collateral constraint and maintaining financial flexibility for ‘bad’ states as a form of insurance [Benmelech, Kumar, and Rajan, 2022, 2024]. Ultimately, this translates into a more conservative modeling choice that underestimates the efficacy of potential secured debt intervention, which otherwise has more impact in economies with more freely available collateral.

Despite this, I find that secured debt intervention, which entails public lending against collateral valued above market prices,¹⁰ boosts firm investment through direct and indirect channels. First, secured debt intervention makes secured debt issuance more valuable, directly incentivizing the firm to invest and raise collateral to relax its collateral constraint. Second, because secured debt issuance has implicit commitment, the firm is able to benefit from greater proceeds from fully collateralized secured debt issuance, without increasing default risk. This results in a higher equity value, as well as a higher value of Tobin’s q . Since capital is perceived as more productive, investment indirectly increases, as well.

In terms of longer-term dynamics, secured debt intervention leads to higher expected average equity prices, debt prices, investment rates, and lower default rates, relative to the case of no intervention and especially, compared to the case of unsecured debt intervention. Since unsecured debt intervention accelerates debt issuance and leads firm to accumulate leverage, the longer-term dynamics are actually more unfavorable compared to the benchmark of no intervention. While secured debt intervention also leads to higher unsecured debt issuance and payouts, the investment response is stronger over much of the state space, while firms’ tolerate higher debt levels before defaulting, reinforcing the more

10. The nature of the secured debt intervention described here is analogous to the Bank Term Funding Program (BTFP) administered by the Fed to provide loans to financial institutions against collateral valued at par (hence, above market prices): <https://www.federalreserve.gov/newsevents/pressreleases/files/monetary20240124a1.pdf>.

favorable default dynamics.

If firms could commit to covenants limiting issuance, they would benefit more from unsecured debt intervention. However, I maintain the assumption that firms would not voluntarily agree to such covenants, consistent with the empirical behavior of IG issuers. Instead, this motivates studying unsecured debt intervention with payouts limited by dividend restrictions, which generates higher investment, higher unsecured debt prices, and lower default rates. However, it induces firms to repurchase debt and also leads to lower equity valuations. Restricting debt repurchases further improves investment dynamics (though, it does not improve equity valuations) and firms choose not to issue unsecured debt when they would have otherwise repurchased debt. All together, the numerical solutions suggest firms would not voluntarily participate in an unsecured debt intervention program with dividend restrictions.

This paper contributes to the extensive literature on the financial and real effects of central bank corporate bond purchase programs referenced earlier in this section. To the best of my knowledge, this is the first paper to connect the stylized empirical facts of the real effects of these programs to the nature of the intervention itself (unsecured debt intervention in financially unconstrained firms). It is also the first to suggest that secured debt intervention, rather than unsecured debt intervention, would have improved investment outcomes. Crouzet and Tourre [2021] take a broader view on corporate credit interventions to include the Main Street Lending Program (MSLP) and Paycheck Protection Program (PPP), which featured subsidized bank lending to smaller, generally non-rated firms. They find that credit interventions can prevent inefficient firm restructurings during a credit shock, quantitatively dominating longer-run drags on investment due to debt overhang. Li and Li [2024] also broadly analyze corporate credit programs and highlight the potential negative long-run implications of rescuing low-quality firms that exacerbates future intervention costs. Greenwald, Krainer, and Paul [2023] develop a structural corporate fi-

nance model with bank term loans, credit lines, and corporate bonds. Interestingly, they also find that corporate bond intervention generates higher corporate bond issuance by the financially unconstrained firms that issue them, largely without generating additional investment. However, they show that such an intervention can still indirectly stimulate investment by freeing up bank credit lines for more constrained firms.

This paper also contributes to the literature on dynamic capital structure models where firms lack commitment to an *ex ante* debt issuance policy. Demarzo and He [2021] build on the seminal work of Leland [1994] to show that firms cannot benefit from the debt tax shield when they lack commitment, although firms still issue debt in equilibrium. Demarzo, He, and Tourre [2023] explore the ramifications of Demarzo and He [2021] in the context of sovereign debt, while Crouzet and Tourre [2021] extends the model to include continuous investment policies subject to convex adjustment costs. They structurally estimate their model and show that the model-implied moments align well with key empirical moments. I further extend Crouzet and Tourre [2021] to include both continuous investment subject to convex adjustment costs as well as secured debt¹¹ and show that the numerically estimated model delivers similar quantitative performance.

The third strand of literature this paper contributes to is on the effects of accommodative monetary policy on payouts.¹² Elgouacem and Zago [2023] show empirically that firms finance share buybacks by issuing corporate bonds. They find that accommodative monetary policy increases buybacks. Acharya and Plantin [2025] also note that the increase in firm payouts have occurred a low-yield environment where the corporate bond market has significantly expanded, while investment has remained depressed. They ratio-

11. Demarzo [2019] first models secured debt in the context of Leland-type models without commitment. There, investment opportunities arrive according to a Poisson process and do not follow *q*-theory dynamics.

12. Other papers studying payouts financed through capital issuance include Farre-Mensa, Michaely, and Schmalz [2024] and Ma [2019].

nalize these dynamics in a parsimonious model featuring agency frictions and moral hazard that arise due to the increasing relationship between investment returns and shareholders' costly private effort. Pazarbasi [2025] shows empirically that cash-rich firms have higher equity payouts and finds that this can be explained in a New Keynesian model where accommodative monetary policy reduces firms' precautionary cash demand, triggering payouts.

The rest of the paper is organized as follows. Section 3.2 sets up the model with short-term secured debt. Section 3.3 explores crisis dynamics in the model. Section 3.4 presents the numerical solution to the model. Section 3.5 concludes.

3.2 Model with Short-Term Secured Debt

3.2.1 Setup

In the baseline model with short-term secured debt, I assume shareholders and creditors are risk-neutral with discount rate r . Shareholders have the option to default on both unsecured and secured creditors at any point. At default, I assume shareholders and unsecured creditors have zero recovery value, while secured creditors receive the collateral backing their debt. Following the standard assumption in Leland models, equity investors are deep-pocketed and can support the firm with liquidity injections. As a result, firms can be viewed as financially unconstrained, given their ability to raise debt and equity to finance operations, so long as its continuation value is positive.

Firms' production technology, in revenue per unit of time, is given by:

$$Y_t = AK_t$$

where the productivity parameter A is deterministic. Capital, K_t , is measured in efficiency

units and follows a geometric Brownian motion given by:

$$\frac{dK_t}{K_t} = (g_t - \delta)dt + \sigma dZ_t$$

where g_t is the endogenous investment rate and δ is the capital depreciation rate, where $\delta \in (0, 1)$. dZ_t is the increment of a Brownian motion and is distributed as $dZ_t \sim N(0, dt)$. The price of capital is fixed at 1, as in Crouzet and Tourre [2021].

Shareholders choose a rate of investment, subject to a convex cost, parameterized as:

$$\Phi(g) = \frac{1}{2}\gamma g^2$$

This parameterization of investment costs ensures investment is nonnegative in equilibrium (and hence, capital is never liquidated). This is in contrast to Crouzet and Tourre [2021], where the firm liquidates its capital at points over the state space (i.e. $g < 0$).¹³

The firm's stock of unsecured debt has an aggregate face value F_t and is an endogenous state variable. Unsecured debt matures at a Poisson rate m^u and has a price p_t . It is issued at a face value equal to 1 with a coupon equal to the risk-free rate, $c^u = r$. Given potential default risk, $p_t \leq 1$. Unsecured debt stock evolves as:

$$dF_t = \underbrace{-m^u F_t dt}_{\text{maturing debt}} + \underbrace{d\Gamma_t^u}_{\text{active debt management}}$$

Following Demarzo and He [2021], I focus on a ‘smooth’ equilibrium where endogenous

13. The chief motivation for this modification is to ensure that long-term secured debt is risk-free in the extension to the model examined in Section 3.6.3 of the Appendix, keeping the modeling tractable. With instantaneously maturing ‘short-term’ secured debt, the level of the secured debt adjusts with capital liquidation, so this parameterization is not critical. With long-term secured debt, capital liquidation would cause initially fully collateralized debt to become under-collateralized, absent restrictions on the firm from doing so.

unsecured debt is assumed to be continuous. Hence, $d\Gamma_t^u = B_t^u dt$, where B_t^u is the endogenous unsecured debt issuance policy.

Secured debt has an aggregate face value of S_t and is another endogenous state variable. Short-term secured debt is assumed to mature instantaneously with maturity dt . When issued at par with face value equal to 1 and paying a coupon equal to the risk-free rate, $c^s = r$, short-term secured debt is risk-free with price equal to 1.¹⁴ Let $S_{t-} \equiv \lim_{dt \searrow 0} S_{t-dt}$ be the value of secured debt issued at the instant before time t , then secured debt evolves as $dS_t = S_t - S_{t-} \equiv B_t^s dt$.¹⁵

Additionally, I assume that the firm faces a non-state contingent collateral constraint when issuing secured debt that is proportional to its capital stock:

$$S_t \leq \alpha K_t$$

where $\alpha \in (0, 1)$ is the proportion of the capital stock pledgeable as collateral to secured creditors.

14. In this setup, instantaneously maturing debt is risk-free so long as priced shocks to the income/production process are continuous, which is the case when shocks are determined by increments of a Brownian motion [DeMarzo, He, and Tourre, 2023, Hu, Varas, and Ying, 2024]. However, this is not necessarily the case if there is priced jump risk [Abel, 2016, 2018, Hu, Varas, and Ying, 2024]. In the presence of jump risks, instantaneously maturity debt becomes risk-free if fully collateralized Abel [2018]. See Section 3.2.3 for further discussion.

15. For the purpose of exposition, I initially treat short-term secured debt as a state variable; however, I will show that its value will be a constant proportion of capital, consistent with Abel [2018] and Hu, Varas, and Ying [2024].

3.2.2 Equity's Problem

Let θ equal the corporate tax rate. Then, equity's flow payoffs are:

$$\begin{aligned}
& \left[\underbrace{AK_t}_{\text{revenue}} - \underbrace{\theta(AK_t - c^u F_t - c^s S_{t-})}_{\text{corporate taxes}} - \underbrace{\Phi(g_t) K_t}_{\text{investment cost}} \right. \\
& - \underbrace{(c^u + m^u) F_t}_{\text{unsecured debt interest \& principal}} + \underbrace{p_t B_t^u}_{\text{unsecured debt net issuance}} \\
& \left. - \underbrace{c^u S_t}_{\text{secured debt interest}} + \underbrace{B_t^s}_{\text{secured debt net issuance}} \right] dt
\end{aligned}$$

Shareholders maximize the present discounted cash flows, taking unsecured debt price, p_t , as given, and choose policies for investment, unsecured debt issuance, secured debt issuance (subject to collateral constraint), and default time, τ . The sequence formulation of the stochastic control and optimal stopping problem is:

$$\begin{aligned}
J(K, F, S) = & \max_{\tau, g, B^u, B^s} \mathbb{E}_0 \left[\int_0^\tau \exp(-rt) [AK_t - \theta(AK_t - c^u F_t - c^s S_t) - \Phi(g_t) K_t \right. \\
& \left. - (c^u + m^u) F_t + p_t B_t^u - c^s S_t + B_t^s] dt \middle| K_0 = K, F_0 = F, S_0 = S \right] \quad (3.1) \\
& s.t. \\
& \frac{dK_t}{K_t} = (g_t - \delta) dt + \sigma dZ_t \\
& dF_t = -m^u F_t dt + B_t^u dt \\
& dS_t = B_t^s dt \\
& S_t \leq \alpha K_t
\end{aligned}$$

As noted by Abel [2018], the value of shareholders' equity is given by $J - S$, where S is the value of short-term debt. However, in solving for optimal policies, shareholders jointly maximize the value of equity and short-term creditors because they immediately receive

the proceeds from the issuance of short-term debt.¹⁶

To show that the value function is homogeneous of degree 1 in K , note that capital is given by:

$$K_t = K_0 \exp \left(\int_0^t \left(g_t - \delta - \frac{1}{2} \sigma^2 \right) dt + \int_0^t \sigma dZ_t \right).$$

Then, substitute this expression into the firm's objective given by Equation (3.1) and factor out $K_0 = K$. Rescale the state variables and controls by K_t :

$$f_t \equiv \frac{F_t}{K_t}, \quad s_t \equiv \frac{S_t}{K_t}, \quad b_t^u \equiv \frac{B_t^u}{K_t}, \quad b_t^s \equiv \frac{B_t^s}{K_t},$$

Under the change of measure $dZ_t \equiv d\tilde{Z}_t + \sigma dt$, the evolution of the state variables are given by:

$$df_t = [b_t^u - (g_t - \delta + m^u) f_t dt] - \sigma f_t d\tilde{Z}_t$$

$$ds_t = [b_t^s - (g_t - \delta)] s_t dt - s_t \sigma d\tilde{Z}_t$$

Then, the rescaled value function is given by:

$$j(f, s) = \max_{\tau, g, b^u, b^s} \tilde{\mathbb{E}}_0 \left[\int_0^\tau \exp \left(- \left(r - \int_0^t g_s ds + \delta \right) t \right) [A - \theta(A - c^u f_t - c^s s_t) - \Phi(g_t) - (c^u + m^u) f_t + p_t b_t^u - c^s s_t + b_t^s] dt \middle| f_0 = f, s_0 = s \right] \quad (3.2)$$

16. See also Hu, Varas, and Ying [2024] for similar arguments.

Such that:

$$df_t = [b_t^u - (g_t - \delta + m^u)f_t]dt - f_t\sigma d\tilde{Z}_t$$

$$ds_t = [b_t^s - (g_t - \delta)s_t]dt - s_t\sigma d\tilde{Z}_t$$

$$s_t \leq \alpha$$

Consequently, the Hamilton-Jacobi-Bellman (HJB) equation characterizing equity's problem in the continuation region is given by:

$$0 = \max_{g, b^u, b^s} \left\{ \begin{aligned} & - (r - g + \delta)j - (s - \alpha)l^s \\ & + \underbrace{A - \theta(A - c^u f - c^s s) - \Phi(g) - (c^u + m^u)f + pb^u - c^s s + b^s}_{\text{cash flows per unit of capital}} \\ & + \underbrace{[b^u - (g - \delta + m^u)f]j_f + \frac{1}{2}\sigma^2 f^2 j_{ff}}_{\text{evolution of unsecured debt per unit of capital}} \\ & + \underbrace{[b^s - (g - \delta)s]j_s + \frac{1}{2}\sigma^2 s^2 j_{ss}}_{\text{evolution of secured debt per unit of capital}} \end{aligned} \right\} \quad (3.3)$$

where l^s is the Lagrange multiplier on the collateral constraint.

Proposition 1 (Collateral Constraint Binds). *The collateral constraint binds, and the HJB equation becomes:*

$$0 = \max_{g, b^u} \left\{ \begin{aligned} & - (r - g + \delta)j + A - \theta(A - c^u f - c^s \alpha) - \Phi(g) - (c^u + m^u)f + pb^u - c^s \alpha + \alpha(g - \delta) \\ & + [b^u - (g - \delta + m^u)f]j_f + \frac{1}{2}\sigma^2 f^2 j_{ff} \end{aligned} \right\} \quad (3.4)$$

Proof. See Section 3.6.2 in the Appendix for the full derivation. The solution method can be summarized as:

1. Take derivative of equity's HJB in continuation region with respect to secured debt issuance policy → obtain equilibrium derivative conditions for equity value function.
2. Take derivative of HJB with respect to s and use equilibrium derivative conditions. Obtain Lagrange multiplier on constraint.
3. Assuming Lagrange multiplier binds, substitute in value for s and use equilibrium derivative conditions to obtain equity HJB reduced by 1 state variable and 1 control variable.

□

Corollary 1 (Value of Commitment). *The value of commitment, as suggested by the Lagrange multiplier, is equal to the marginal value of the debt tax shield ($l^s = \theta c^s$). That is, relaxing the collateral constraint and allowing the firm to issue additional secured debt generates additional tax shield benefits.*

Proof. Follows from the proof of Proposition 1. □

Equivalent results to Proposition 1 and Corollary 1 hold in the case when the firm can issue long-term riskless secured debt, as shown in Appendix 3.6.3. That is, the collateral constraint binds, and the value of the Lagrange multiplier equals the debt tax shield. However, modeling secured debt as instantaneously maturing simplifies the numerical solution and discussion of the results.¹⁷

The ability of collateral to induce commitment, allowing the firm to enjoy the tax shield benefits from issuing secured debt was first made by Demarzo [2019], in the context of Leland-type models. This contrasts with the main finding in Demarzo and He [2021], that absent commitment to an ex ante debt issuance policy, the firm cannot monetize the tax

17. Future extensions of this model can model risky, long-term secured debt where risk is driven by fluctuating capital quality or capital prices.

shield benefits from issuing unsecured debt, as shown in Section 3.2.5. This is because unsecured creditors immediately discount the price of unsecured debt by the same value as the debt tax shield, owing to the larger bankruptcy costs engendered by the additional issuance of risky, unsecured debt.

3.2.3 Discussion on Collateral Constraint and Financial Slack

I model collateral constraints in a non-state contingent fashion, as in Kiyotaki and Moore [1997], and obtain a similar result that the collateral constraint binds when there is a motivation to trade, either due to a difference in discount rates or the presence of a debt tax shield. In the models considered here, both short-term and long-term secured debt are risk-free. As such, the marginal cost of issuing secured debt is zero, since there is no impact from increased exposure to bankruptcy. At the same time, the marginal benefit is the interest tax shield. As a result, firms issue up to their collateral constraint, completely exhausting debt capacity.

Rampini and Viswanathan [2010] feature state-contingent debt and collateral constraints, where firms also face non-negativity constraints on dividends. All agents in the model have the same discount rate and there are no taxes. Firms can borrow in the current state by issuing promises to pay in future states, subject to the collateral constraint, which ensures that debt is risk-free. The benefit to issuing debt is the expected returns to investment in the current and future period, while the cost is the expected return from conserving net worth and increasing investment in certain future states. Consequently, the authors show that latter may dominate, leading firms to maintain slack in the collateral constraint in some states.

However, as shown in Appendix 3.6.5, when the Rampini and Viswanathan [2010] environment is modified to allow dividends to be unconstrained, so that the firm can receive cash infusions from equity investors, as is the case in the model presented in this section,

and a debt tax shield is introduced, one recovers the result that collateral constraints bind, even with state-contingency. Removing the nonnegativity constraints on dividends eases the firm's financial constraints. Since debt is risk-free, and the firm receives benefit from the debt tax shield, the firm issues up to the collateral constraint.

Empirically, firms issued both corporate bonds, as well as, equity during the COVID-19 pandemic.¹⁸ Moreover, as argued in Section 3.1, corporate bond purchase programs generally directed monetary stimulus to relatively unconstrained firms (IG-rated firms). All together, the standard assumptions of Leland-type models seem more appropriate.

As noted by Hu, Varas, and Ying [2024], unsecured short-term debt is risk-free whenever shocks to the firm's earnings process is governed by an Itô process, as is the case in the model presented in this section. Consequently, if firms have a motive to borrow due to a difference in discount rates or a debt tax shield, they will exhaust the borrowing capacity imposed by limited liability. To induce risky unsecured short-term debt, Abel [2018] and Hu, Varas, and Ying [2024] introduce possible downward jumps in firm earnings. With this modification, issuing unsecured short-term debt can expose the firm to potential bankruptcy costs and so, the firm may choose to not exhaust its borrowing capacity. However, if short-term debt is fully collateralized, then it is risk-free even in the presence of jumps, and the firm will exhaust its borrowing capacity.¹⁹

Empirically, secured debt issuance is countercyclical, with firms maintaining slack in the

18. Papers documenting record bond issuance include: Becker and Benmelech [2021], Boyarchenko, Kovner, and Shachar [2022], Darmouni and Siani [2024], Dutordoir et al. [2024], Halling, Yu, and Zechner [2020], Hotchkiss, Nini, and Smith [2022]. Papers documenting equity issuance, particularly for more financially constrained firms, include: Dutordoir et al. [2024], Halling, Yu, and Zechner [2020], Hotchkiss, Nini, and Smith [2022]

19. This can be seen in [Abel, 2018, p. 104] Equation (11) by setting the fraction of deadweight losses from default, α , equal to zero. Then, the derivative of the trade-off function with respect to debt is equal to the debt tax shield and strictly positive.

collateral constraint, maintaining financial flexibility for ‘bad’ states as a form of insurance [Benmelech, Kumar, and Rajan, 2022, 2024]. More realistic model dynamics would necessitate generating a slack in the collateral constraint, which could be done by introducing frictions to collateralizing capital, issuing secured debt, etc. However, this would imply a stronger response from secured debt intervention in the crisis period (characterized in Section 3.3) as firms would enter this state with greater capacity to issue secured debt. Indeed, a firm’s limited capacity to issue secured debt is precisely what disciplines and enables it to benefit from secured debt intervention; in contrast, unsecured debt intervention debt accelerates issuance to the point where any potential benefits are exactly offset by higher bankruptcy costs incurred from greater indebtedness. Consequently, a more conservative and parsimonious modeling approach is followed where the collateral constraints bind.

3.2.4 Unsecured Creditors’ Problem

Unsecured creditors take equity’s optimal policies as given and price unsecured debt rationally (i.e. anticipating future default). The price of 1 unit of unsecured debt with face value 1 is given by:

$$\begin{aligned}
 p(K, F) &\equiv \mathbb{E}_0 \left[\int_0^\tau \exp(-(r + m^u)t) (c^u + m^u) dt \middle| K_0 = K, F_0 = F \right] \\
 &\quad s.t. \\
 \frac{dK_t}{K_t} &= (g_t - \delta) dt + \sigma dZ_t \\
 dF_t &= -m^u F_t dt + B_t^u dt
 \end{aligned}$$

The unsecured debt price is homogeneous of degree zero in capital: $p(1, F/K) = p(f)$. Given the drift for df_t , the HJB for the debt value function in the continuation region is

given by:

$$(r + m^u)p = c^u + m^u + [b^u - (g + m^u - \delta - \sigma^2)f]p_f + \frac{1}{2}\sigma^2 f^2 p_{ff} \quad (3.5)$$

3.2.5 Optimal Policies

The first order condition for the HJB equation shown in Equation (3.4) with respect to g yields:

$$\begin{aligned}\Phi'(g) &= j - f j_f + \alpha \\ g &= \frac{1}{\gamma}(j - f j_f + \alpha)\end{aligned}$$

Tobin's q is given by the marginal derivative of J with respect to K (with the price of capital fixed at one):

$$\begin{aligned}q \equiv \partial_K J &= \frac{\partial J(K, F)}{\partial K} = \frac{\partial(Kj(f = F/K))}{\partial K} \\ &= j(f) - f j_f(f)\end{aligned}$$

With a binding collateral constraint, collateralized borrowing provides a direct motivation to invest in order to relax the collateral constraint. Hence, the ability to monetize a portion of the capital stock through secured debt issuance increases optimal investment by a factor proportional to α , relative to Tobin's q .

Similarly, Abel [2016] finds that the availability of instantaneously maturity, short-term bond financing boosts firm investment indirectly via increasing the joint value of equity and short-term debt. In contrast, this channel is absent in Crouzet and Tourre [2021] who only allow firms to issue unsecured debt. As shown below, absent commitment, firms do not benefit from unsecured debt issuance.

The FOC of equity's problem with respect to b^u :

$$\underbrace{p}_{\text{MB of issuance}} + \underbrace{j_f}_{\text{MC on future value}} = 0$$

This holds for all equilibria; in particular, it holds for the no-trade equilibrium where equity does not issue unsecured debt (i.e. $b^u = 0$). The economic content of this result is that the marginal benefit equity gains from issuing debt (the amount raised) is completely offset by the marginal impact on equity due to higher unsecured debt levels. Stated otherwise, lenders anticipate the firms issuance policy and price in higher default risk at issuance. Consequently, this allows one to solve for the equity value assuming no-trade.

Nonetheless, while equity value is unaffected by unsecured debt issuance, in equilibrium, equity does issue unsecured debt, given the presence of the debt tax shield. Likewise, unsecured creditors require knowledge of this policy to accurately price unsecured debt; otherwise, the equilibrium condition $p = -j_f$ does not hold.

To solve for the optimal issuance policy, first take the derivative of the HJB equation characterizing equity's problem without trade (setting $b^u = 0$ in Equation (3.4) and using the envelope theorem with respect to optimal investment):

$$\begin{aligned} (r - g + \delta)j_f &= \theta c^u - (c^u + m^u) - (g - \delta + m^u)j_f - (g - \delta + m^u)fj_{ff} + \sigma^2 f j_{ff} \\ &\quad + \frac{1}{2}\sigma^2 f^2 j_{fff} \\ \Rightarrow (r + m^u)j_f &= \theta c^u - (c^u + m^u) - (g - \delta + m^u - \sigma^2)fj_{ff} + \frac{1}{2}\sigma^2 f^2 j_{fff} \end{aligned}$$

Then, substitute in the equilibrium condition $p = -j_f$ into Equation (3.5):

$$-(r + m^u)j_f = c^u + m^u - [b^u - (g + m^u - \delta - \sigma^2)f]j_{ff} - \frac{1}{2}\sigma^2 f^2 j_{fff}$$

Combine these two results and obtain the optimal unsecured debt issuance rate:

$$0 = \theta c^u - b^u j_{ff}$$

$$\Rightarrow b^u = \frac{\theta c^u}{j_{ff}} = \frac{\theta c^u}{-p_f} > 0$$

Given a strictly convex value function for equity (see Proposition 8 in the Appendix) and short-term debt ($j_{ff} > 0$), unsecured debt issuance is strictly positive in the continuation region (outside of default).

Taking the derivative of unsecured debt issuance policy with respect to f yields:

$$b_f^u = \frac{\theta c^u}{p_f^2} p_{ff}$$

Thus, the monotonicity of unsecured debt issuance depends on the convexity or concavity of debt prices. If debt prices are convex, then unsecured debt issuance increases with leverage; if they are concave, it decreases. The convexity or concavity of debt prices depends on the parameter values used in estimating the model.

3.3 Crisis Dynamics with Short-Term Debt

A crisis is modelled as an unforeseen shock which causes productivity, A , to drop to ηA , where $\eta < 1$. The economy jumps back to its pre-shock equilibrium at the Poisson rate λ so that the expected length of the crisis is $1/\lambda$.

Additionally, let p_s^* equal the exogenous price of 1 unit of short-term secured debt during a crisis. If $p_s^* < 1$, then this is equivalent to investors demanding a haircut when lending to firms against their collateral, similar to repo haircuts. Short-term secured debt is issued at a premium if $p_s^* > 1$, which may be the case in the event of intervention. Note that absent an exogenous change in price, the endogenous price of short-term secured debt

would still be risk-free with price equal to one.

Proposition 2 (Crisis HJB with Binding Constraint). *The collateral constraint binds in a crisis regime, if p_s^* satisfies:*

$$\frac{\theta r}{1+r+\lambda} > 1 - p_s^* \quad (3.6)$$

That is, if the discounted value of the debt tax shield is greater than the haircut, the collateral constraint binds.

Given p_s^* so that the collateral constraint binds, the crisis joint equity and short-term debt HJB in the continuation region is:

$$\begin{aligned} 0 = \max_{b^u, g} \left\{ & - (r - g + \delta + \lambda)j + \eta A - \theta(\eta A - c^u f - c^s \alpha) - \Phi(g) \right. \\ & - (c^u + m^u)f + pb^u - c^s \alpha + \alpha(p_s^* - 1) + p_s^* \alpha(g - \delta) + \lambda \bar{j} \\ & \left. + [b^u - (g + m^u - \delta)f]j_f + \frac{1}{2} \sigma^2 f^2 j_{ff} \right\} \end{aligned} \quad (3.7)$$

where \bar{j} is the pre-shock value of equity and short-term debt. Note that \bar{j} can be solved independently of j .

Proof. See Section 3.6.6 in the Appendix. \square

The first order condition with respect to g is:

$$\begin{aligned} 0 = & j - f j_f - \Phi'(g) + p_s^* \alpha \\ \Rightarrow \Phi'(g) = & j - f j_f + p_s^* \alpha \end{aligned}$$

Thus, the exogenous price of secured debt directly impacts investment policy, while also indirectly affecting it through changes in the value function and hence, q .

Additionally, note that the crisis HJB for unsecured debt price is given by:

$$(r + m^u)p = c^u + m^u + [b^u - (g + m^u - \delta - \sigma^2)f]p_f + \frac{1}{2} \sigma^2 f^2 p_{ff} + \lambda(\bar{p} - p) \quad (3.8)$$

where \bar{p} is the pre-shock unsecured debt price consistent with \bar{j} .

3.3.1 Secured Debt Intervention

Proposition 3 (Secured Debt Intervention Strictly Increases Equity Value). *Consider an intervention in secured debt that results in an increase in the price of secured debt to a level higher than before intervention, such that Equation 3.6 is satisfied. As a result, the collateral constraint binds and there is a strict increase in both the joint value of equity and short-term debt, and the value of equity.*

Proof. See Section 3.6.7 in the Appendix. \square

Secured debt intervention is modeled as the central bank temporarily purchasing secured debt at a premium relative to the prevailing market price for the duration of a crisis.²⁰ Proposition 3 states that if such an intervention is sufficiently strong such that firms have an incentive to issue secured debt (i.e. Proposition 2 holds), then both the joint value of equity and short-term debt as well as just the value of equity are strictly increased. The result is not surprising, since the firm receives more proceeds from secured debt issuance when prices are higher, on the intensive margin, and on the extensive margin, sufficiently high secured debt prices make issuance worthwhile for the firm. Given these results, secured debt intervention is modeled as a premium offered above par in the numerical estimation, for simplicity.

Proposition 4 (Secured Debt Intervention Strictly Increases Investment). *Provided that Proposition 3 holds, investment is strictly increasing in the amount of secured debt intervention. Furthermore, the increase can be decomposed into direct and indirect channels.*

20. The nature of the secured debt intervention described here is analogous to the Bank Term Funding Program (BTFP) administered by the Fed to provide loans to financial institutions against collateral valued at par (hence, above market prices): <https://www.federalreserve.gov/newsevents/pressreleases/files/monetary20240124a1.pdf>.

- *Direct Channel: Higher proceeds from secured debt issuance directly boost investment by strengthening the motivation for the firm to invest and relax the collateral constraint.*
- *Indirect Channel: Higher value of Tobin's q , i.e. higher marginal value of capital, indirectly boosts investment.*

Proof. See Section 3.6.8 in the Appendix. □

Proposition 4 states that secured debt intervention strictly increases investment. Moreover, the higher the premium offered in the intervention, the higher the increase in investment. Secured debt intervention increases investment directly and indirectly. First, by making secured debt issuance more lucrative, intervention directly increases the motivation of the firm to invest and relax its collateral constraint. Second, secured debt intervention increases the value of Tobin's q , implying a higher marginal value of capital, thus indirectly stimulating investment.

Firms are still permitted to issue unsecured debt at market prices when secured debt intervention is operative. In the numerical results shown in Section 3.4, I find that firms receiving secured debt intervention experience an indirect increase in unsecured debt prices and increase both unsecured debt issuance and payouts. However, the investment response is stronger over much of the state space, implying declining leverage ratios, while firms' debt capacity (i.e. their default threshold) is further enhanced relative to the case without intervention. These two forces together lead to more favorable default dynamics.

3.3.2 Unsecured Debt Intervention

As in Crouzet and Tourre [2021], I model an unsecured debt intervention as the government becoming the marginal buyer in the unsecured debt market during a crisis period.

This results in segmented equity and credit markets. Hence, we would have different discount rates corresponding to equity investors, $r^{(e)}$, and unsecured debt investors, $r^{(d)}$.

Proposition 5 (Unsecured Debt Intervention Accelerates Issuance). *In the case where unsecured debt intervention segments equity and credit markets with the government becoming the marginal buyer of debt, the endogenous unsecured debt issuance policy becomes:*

$$b^u = \frac{\theta c^u}{-p_f} + \frac{(r^{(e)} - r^{(d)})p}{-p_f}$$

and is increasing in the wedge between the discount rates of equity investors, $r^{(e)}$, and the discount rate implied by the government's subsidy, $r^{(d)}$. Unsecured debt intervention implies $r^{(d)} < r^{(e)}$ and hence, higher issuance in the continuation region since p is decreasing in leverage and $p > 0$ outside of default.

Proof. See Section 3.6.9 in the Appendix. □

The nature of the unsecured debt intervention considered in Proposition 5 leads to an equilibrium increase in firms' unsecured debt issuance, but does not imply a higher price for unsecured debt. Indeed, the potential improvement in unsecured debt price implied by government intervention at lower discount rates is exactly offset by accelerated issuance which leaves unsecured debt price unchanged. This is a stark consequence of a lack of commitment to ex ante debt policy. Empirically, debt issuance does not completely offset the price impact of unsecured debt intervention, although it does accelerate significantly.

Proposition 6 (Unsecured Debt Intervention Accelerates Firm Payouts to Shareholders).

Proposition 5 shows that unsecured debt intervention accelerates the issuance of unsecured debt, while the price of unsecured debt is unaffected due to the intervention. This results in higher proceeds from unsecured debt issuance. Firms do not use these proceeds for investment but rather pay these out to shareholders. Higher payouts are exactly offset by a lower

joint continuation value for equity and short-term debt due to higher default costs induced by higher leverage.

Proof. See Section 3.6.10 in the Appendix. □

Proposition 6 implies that unsecured debt intervention increases firm leverage and defaults, relative to non-intervention, a prediction which is verified in the numerical estimation. While unsecured debt intervention does not affect the discounted equity price, since higher payouts and higher default costs due to higher leverage are exactly offset, it does imply negative dynamics for future investment.

If firms were able to commit to debt covenants limiting issuance, then more favorable dynamics would materialize: payouts would fall and investment would improve. This echoes the findings of DeMarzo, He, and Tourre [2023] in the sovereign debt context where restrictions on issuance lead to welfare improvements. Empirically, IG issuers have little to no financial or operating covenants on their corporate bond debt [Deng et al., 2016].²¹ Hence, I maintain the assumption that firms would not voluntarily commit to such covenants. Instead, I consider the case where unsecured debt intervention entails restrictions on firm operations, similar to imposing covenants.

3.3.3 Dividend Restriction

An alternative method to induce commitment is the use of dividend restrictions which prevents unsecured debt issuance from immediately being paid out as dividends. While a permanent dividend restriction will cause equity price to fall to 0, a temporary dividend restriction can be implemented during the crisis period while still maintaining positive equity prices. Given that unsecured debt intervention distorts firm incentives to accelerate

21. See also <https://www.lexisnexis.com/community/insights/legal/practical-guidance-journal/b/pa/posts/high-yield-vs-investment-grade-covenants>.

issuance to increase payouts to shareholders, a natural question is whether this force can be curtailed through the use of dividend restrictions, causing firms to increase investment instead.

Proposition 7 (Optimal Policies with Dividend Restrictions). *With dividend restrictions, investment (g) and unsecured debt issuance policies (b^u) satisfy:*

$$\begin{aligned}\pi(b^u, g) \equiv & \eta A - \theta(\eta A - c^u f - c^s \alpha) - \Phi(g) \\ & - (c^u + m^u)f + pb^u - c^s \alpha + \alpha(p_s^* - 1) + p_s^* \alpha(g - \delta) \leq 0\end{aligned}\tag{3.9}$$

Let l be the Lagrange multiplier on this constraint, where $l \geq 0$, with equality when the constraint is slack. Taking l as given, the crisis joint equity and short-term debt HJB with a temporary dividend restriction is:

$$0 = \max_{b^u, g} \left\{ -(r - g + \delta + \lambda)j + (1 - l)\pi(b^u, g) + \lambda\bar{j} + [b^u - (g - \delta + m^u)f]j_f + \frac{1}{2}\sigma^2 f^2 j_{ff} \right\} \tag{3.10}$$

The expressions for unsecured debt price, unsecured debt issuance, and investment are given by:

$$\begin{aligned}p &= -\frac{j_f}{1 - l} \\ g &= \frac{1}{\gamma} \left(\frac{j - f j_f}{1 - l} + p_s^* \alpha \right) \\ b^u &= (1 - l) \frac{\theta c^u}{j_{ff}} + l \frac{\lambda \bar{j}_f}{j_{ff}}\end{aligned}$$

Proof. See Section 3.6.11 in the Appendix. □

As a result of the dividend constraint, it is no longer the case that equity prices are invariant to unsecured debt policy. Additionally, given $l \in [0, 1)$, relative to the unconstrained case $l = 0$, unsecured debt price is higher, investment is higher, and unsecured

debt issuance is lower. In particular, Section 3.6.11 in the Appendix shows that investment is increasing in unsecured debt issuance when the dividend constraint binds.

Unlike before, it is possible that shareholders may wish to buy back debt when a dividend constraint is in place. Consequently, deviations of unsecured debt management from an unrestricted benchmark can be thought as having two drivers:

$$b^{\text{rest}} - b^{\text{unrest}} = - \underbrace{l \frac{\theta c^u}{j_{ff}}}_{\text{Reduced issuance motive}} - \underbrace{l \frac{\lambda \bar{p}}{j_{ff}}}_{\text{Debt repurchase motive}}$$

Interpreting l as the value shareholders assign to relaxing the dividend constraint, the more value shareholders assign to relaxing the constraint (and thereby being able to payout dividends), the more intense is their motivation to reduce issuance and to even buy-back debt. This decision can be pinned down by the following inequality:

$$\begin{aligned} (1 - l) \frac{\theta c^u}{j_{ff}} &< l \frac{\lambda \bar{p}}{j_{ff}} \\ \Rightarrow \theta c^u &< \frac{l}{1 - l} \lambda \bar{p} \end{aligned}$$

That is, when the debt tax shield is below some threshold defined by shadow value of issuing dividends and the jump probability weighted pre-crisis debt price, the firm will find it beneficial to make net repurchases of unsecured debt.

Section 3.4.3 discusses the numerical results for models with dividend restrictions accompanying unsecured debt intervention, with and without debt repurchase restrictions. As mentioned, the motivation is to see if firms will redirect the proceeds from unsecured debt intervention to investment from payouts when dividend restrictions are in place. While this does occur, the value of equity also falls. Moreover, firms engage in net repurchases of unsecured debt and when repurchases are restricted, they choose not to issue at all. Hence, while investment and default dynamics improve when unsecured debt intervention

is combined with dividend restrictions, the numerical analysis suggests that firms may not voluntarily participate in such a program.

3.4 Numerical Results

3.4.1 Model Calibration and Fit

Table 3.1: Calibrated Parameters

Parameter	Description	Value	Source
γ	Adjustment Cost Curvature	16	Caballero and Engel [1999]
A	Capital Productivity	0.24	Crouzet and Tourre [2021]
α	Capital Stock Pledgeability	0.20	Catherine et al. [2022]
σ	Capital Quality Volatility	0.31	Crouzet and Tourre [2021]
θ	Corporate Income Tax Rate	0.35	OECD [2020]
m^u, m^s	Debt Amortization Rate	0.10	Saretto and Tookes [2013]
δ	Depreciation Rate	0.10	Hennessy and Whited [2005]
r	Risk-Free Rate	0.05	Crouzet and Eberly [2020]

The table reports the calibrated parameters used in the numerical solution of the model presented in Section 3.4. The parameters are chosen to correspond with those used by Crouzet and Tourre [2021], with the exception of the curvature of the capital adjustment cost function, γ , the proportion of the capital stock pledgeable as collateral, α , and the initial distribution of debt to capital, f . Crouzet and Tourre [2021] estimate γ , the productivity of capital, A , and the volatility of capital quality, σ , targeting the slope of investment with respect to (net) debt to EBITDA, the average investment rate, and the average (net) debt to EBITDA as empirical moments for identification (see Table 3.2). The capital adjustment costs differ in this paper to ensure that investment is non-negative in equilibrium, which simplifies the modeling of fully collateralized secured debt. The selected value for γ lies in the range reported by Falato et al. [2022] of 2 to 20, matching the value of 16 estimated by Caballero and Engel [1999]. The selected value for α corresponds to the lower-bound of the range (0.20 to 0.25) estimated by Catherine et al. [2022]. This parameter is not present in Crouzet and Tourre [2021], since they do not model secured debt. The initial distribution of debt to capital is shown in Figure 3.13. It is proxied by gross liabilities to assets taken from Compustat.

Table 3.1 reports the calibrated parameters used in the numerical solution of the model reported in this section. The parameters are chosen to correspond with those used by Crouzet and Tourre [2021], with the exception of the curvature of the capital adjustment cost function, γ , the proportion of the capital stock pledgeable as collateral, α , and the initial distribution of debt to capital, f . Crouzet and Tourre [2021] estimate γ , the productivity of capital, A , and the volatility of capital quality, σ , targeting the slope of investment with respect to net debt to EBITDA, the average investment rate, and the average net debt to EBITDA as empirical moments for identification (see Table 3.2).

The specification for capital adjustment costs differs in this paper to ensure that invest-

ment is non-negative in equilibrium, which simplifies the modeling of fully collateralized secured debt. The selected value for γ lies in the range reported by Falato et al. [2022] of 2 to 20, matching the value of 16 estimated by Caballero and Engel [1999]. The selected value for α corresponds to the lower-bound of the range (0.20 to 0.25) estimated by Catherine et al. [2022]. This parameter is not present in Crouzet and Tourre [2021], since they do not model secured debt.

The initial distribution of debt to capital is shown in Figure 3.13. It is proxied by gross liabilities to assets taken from Compustat. The choice of initial distribution does not impact the model solution but does affect the calculation of the model implied moments. While Crouzet and Tourre [2021] target debt net of cash holdings for empirical moments, initializing the model with the empirical distribution of net debt to capital would lead to negative values for the state variable, which is ruled out by assumption and presents complications (i.e. net lending by non-financial firms) that are out of scope for this paper.

Table 3.2 reports the implied moments from the model presented in this paper (column corresponding to ‘Model’) and compares these against the empirical moments computed by Crouzet and Tourre [2021] (‘Data’), as well as the moments implied by their model (‘CT21’). Since Crouzet and Tourre [2021] target the average net debt to EBITDA, the average investment rate, and the slope of investment with respect to net debt to EBITDA in their estimation of parameters, these moments are particularly well-matched for their model. Since this paper initializes the distribution of debt to capital with the empirical gross leverage ratio, instead of net debt, the model implied moments are larger for debt to EBITDA and inverse interest coverage ratio.

The default rate comes from S&P [2025] data for 2019. While the values are similar, the model implied default rate is lower for this paper, despite higher starting debt levels. This is consistent with secured debt enhancing overall debt capacity. Similarly, the model implied average credit spreads are slightly lower in this paper than in Crouzet and Tourre

Table 3.2: Model Fit

Description	Source	Data	CT21	Model
Average Credit Spreads	Feldhütter and Schaefer [2018]	0.87-4.17	4.98	4.76
Average Debt Issuance Rate	Compustat	25.7	17.9	23.1
Average Debt to EBITDA	Compustat	2.13	2.14	3.08
Average Equity Payout Rate	Compustat	4.6	3.0	5.0
Average Inverse Interest Coverage Ratio	Compustat	11.3	10.7	15.4
Average Investment Rate	Compustat	11.28	11.28	9.55-16.88
Default Rate (2019)	S&P [2025]	1.3	1.5	1.3
Slope of Inv. wrt Debt to EBITDA	Compustat	-1.04	-1.04	-1.15

The table reports the implied moments from the model presented in this paper (column corresponding to ‘Model’) and compares these against the empirical moments computed by Crouzet and Tourre [2021] (‘Data’), as well as the moments implied by their model (‘CT21’). Crouzet and Tourre [2021] estimate γ , the productivity of capital, A , and the volatility of capital quality, σ , reported in Table 3.1, targeting the slope of investment with respect to debt-to-EBITDA, the average investment rate, and the average debt-to-EBITDA as empirical moments for identification. As a result, the ‘Data’ and ‘CT21’ moments closely match for these variables. Crouzet and Tourre [2021] reports empirical moment for debt to EBITDA for debt net of cash. In contrast, this paper uses the initial debt to capital distribution for gross book leverage, to avoid negative net debt values (see Figure 3.13). This results in higher model implied moments for debt to EBITDA and inverse interest coverage ratio. The default rate comes from S&P [2025] data for 2019. While the values are similar, the model implied default rate is lower for this paper, despite higher starting debt levels. This can be due to two forces: 1. firm restructuring, rather than liquidation, after default, in Crouzet and Tourre [2021] and 2. secured debt enhancing overall debt capacity in this paper. Similarly, the model implied average credit spreads are slightly lower in this paper than in Crouzet and Tourre [2021]. The empirical moments for average credit spreads come from Feldhütter and Schaefer [2018] and cover the range of credit spreads for investment-grade (IG) and high-yield (HY) firms. Crouzet and Tourre [2021] present investment rates gross of capital adjustment costs. The range of investment rates with and without capital adjustment costs are reported for this paper; the interval contains both the empirical and model moments reported by Crouzet and Tourre [2021]. Higher gross investment rates in this paper are driven by the presence of secured debt which incentivizes higher investment to generate more pledgeable collateral. The moments for average debt issuance, average equity payout rate, and the slope of investment with respect to debt to EBITDA are broadly aligned across the three estimates.

[2021]. The empirical moments for average credit spreads come from Feldhütter and Schaefer [2018] and cover the range of credit spreads for investment-grade (IG) and high-yield (HY) firms.

Crouzet and Tourre [2021] present investment rates gross of capital adjustment costs. The range of investment rates with and without capital adjustment costs are reported for this paper; the interval contains both the empirical and model moments reported by Crouzet and Tourre [2021]. Higher gross investment rates in this paper are driven by the presence of secured debt which incentivizes higher investment to generate more pledgeable collateral. The moments for average debt issuance, average equity payout rate, and the slope of investment with respect to debt to EBITDA are broadly aligned across the three estimates.

3.4.2 Numerically Solved Model and Dynamics

Section 3.6.13 in the Appendix presents the details for numerically solving equity and unsecured debt prices in the model with short-term debt, as well as the model with dividend restrictions. Additional parameters are reported in Section 3.6.14 in the Appendix across the different economic environments considered for the model dynamics. As a preview of the results, secured debt intervention leads to higher equity values and investment, relative to no intervention. In addition, it leads to more favorable firm dynamics with longer-term improvements in investment and lower default rates. In contrast, while unsecured debt intervention does not alter current equity values and investment, it does lead to worse longer-term outcomes, driven by higher leverage and default rates among firms.

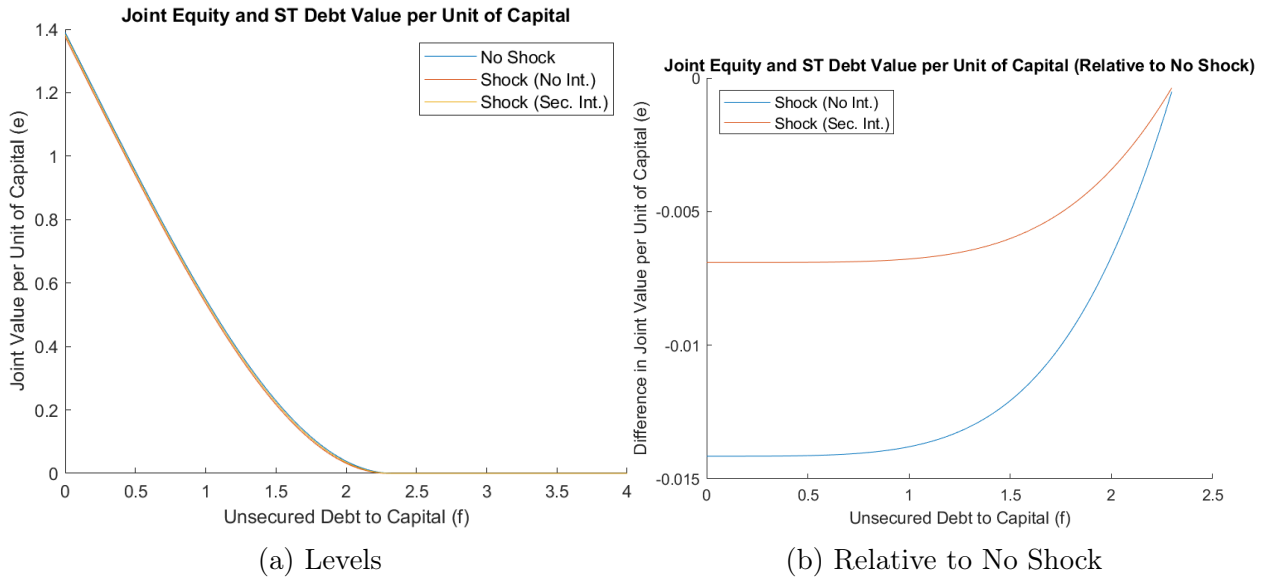


Figure 3.1: Secured Debt Intervention Boosts Equity Prices After Shock

I estimate both current prices and investment policies, as well as the dynamics. Figure 3.1 shows the joint value of equity and short-term debt for the different economies considered in the baselines analysis: prices with no shock, with shock but no secured debt intervention, and with shock and secured debt intervention. Prices are unaffected by trading or unsecured debt interventions. That is, the trade and no trade solutions for the joint value

of equity and short-term debt coincides. Consequently, secured debt intervention improves the joint value of equity and short-term debt relative to both no intervention and uncured debt intervention, as emphasized in Figure 3.1b.

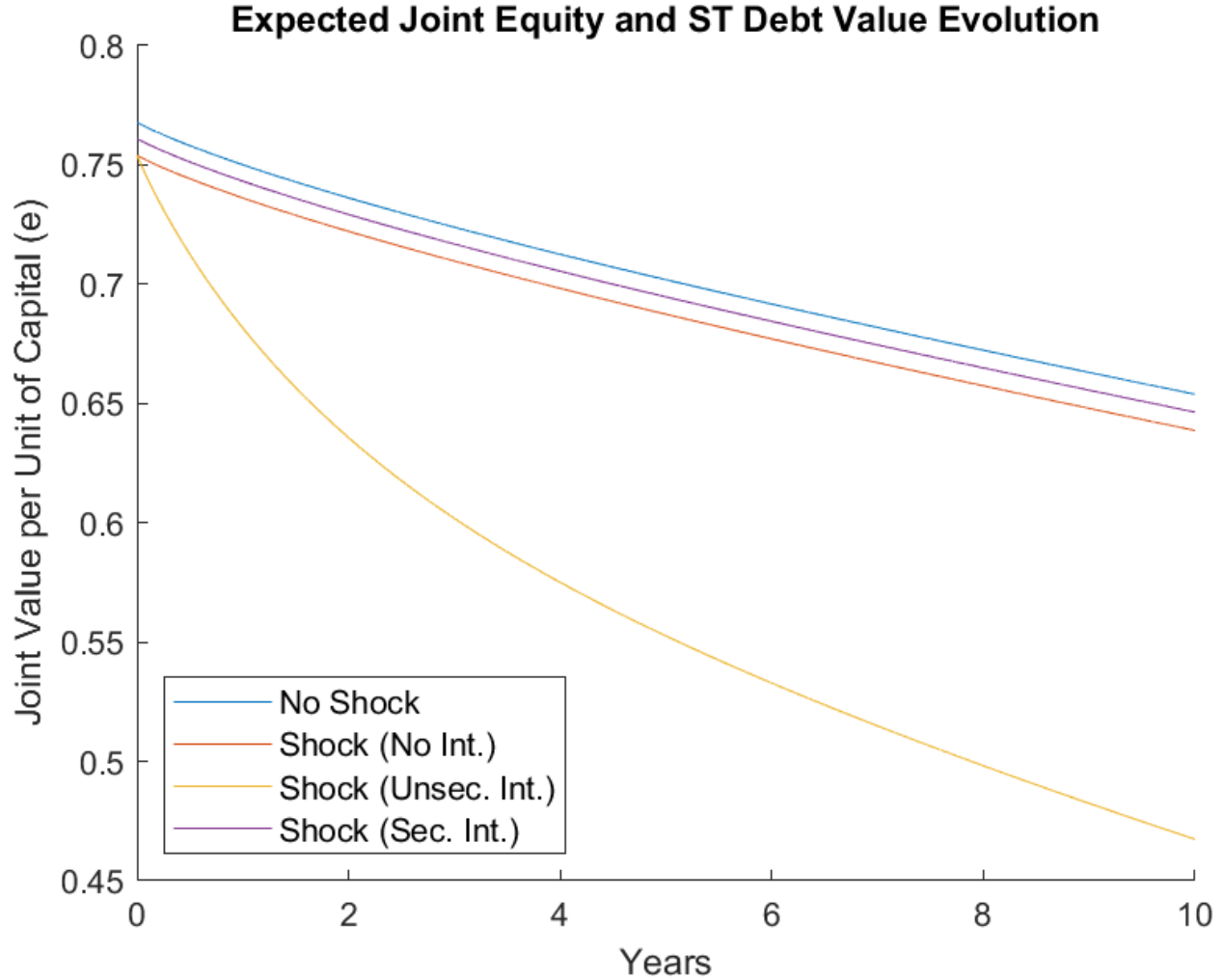


Figure 3.2: Expected Equity Value Evolution Higher with Secured Debt Intervention

Figure 3.2 shows the long-run dynamics in average expected joint value of equity and short-term debt. The evolution of joint values shows that the economy with secured debt intervention dominates the economies with no intervention or unsecured debt intervention. In fact, the evolution of expected joint values are worst with unsecured debt interventions, reflecting the perverse effects induced by no commitment: unsecured debt intervention boosts dividend payments exactly at the same rate as it accelerates the firms movement

toward default.

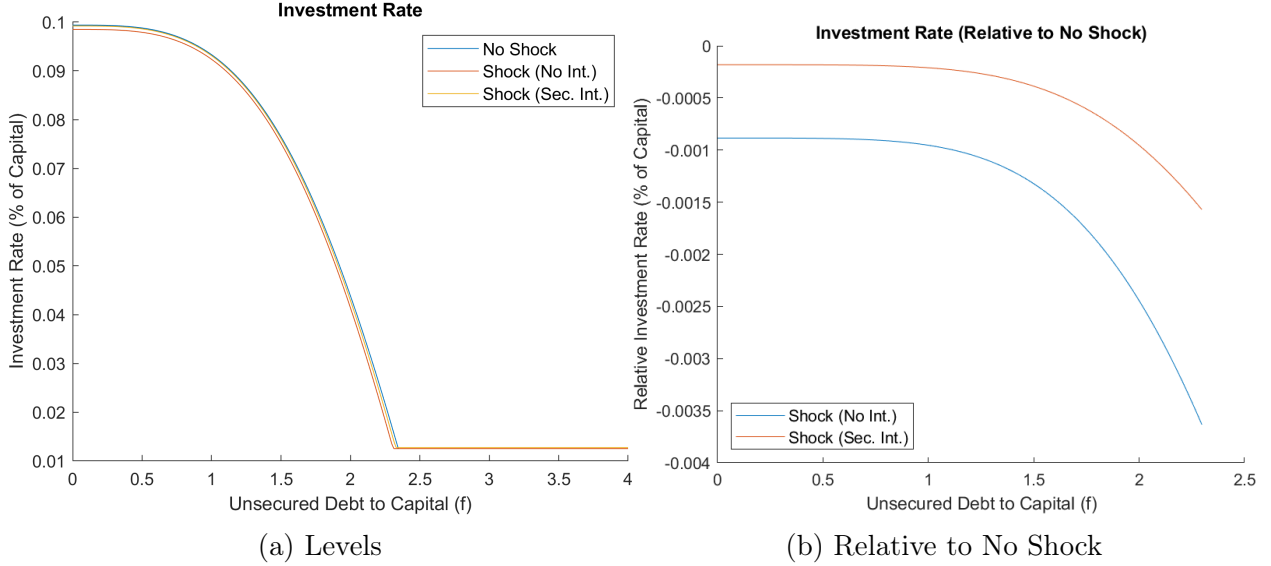


Figure 3.3: Investment Rate Higher with Secured Debt Intervention

Consistent with Figure 3.3, we see that secured debt intervention boosts investment relative to no intervention (and hence, unsecured debt intervention) after an economy experiences a shock.

The evolution of expected investment rates, shown in Figure 3.4, is analogous to that of equity prices, with secured debt intervention resulting in a higher path of expected investment versus no intervention and, especially, unsecured debt intervention.

Unsecured debt prices are shown in Figure 3.5. In contrast to joint equity and short-term debt prices, dispersion in unsecured debt prices is initially low for lower leverage and increases closer to the default threshold. Given the parameter values used, debt prices are concave and lead to monotonically decreasing issuance rates, as seen in Figure 3.6a. Following the shock, unsecured debt issuance falls for the cases with no intervention and secured debt intervention but rises with unsecured debt intervention, as seen in Figure 3.6b.

As with equity prices, the evolution of unsecured debt prices is higher with secured debt intervention than unsecured debt intervention, as seen in Figure 3.7. In fact, the economy with unsecured debt intervention has lower future expected prices. This underscores how

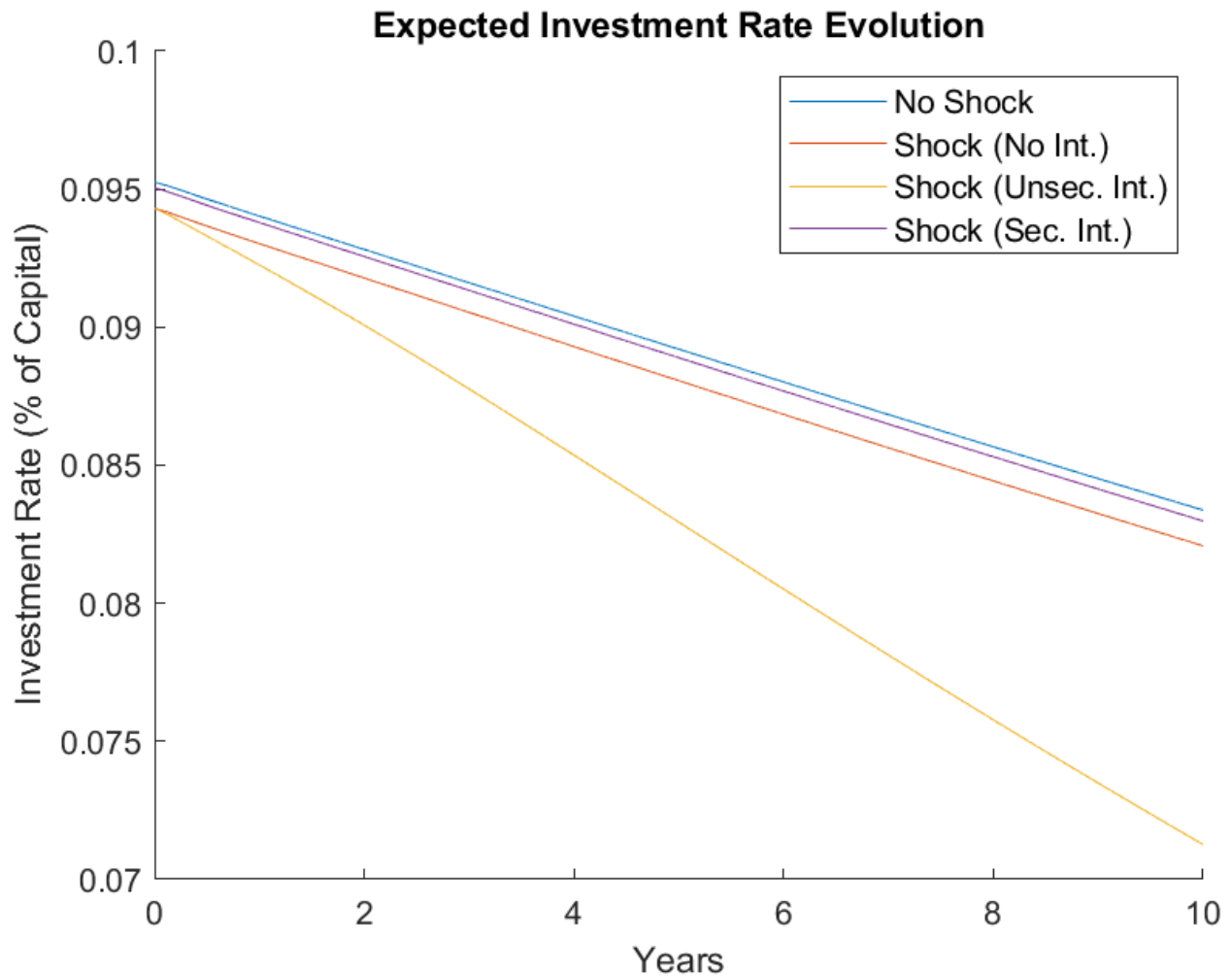


Figure 3.4: Evolution of Expected Investment Rates Higher with Secured Debt Intervention

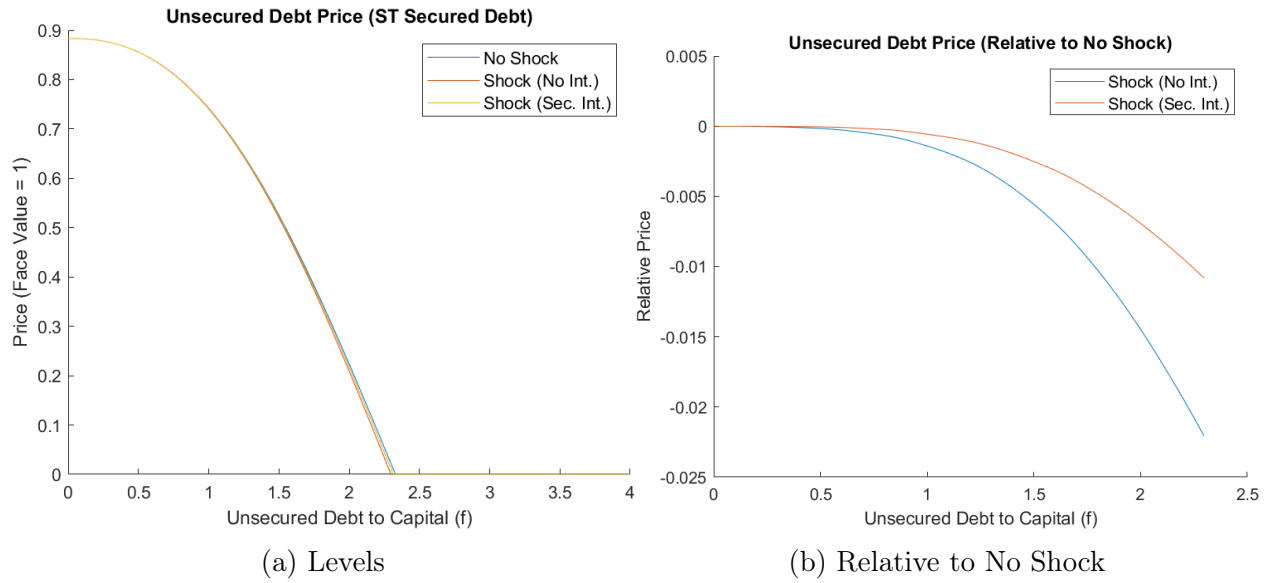


Figure 3.5: Unsecured Debt Prices Higher With Secured Debt Intervention for More Leveraged Firms

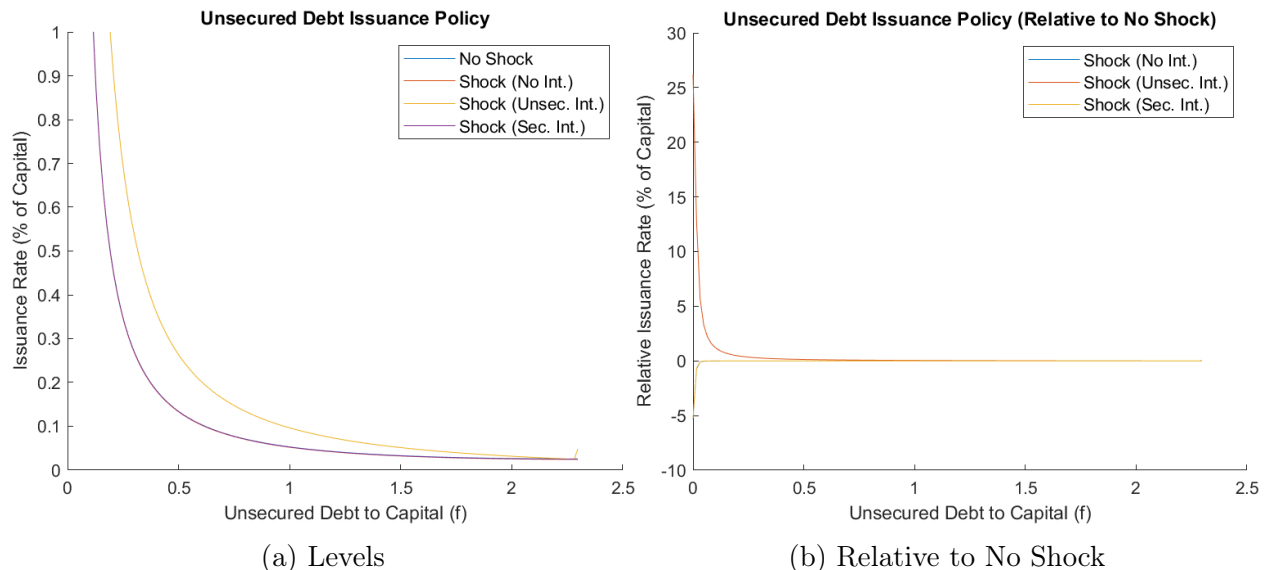


Figure 3.6: Unsecured Debt Issuance Rate Higher with Intervention

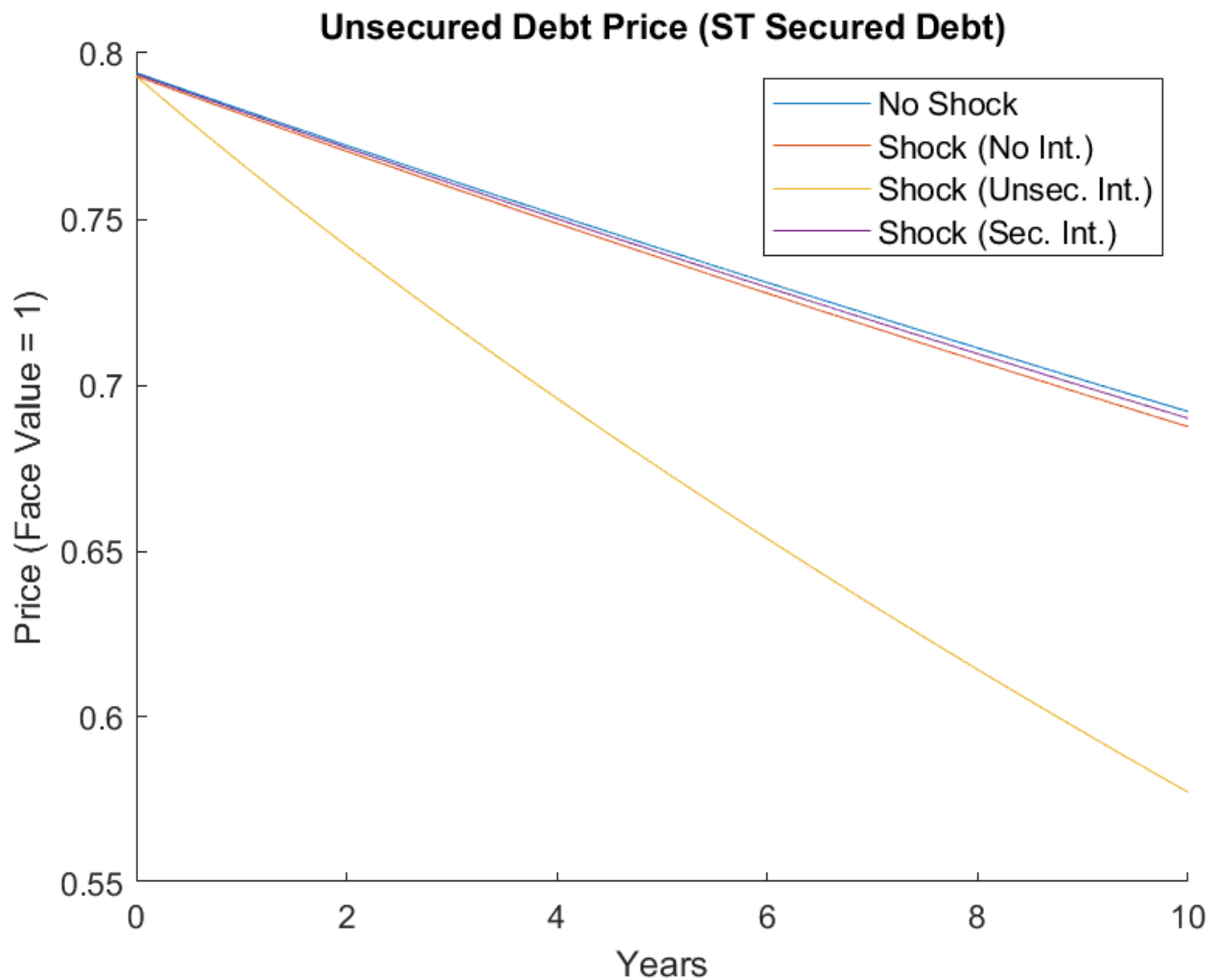


Figure 3.7: Secured Debt Intervention Boosts Unsecured Debt Price More Than Unsecured Debt Intervention

unsecured debt intervention may be counter-productive: firms increase debt issuance in response to the government becoming the marginal buyer at lower discount rates, which increases in default risk. The proceeds from accelerated debt issuance are paid out to shareholders while firms indebtedness increases; these two forces exactly offset each other, such that the unsecured debt price with unsecured debt intervention is unchanged from the no trade unsecured debt price.

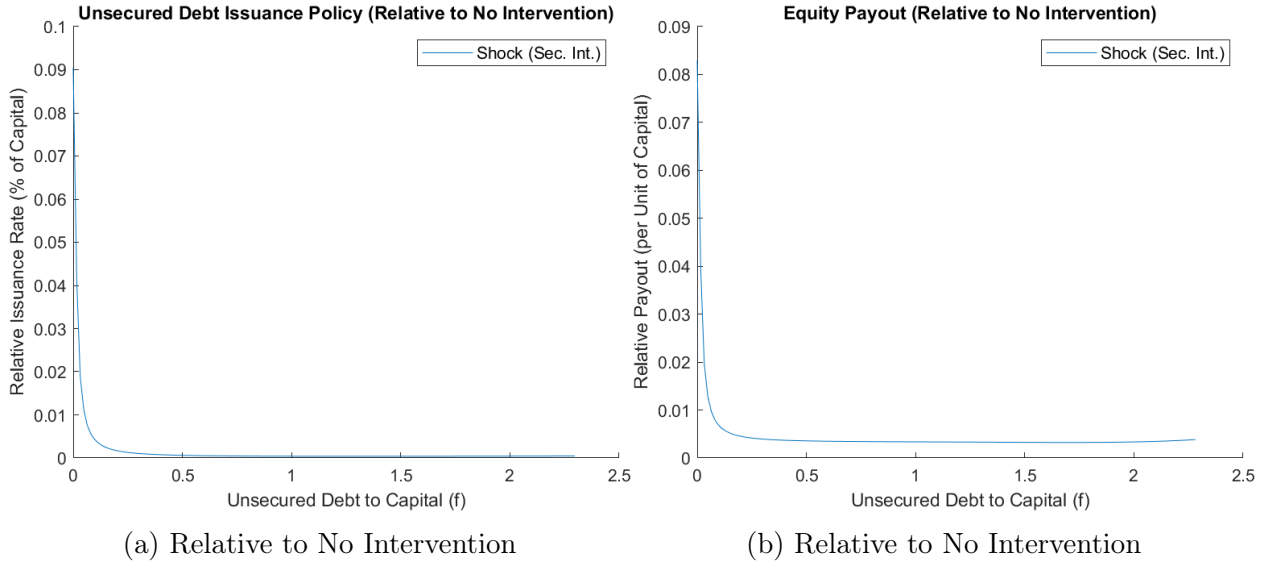


Figure 3.8: Secured Debt Intervention Increases Unsecured Debt Issuance and Payouts

Figure 3.5 shows that secured debt intervention also boosts the price of unsecured debt, while Figure 3.8 shows that, relative to no intervention, secured debt intervention leads to higher unsecured debt issuance and payouts. Nonetheless, the increase in investment, as shown in Figure 3.3, exceeds increased unsecured debt issuance over much of the state space, implying decreasing leverage ratios. Additionally, secured debt intervention also increases the debt tolerance of firms, as shown in Figure 3.9. While the default threshold decreases post-shock, the decrease is lower with secured debt intervention than no intervention, as seen in Figure 3.9b. This provides another benefit of secured debt intervention in addition to directly boosting investment.

Consistent with higher default thresholds, cumulative default is lower with secured debt

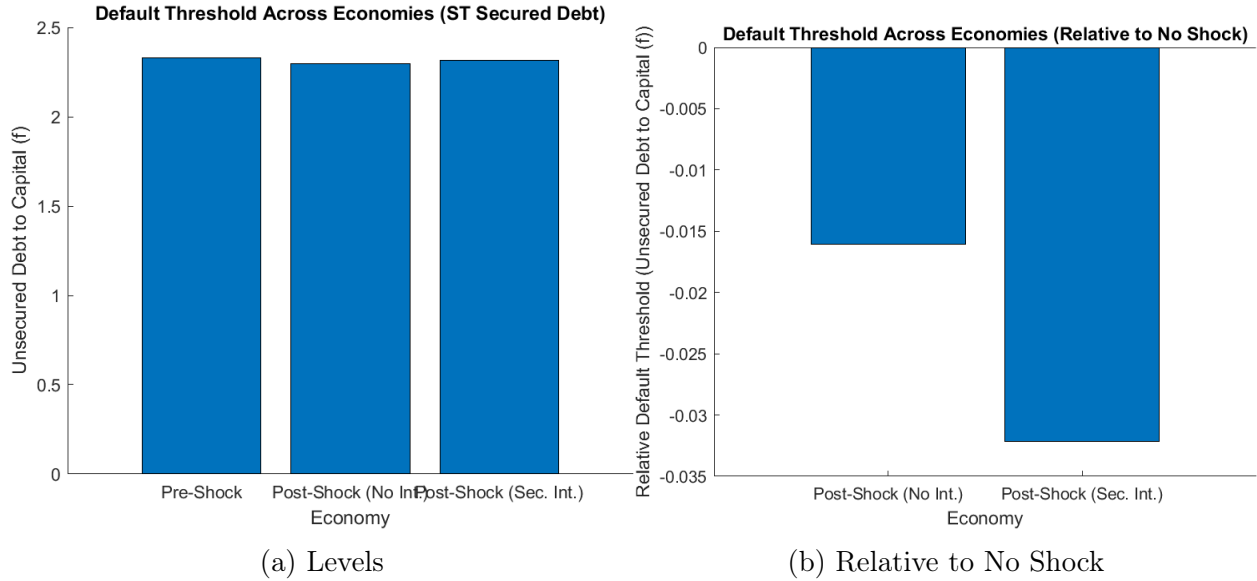


Figure 3.9: Secured Debt Intervention Pushes Back Default Threshold

intervention, as seen in Figure 3.10. Echoing the evolution of unsecured debt prices, unsecured debt intervention results in the greatest number of cumulative defaults, despite not affecting the default threshold. Instead, unsecured debt intervention accelerates the path to default by encouraging unsecured debt issuance.

Figure 3.11 depicts the long-run distribution of surviving firms. All of the distributions are right-skewed because of the mean reverting nature of the dynamics, and the proportionally slower rate of issuance for more indebted firms.

Figure 3.12 shows the CDFs of surviving firms. Unsecured debt intervention results in a notable rightward shift in the CDF of surviving firms, suggesting that these firms have higher levels of leverage. Figure 3.12b computes the difference between the CDF for the economy where there is secured debt intervention versus the economy with no intervention. The non-negative values indicate that the CDF for the economy with secured debt intervention exhibits (weak) first order stochastic dominance over the corresponding distribution for the economy with no intervention, as well as the economy with unsecured debt intervention.

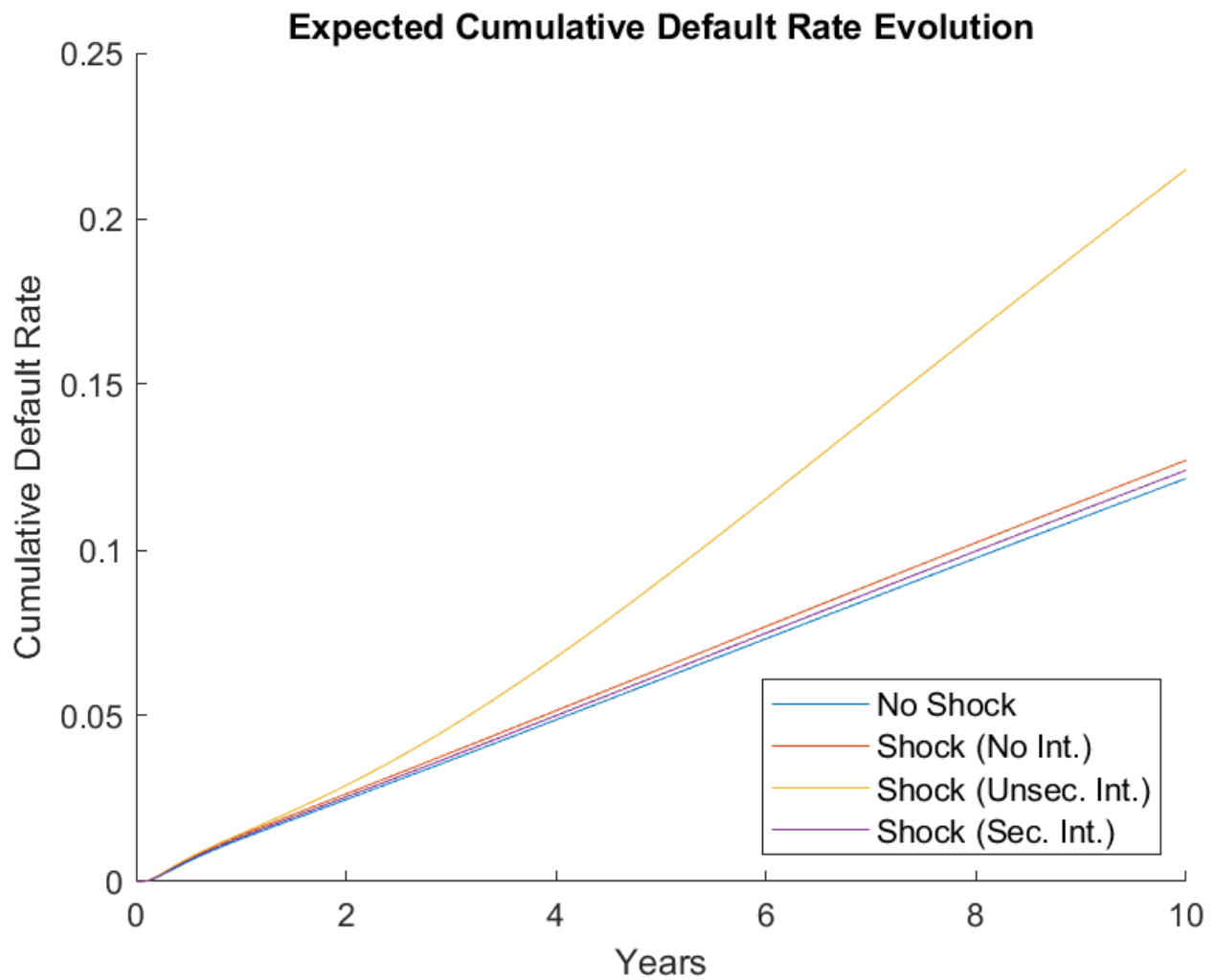


Figure 3.10: Secured Debt Intervention Reduces Expected Cumulative Default Rates

Surviving Firm Distribution after 10 Years (ST Secured Deb)

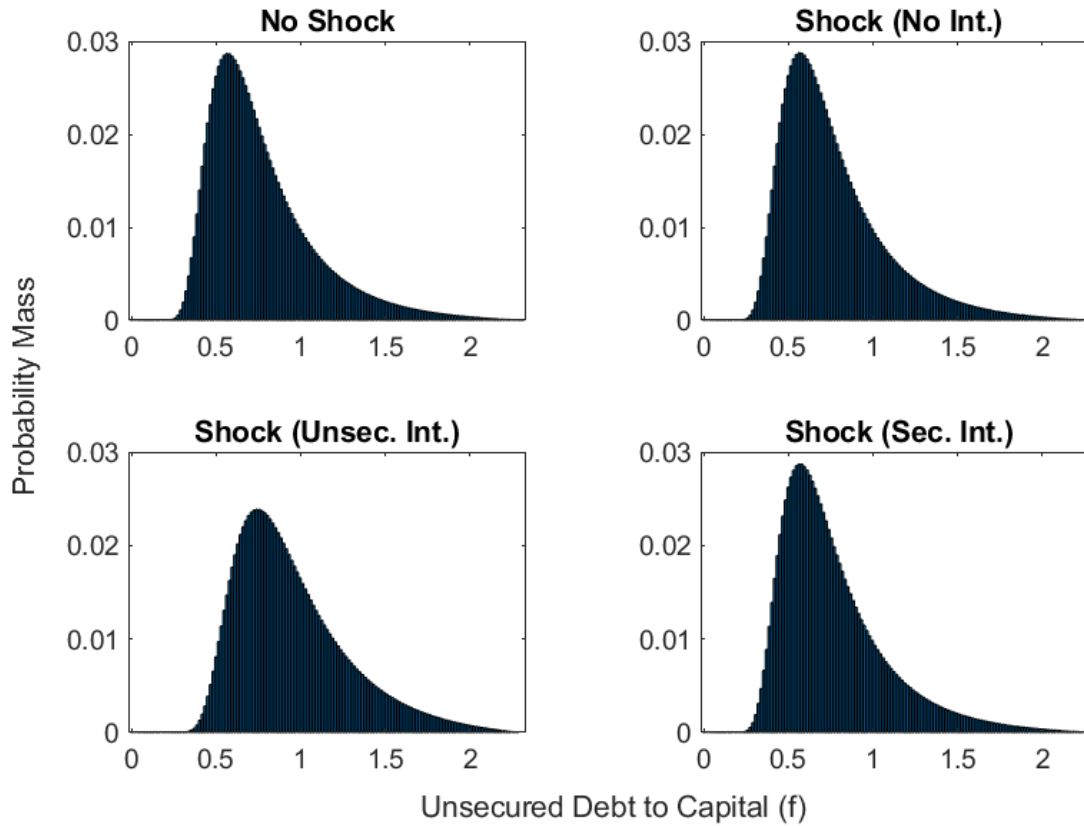


Figure 3.11: Secured Debt Intervention Supports Higher Leverage Ratios

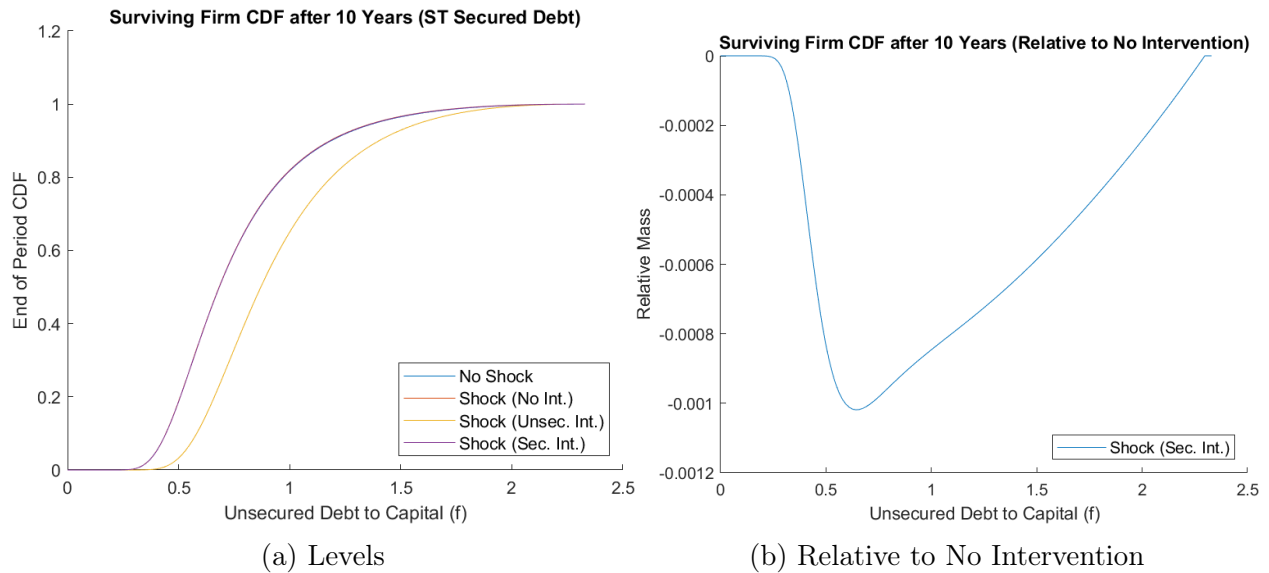


Figure 3.12: Secured Debt Intervention Distribution Features First Order Stochastic Dominance Over Unsecured Debt Intervention

3.4.3 *Dividend and Debt Repurchase Restrictions with Unsecured Debt Intervention*

Section 3.6.13 in the Appendix provides details on the numerical solution method to solve the extension to the baseline model with nonlinear policy constraints. I consider both dividend restrictions with and without a constraint on unsecured debt repurchases. Both economies with dividend restrictions also feature unsecured debt intervention (see Section 3.6.14 in the Appendix). Critically, the dividend restriction is only in place for the duration of the crisis; otherwise, if it were permanent, equity prices would fall to zero as shareholders would derive no value from owning equity.

Dividend restrictions lead to more beneficial investment outcomes, lower leverage, and more favorable investment and default dynamics. Unlike before, unsecured debt prices are also higher with intervention. However, they lead to lower equity prices and even create an incentive for firms to repurchase unsecured debt. If debt repurchases are further restricted, firms choose not to issue unsecured debt when they otherwise would have repurchased debt. All together, the numerical solutions suggest firms would not voluntarily participate in an unsecured debt intervention program with dividend restrictions.

3.5 Conclusion

Empirical research has shown that central bank corporate bond purchase programs in Europe and the United States led to an increase in leverage for directly targeted firms. The payouts of these firms to shareholders increased relative to other firms, while investment did not. A commonality of both programs is that they primarily involved interventions in the unsecured debt of financially unconstrained firms. This paper shows that a dynamic capital structure model where firms cannot commit to a debt issuance policy *ex ante* can reproduce these stylized facts.

Without commitment, firms accelerate the issuance of unsecured debt following intervention. The additional proceeds are distributed to shareholders and are not used for investment. Higher firm payouts and higher leverage directly offset each other to leave the firm's current discounted equity valuation unchanged. However, the greater debt burden translates into worse investment and default dynamics for firms. In contrast, secured debt issuance features implicit commitment induced by the firm's collateral constraint. While the scope of secured debt intervention is far more limited, I show theoretically and numerically that secured debt intervention can improve investment outcomes and default dynamics for firms, both relative to the case of no intervention and especially the case of unsecured debt intervention.

Imposing dividend restrictions while intervening in unsecured debt reduces the negative impact of the lack of firms' commitment to an *ex ante* debt policy, leading to higher unsecured debt prices, greater investment, and more favorable credit dynamics. However, dividend restrictions also lead to a drop in firms' equity valuation and actually induce firms to repurchase unsecured debt. Restricting debt repurchases further increases investment but does not improve equity valuation. These results suggest that firms would not voluntarily participate in unsecured debt intervention programs with dividend restrictions, since it would not be optimal from a valuation standpoint.

To the extent that central banks motivated their interventions by arguing real outcomes would be improved from loosening financial conditions, the findings in this paper on the improved dynamics generated by secured debt intervention, compared to unsecured debt intervention, are important. However, this paper abstracts away from any potential moral hazard induced by such credit programs. Nor does it address other concerns around directing monetary stimulus to relatively unconstrained and large firms, such as negative effects on competitiveness or welfare implications. Policymakers will need to balance these concerns against any potential benefits in future interventions in corporate credit markets.

3.6 Appendix

3.6.1 Strict Convexity of the Joint Value Function

Proposition 8 (Strict Convexity of the Joint Value Function). *Let $j(f)$ denote the maximized joint value function of the firm given a debt to capital ratio f . Then, $j(f)$ is strictly convex in the continuation region (outside of default); that is, for any two feasible leverage levels f_1 and f_2 and for any $\lambda \in (0, 1)$, if we define*

$$f_\lambda = \lambda f_1 + (1 - \lambda) f_2,$$

we have

$$\lambda j(f_1) + (1 - \lambda) j(f_2) > j(f_\lambda).$$

Proof. Let the firm's optimized joint value function be given by $j(f)$ with values $j(f_1)$ and $j(f_2)$ for feasible leverage values f_1 and f_2 . Consider the convex combination

$$f_\lambda = \lambda f_1 + (1 - \lambda) f_2,$$

which is a feasible debt level by the continuity of j .

Since $j(f_1)$ and $j(f_2)$ represent optimized values, any deviation from the optimal policies cannot produce a higher value. That is, if the firm with leverage f_1 deviates to f_λ , then

$$j(f_1) > j(f_\lambda) + (f_\lambda - f_1)p(f_\lambda),$$

where $p(f_\lambda)$ is the price of unsecured debt given leverage f_λ . Since f_λ lies in the continuation region, $p(f_\lambda) > 0$. Then, $(f_\lambda - f_1)p(f_\lambda)$ is the incremental proceeds from deviating to

f_λ from f_1 . Analogously, a deviation from f_2 gives

$$j(f_2) > j(f_\lambda) + (f_\lambda - f_2)p(f_\lambda).$$

Take the weighted average of these two inequalities by multiplying the first by λ and the second by $(1 - \lambda)$. Add the two together to obtain:

$$\lambda j(f_1) + (1 - \lambda)j(f_2) > \lambda j(f_\lambda) + \lambda(f_\lambda - f_1)p(f_\lambda) + (1 - \lambda)j(f_\lambda) + (1 - \lambda)(f_\lambda - f_2)p(f_\lambda).$$

This simplifies to:

$$\lambda j(f_1) + (1 - \lambda)j(f_2) > j(f_\lambda) + [\lambda(f_\lambda - f_1) + (1 - \lambda)(f_\lambda - f_2)] p(f_\lambda).$$

Note that by the definition of f_λ ,

$$\lambda(f_\lambda - f_1) + (1 - \lambda)(f_\lambda - f_2) = 0.$$

Thus, the inequality reduces to:

$$\lambda j(f_1) + (1 - \lambda)j(f_2) > j(f_\lambda).$$

Since the above inequality holds for any $\lambda \in [0, 1]$ and any two feasible leverage levels f_1 and f_2 , it follows by definition that the function $j(f)$ is strictly convex in the continuation region (outside of default). \square

3.6.2 Collateral Constraint with Short-Term Secured Debt

This section provides the proof for Proposition 1.

Proof. Note that by the complementary slackness condition:

$$-l^s(s - \alpha) = 0, l^s \geq 0$$

That is, either the constraint binds, $l^s > 0, s = \alpha$, or there is slack, $l^s = 0, s < \alpha$.

To obtain equilibrium conditions on the derivatives of the value function, take the first order condition with respect to b^s and take successive derivatives to obtain:

$$j_s = -1$$

$$j_{ss} = 0$$

$$j_{sss} = 0$$

$$j_{ffs} = 0$$

$$j_{fs} = 0$$

To obtain the value for p_s , take the first order condition of the HJB with respect to b^u , which yields $p = -j_f$. Differentiating with respect to s and using the expression for $j_{fs} = 0$ yields $p_s = 0$. Intuitively, this follows because the issuance of secured short-term debt does not entail additional bankruptcy costs.²²

To obtain an expression for the Lagrange multiplier, l^s , differentiate the HJB equation with respect to s , appealing to the envelope condition for the controls and using the equi-

22. This contrasts with Hu, Varas, and Ying [2024] where unsecured short-term debt is exposed to default risk via jumps, and the firm has the ability to issue risky short-term debt.

librium derivative conditions for j :

$$\begin{aligned}
0 &= -(r - g + \delta)j_s - l^s + \theta c^s - c^s - (g - \delta)e_s \\
&= (r - g + \delta) - l^s + \theta c^s - c^s + (g - \delta) \\
\Rightarrow l^s &= r - c^s + \theta c^s
\end{aligned}$$

Since $c^s = r$, $l^s > 0$, and the collateral constraint always binds.²³

$$l^s = \theta c^s$$

Interpreting l^s as the value of the collateral constraint, it is intuitively equal to the debt tax shield when the coupon is set equal to the discount rate and the discount rate when the coupon equals zero.

With $s = \alpha$, and given the equilibrium derivative conditions, obtain:

$$\begin{aligned}
0 = \max_{g, b^u} \left\{ & - (r - g + \delta)j + A - \theta(A - c^u f - c^s \alpha) - \Phi(g) - (c^u + m^u)f + pb^u - c^s \alpha \right. \\
& \left. + \alpha(g - \delta) + [b^u - (g - \delta + m^u)f]j_f + \frac{1}{2}\sigma^2 f^2 j_{ff} \right\}
\end{aligned}$$

Appendix 3.6.4 shows that this is the same HJB equation that is obtained if one starts by assuming that the collateral constraint always binds before deriving the HJB equation.

□

23. Alternatively, if markets are segmented and lenders discount at a lower rate than borrowers, such that $c^s = \rho > r$, the collateral constraint still binds without the debt tax shield, i.e. $\theta = 0$

3.6.3 Collateral Constraint with Long-Term Secured Debt

As before, shareholders and creditors are risk-neutral with discount rate r . Shareholders have the option to default on any security and at default, unsecured creditors have no recovery value while secured creditors receive the value of collateral. Equity investors are deep-pocketed. Capital adjustment costs are parameterized so that investment is nonnegative.

Firms' production technology, in revenue per unit of time, is given by:

$$Y_t = A_t K_t$$

The productivity parameter A_t evolves as:

$$\frac{dA_t}{A_t} = \mu dt + \sigma dZ_t$$

where μ is the constant rate of drift and dZ_t is the increment of a Brownian motion with distribution given by $dZ_t \sim N(0, dt)$.

Capital K_t evolves as:

$$\frac{dK_t}{K_t} = (g_t - \delta)dt$$

where g_t is the endogenous investment rate (the capital stock rate of growth) and δ is the capital depreciation rate. The price of capital is fixed at 1. The absence of shocks to the capital process renders it locally deterministic. This helps to simplify the pricing of long-term secured debt.

Investing entails paying capital adjustment costs (per unit of capital), which are increas-

ing and convex:

$$\Phi(g_t) = \frac{1}{2}\gamma g_t^2$$

where $\gamma > 0$ drives the cost of adjustment.

Unsecured debt has aggregate face value F_t and is endogenous. It matures at a Poisson rate m^u and hence, has expected maturity $1/m^u$. Individual bonds have face value equal to 1 and pay coupon rate $c^u = r$. Given default risk, unsecured debt is risky and pays $p_t < 1$. The evolution of unsecured debt stock is given by:

$$dF_t = \underbrace{-m^u F_t dt}_{\text{maturing debt}} + \underbrace{d\Gamma_t^u}_{\text{active debt management}}$$

I restrict my attention to the ‘smooth’ equilibrium where $d\Gamma_t^u = B_t^u dt$.

Firms can issue secured debt maturity at the rate $m^s = \delta$ and coupon rate equal to $c^s = r$. The collateral constraint is $S_t \leq \alpha K_t$, where S_t is the value of secured debt and α is the proportion of the capital stock that can be pledged. Since the investment rate g_t will be non-negative (in equilibrium), the assumption that secured debt matures at the same rate as capital depreciates, no shocks to the capital stock (so, capital is locally deterministic), and because α is constant, secured debt will always be exactly collateralized. Hence, with $c^s = r$, secured debt is risk-free and issued at par equal to 1 for face value equal to 1. The secured debt stock evolves as:

$$dS_t = \underbrace{-m^s S_t dt}_{\text{maturing debt}} + \underbrace{B_t^s dt}_{\text{active debt management}}$$

Given constant corporate tax rate θ , firm pays $\theta(Y_t - c^u F_t - c^s S_t)$ in corporate taxes.

Equity payout ($Payout_t$) equals:

$$\begin{aligned}
& \underbrace{A_t K_t}_{\text{cash flows}} - \underbrace{\theta(A_t K_t - c^u F_t - c^s S_t)}_{\text{corporate taxes}} - \underbrace{\Phi(g_t) K_t}_{\text{investment cost}} \\
& - \underbrace{(c^u + m^u) F_t}_{\text{unsecured debt interest \& principal}} - \underbrace{(c^s + m^s) S_t}_{\text{secured debt interest \& principal}} \\
& + \underbrace{p_t B_t^u}_{\text{unsecured debt issuance/repurchase}} + \underbrace{B_t^s}_{\text{secured debt issuance/repurchase}}
\end{aligned}$$

If positive, equity pays out dividends to investors. If negative, equity receives a cash infusion from deep pocketed investors.

Shareholders take debt price p_t as given and maximize:

$$\begin{aligned}
E(A, K, F, S) &= \max_{g, B^u, B^s, \tau} \left\{ \mathbb{E}_0 \left[\int_0^\tau \exp(-rt) (Payout_t) dt \middle| A_0 = A, K_0 = K, F_0 = F, S_0 = S \right] \right\} \\
\frac{dA_t}{A_t} &= \mu dt + \sigma dZ_t \\
\frac{dK_t}{K_t} &= (g_t - \delta) dt \\
dF_t &= (-m^u F_t + B_t^u) dt \\
dS_t &= (-m^s S_t + B_t^s) dt \\
S_t &\leq \alpha K_t
\end{aligned}$$

where τ is equity's endogenous default time.

Observe that capital K_t satisfies:

$$K_t = K_0 \exp \left(\int_0^t (g(s) - \delta) ds \right)$$

Then, we can show that the equity valuation equation is homogeneous of degree 1 in

capital:

$$\begin{aligned}
E(A, K, F, S) &= \max_{g, B^u, B^s, \tau} \left\{ \mathbb{E}_0 \left[\int_0^\tau \exp(-rt) (Payout_t) dt \middle| A_0 = A, K_0 = K, F_0 = F \right] \right\} \\
&= K \max_{g, B^u, B^s, \tau} \left\{ \mathbb{E}_0 \left[\int_0^\tau \exp \left(- \int_0^t (r - g_u + \delta) du \right) \times \right. \right. \\
&\quad \left. \left. (Payout_t / K_t) dt \middle| A_0 = A, f_0 = f, s_0 = 0 \right] \right\} \\
&= K e(A, f, s)
\end{aligned}$$

where,

$$f_t \equiv F_t / K_t$$

$$s_t \equiv S_t / K_t$$

$$b_t^u \equiv B_t^u / K_t$$

$$b_t^s \equiv B_t^s / K_t$$

By applying Ito's lemma to the new state variables f and s , obtain:

$$df_t = (b_t^u - (g_t + m^u - \delta)f_t)dt$$

$$ds_t = (b_t^s - (g_t + m^s - \delta)s_t)dt$$

Equity's HJB in the continuation region is given by:

$$\begin{aligned}
0 = \max_{g, b^u, b^s} \left\{ & - (r - g + \delta) e(A, f, s) - l(s - \alpha) \right. \\
& + A - \theta(A - c^u f - c^s s) - \Phi(g) - (c^u + m^u) f - (c^s + m^s) s + p(A, f, s) b^u + b^s \\
& + \mu A e_A(A, f, s) + \frac{1}{2} \sigma^2 A^2 e_{AA}(A, f, s) \\
& + [b^u - (g + m^u - \delta) f] e_f(A, f, s) \\
& \left. + [b^s - (g + m^s - \delta) s] e_s(A, f, s) \right\}
\end{aligned}$$

where l is the Lagrange multiplier on the collateral constraint.

Taking the first order condition with respect to b^s to obtain e_s and take additional derivatives, as before.

$$e_s = -1$$

$$e_{sA} = 0$$

$$e_{sAA} = 0$$

$$e_{fs} = 0$$

$$e_{ss} = 0$$

To obtain the value for p_s , differentiate the equity HJB with respect to b^u and obtain $p = -e_f$. Differentiate again with respect to s and use $e_{fs} = 0$ to obtain $p_s = 0$. As with secured short-term debt, the impact on unsecured debt from the issuance of secured debt is zero because secured debt is risk-free and its issuance does not incur additional bankruptcy costs.

Differentiate the HJB equation with respect to s , using the envelope condition for the

controls, and the values for the derivatives of e above to obtain:

$$0 = -l + \theta c^s - (c^s + m^s) + (r - g + \delta) + (g + m^s - \delta)$$

$$0 = -l + \theta c^s + r - c^s$$

$$\Rightarrow l = \theta c^s$$

Consequently, the collateral constraint binds, and the Lagrange multiplier on the collateral constraint equals the debt tax shield.

3.6.4 Deriving Equity HJB By Assuming Collateral Constraint Always

Binds

Suppose that the collateral constraint binds, then $S_t = \alpha K_t$, and the problem can be reduced to two state variables, F_t and K_t . Given corporate taxes rates θ , the flow payoffs are:

$$\begin{aligned} & \left[\begin{array}{c} \underbrace{AK_t}_{\text{cash flows}} - \underbrace{\theta(AK_t - c^u F_t)}_{\text{corporate taxes}} - \underbrace{\Phi(g_t) K_t}_{\text{investment cost}} \\ - \underbrace{(c^u + m^u) F_t}_{\text{unsecured debt interest \& principal}} + \underbrace{p_t B_t}_{\text{unsecured debt issuance/repurchase}} \end{array} \right] dt \\ & + \underbrace{\alpha d K_t}_{\text{secured debt net issuance}} \end{aligned}$$

Shareholders take unsecured debt price as given and solve the optimal control problem to maximize equity value, by choosing investment rate, unsecured debt issuance, and de-

fault timing.

$$\begin{aligned}
E(K, F) = \max_{\tau, g, B} & \mathbb{E} \left[\int_0^\tau \exp(-rt) [AK_t - \theta(AK_t - c^u F_t) - \Phi(g_t)K_t - (c^u + m^u)F_t + p_t B_t] dt \right. \\
& \left. + \alpha \int_0^\tau \exp(-rt) dK_t \middle| K_0 = K, F_0 = F \right] \\
& s.t. \\
& \frac{dK_t}{K_t} = (g_t - \delta)dt + \sigma dZ_t \\
& dF_t = -m^u F_t dt + B_t dt
\end{aligned}$$

where τ is the optimal stopping time for equity to default on its secured and unsecured debt obligations and cease operations.

The last term in the objective function captures the net cumulative proceeds from secured debt operations. To simplify, substitute in the expression for dK_t and then appeal to the linearity of the expectations operator and apply the stochastic version of Fubini's Theorem²⁴ to obtain:

$$\begin{aligned}
E(K, F) = \max_{\tau, g, B} & \mathbb{E} \left[\int_0^\tau \exp(-rt) [AK_t - \theta(AK_t - c^u F_t) - \Phi(g_t)K_t - (c^u + m^u)F_t + p_t B_t \right. \\
& \left. + \alpha(g_t - \delta)K_t] dt \middle| K_0 = K, F_0 = F \right] \\
& s.t. \\
& \frac{dK_t}{K_t} = (g_t - \delta)dt + \sigma dZ_t \\
& dF_t = -m^u F_t dt + B_t dt
\end{aligned}$$

Hence, for secured debt operations, shareholders need only consider the endogenous drift

24. By the optional stopping theorem, τ is almost surely bounded above and has a finite expectation.

in the evolution of capital, which is determined by the investment and depreciation rates.

Let $f_t \equiv F_t/K_t$ and $B_t \equiv B_t/K_t$ be rescaled variables per unit of capital. Notice:

$$K_t = K_0 \exp \left(\int_0^t (g_t - \delta - \frac{1}{2}\sigma^2) dt + \int_0^t \sigma dZ_t \right)$$

Substitute in K_t to the objective function and factor out $K_0 = K$ to find that equity value is homogeneous of degree 1 in capital (i.e. $E(1, F/K) = Ke(f)$). Further divide by K and employ a change of measure $dZ_t \equiv d\tilde{Z}_t + \sigma dt$ to obtain:

$$\begin{aligned} e(f) = \max_{\tau, g, b} \tilde{\mathbb{E}} \left[\int_0^\tau \exp \left(- \left(r - \int_0^t g_s ds + \delta \right) t \right) [A - \theta(A - c^u f_t) - \Phi(g_t) - (c^u + m^u) f_t + p_t b_t \right. \\ \left. + \alpha(g_t - \delta)] dt \middle| f_0 = f \right] \\ s.t. \end{aligned}$$

$$df_t = (b_t - (g_t - \delta + m^u) f_t) dt - f_t \sigma d\tilde{Z}_t$$

Hence, the recursive HJB formulation of the non-recursive problem in the continuation region where the firm is in operation is given by:

$$\begin{aligned} 0 = \max_{b, g} \left\{ - (r - g + \delta) e + A - \theta(A - c^u f) - \Phi(g) - (c^u + m^u) f + pb + \alpha(g - \delta) \right. \\ \left. + [b - (g - \delta + m^u) f] e_f + \frac{1}{2} \sigma^2 f^2 e_{ff} \right\} \end{aligned}$$

3.6.5 Binding Collateral Constraints in Rampini and Viswanathan (2010)

In this section, I show that collateral constraints bind in the setup of Rampini and Viswanathan [2010] with a debt tax shield on interest expenses and unconstrained dividends (where negative dividends represent inflows to the firm from equity investors). With unconstrained dividends, the motive for the firm to conserve debt capacity is diminished. Issuing debt

allows the firm to enjoy the benefit of the debt tax shield and since debt is risk-free, the firm issues up to the collateral constraint. This holds even with state-contingent debt and collateral constraints.

The firm maximizes the sum of discounted dividends over three periods ($t = 0, 1, 2$) by choosing the value of state-contingent dividends ($d_t(s)$) in each period, as well as, capital ($k_t(s)$) and the issuance of debt ($b_t(s)$) which matures in one period, where states are denoted by $s \in \mathcal{S}$. All agents are risk-neutral with discount factor $\beta \in (0, 1)$, and lenders price state-contingent debt competitively, such that, the interest rate on debt is equal to the gross-risk free rate, $R \equiv \beta^{-1} > 1$. State-contingent debt is issued against state-contingent collateral constraints: $q_t(s)\theta k_{t-1}(s) \geq Rb_t(s)$, where $q_t(s)$ is the state-contingent capital price and θ is the fraction of capital value that can be pledged as collateral.

Capital has a nonnegativity constraint and is used for production in the period ahead, such that, output is given by $A_t(s)f(k_{t-1}(s))$, where f denotes the firms production technology and is scaled by a factor A . The firm pays taxes, $\tau > 0$, on output less interest expenses, where $r \equiv R - 1$ denotes the net interest rate. Finally, the firm is subject to wealth constraints in each period and state, whereby the dividends, capital expenditures, and debt servicing costs cannot exceed output and any new borrowing.

The firm's problem is given by

$$\max_{b,d,k} \left(d_0 + \beta \mathbb{E}[d_1] + \beta^2 \mathbb{E}[d_2] \right)$$

subject to constraints in period 0, 1, and 2.

Period 0 constraints:

$$w_0 \geq d_0 + q_0 k_0 - b_1(s)$$

$$k_0 \geq 0$$

where w_0 is the given level of initial wealth.

Period 1 constraints:

$$q_1(s)\theta k_0 \geq Rb_1(s)$$

$$A_1(s)f(k_0) + q_1(s)k_0 - \tau(A_1(s)f(k_0) - rb_1(s)) \geq d_1(s) + q_1(s)k_1(s) - b_2(s) + Rb_1(s)$$

$$k_1(s) \geq 0$$

Period 2 constraints:

$$q_2(s)\theta k_1(s) \geq Rb_2(s)$$

$$A_2(s)f(k_1(s)) + q_2(s)k_1(s) - \tau(A_2(s)f(k_1(s)) - rb_2(s)) \geq d_2(s) + Rb_2(s)$$

$$k_2(s) = 0$$

Denote by $\pi(s)$ the probability of realizing state s . Let the multipliers on the wealth constraints be μ_0 , $\pi(s)\mu_1(s)$, and $\pi(s)\mu_2(s)$. Similarly, let the multipliers on the collateral constraints be $\pi(s)\lambda_1(s)$ and $\pi(s)\lambda_2(s)$. Finally, let the multipliers on the nonnegativity constraints for capital be ν_0^k and $\pi(s)\nu_1^k(s)$. Then, the Lagrangian for the firm's problem is given by:

$$\begin{aligned} \mathcal{L} = & d_0 + \beta \sum \pi(s)d_1(s) + \beta^2 \sum \pi(s)d_2(s) \\ & - \mu_0(d_0 + q_0k_0 - \sum \pi(s)b_1(s) - w_0) \\ & - \sum \pi(s)\mu_1(s)(d_1(s) + q_1(s)k_1(s) - b_2(s) + Rb_1(s)) \\ & - A_1(s)f(k_0) - q_1(s)k_0 + \tau(A_1(s)f(k_0) - rb_1(s)) \\ & - \sum \pi(s)\mu_2(s)(d_2(s) + Rb_2(s) - A_2(s)f(k_1(s)) - q_2(s)k_1(s) + \tau(A_2(s)f(k_1(s)) - rb_2(s))) \\ & - \sum \pi(s)\lambda_1(s)(Rb_1(s) - q_1(s)\theta k_0) \\ & - \sum \pi(s)\lambda_2(s)(Rb_2(s) - q_2(s)\theta k_1(s)) \\ & + \nu_0^k k_0 + \sum \pi(s)\nu_1^k(s)k_1(s) \end{aligned}$$

Computing the derivatives of the Lagrangian with respect to dividends yields:

$$\mu_0 = 1$$

$$\mu_1(s) = \beta, \forall s \in \mathcal{S}$$

$$\mu_2(s) = \beta^2, \forall s \in \mathcal{S}$$

And computing the derivatives of the Lagrangian with respect to debt yields:

$$\mu_0 = (R - \tau r)\mu_1(s) + R\lambda_1(s), \forall s \in \mathcal{S}$$

$$\mu_1(s) = (R - \tau r)\mu_2(s) + R\lambda_2(s), \forall s \in \mathcal{S}$$

Solving for $\lambda_1(s)$ and $\lambda_2(s)$ yields:

$$\lambda_1(s) = \tau r \beta^2 > 0$$

$$\lambda_2(s) = \tau r \beta^3 > 0$$

Hence, the Lagrange multipliers on the collateral constraints are proportional to the interest tax shield and are strictly positive. This implies that the collateral constraints bind for each time period and state.

3.6.6 Crisis Collateral Constraint in Model with Short-Term Secured Debt

This section provides the proof for Proposition 2.

Proof. The crisis HJB characterizing the joint value of equity and short-term debt in the

continuation region is given by:

$$\begin{aligned}
0 = \max_{b^u, b^s, g} & \left\{ - (r - g + \delta + \lambda)j + \eta A - \theta(\eta A - c^u f - c^s s) - \Phi(g) \right. \\
& - (c^u + m^u)f + pb^u - c^s s + p_s^* b^s - (1 - p_s^*)s \\
& + [b^u - (g + m^u - \delta)f]j_f + \frac{1}{2}\sigma^2 f^2 j_{ff} \\
& + [b^s - (g - \delta)s]j_s + \frac{1}{2}\sigma^2 s^2 j_{ss} \\
& \left. + \lambda \bar{j} - l_s(s - \alpha) \right\}
\end{aligned}$$

where p_s^* is the exogenous price of short-term secured debt and l_s is the Lagrange multiplier on the constraint $s \leq \alpha$.

FOC with respect to b^s :

$$\begin{aligned}
0 &= p_s^* + j_s \\
\Rightarrow j_s &= -p_s^* \\
\Rightarrow j_{ss} &= 0 \\
\Rightarrow j_{sf} &= 0 \\
\Rightarrow j_{sss} &= 0
\end{aligned}$$

To obtain p_s , compute the FOC with respect to b^u to obtain $p = -j_f$. Then, differentiate with respect to s and use $j_{sf} = 0$ to conclude $p_s = 0$.

Take FOC with respect to s , using envelope condition for controls, recalling $\bar{j}_s = -1$ and

$c^s = r$:

$$\begin{aligned}
0 &= -(r - g + \delta + \lambda)j_s + \theta c^s - c^s - (1 - p_s^*) - (g - \delta)j_s + \lambda \bar{j}_s - l_s \\
0 &= (r - g + \delta + \lambda)p_s^* + \theta c^s - c^s - (1 - p_s^*) + (g - \delta)p_s^* - \lambda - l_s \\
\Rightarrow l_s &= rp_s^* + \lambda p_s^* + \theta r - r - 1 + p_s^* - \lambda \\
&= p_s^*(1 + r + \lambda) + \theta r - (1 + r + \lambda)
\end{aligned}$$

The collateral constraint binds when $l_s > 0$, this occurs when:

$$\begin{aligned}
p_s^*(1 + r + \lambda) + \theta r - (1 + r + \lambda) &> 0 \\
p_s^* + \frac{\theta r}{1 + r + \lambda} &> 1 \\
\frac{\theta r}{1 + r + \lambda} &> 1 - p_s^*
\end{aligned}$$

Assuming this holds, the collateral constraint binds and $s = \alpha$. Plugging this back in and using the equilibrium conditions for the derivatives of j gives:

$$\begin{aligned}
0 &= \max_{b^u, g} \left\{ -(r - g + \delta + \lambda)j + \eta A - \theta(\eta A - c^u f - c^s \alpha) - \Phi(g) \right. \\
&\quad \left. - (c^u + m^u)f + pb^u - c^s \alpha + \alpha(p_s^* - 1) + p_s^* \alpha(g - \delta) + \lambda \bar{j} \right. \\
&\quad \left. + [b^u - (g + m^u - \delta)f]j_f + \frac{1}{2} \sigma^2 f^2 j_{ff} \right\}
\end{aligned}$$

In case the collateral condition does not bind, $l_s = 0$, then the firm does not issue short-

term debt and $s = 0$. The crisis HJB then becomes:

$$0 = \max_{b^u, g} \left\{ -(r - g + \delta + \lambda)j + \eta A - \theta(\eta A - c^u f) - \Phi(g) \right. \\ \left. - (c^u + m^u) f + pb^u + \lambda \bar{j} \right. \\ \left. + [b^u - (g + m^u - \delta) f] j_f + \frac{1}{2} \sigma^2 f^2 j_{ff} \right\}$$

□

3.6.7 Secured Debt Intervention Strictly Increases Value Function

This section provides the proof for Proposition 3.

Proof. Let $b^u(f, p_s^*)$ and $g(f, p_s^*)$ denote the optimal policies for unsecured debt issuance and investment when debt-to-capital is f and the exogenous price of secured debt is p_s^* . Let $j(f, p_s^*; p_s^{*'})$ be the joint value of equity and short-term debt when optimal policies are given by the arguments (f, p_s^*) , but the proceeds of secured debt issuance are determined by $p_s^{*'}.$ Moreover, the derivatives of j with respect to f are evaluated for the function j when debt-to-capital is f and secured debt price is $p_s^*.$

Secured debt intervention is identified as the case when $p_s^{*'}$ is greater than $p_s^*.$ Assuming that the collateral constraint binds at $p_s^{*'},$ then we can simplify the proof that the value function increases in intervention by assuming the collateral constraints also bind at $p_s^*.$ If the collateral constraints do not bind at $p_s^{*'},$ then by Equation 3.6, they also would not bind at $p_s^*,$ and it is no longer the case that secured debt intervention increases the value function.

The joint equity and short-term debt HJB during a crisis, given by Equation 3.7, can be

restated as:

$$\begin{aligned}
j(f, p_s^*; p_s^*) &= \max_{b^u, g} \left\{ \frac{1}{r - g + \delta + \lambda} \left[\eta A - \theta(\eta A - c^u f - c^s \alpha) - \Phi(g) \right. \right. \\
&\quad - (c^u + m^u) f + p b^u - c^s \alpha + \alpha(p_s^* - 1) + p_s^* \alpha(g - \delta) + \lambda \bar{j} \\
&\quad \left. \left. + [b^u - (g + m^u - \delta) f] j_f + \frac{1}{2} \sigma^2 f^2 j_{ff} \right] \right\} \\
&= \frac{1}{r - g(f, p_s^*) + \delta + \lambda} \left[\eta A - \theta(\eta A - c^u f - c^s \alpha) - \Phi(g(f, p_s^*)) \right. \\
&\quad - (c^u + m^u) f + p b^u(f, p_s^*) - c^s \alpha + \alpha(p_s^* - 1) + p_s^* \alpha(g(f, p_s^*) - \delta) + \lambda \bar{j} \\
&\quad \left. + [b^u(f, p_s^*) - (g(f, p_s^*) + m^u - \delta) f] j_f + \frac{1}{2} \sigma^2 f^2 j_{ff} \right]
\end{aligned}$$

By construction, $j(f, p_s^*; p_s^{*\prime}) \leq j(f, p_s^{*\prime}; p_s^{*\prime})$. Compare $j(f, p_s^*; p_s^{*\prime})$ and $j(f, p_s^*; p_s^*)$, where $p_s^{*\prime} - p_s^* > 0$:

$$\begin{aligned}
j(f, p_s^*; p_s^{*\prime}) - j(f, p_s^*; p_s^*) &\propto \alpha(p_s^{*\prime} - 1) - \alpha(p_s^* - 1) + (p_s^{*\prime} - p_s^*) \alpha(g(f, p_s^*) - \delta) \\
&= \alpha[(p_s^{*\prime} - 1) - (p_s^* - 1)] + (p_s^{*\prime} - p_s^*) \alpha(g(f, p_s^*) - \delta) \\
&= \alpha(p_s^{*\prime} - p_s^*) + (p_s^{*\prime} - p_s^*) \alpha(g(f, p_s^*) - \delta) \\
&= (\alpha(p_s^{*\prime} - p_s^*))(1 + g(f, p_s^*) - \delta)
\end{aligned}$$

Hence, the difference is the product of two terms. Since $\alpha \in (0, 1)$ and $p_s^{*\prime} - p_s^* > 0$, the first term is positive: $\alpha(p_s^{*\prime} - p_s^*) > 0$.

To determine the sign of the second term, first differentiate the investment policy function with respect to f yields $g_f(f, p_s^*) = \frac{1}{\gamma}(j_f - f j_{ff} - j_f) = \frac{1}{\gamma}(-f j_{ff})$. By Proposition 8, j is strictly convex. Thus, $j_{ff} > 0$ and investment decreases as f increases, attaining a minimum at the default threshold \bar{f} . In the default region, $j(\bar{f}) = 0$ and $j_f(\bar{f}) = 0$. Thus, the minimum value of investment is strictly positive: $g^{\min} = \frac{1}{\gamma} p_s^* \alpha > 0$. Furthermore, $\delta \in (0, 1)$, $1 - \delta > 0$. Therefore, $1 + g(f, p_s^*) - \delta > 0$. Consequently, $j(f, p_s^*; p_s^{*\prime}) > j(f, p_s^*; p_s^*)$.

All together:

$$j(f, p_s^{*'}; p_s^{*'}) \geq j(f, p_s^*; p_s^{*'}) > j(f, p_s^*; p_s^*)$$

Hence, secured debt intervention, such that $p_s^{*'} - p_s^* > 0$, strictly increases the joint value of equity and short-term debt. Since equity value is given by $e = j - \alpha$, it is also the case that:

$$e(f, p_s^{*'}; p_s^{*'}) \geq e(f, p_s^*; p_s^{*'}) > e(f, p_s^*; p_s^*)$$

Thus, secured debt intervention strictly increases the value of equity.

□

3.6.8 Secured Debt Intervention Boosts Investment Via Direct and Indirect Channels

This section provides the proof for Proposition 4.

Proof. Following the notation in Appendix 3.6.7, the investment policy $g(f, p_s^{*'})$ and $g(f, p_s^*)$ are given by:

$$\begin{aligned} g(f, p_s^{*'}) &= \frac{1}{\gamma} (j(f, p_s^{*'}; p_s^{*'}) - f j_f(f, p_s^{*'}; p_s^{*'}) + p_s^{*'} \alpha) \\ &= \frac{1}{\gamma} (j(f, p_s^{*'}; p_s^{*'}) + f p(f, p_s^{*'}; p_s^{*'}) + p_s^{*'} \alpha) \\ g(f, p_s^*) &= \frac{1}{\gamma} (j(f, p_s^*; p_s^*) - f j_f(f, p_s^*; p_s^*) + p_s^* \alpha) \\ &= \frac{1}{\gamma} (j(f, p_s^*; p_s^*) + f p(f, p_s^*; p_s^*) + p_s^* \alpha) \end{aligned}$$

in the case where $p_s^{*'} > p_s^*$, and the collateral constraints bind for both $p_s^{*'} \text{ and } p_s^*$. Note that the optimality condition $p = -j_f$, where p is the price of unsecured debt, is used in

each case to restate the expressions.

The difference between the two policies can be expressed as:

$$\begin{aligned}
g(f, p_s^{*'}) - g(f, p_s^*) &= \frac{1}{\gamma} \left[(j(f, p_s^{*'}; p_s^{*'}) + fp(f, p_s^{*'}; p_s^{*'}) + p_s^{*'}\alpha) \right. \\
&\quad \left. - (j(f, p_s^*; p_s^*) + fp(f, p_s^*; p_s^*) + p_s^*\alpha) \right] \\
&= \frac{1}{\gamma} \left[\underbrace{j(f, p_s^{*'}; p_s^{*'}) - j(f, p_s^*; p_s^*)}_{\text{indirect channel}} + \underbrace{(p_s^{*'} - p_s^*)\alpha}_{\text{direct channel}} \right]
\end{aligned}$$

The change in investment can be decomposed into a direct channel and an indirect channel. Since $\gamma > 0$ and $p_s^{*'} > p_s^*$, there is a direct increase to investment arising from greater proceeds from secured debt issuance.

Indirectly, an increase in the joint value for equity and short-term debt and an increase in the price of unsecured debt can lead to higher investment. To see this, first note that by Proposition 3, as shown in Appendix 3.6.7, $j(f, p_s^{*'}; p_s^{*'}) > j(f, p_s^*; p_s^*)$. Second, recall that the price of unsecured debt, p , as defined in Section 3.2.4, is increasing in the default time τ . Since $j(f, p_s^{*'}; p_s^{*'}) > j(f, p_s^*; p_s^*)$, $\tau(f, p_s^{*'}; p_s^{*'}) \geq \tau(f, p_s^*; p_s^*)$ and so, $p(f, p_s^{*'}; p_s^{*'}) - p(f, p_s^*; p_s^*) \geq 0$. Equivalently, recalling the definition for Tobin's q , we can conclude that $q(f, p_s^{*'}; p_s^{*'}) > q(f, p_s^*; p_s^*)$; that is, Tobin's q is higher under secured debt intervention.

In sum, $g(f, p_s^{*'}) - g(f, p_s^*) > 0$ and investment is strictly increasing in secured debt intervention. This increase can be decomposed into direct and indirect channels. \square

3.6.9 Segmented Markets in Model with Short-Term Secured Debt

This section provides the proof for Proposition 5.

Proof. First, we verify that changing unsecured debt issuance does not change the joint equity and short-term debt value function. This can be seen from differentiating Equation

(3.7) with respect to b^u and obtaining the optimality condition $p = -j_f$. Plugging this into (3.7) shows that the value function is invariant to the choice of b^u , although the equilibrium values of b^u are different in the case without and with unsecured debt intervention.

Given the above, differentiate the no-trade crisis state HJB equation for equity and short-term debt, as characterized by Equation (3.7) with $b^u = 0$, with respect to f and where the discount rate is given by $r^{(e)}$, using the envelope condition for investment:

$$\begin{aligned} (r^{(e)} - g^* + \delta + \lambda)j_f &= \theta c^u - (c^u + m^u) - (g^* + m^u - \delta) f j_{ff} - (g^* + m^u - \delta) e_f \\ &\quad + \sigma^2 f j_{ff} + \frac{1}{2} \sigma^2 f^2 j_{fff} + \lambda \bar{e}_f \\ \Rightarrow (r^{(e)} + m^u + \lambda)j_f &= \theta c^u - (c^u + m^u) - (g^* + m^u - \delta - \sigma^2) f j_{ff} + \frac{1}{2} \sigma^2 f^2 j_{fff} + \lambda \bar{j}_f \end{aligned}$$

Substitute in the first order condition for b^u , $p = -j_f$ and $\bar{p} = -\bar{j}_f$, into the crisis HJB equation for unsecured debt price, as in Equation (3.8), but priced with discount rate r^d :

$$-(r^{(d)} + m^u + \lambda)j_f = c^u + m^u - [b^u - (g^* + m^u - \delta - \sigma^2) f] j_{ff} - \frac{1}{2} \sigma^2 f^2 j_{fff} - \lambda \bar{j}_f$$

Add these two expression together:

$$\begin{aligned} (r^{(e)} - r^{(d)})j_f &= \theta c^u - b^u j_{ff} \\ \Rightarrow b^u &= \frac{\theta c^u}{j_{ff}} - \frac{(r^{(e)} - r^{(d)})j_f}{j_{ff}} \end{aligned}$$

□

3.6.10 Unsecured Debt Intervention and Joint Equity and Short-Term Debt Value Function

This section provides the proof for Proposition 6.

Proof. Appendix 3.6.9 verifies that the joint equity and short-term debt value functions are invariant to unsecured debt issuance policy and derives the general expression for this policy in segmented markets.

Without unsecured debt intervention, $r^{(e)} = r^{(d)}$ and:

$$b^{\text{no int}} = \frac{\theta c^u}{j_{ff}}$$

In the case of unsecured debt intervention, $r^{(e)} > r^{(d)}$ and

$$\begin{aligned} b^{\text{int}} &= \frac{\theta c^u}{j_{ff}} - \frac{(r^{(e)} - r^{(d)})j_f}{j_{ff}} \\ &= \frac{\theta c^u}{j_{ff}} + \frac{(r^{(e)} - r^{(d)})p}{j_{ff}} \end{aligned}$$

The difference between the issuance policies is given by:

$$b^{\text{int}} - b^{\text{no int}} = \frac{(r^{(e)} - r^{(d)})p}{j_{ff}} > 0$$

which is strictly positive in the continuation region because debt price $p > 0$ and j is convex.

Given that j is invariant to issuance policy, the optimal investment policy is invariant to issuance and is denoted as $g^*(f)$. Let $j(f; b^{\text{int}})$ denote the value function given issuance policy under unsecured debt intervention; similarly, denote $j(f; b^{\text{no int}})$. The difference between these two value function is equal to zero and given by:

$$j(f; b^{\text{int}}) - j(f; b^{\text{no int}}) \propto pb^{\text{int}} - pb^{\text{no int}} + \mathcal{A}(b^{\text{int}})j(f; b^{\text{int}}) - \mathcal{A}(b^{\text{no int}})j(f; b^{\text{no int}}) = 0$$

where \mathcal{A} is the infinitesimal generator of j , such that $\mathcal{A}(b^u)j = [b^u - (g + m^u - \delta)f]j_f +$

$\frac{1}{2}\sigma^2 f^2 j_{ff}$ is the continuation value of j . Rearranging, we have:

$$p(b^{\text{int}} - b^{\text{no int}}) = \mathcal{A}(b^{\text{no int}})j(f; b^{\text{no int}}) - \mathcal{A}(b^{\text{int}})j(f; b^{\text{int}})$$

Since $b^{\text{int}} - b^{\text{no int}} > 0$ and $p > 0$ in the continuation region, the continuation value under $b^{\text{no int}}$ is strictly greater than the continuation value under b^{int} : $\mathcal{A}(b^{\text{no int}})j(f; b^{\text{no int}}) > \mathcal{A}(b^{\text{int}})j(f; b^{\text{int}})$.

Consequently, unsecured debt intervention accelerates payouts immediately by stimulating greater issuance at the cost of a lower continuation value. This also suggests implications for the evolution of the distribution of firms over the state space, that is, the distribution of firms' unsecured debt-to-capital. Heuristically, a lower continuation value implies higher levels of leverage, which in turn implies higher default rates. Numerical results confirm this conjecture.

□

3.6.11 Dividend Restriction in Model with Short-Term Secured Debt

This section provides the proof for Proposition 7.

Complementary Slackness Condition

- The complementary slackness condition corresponding to the constraint given by Equation (3.9) and Lagrange multiplier l is:

$$l\pi(b^u, g) = 0$$

$$l \geq 0, \pi(b^u, g) \leq 0$$

Then,

$$\pi < 0 \Rightarrow l = 0$$

$$\pi = 0 \Rightarrow l > 0$$

Note:

$$\pi_{b^u} = p$$

$$\pi_g = -\Phi'(g) + p_s^* \alpha$$

$$\pi_f = \theta c^u - (c^u + m^u) + p_f b^u$$

FOCs for Joint Equity and Short-Term Debt HJB

- Taking the Lagrange multiplier l as given, the control problem for shareholders becomes:

$$0 = \max_{b^u, g} \left\{ -(r - g + \delta + \lambda)j + (1 - l)\pi(b^u, g) + \lambda \bar{j} + [b^u - (g - \delta + m^u)f]j_f + \frac{1}{2}\sigma^2 f^2 j_{ff} \right\}$$

- FOC w/r/t g :

$$\begin{aligned} 0 &= j - f j_f + (1 - l)\pi_g \\ &= j - f j_f - (1 - l)\Phi'(g) + (1 - l)p_s^* \alpha \\ \Rightarrow \Phi'(g) &= \frac{j - f j_f}{1 - l} + p_s^* \alpha \\ g &= \frac{1}{\gamma} \left(\frac{j - f j_f}{1 - l} + p_s^* \alpha \right) \end{aligned}$$

- FOC w/r/t b^u :

$$0 = j_f + (1 - l)\pi_{b^u}$$

$$\begin{aligned} -(1 - l)\pi_{b^u} &= j_f \\ \Rightarrow p &= -\frac{j_f}{1 - l} \\ \Rightarrow l &= 1 + \frac{j_f}{p} \end{aligned}$$

Note:

$$\begin{aligned} p_f &= -\frac{j_{ff}}{1 - l} \\ p_{ff} &= -\frac{j_{fff}}{1 - l} \end{aligned}$$

Optimal Issuance

- The crisis HJB for debt is:

$$(r + m^u + \lambda)p = c^u + m^u + \lambda\bar{p} + [b - (g + m^u - \delta - \sigma^2)f]p_f + \frac{1}{2}\sigma^2f^2p_{ff}$$

- Substitute in the expression for p, p_f, p_{ff} and \bar{p} :

$$\begin{aligned} (r + m^u + \lambda) \left(-\frac{j_f}{1 - l} \right) &= c^u + m^u - \lambda\bar{j}_f + [b^u - (g + m^u - \delta - \sigma^2)f] \left(-\frac{j_{ff}}{1 - l} \right) \\ &\quad + \frac{1}{2}\sigma^2f^2 \left(-\frac{j_{fff}}{1 - l} \right) \\ \Rightarrow -(r + m^u + \lambda)j_f &= (1 - l)(c^u + m^u) - (1 - l)\lambda\bar{j}_f - b^u j_{ff} \\ &\quad + (g + m^u - \delta - \sigma^2)fj_{ff} - \frac{1}{2}\sigma^2f^2j_{fff} \end{aligned}$$

- Take derivative of crisis equity HJB w/r/t f :

$$\begin{aligned}
0 &= -(r - g + \delta + \lambda)j_f + (1 - l)\pi_f + \lambda\bar{j}_f \\
&\quad + b^u j_{ff} - (g - \delta + m^u)j_f - (g - \delta + m^u)fj_{ff} + \sigma^2 f j_{ff} + \frac{1}{2}\sigma^2 f^2 j_{fff} \\
\Rightarrow (r + m^u + \lambda)j_f &= (1 - l)\pi_f + \lambda\bar{j}_f + [b^u - (g - \delta + m^u - \sigma^2)f]j_{ff} + \frac{1}{2}\sigma^2 f^2 j_{fff} \\
&= (1 - l)(\theta c^u - (c^u + m^u) + p_f b^u) + \lambda\bar{j}_f \\
&\quad + [b^u - (g - \delta + m^u - \sigma^2)f]j_{ff} + \frac{1}{2}\sigma^2 f^2 j_{fff} \\
&= (1 - l)\theta c^u - (1 - l)(c^u + m^u) - j_f b^u + \lambda\bar{j}_f \\
&\quad + [b^u - (g - \delta + m^u - \sigma^2)f]j_{ff} + \frac{1}{2}\sigma^2 f^2 j_{fff} \\
&= (1 - l)\theta c^u - (1 - l)(c^u + m^u) + \lambda\bar{j}_f - (g - \delta + m^u - \sigma^2)fj_{ff} \\
&\quad + \frac{1}{2}\sigma^2 f^2 j_{fff}
\end{aligned}$$

- Add these two equations together:

$$\begin{aligned}
0 &= (1 - l)\theta c^u + l\lambda\bar{j}_f - b^u j_{ff} \\
\Rightarrow b^u &= (1 - l)\frac{\theta c^u}{j_{ff}} + l\frac{\lambda\bar{j}_f}{j_{ff}} \\
&= (1 - l)\frac{\theta c^u}{j_{ff}} - l\frac{\lambda\bar{p}}{j_{ff}}
\end{aligned}$$

Solution with Binding Constraint

- When constraint binds:

$$\begin{aligned}\pi(b^u, g) &= -\frac{1}{2}\gamma g^2 + p_s^* \alpha g + \eta A - \theta(\eta A - c^u f - c^s \alpha) - (c^u + m^u) f + pb^u - c^s \alpha \\ &\quad + (p_s^* - 1)\alpha - p_s^* \alpha \delta = 0 \\ \zeta(b^u) &\equiv \eta A - \theta(\eta A - c^u f - c^s \alpha) - (c^u + m^u) f + pb^u - c^s \alpha + (p_s^* - 1)\alpha - p_s^* \alpha \delta \\ \Rightarrow g &= \frac{-p_s^* \alpha - \sqrt{(p_s^* \alpha)^2 + 2\gamma \zeta(b^u)}}{-\gamma} \\ &= \frac{p_s^* \alpha + \sqrt{(p_s^* \alpha)^2 + 2\gamma \zeta(b^u)}}{\gamma}\end{aligned}$$

- Investment increases in unsecured debt issuance:

$$\begin{aligned}\frac{\partial g}{\partial b^u} &= \frac{1}{\gamma} \frac{1}{2} ((p_s^* \alpha)^2 + 2\gamma \zeta(b^u))^{-1/2} (2\gamma) \zeta'(b^u) \\ &= \frac{p}{\sqrt{(p_s^* \alpha)^2 + 2\gamma \zeta(b^u)}}\end{aligned}$$

- Ensuring that investment is non-negative requires $\zeta(b^u) \geq 0$:

$$\begin{aligned}0 &\leq \zeta(b^u) \\ &\leq \eta A - \theta(\eta A - c^u f - c^s \alpha) - (c^u + m^u) f + pb^u - c^s \alpha + (p_s^* - 1)\alpha - p_s^* \alpha \delta \\ \Rightarrow b^u &\geq -\frac{1}{p} (\eta A - \theta(\eta A - c^u f - c^s \alpha) - (c^u + m^u) f - c^s \alpha + (p_s^* - 1)\alpha - p_s^* \alpha \delta)\end{aligned}$$

- I also consider a restriction on unsecured debt repurchases while the dividend restriction is in place (i.e. $b^u \geq 0$). This ensures strictly positive investment.

3.6.12 Dividend Restriction and Unsecured Debt Repurchase Restriction in Model with Short-Term Secured Debt

Let l_1 be the Lagrange multiplier on the dividend constraint Equation (3.9) and l_2 be the Lagrange multiplier on the unsecured debt issuance constraint: $b^u \geq 0$.

Then, the complementary complementary slackness condition for the dividend constraint is:

$$l_1 \pi(b^u, g) = 0$$

$$l_1 \geq 0, \pi(b^u, g) \leq 0$$

and the complementary slackness condition for the unsecured debt issuance constraint is:

$$-l_2 b^u = 0$$

$$l_2 \geq 0, -b^u \leq 0$$

Using the Lagrange multipliers, l_1 and l_2 , the control problem in the continuation region can be express as:

$$0 = \max_{b^u, g} \left\{ -(r - g + \delta + \lambda)j + (1 - l_1)\pi(b^u, g) + l_2 b^u + \lambda \bar{j} + [b^u - (g - \delta + m^u)f]j_f + \frac{1}{2}\sigma^2 f^2 j_{ff} \right\}$$

The FOC with respect to optimal investment, g , is:

$$\begin{aligned}
0 &= j - f j_f + (1 - l_1) \pi_g \\
&= j - f j_f - (1 - l_1) \Phi'(g) + (1 - l_1) p_s^* \alpha \\
\Rightarrow \Phi'(g) &= \frac{j - f j_f}{1 - l_1} + p_s^* \alpha \\
g &= \frac{1}{\gamma} \left(\frac{j - f j_f}{1 - l_1} + p_s^* \alpha \right)
\end{aligned}$$

An expression for l_1 can be obtained in terms of g :

$$\begin{aligned}
g\gamma &= \frac{j - f j_f}{1 - l_1} + p_s^* \alpha \\
g\gamma(1 - l_1) &= j - f j_f + (1 - l_1) p_s^* \alpha \\
l_1(p_s^* \alpha - g\gamma) &= j - f j_f + p_s^* \alpha - g\gamma \\
l_1 &= 1 + \frac{j - f j_f}{p_s^* \alpha - g\gamma}
\end{aligned}$$

The FOC with respect to optimal unsecured debt issuance, b^u , is:

$$\begin{aligned}
0 &= j_f + (1 - l_1) \pi_{b^u} + l_2 \\
-(1 - l) \pi_{b^u} &= j_f + l_2 \\
\Rightarrow p &= -\frac{j_f + l_2}{1 - l_1} \\
\Rightarrow l_1 &= 1 + \frac{j_f + l_2}{p}
\end{aligned}$$

If the dividend constraint binds, $l_1 > 0$, then:

$$\begin{aligned}
0 &< p + j_f + l_2 \\
-p - j_f &< l_2
\end{aligned}$$

If the dividend constraint doesn't bind, $l_1 = 0$, then:

$$0 = p + j_f + l_2$$

Note:

$$p_f = -\frac{j_{ff}}{1 - l_1}$$

$$p_{ff} = -\frac{j_{fff}}{1 - l_1}$$

The crisis HJB for debt is:

$$(r + m^u + \lambda)p = c^u + m^u + \lambda\bar{p} + [b^u - (g + m^u - \delta - \sigma^2)f]p_f + \frac{1}{2}\sigma^2 f^2 p_{ff}$$

Substitute in the expression for p, p_f, p_{ff} and \bar{p} :

$$(r + m^u + \lambda) \left(-\frac{j_f + l_2}{1 - l_1} \right) = c^u + m^u - \lambda\bar{j}_f + [b^u - (g + m^u - \delta - \sigma^2)f] \left(-\frac{j_{ff}}{1 - l_1} \right) + \frac{1}{2}\sigma^2 f^2 \left(-\frac{j_{fff}}{1 - l_1} \right)$$

$$\Rightarrow -(r + m^u + \lambda)(j_f + l_2) = (1 - l_1)(c^u + m^u) - (1 - l_1)\lambda\bar{j}_f - b^u j_{ff} + (g + m^u - \delta - \sigma^2)f j_{fff} - \frac{1}{2}\sigma^2 f^2 j_{fff}$$

Take derivative of crisis equity HJB w/r/t f :

$$\begin{aligned}
0 &= -(r - g + \delta + \lambda)j_f + (1 - l_1)\pi_f + \lambda\bar{j}_f \\
&\quad + b^u j_{ff} - (g - \delta + m^u)j_f - (g - \delta + m^u)fj_{ff} + \sigma^2 f j_{ff} + \frac{1}{2}\sigma^2 f^2 j_{fff} \\
\Rightarrow (r + m^u + \lambda)j_f &= (1 - l_1)\pi_f + \lambda\bar{j}_f + [b^u - (g - \delta + m^u - \sigma^2)f]j_{ff} + \frac{1}{2}\sigma^2 f^2 j_{fff} \\
&= (1 - l_1)(\theta c^u - (c^u + m^u) + p_f b^u) + \lambda\bar{j}_f \\
&\quad + [b^u - (g - \delta + m^u - \sigma^2)f]j_{ff} + \frac{1}{2}\sigma^2 f^2 j_{fff} \\
&= (1 - l_1)\theta c^u - (1 - l_1)(c^u + m^u) - j_{ff}b^u + \lambda\bar{j}_f \\
&\quad + [b^u - (g - \delta + m^u - \sigma^2)f]j_{ff} + \frac{1}{2}\sigma^2 f^2 j_{fff} \\
&= (1 - l_1)\theta c^u - (1 - l_1)(c^u + m^u) + \lambda\bar{j}_f - (g - \delta + m^u - \sigma^2)fj_{ff} \\
&\quad + \frac{1}{2}\sigma^2 f^2 j_{fff}
\end{aligned}$$

Add these two equations together:

$$\begin{aligned}
-l_2(r + m^u + \lambda) &= (1 - l_1)\theta c^u + l_1\lambda\bar{j}_f - b^u j_{ff} \\
\Rightarrow b^u &= (1 - l_1)\frac{\theta c^u}{j_{ff}} + l_1\frac{\lambda\bar{j}_f}{j_{ff}} + l_2\frac{r + m^u + \lambda}{j_{ff}} \\
&= (1 - l_1)\frac{\theta c^u}{j_{ff}} - l_1\frac{\lambda\bar{p}}{j_{ff}} + l_2\frac{r + m^u + \lambda}{j_{ff}}
\end{aligned}$$

When the debt repurchase restriction binds, $b^u = 0$ and:

$$\begin{aligned}
l_2\frac{r + m^u + \lambda}{j_{ff}} &= l_1\frac{\lambda\bar{p}}{j_{ff}} - (1 - l_1)\frac{\theta c^u}{j_{ff}} \\
l_2 &= l_1\frac{\lambda\bar{p}}{r + m^u + \lambda} - (1 - l_1)\frac{\theta c^u}{r + m^u + \lambda} \geq 0
\end{aligned}$$

3.6.13 Numerical Solution for Model with Short-Term Debt

- Endogenous state f : $\Delta f : \{f_1, \dots, f_I\}$, where:

$$f_1 = f_{i-1} + \Delta f = f_1 + (i-1)\Delta f$$

for $2 \leq i \leq I$, where $f_1 = 0$. Policy on boundary such that process obeys the state constraint.

Solution with No-Trade

Discrete Dynamics of Endogenous State Variable

- Drift for endogenous state f : $\iota(f_i) = -(g(f_i) + m^u - \delta)f_i = -(\frac{1}{\gamma}(j_i - f\partial j_i + \alpha) + m^u - \delta)f_i$.
- Forward approximation for $\partial_F j_i$:

$$\partial_F j_i \equiv \frac{j_{i+1} - j_i}{\Delta f}$$

- Backward approximation for $\partial_B j_i$:

$$\partial_B j_i \equiv \frac{j_i - j_{i-1}}{\Delta f}$$

- Second derivative (central):

$$\frac{\partial^2 j(f)}{\partial f^2} \approx \partial_{ff} j_i \equiv \frac{j_{i+1} + j_{i-1} - 2j_i}{(\Delta f)^2}$$

- Choice of approximation depends on sign of ι_i (per upwind scheme):

- $\iota_{i,F} = -(\frac{1}{\gamma}(j_i - f_i \partial_F j_i + \alpha) + m^u - \delta) f_i > 0 \Rightarrow g_i = \frac{1}{\gamma}(j_i - f_i \partial_F j_i + \alpha).$
- $\iota_{i,B} = -(\frac{1}{\gamma}(j_i - f_i \partial_B j_i + \alpha) + m^u - \delta) f_i < 0 \Rightarrow g_i = \frac{1}{\gamma}(j_i - f_i \partial_B j_i + \alpha).$
- $\iota_i = -(\frac{1}{\gamma}(j_i - f_i \partial_B j_i + \alpha) + m^u - \delta) f_i = 0 \Rightarrow g_i = -m^u + \delta.$

Discretized HJB Equation

- Let $\Psi_i^n = A - \theta(A - c^u f_i - c^s \alpha) - \Phi(g_i^n) - (c^u + m^u) f_i - c^s \alpha + \alpha(g_i^n - \delta).$
- Given time step Δ , the discretized HJB equation in the continuation is given by:

$$\begin{aligned}
\frac{j_i^{n+1} - j_i^n}{\Delta} + (r - g_i^n + \delta) j_i^{n+1} &= \Psi_i^n + \iota_{i,F}^n \mathbb{1}_{\iota_{i,F}^n > 0} \partial_F j_i^{n+1} + \iota_{i,B}^n \mathbb{1}_{\iota_{i,B}^n < 0} \partial_B j_i^{n+1} \\
&\quad + \frac{1}{2} \sigma^2 f_i^2 j_{ff} \\
&= \Psi_i^n + \iota_{i,F}^n \mathbb{1}_{\iota_{i,F}^n > 0} \frac{j_{i+1}^{n+1} - j_i^{n+1}}{\Delta f} \\
&\quad + \iota_{i,B}^n \mathbb{1}_{\iota_{i,B}^n < 0} \frac{j_i^{n+1} - j_{i-1}^{n+1}}{\Delta f} \\
&\quad + \frac{\sigma^2 f_i^2}{2} \frac{j_{i+1}^{n+1} + j_{i-1}^{n+1} - 2j_i^{n+1}}{(\Delta f)^2}
\end{aligned}$$

- Collecting terms:

$$\begin{aligned}
&\left(-\frac{\iota_{i,B}^n \mathbb{1}_{\iota_{i,B}^n < 0}}{\Delta f} + \frac{1}{2} \frac{\sigma^2 f_i^2}{(\Delta f)^2} \right) j_{i-1}^{n+1} + \left(-\frac{\iota_{i,F}^n \mathbb{1}_{\iota_{i,F}^n > 0}}{\Delta f} + \frac{\iota_{i,B}^n \mathbb{1}_{\iota_{i,B}^n < 0}}{\Delta f} - \frac{\sigma^2 f_i^2}{(\Delta f)^2} \right) j_i^{n+1} \\
&\quad + \left(\frac{\iota_{i,F}^n \mathbb{1}_{\iota_{i,F}^n > 0}}{\Delta f} + \frac{1}{2} \frac{\sigma^2 f_i^2}{(\Delta f)^2} \right) j_{i+1}^{n+1}
\end{aligned}$$

- Define:

$$\begin{aligned}\xi_i &= -\frac{\iota_{i,B}^n \mathbb{1}_{\iota_{i,B}^n < 0}}{\Delta f} + \frac{1}{2} \frac{\sigma^2 f_i^2}{(\Delta f)^2} \\ \beta_i &= -\frac{\iota_{i,F}^n \mathbb{1}_{\iota_{i,F}^n > 0}}{\Delta f} + \frac{\iota_{i,B}^n \mathbb{1}_{\iota_{i,B}^n < 0}}{\Delta f} - \frac{\sigma^2 f_i^2}{(\Delta f)^2} \\ \zeta_i &= \frac{\iota_{i,F}^n \mathbb{1}_{\iota_{i,F}^n > 0}}{\Delta f} + \frac{1}{2} \frac{\sigma^2 f_i^2}{(\Delta f)^2}\end{aligned}$$

- In matrix notation,

$$\frac{\mathbf{j}^{n+1} - \mathbf{j}^n}{\Delta} + \text{diag}((r + \delta)\mathbf{1} - \mathbf{g}^n)\mathbf{j}^{n+1} = \Psi^n + \mathbf{C}\mathbf{j}^{n+1}$$

where,

$$\begin{aligned}\mathbf{j}, \mathbf{1}, \mathbf{g}, \Psi^n, \mathbf{j}^{n+1} &\in \mathbb{R}^{I \times 1} \\ \mathbf{C} &\in \mathbb{R}^{I \times I} \\ \text{diag}((r + \delta)\mathbf{1} - \mathbf{g}^n) &\in \mathbb{R}^{I \times I}\end{aligned}$$

- Matrix \mathbf{C} is the discrete-space approximation of the infinitesimal generator \mathcal{C} .
- System can also be written as:

$$\mathbf{B}^n \mathbf{j}^{n+1} = \mathbf{b}^n$$

where,

$$\begin{aligned}\mathbf{B}^n &= \text{diag} \left(\left(\frac{1}{\Delta} + r + \delta \right) \mathbf{1} - \mathbf{g}^n \right) - \mathbf{C}^n \\ \mathbf{b}^n &= \Psi^n + \frac{1}{\Delta} \mathbf{j}^n\end{aligned}$$

- The HJBVI which takes into account the default option can be expressed in the standard form of a linear complementarity problem (LCP):

$$\mathbf{j}^{n+1\prime}(\mathbf{B}^n \mathbf{j}^{n+1} + (-\mathbf{b}^n)) = 0$$

$$\mathbf{j}^{n+1} \geq 0$$

$$\mathbf{B}^n \mathbf{j}^{n+1} + (-\mathbf{b}^n) \geq 0$$

Boundary Conditions

- Assuming we've solved for the equilibrium transition rate matrix, \mathbf{C} , take as given the default threshold, $f_D \in (f_1, f_I)$, where we assume that the state grid is sufficiently constructed so that f_D lies in the interior.
- We have the following state constraint at the lower boundary (there is no negative drift in df):

$$f \geq f_1 = 0 \Rightarrow \iota_{1,B} = 0$$

Also, $f_1 = 0 \Rightarrow \iota_{1,F} = 0$. Therefore,

$$\xi_1 = 0$$

$$\beta_1 = 0$$

$$\zeta_1 = 0$$

- A firm entering default cannot resume operations or accumulate more debt:

$$f = f_D, \forall t \Rightarrow \begin{bmatrix} \xi_D & \beta_D & \zeta_D \end{bmatrix} = 0$$

Solution with Trade and No Market Segmentation

- Upwind scheme unchanged. Unsecured debt issuance policy only affects drift.

Discretized HJB Equation

- Let $\Psi_i^n = A - \theta(A - c^u f_i - c^s \alpha) - \Phi(g_i^n) - (c^u + m^u) f_i - c^s \alpha + p_i^n b_i^n + \alpha(g_i^n - \delta)$.
- Given time step Δ , the discretized HJB equation in the continuation is given by:

$$\begin{aligned}
\frac{j_i^{n+1} - j_i^n}{\Delta} + (r - g_i^n + \delta) j_i^{n+1} &= \Psi_i^n + b_i^n \partial_F j_i^{n+1} + \iota_{i,F}^n \mathbb{1}_{\iota_{i,F}^n > 0} \partial_F j_i^{n+1} \\
&\quad + \iota_{i,B}^n \mathbb{1}_{\iota_{i,B}^n < 0} \partial_B j_i^{n+1} + \frac{1}{2} \sigma^2 f_i^2 j_{ff} \\
&= \Psi_i^n + b_i^n \frac{j_{i+1}^{n+1} - j_i^{n+1}}{\Delta f} + \iota_{i,F}^n \mathbb{1}_{\iota_{i,F}^n > 0} \frac{j_{i+1}^{n+1} - j_i^{n+1}}{\Delta f} \\
&\quad + \iota_{i,B}^n \mathbb{1}_{\iota_{i,B}^n < 0} \frac{j_i^{n+1} - j_{i-1}^{n+1}}{\Delta f} \\
&\quad + \frac{\sigma^2 f_i^2}{2} \frac{j_{i+1}^{n+1} + j_{i-1}^{n+1} - 2j_i^{n+1}}{(\Delta f)^2}
\end{aligned}$$

- Collecting terms:

$$\begin{aligned}
&\left(-\frac{\iota_{i,B}^n \mathbb{1}_{\iota_{i,B}^n < 0}}{\Delta f} + \frac{1}{2} \frac{\sigma^2 f_i^2}{(\Delta f)^2} \right) j_{i-1}^{n+1} + \\
&\left(-\frac{b_i^n}{\Delta f} - \frac{\iota_{i,F}^n \mathbb{1}_{\iota_{i,F}^n > 0}}{\Delta f} + \frac{\iota_{i,B}^n \mathbb{1}_{\iota_{i,B}^n < 0}}{\Delta f} - \frac{\sigma^2 f_i^2}{(\Delta f)^2} \right) j_i^{n+1} + \\
&\left(\frac{b_i^n}{\Delta f} + \frac{\iota_{i,F}^n \mathbb{1}_{\iota_{i,F}^n > 0}}{\Delta f} + \frac{1}{2} \frac{\sigma^2 f_i^2}{(\Delta f)^2} \right) j_{i+1}^{n+1}
\end{aligned}$$

- Define:

$$\begin{aligned}\xi_i &= -\frac{\iota_{i,B}^n \mathbb{1}_{\iota_{i,B}^n < 0}}{\Delta f} + \frac{1}{2} \frac{\sigma^2 f_i^2}{(\Delta f)^2} \\ \beta_i &= -\frac{b_i^n}{\Delta f} - \frac{\iota_{i,F}^n \mathbb{1}_{\iota_{i,F}^n > 0}}{\Delta f} + \frac{\iota_{i,B}^n \mathbb{1}_{\iota_{i,B}^n < 0}}{\Delta f} - \frac{\sigma^2 f_i^2}{(\Delta f)^2} \\ \zeta_i &= \frac{b_i^n}{\Delta f} + \frac{\iota_{i,F}^n \mathbb{1}_{\iota_{i,F}^n > 0}}{\Delta f} + \frac{1}{2} \frac{\sigma^2 f_i^2}{(\Delta f)^2}\end{aligned}$$

Boundary Conditions

- We have the following state constraint at the lower boundary (there is no negative drift in df):

$$f \geq f_1 = 0 \Rightarrow \iota_{1,B} = 0$$

However, unlike before, at $f_1 = 0 \Rightarrow \iota_{1,F} = b_1^* > 0$. Therefore,

$$\begin{aligned}\xi_1 &= 0 \\ \beta_1 &= -\frac{b_1^n}{\Delta f} \\ \zeta_1 &= \frac{b_1^n}{\Delta f}\end{aligned}$$

- As before, a firm entering default cannot resume operations or accumulate more debt:

$$f = f_D, \forall t \Rightarrow \begin{bmatrix} \xi_D & \beta_D & \zeta_D \end{bmatrix} = 0$$

Finite difference method for debt price

- With a dividend restriction, it is no longer the case that the no-trade equity value is equal to the equity value with trade.
- As a result, the debt price needs to be solved for taking equity's optimal policies as given.
- The HJB for debt in the crisis region is:

$$(r + m^u + \lambda)p = c^u + m^u + [b - (g + m^u - \delta - \sigma^2)f]p_f + \frac{1}{2}\sigma^2 f^2 p_{ff} + \lambda\bar{p}$$

- Then given time step Δ , the discretized HJB equation in the continuation is given by:

$$\begin{aligned} \frac{p_i^{n+1} - p_i^n}{\Delta} + (r + m^u + \lambda)p_i^{n+1} &= c^u + m^u + \lambda\bar{p} + [b_i^n - (g_i^n + m^u - \delta - \sigma^2)f_i]\partial p_i^{n+1} \\ &\quad + \frac{1}{2}\sigma^2 f_i^2 \partial^2 p_i^{n+1} \\ &= c^u + m^u + \lambda\bar{p} + [b_i^n - (g_i^n + m^u - \delta - \sigma^2)f_i]\frac{p_{i+1}^{n+1} - p_i^{n+1}}{\Delta f} \\ &\quad + \frac{\sigma^2 f_i^2}{2} \frac{p_{i+1}^{n+1} + p_{i-1}^{n+1} - 2p_i^{n+1}}{(\Delta f)^2} \end{aligned}$$

- Collecting terms:

$$\begin{aligned} \left(\frac{\sigma^2 f_i^2}{2(\Delta f)^2} \right) p_{i-1}^{n+1} + \left(-\frac{[b_i^n - (g_i^n + m^u - \delta - \sigma^2)f_i]}{\Delta f} - \frac{\sigma^2 f_i^2}{(\Delta f)^2} \right) p_i^{n+1} \\ + \left(\frac{[b_i^n - (g_i^n + m^u - \delta - \sigma^2)f_i]}{\Delta f} + \frac{\sigma^2 f_i^2}{2(\Delta f)^2} \right) p_{i+1}^{n+1} \end{aligned}$$

- Denote:

$$\begin{aligned}\xi_i^p &= \frac{\sigma^2 f_i^2}{2(\Delta f)^2} \\ \beta_i^p &= -\frac{[b_i^n - (g_i^n + m^u - \delta - \sigma^2)f_i]}{\Delta f} - \frac{\sigma^2 f_i^2}{(\Delta f)^2} \\ \zeta_i^p &= \frac{[b_i^n - (g_i^n + m^u - \delta - \sigma^2)f_i]}{\Delta f} + \frac{\sigma^2 f_i^2}{2(\Delta f)^2}\end{aligned}$$

- In matrix notation,

$$\frac{\mathbf{p}^{n+1} - \mathbf{p}^n}{\Delta} + (r + m^u + \lambda)\mathbf{p}^{n+1} = (c^u + m^u)\mathbf{1} + \lambda\bar{\mathbf{p}} + \mathbf{C}^p \mathbf{p}^{n+1}$$

where,

$$\mathbf{p}, \bar{\mathbf{p}}, \mathbf{1} \in \mathbb{R}^{I \times 1}$$

$$\mathbf{C}^p \in \mathbb{R}^{I \times I}$$

- Rewrite system:

$$\begin{aligned}\frac{\mathbf{p}^{n+1}}{\Delta} + (r + m^u + \lambda)\mathbf{p}^{n+1} - \mathbf{C}^p \mathbf{p}^{n+1} &= (c^u + m^u)\mathbf{1} + \lambda\bar{\mathbf{p}} + \frac{1}{\Delta}\mathbf{p}^n \\ \left(\text{diag} \left(\frac{1}{\Delta} + (r + m^u + \lambda) \right) - \mathbf{C}^p \right) \mathbf{p}^{n+1} &= (c^u + m^u)\mathbf{1} + \lambda\bar{\mathbf{p}} + \frac{1}{\Delta}\mathbf{p}^n \\ \mathbf{B}^{p,n} \mathbf{p}^{n+1} &= \mathbf{b}^{p,n}\end{aligned}$$

where,

$$\mathbf{B}^{p,n} = \text{diag} \left(\frac{1}{\Delta} + (r + m^u + \lambda) \right) - \mathbf{C}^p$$

$$\mathbf{b}^{p,n} = (c^u + m^u) \mathbf{1} + \lambda \bar{\mathbf{p}} + \frac{1}{\Delta} \mathbf{p}^n$$

- In the standard form of a LCP:

$$\mathbf{p}^{n+1'} (\mathbf{B}^{p,n} \mathbf{p}^{n+1} + (-\mathbf{b}^{p,n})) = 0$$

$$\mathbf{p}^{n+1} \geq 0$$

$$\mathbf{B}^{p,n} \mathbf{p}^{n+1} + (-\mathbf{b}^{p,n}) \geq 0$$

Boundary Conditions

- A firm entering default cannot resume operations or accumulate more debt:

$$f = f_D, \forall t \Rightarrow \begin{bmatrix} \xi_D^p & \beta_D^p & \zeta_D^p \end{bmatrix} = 0$$

where, f_D corresponds to the region of the state space where the firm is defaulted.

Solution for Joint Equity and Short-Term Debt Value Function and Investment Policy at No-Debt Boundary

- The HJB in the continuation region for the no-debt, no-trade equilibrium is:

$$0 = \max_g \left\{ -(r - g + \delta)j + A - \theta(A - c^s \alpha) - \Phi(g) - c^s \alpha + \alpha(g - \delta) \right\}$$

- FOC with respect to investment policy:

$$\Phi'(g) = j + \alpha$$

$$\Rightarrow j = \Phi'(g) - \alpha$$

- Joint equity and short-term debt value function for a firm that never takes on debt (and so does not default):

$$\begin{aligned} j &= \mathbb{E} \left[\int_0^\infty \exp(-(r - g^* + \delta)t) [[A - \theta(A - c^s \alpha) - \Phi(g^*) - c^s \alpha + \alpha(g^* - \delta)] dt + \alpha \sigma dZ_t] \right] \\ &= \int_0^\infty \exp(-(r - g^* + \delta)t) [A - \theta(A - c^s \alpha) - \Phi(g^*) - c^s \alpha + \alpha(g^* - \delta)] dt \\ &= \frac{A - \theta(A - c^s \alpha) - \Phi(g^*) - c^s \alpha + \alpha(g^* - \delta)}{r - g^* + \delta} \end{aligned}$$

- Combining these two equations, we have:

$$r + \delta = g^* + \frac{1}{\Phi'(g^*) - \alpha} [A - \theta(A - c^s \alpha) - \Phi(g^*) - c^s \alpha + \alpha(g^* - \delta)]$$

- Since $\Phi'(g^*) - \alpha = \gamma g^* - \alpha$ is strictly increasing in g^* and $g^* > \alpha/\gamma$, RHS is increasing in g^* if:

$$r + \delta > g^* > \alpha/\gamma \Rightarrow \Phi(r + \delta) > \Psi > \Phi(\alpha/\gamma)A - \theta(A - c^s \alpha) - \Phi(g^*) - c^s \alpha$$

$$+ \alpha(g^* - \delta) > 0$$

$$(1 - \theta)A - ((1 - \theta)c^s + \delta)\alpha > \Phi(g^*) - \alpha g^*$$

- Then, $g^* \in (\alpha/\gamma, r + \delta)$:

$$\Phi(\alpha/\gamma) - \alpha(\alpha/\gamma) < (1 - \theta)A - ((1 - \theta)c^s + \delta)\alpha < \Phi(r + \delta) - \alpha(r + \delta)$$

- Rearrange terms and express the equation as a quadratic function in g^* :

$$-\gamma g^{*2} + 2\gamma(r + \delta)g^* + 2\alpha[(1 - \theta)c^s - r] - 2(1 - \theta)A = 0$$

- Then, we choose the smaller root so that $g^* \in (\alpha/\gamma, r + \delta)$:

$$\begin{aligned} g^* &= \frac{-2\gamma(r + \delta) + \sqrt{(2\gamma(r + \delta))^2 - 4(-\gamma)(2\alpha[(1 - \theta)c^s - r] - 2(1 - \theta)A)}}{-2\gamma} \\ &= \frac{\gamma(r + \delta) - \sqrt{(\gamma(r + \delta))^2 + 2\gamma(\alpha[(1 - \theta)c^s - r] - (1 - \theta)A)}}{\gamma} \end{aligned}$$

No-Debt Boundary Optimal Investment in Crisis

- The HJB in the continuation region for the no-debt, no-trade equilibrium with crisis dynamics is:

$$0 = \max_g \left\{ -(r - g + \delta)j + \eta A - \theta(\eta A - c^s \alpha) - \Phi(g) - c^s \alpha + (p_s^* - 1)\alpha + p_s^* \alpha(g - \delta) + \lambda(\bar{j} - j) \right\}$$

where \bar{j} is the pre-shock joint equity and short-term debt value.

- FOC with respect to investment policy:

$$\Phi'(g) = j + p_s^* \alpha$$

$$\Rightarrow j = \Phi'(g) - p_s^* \alpha = \gamma g - p_s^* \alpha$$

- The joint equity and short-term debt value function for a firm that never takes on debt (and so does not default):

$$j^* = \frac{\eta A - \theta(\eta A - c^s \alpha) - \Phi(g^*) - c^s \alpha + (p_s^* - 1)\alpha + p_s^* \alpha(g^* - \delta) + \lambda \bar{j}}{r - g^* + \delta + \lambda}$$

- Combining these two equations, we have:

$$\begin{aligned} r + \delta + \lambda &= g^* + \frac{1}{\Phi'(g^*) - p_s^* \alpha} [\eta A - \theta(\eta A - c^s \alpha) - \Phi(g^*) - c^s \alpha \\ &\quad + (p_s^* - 1)\alpha + p_s^* \alpha(g^* - \delta) + \lambda \bar{j}] \end{aligned}$$

- As a quadratic function in g^* ,

$$\begin{aligned} r + \delta + \lambda &= g^* + \frac{1}{\gamma g^* - p_s^* \alpha} [\eta A - \theta(\eta A - c^s \alpha) \\ &\quad - \frac{1}{2} \gamma g^{*2} - c^s \alpha + (p_s^* - 1)\alpha \\ &\quad + p_s^* \alpha(g^* - \delta) + \lambda \bar{j}] \\ &= \frac{1}{\gamma g^* - p_s^* \alpha} [\gamma g^{*2} - g^* p_s^* \alpha + \eta A - \theta(\eta A - c^s \alpha) - \frac{1}{2} \gamma g^{*2} - c^s \alpha \\ &\quad + (p_s^* - 1)\alpha + p_s^* \alpha(g^* - \delta) + \lambda \bar{j}] \\ &= \frac{\frac{1}{2} \gamma g^{*2} + \eta A - \theta(\eta A - c^s \alpha) - c^s \alpha + (p_s^* - 1)\alpha - p_s^* \alpha \delta + \lambda \bar{j}}{\gamma g^* - p_s^* \alpha} \\ (r + \delta + \lambda)(\gamma g^* - p_s^* \alpha) &= \frac{1}{2} \gamma g^{*2} + \eta A - \theta(\eta A - c^s \alpha) - c^s \alpha + (p_s^* - 1)\alpha - p_s^* \alpha \delta + \lambda \bar{j} \\ \Rightarrow 0 &= -\gamma g^{*2} + 2\gamma(r + \delta + \lambda)g^* \\ &\quad - 2p_s^* \alpha(r + \lambda) - 2[\eta A - \theta(\eta A - c^s \alpha) - c^s \alpha \\ &\quad + (p_s^* - 1)\alpha + \lambda \bar{j}] \\ 0 &= -\gamma g^{*2} + 2\gamma(r + \delta + \lambda)g^* \\ &\quad - 2\alpha[p_s^*(r + \lambda) - (1 - \theta)c^s + (p_s^* - 1)] - 2[(1 - \theta)\eta A + \lambda \bar{j}] \end{aligned}$$

- Choose smaller root:

$$g^* = \frac{-2\gamma(r + \delta + \lambda) + \sqrt{(2\gamma(r + \delta + \lambda))^2 - 4(-\gamma)(-2\alpha[p_s^*(r + \lambda) + (1 - \theta)c^s + (p_s^* - 1)] - 2[(1 - \theta)\eta A + \lambda \bar{j}])}}{-2\gamma}$$

$$= \frac{\gamma(r + \delta + \lambda) - \sqrt{(\gamma(r + \delta + \lambda))^2 - 2\gamma(\alpha[p_s^*(r + \lambda) + (1 - \theta)c^s + (p_s^* - 1)] + [(1 - \theta)\eta A + \lambda \bar{j}])}}{\gamma}$$

Primal-Dual Interior-Point Method

- To solve extensions to the base model with policy constraints, I marry an interior-point method to solve the resultant nonlinear optimization problem with an upwind finite differences method to solve the HJB and a linear complementary method to solve for the optimal stopping time (i.e. default).
- Below is the formulation for the nonlinear convex optimization problem featuring a dividend restriction, which both policies must satisfy.
- Define:

$$h(b^u, g, \omega) \equiv -(r - g + \delta + \lambda)j + \pi(b^u, g) + \lambda \bar{j} + [b^u - (g - \delta + m^u)f]j_f + \frac{1}{2}\sigma^2 f^2 j_{ff}$$

$$B(b^u, g, \omega) \equiv -h(b^u, g, \omega) - \omega \log(-\pi(b^u, g))$$

Note the change in sign on the objective $B(b^u, g, \omega)$. This is because I'm solving the maximization problem as minimization.

- Compute the gradient of the barrier function $B(b^u, g, \omega)$:

$$\begin{aligned}
\nabla B(b^u, g, \omega) &= -\nabla h(b^u, g, \omega) - \omega \frac{1}{\pi(b^u, g)} \nabla \pi(b^u, g) \\
\begin{bmatrix} \frac{\partial B}{\partial b^u} \\ \frac{\partial B}{\partial g} \end{bmatrix} &= - \begin{bmatrix} \frac{\partial h}{\partial b^u} \\ \frac{\partial h}{\partial g} \end{bmatrix} - \omega \frac{1}{\pi(b^u, g)} \begin{bmatrix} \frac{\partial \pi}{\partial b^u} \\ \frac{\partial \pi}{\partial g} \end{bmatrix} \\
&= - \begin{bmatrix} \pi_{b^u} + j_f \\ j + \pi_g - f j_f \end{bmatrix} - \omega \frac{1}{\pi(b^u, g)} \begin{bmatrix} p \\ -\Phi'(g) + p_s^* \alpha \end{bmatrix} \\
&= - \begin{bmatrix} p + j_f \\ j - \Phi'(g) + p_s^* \alpha - f j_f \end{bmatrix} - \omega \frac{1}{\pi(b^u, g)} \begin{bmatrix} p \\ -\Phi'(g) + p_s^* \alpha \end{bmatrix} \\
&= - \begin{bmatrix} p + j_f \\ j - g\gamma + p_s^* \alpha - f j_f \end{bmatrix} - \omega \frac{1}{\pi(b^u, g)} \begin{bmatrix} p \\ -g\gamma + p_s^* \alpha \end{bmatrix}
\end{aligned}$$

3.6.14 Numerical Results for Model with Short-Term Debt

- Associated with Section 3.4.

Initial Distribution

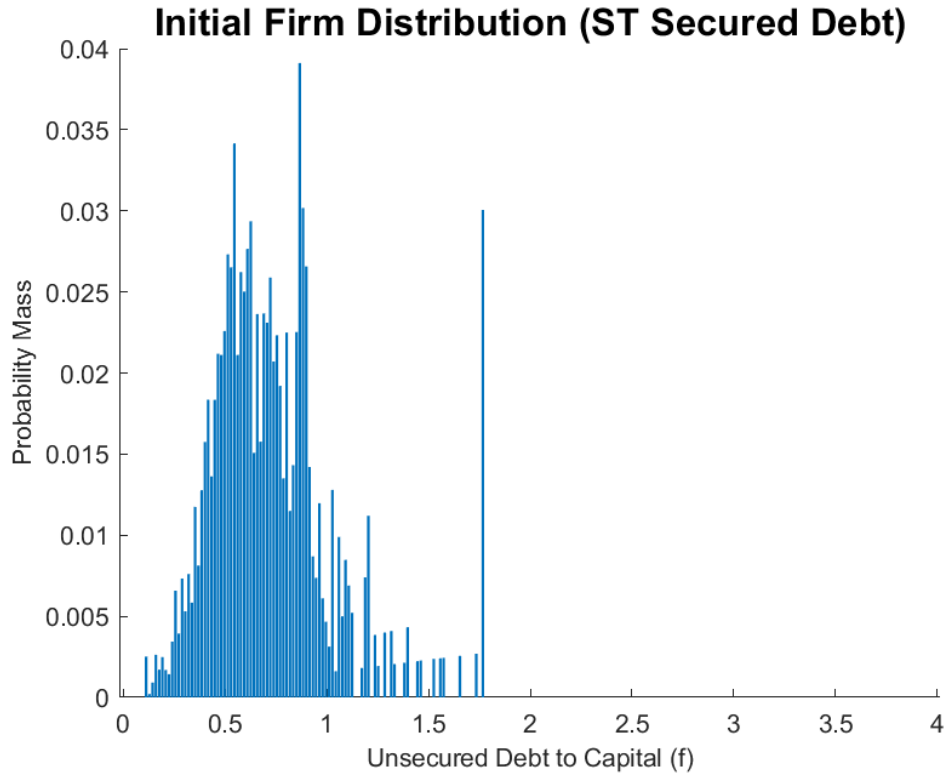


Figure 3.13: Initial Distribution of Firms

The figure plots the initial distribution of unsecured debt to capital. It is proxied by the variable `debt_capital` from the Financial Ratios Suite by Wharton WRDS based on Compustat data for rated firms. Ratings information is obtained from the Mergent FISD database. Data is winsorized at the 1% and 99% levels. The numerator of `debt_capital` is computed as the sum of accounts payable (`ap`), total debt in current liabilities (`d1c`), and total long-term debt (`d1tt`). The denominator is computed as the sum of debt, and the sum of total common equity (`ceq`) and preferred stock (`pstkrv`, `pstk1`, `pstk`). Results are robust to using the variable `debt_assets`, which is computed as the ratio of total liabilities (`ltq`) to total assets (`at`).

Parameters

	Baseline	Crisis No. Int.	Crisis Unsec. Int.	Crisis Sec. Int.	Crisis Div. Rest.
A	0.24	$\eta \times 0.24$	$\eta \times 0.24$	$\eta \times 0.24$	$\eta \times 0.24$
$r^{(e)}$	0.05	0.05	0.05	0.05	0.05
$r^{(d)}$	$r^{(e)}$	$r^{(e)}$	$r^{(e)} - 0.02$	$r^{(e)}$	$r^{(e)} - 0.02$
δ	0.1	0.1	0.1	0.1	0.1
m^u	0.1	0.1	0.1	0.1	0.1
θ	0.35	0.35	0.35	0.35	0.35
α	0.20	0.20	0.20	0.20	0.20
σ	0.31	0.31	0.31	0.31	0.31
γ	16	16	16	16	16
η	1	0.95	0.95	0.95	0.95
λ	0	0.50	0.50	0.50	0.50
p_s^*	1	1	1	1.02	1

Table 3.3: Parameters for Numerical Estimation

3.6.15 Dividend and Debt Repurchase Restrictions with Unsecured Debt Intervention

Figure 3.14 shows that the dividend restriction binds over the same region for both economies with and without unsecured debt repurchase restrictions. Unsurprisingly, payouts are far lower in the case with dividend restrictions.

Figure 3.15 shows firms unsecured debt issuance policies. Recall that the economies featuring dividend restrictions also benefit from unsecured debt intervention. In spite of this, firms in these economies do not choose to issue unsecured debt while the dividend restriction binds. Unable to make payouts, firms either increase investment, repurchase unsecured debt, or do both.

Figure 3.16 shows that dividend restrictions result in lower joint valuations for equity and short-term debt, particularly for the region of the state space where the dividend constraint binds. In fact, the difference between unconstrained and constrained equity prices

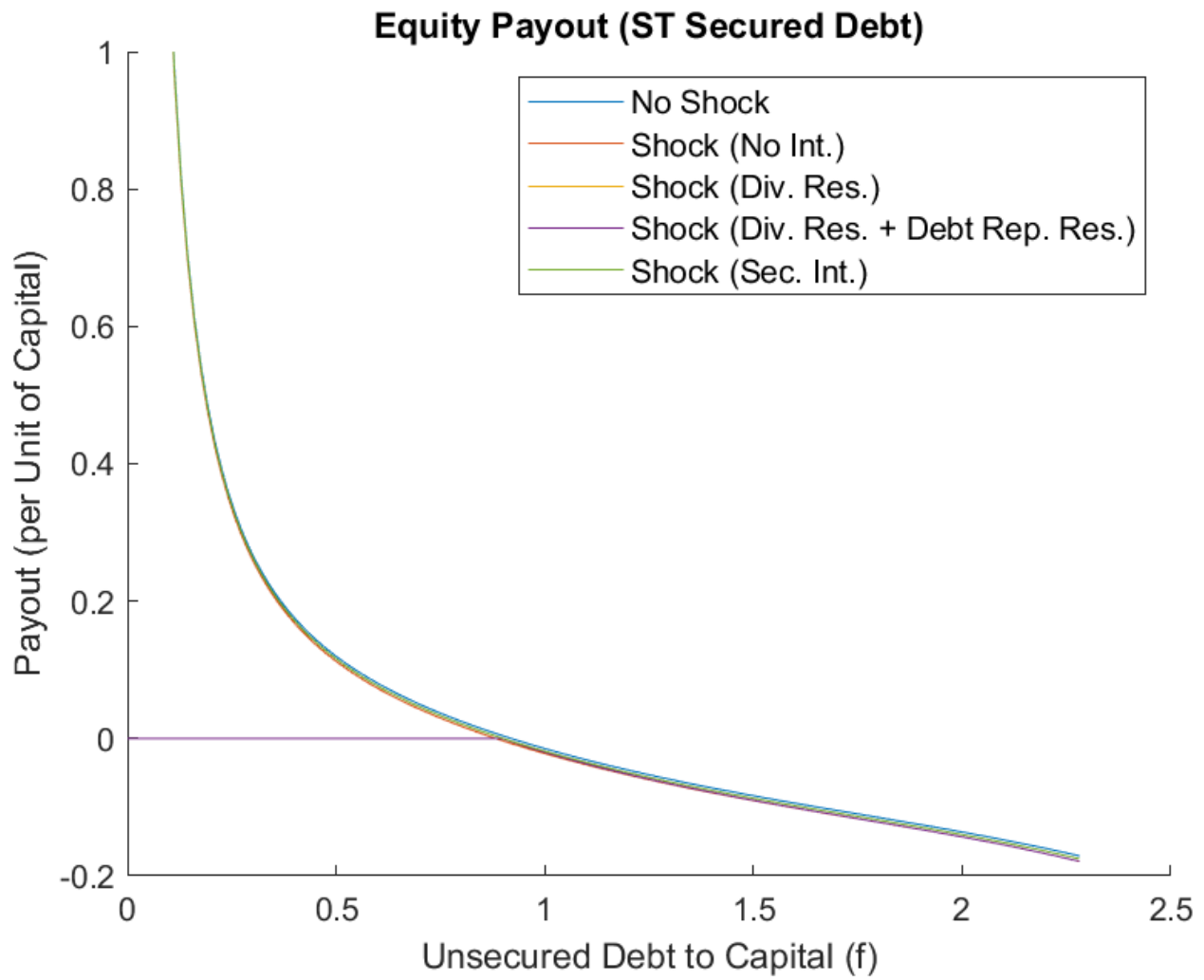


Figure 3.14: Dividend Restriction Binds for Large Portion of State Space

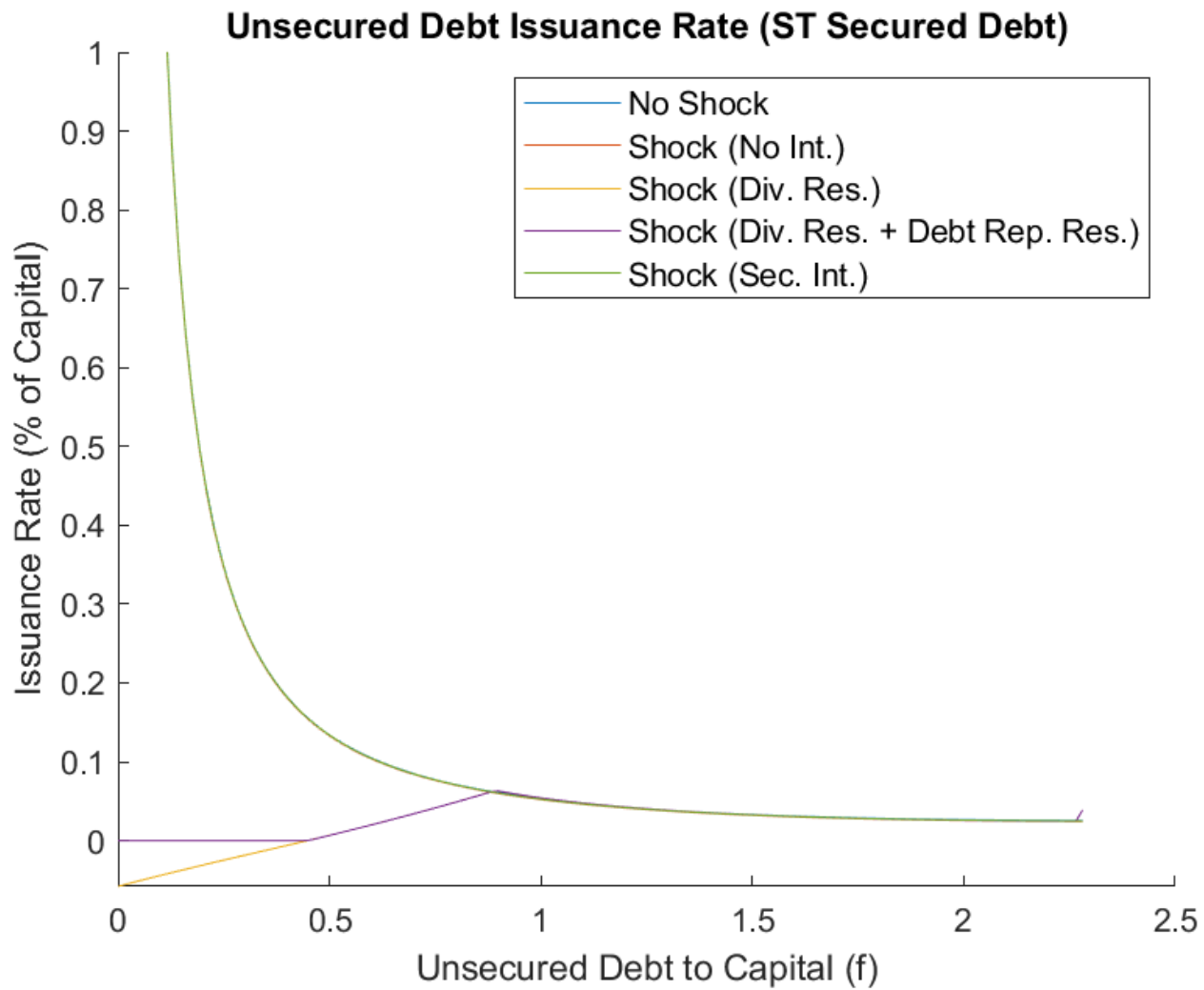


Figure 3.15: Debt Repurchase Motive With Dividend Restriction

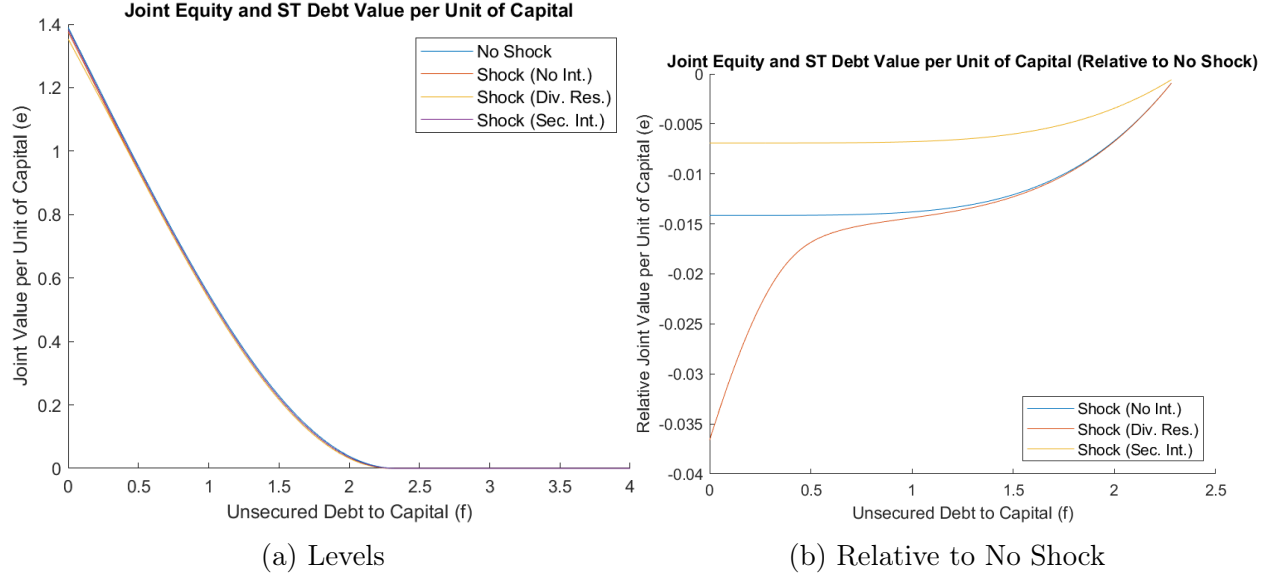


Figure 3.16: Dividend Restriction Decreases Equity Value

increases as distance to the dividend restriction boundary increases. This is consistent with the monotonic pattern implied by the difference in dividends shown in Figure 3.14. The combination of lower equity prices, as well as non-positive unsecured debt issuance, suggest that firms would not voluntarily participate in credit programs featuring dividend and debt repurchase restrictions, which can explain the low uptake of the MSLP (which had less than a 3% utilization rate).

As intended, dividend restrictions sharply boost investment rates, as shown in Figure 3.17. In particular, a restriction on unsecured debt repurchases leads to sizeable increase in investment. This reinforces the debt repurchase motive for firms, as seen in Figure 3.15.

Echoing the differences in investment policy, the expected evolution of average investment rates is higher when dividend restrictions are in place, more so when the firm cannot repurchase unsecured debt. This is shown in Figure 3.18.

While equity prices are shown to fall in Figure 3.16, Figure 3.19 shows that unsecured debt price rises with dividend restrictions. With positive investment rates and no unsecured debt issuance, or even repurchases, the firm deleverages, reducing default risk and improving debt prices.

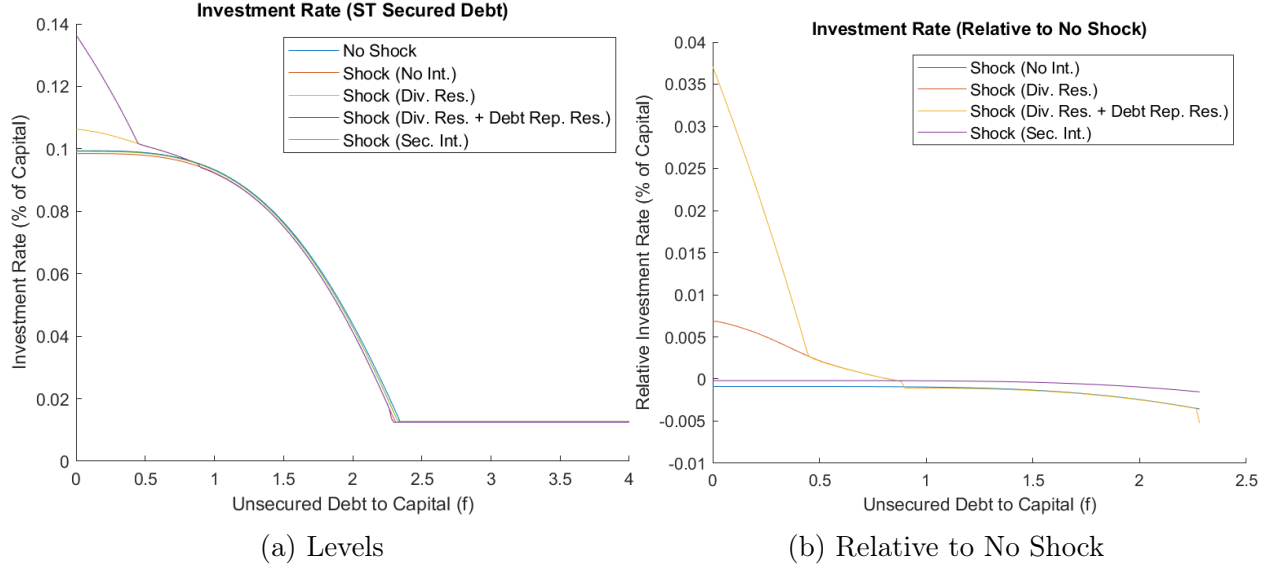


Figure 3.17: Dividend Restriction Sharply Increases Investment Rates

Figure 3.20 shows that dividend restrictions has no impact on the firm's default threshold relative to no intervention.

Figure 3.21 shows that the evolution of expected default rates are eventually lower with dividend restrictions. This is because the restriction forces the firm to grow larger (and hence, hold a smaller proportion of debt to assets). Additionally, when there are no restrictions on unsecured debt repurchases in place, retiring debt results in lower leverage and lowers default risk.

Figure 3.23 shows a stark contrast in the distributions of surviving firms in the economies with and without dividend restrictions. Dividend restrictions cause firms to move away from the default boundary as a result of higher investment. This force is compounded when the firm can repurchase unsecured debt.

Figure 3.23 reinforces these results and gives a sense of how lower of a leverage ratio surviving firms have with dividend restrictions.

While it may be surprising that average expected equity value increases with dividend restrictions, as shown in Figure 3.24, this is because more firms are moving away faster from the boundary than those which are defaulting. This force is strong enough to coun-

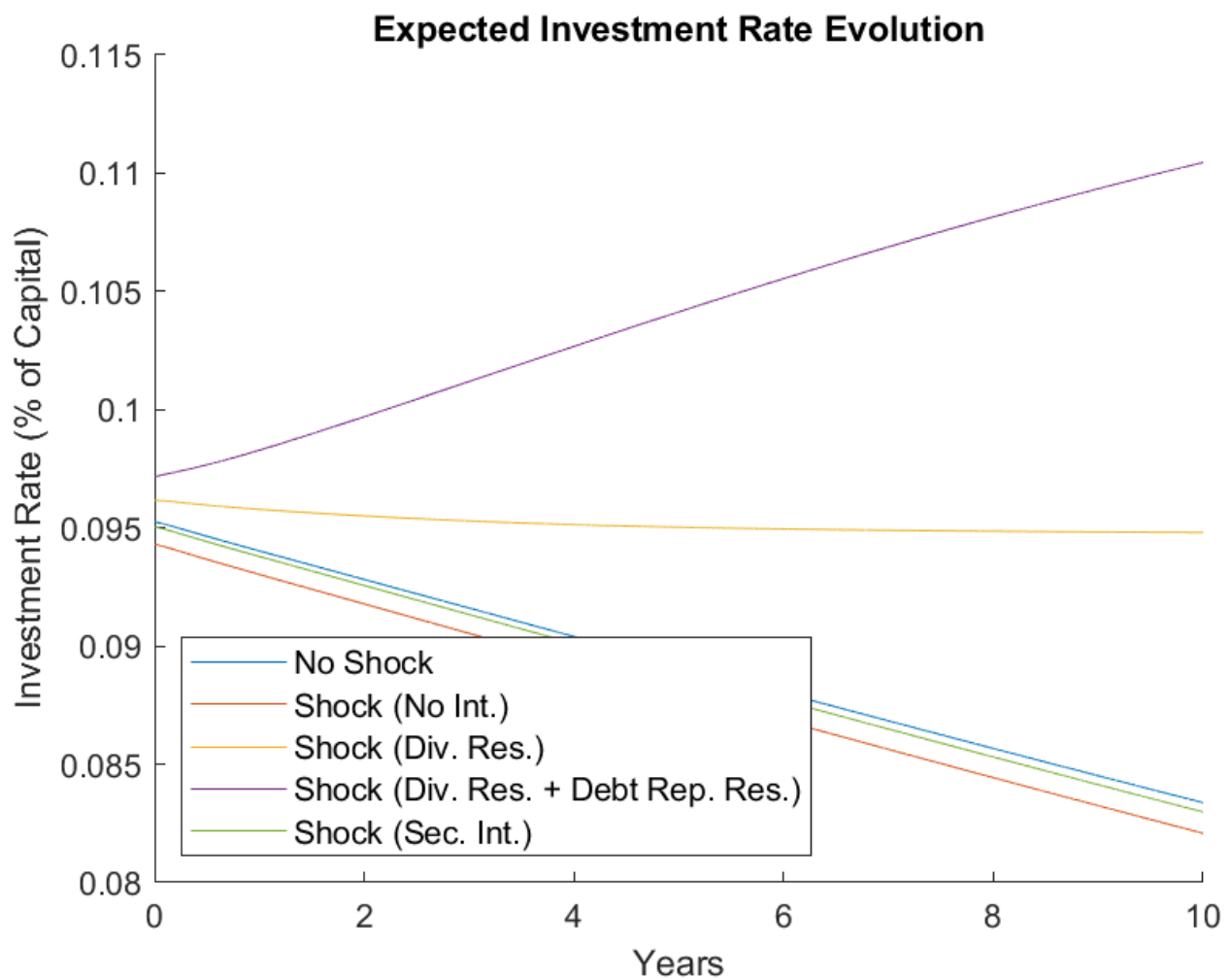


Figure 3.18: Expected Evolution of Investment Rates Also Far Higher

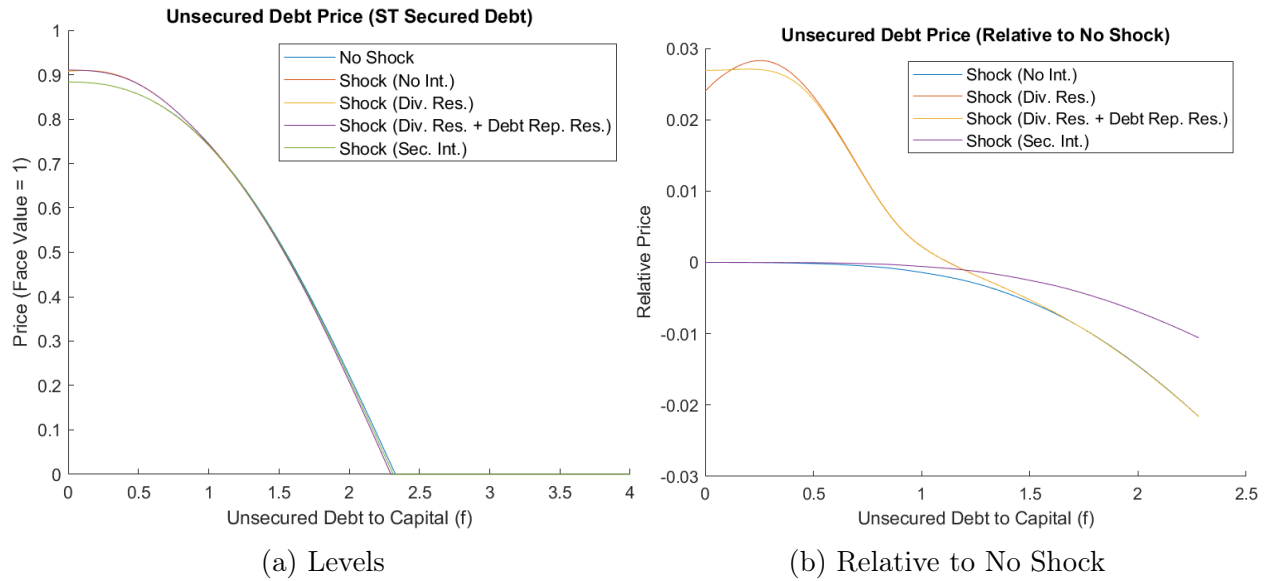


Figure 3.19: Dividend Restriction Increases Unsecured Debt Price

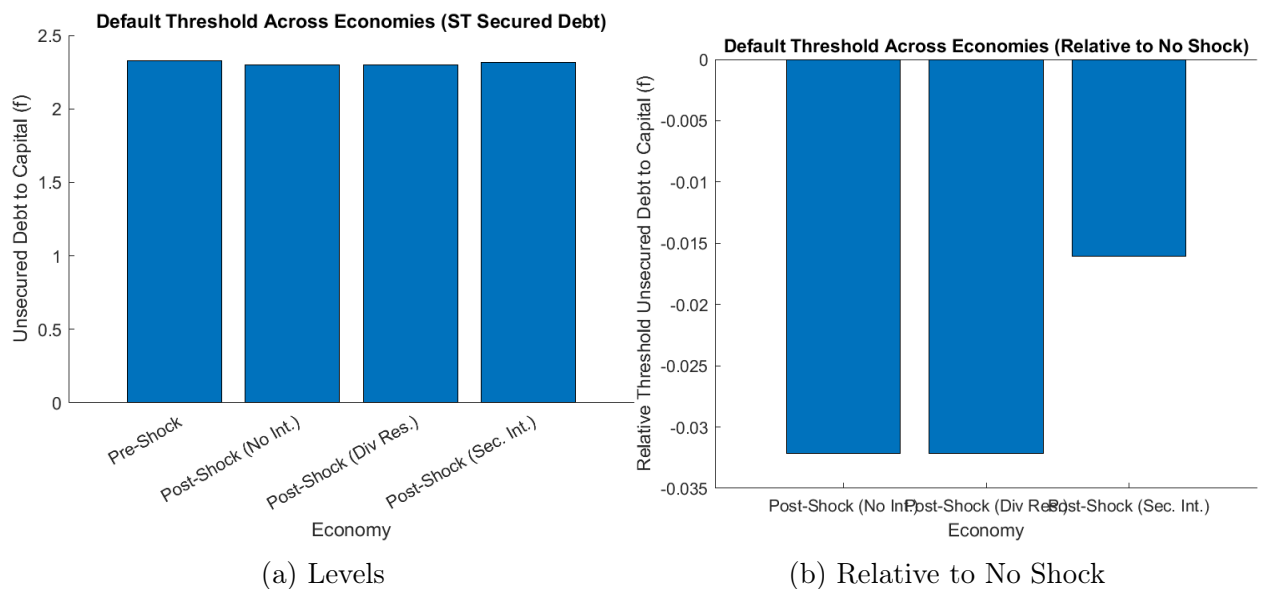


Figure 3.20: Dividend Restriction has No Impact on Default Threshold

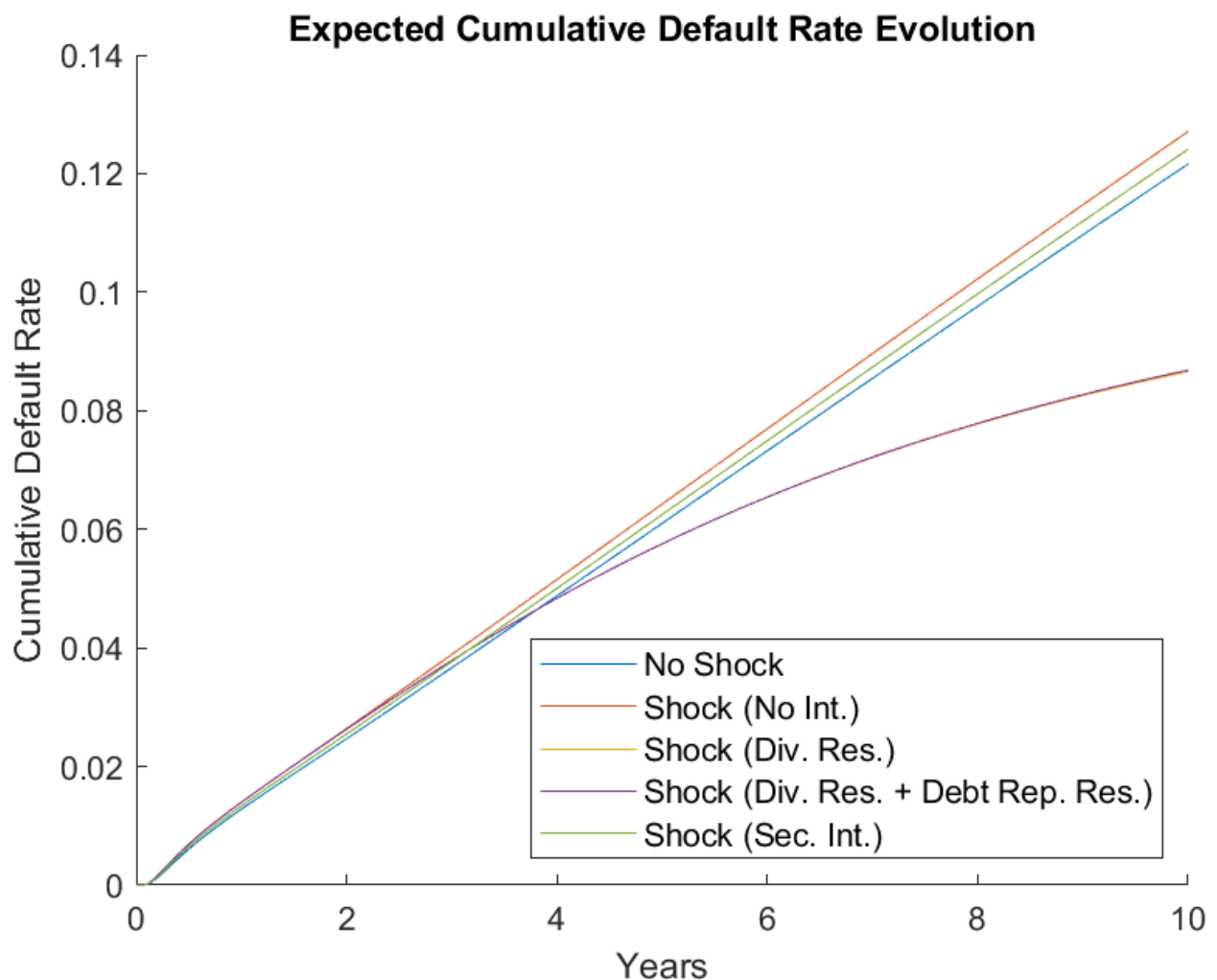


Figure 3.21: Dividend Restriction Sharply Reduces Long-Run Defaults

Surviving Firm Distribution after 10 Years

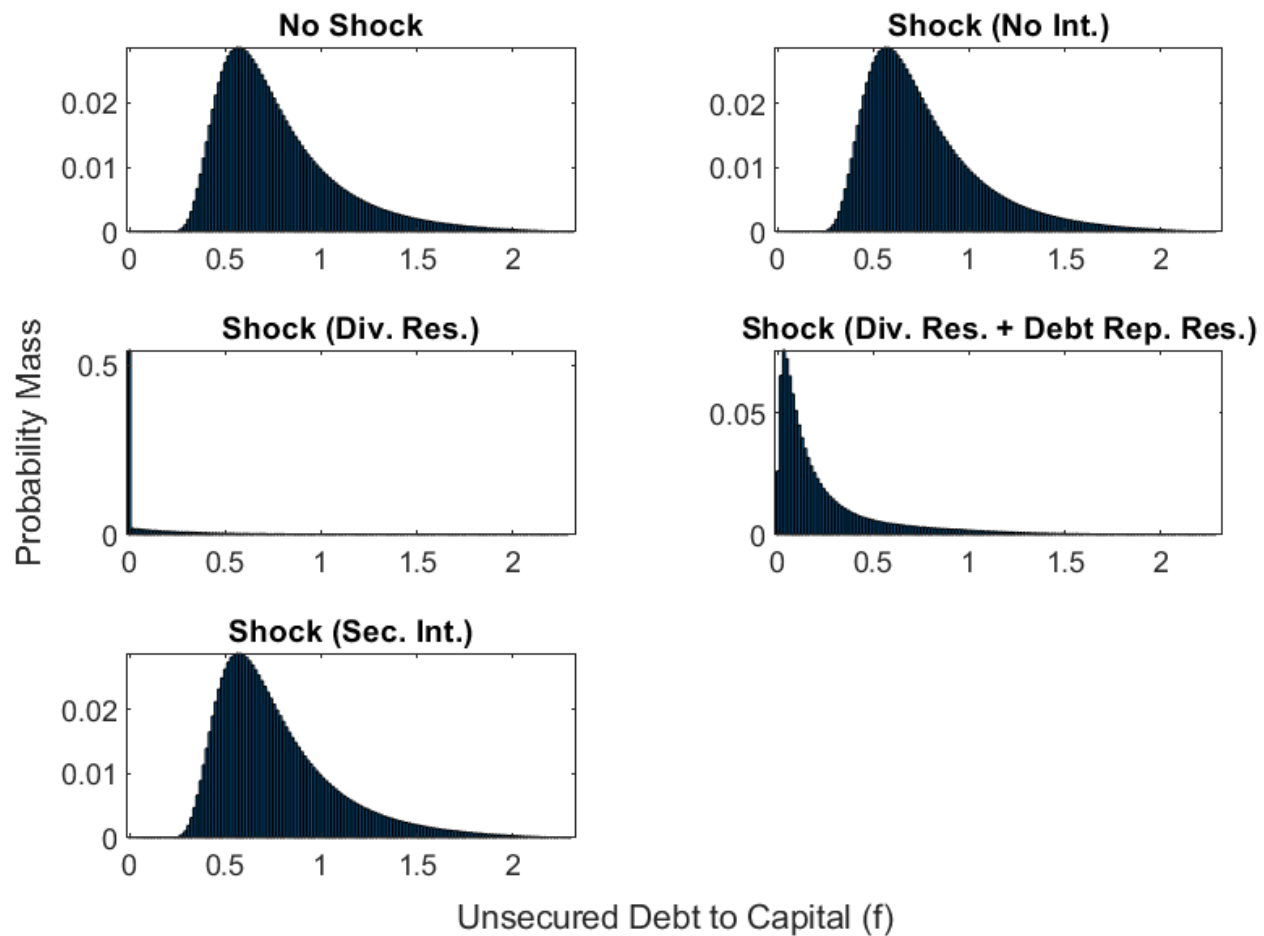


Figure 3.22: Surviving Firms Have Far Lower Leverage With Dividend Restriction; Even Less Without Debt Repurchase Restriction

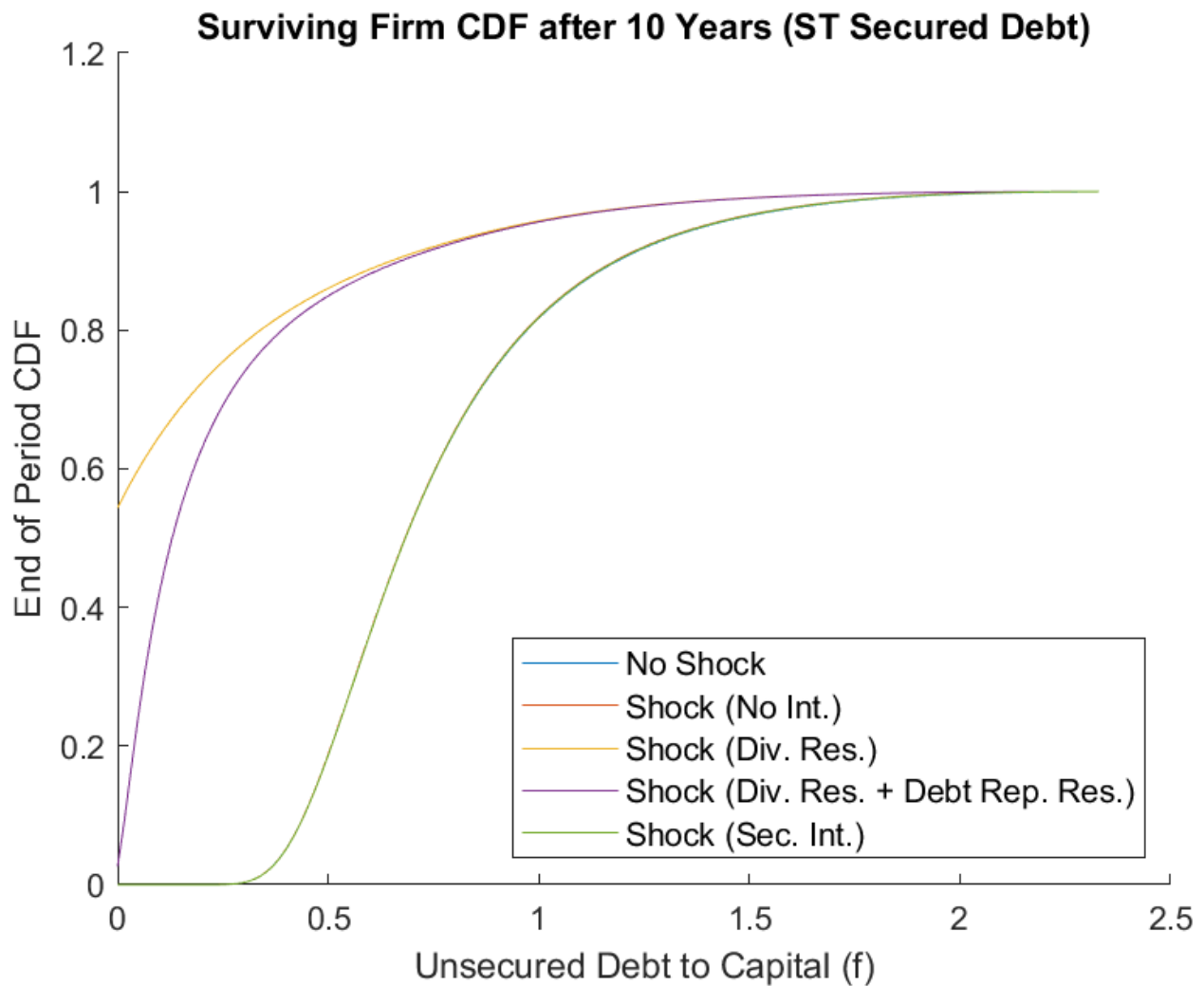


Figure 3.23: Surviving Firms Have Far Lower Leverage With Dividend Restriction; Even Less Without Debt Repurchase Restriction

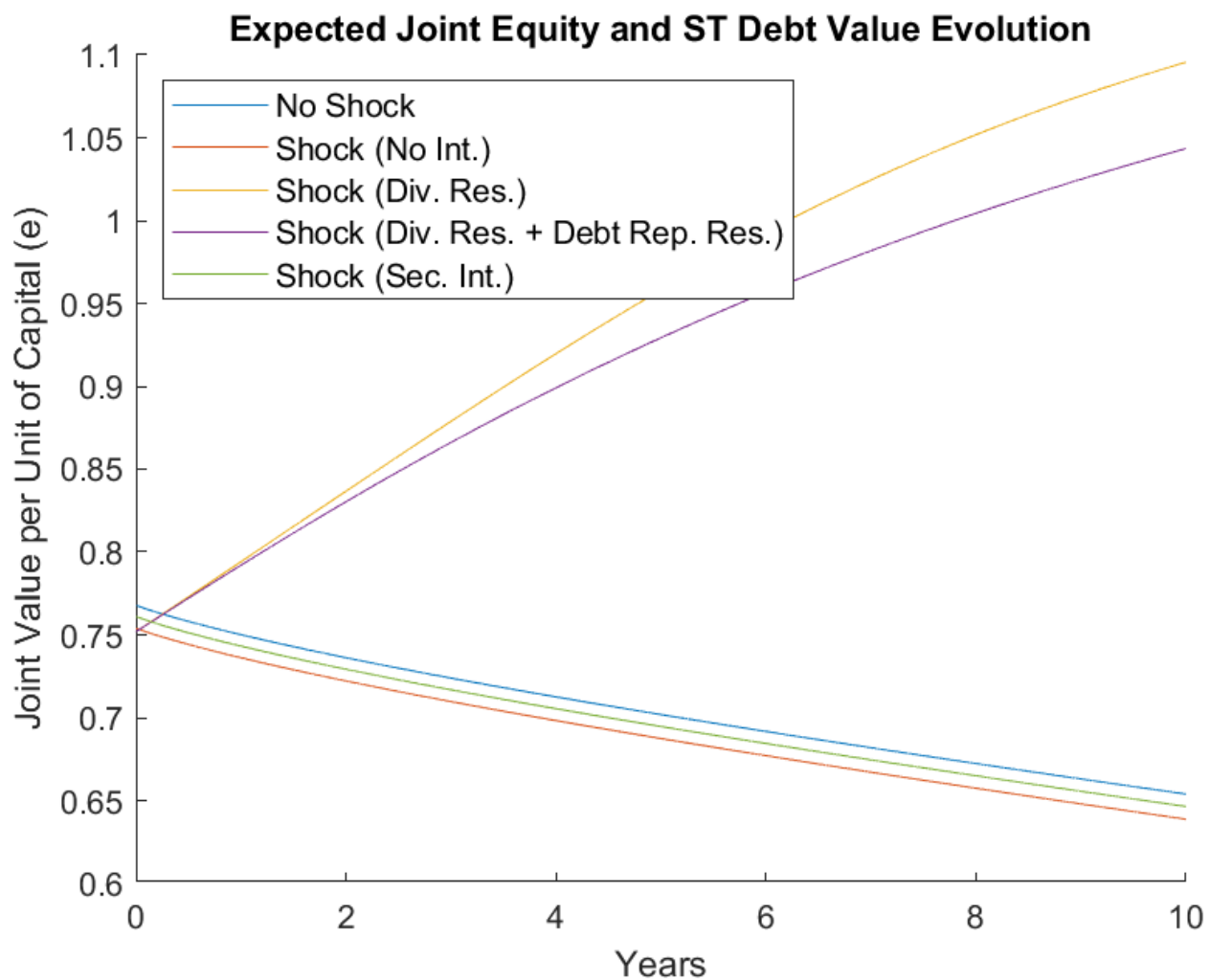


Figure 3.24: Expected Average Equity Values Increase Over Time With Restrictions

teract the relatively lower equity prices from the dividend restriction binding more tightly.

BIBLIOGRAPHY

Abel, Andrew B. 2016. "Investment with Leverage."

Abel, Andrew B. 2018. "Optimal Debt and Profitability in the Trade-Off Theory." *The Journal of Finance* 73 (1): 95–143.

Abidi, Nordine, and Ixart Miquel-Flores. 2018. "Who Benefits from the Corporate QE? A Regression Discontinuity Design Approach." *SSRN Electronic Journal*.

Acharya, Viral, and Guillaume Plantin. 2025. "Monetary Easing, Leveraged Payouts, and Lack of Investment." *Management Science*: mnsc.2022.01440.

Acharya, Viral V, and Sascha Steffen. 2020. "The Risk of Being a Fallen Angel and the Corporate Dash for Cash in the Midst of COVID." *The Review of Corporate Finance Studies* 9 (3): 430–471.

Ali, Heba. 2022. "Corporate dividend policy in the time of COVID-19: Evidence from the G-12 countries." *Finance Research Letters* 46: 102493.

Almeida, Heitor, Murillo Campello, and Michael S. Weisbach. 2004. "The Cash Flow Sensitivity of Cash." *The Journal of Finance* 59 (4): 1777–1804.

Altman, Edward. 2020. "Covid-19 and the credit cycle." *The Journal of Credit Risk*.

Altman, Edward I., and Herbert A. Rijken. 2004. "How rating agencies achieve rating stability." *Journal of Banking & Finance* 28 (11): 2679–2714.

Barry, John W., Murillo Campello, John R. Graham, and Yueran Ma. 2022. "Corporate flexibility in a time of crisis." *Journal of Financial Economics* 144 (3): 780–806.

Becker, Bo, and Efraim Benmelech. 2021. "The Resilience of the U.S. Corporate Bond Market During Financial Crises." Technical Report w28868, National Bureau of Economic Research. Cambridge, MA.

Belloni, Alexandre, Victor Chernozhukov, and Christian Hansen. 2014. "High-Dimensional Methods and Inference on Structural and Treatment Effects." *Journal of Economic Perspectives* 28 (2): 29–50.

Benmelech, Efraim, Nitish Kumar, and Raghuram Rajan. 2022. "The secured credit premium and the issuance of secured debt." *Journal of Financial Economics* 146 (1): 143–171.

Benmelech, Efraim, Nitish Kumar, and Raghuram Rajan. 2024. "The Decline of Secured Debt." *The Journal of Finance* 79 (1): 35–93.

Bilgin, Rumeysa. 2023. "The selection of control variables in capital structure research with machine learning." *Journal of Corporate Accounting & Finance* 34 (4): 244–255. _eprint: <https://onlinelibrary.wiley.com/doi/pdf/10.1002/jcaf.22647>.

Borri, Nicola, Denis Chetverikov, Yukun Liu, and Aleh Tsvybinski. 2024. “One Factor to Bind the Cross-Section of Returns.”

Boyarchenko, Nina, Anna Kovner, and Or Shachar. 2020. “It’s What You Say and What You Buy: A Holistic Evaluation of the Corporate Credit Facilities.”

Boyarchenko, Nina, Anna Kovner, and Or Shachar. 2022. “It’s what you say and what you buy: A holistic evaluation of the corporate credit facilities.” *Journal of Financial Economics* 144 (3): 695–731.

Brunnermeier, Markus, and Arvind Krishnamurthy. 2020. “Corporate Debt Overhang and Credit Policy.” *Brookings Papers on Economic Activity* 2020 (2): 447–502.

Caballero, Ricardo J., and Eduardo M. R. A. Engel. 1999. “Explaining investment dynamics in U.S. manufacturing: A generalized (S,s) approach.” *Econometrica* 67 (4): 783–826.

Caetano, Carolina, Brantly Callaway, Stroud Payne, and Hugo Sant’Anna Rodrigues. 2024. “Difference in Differences with Time-Varying Covariates.” arXiv:2202.02903 [econ].

Campello, Murillo, John R. Graham, and Campbell R. Harvey. 2010. “The real effects of financial constraints: Evidence from a financial crisis.” *Journal of Financial Economics* 97 (3): 470–487.

Catherine, Sylvain, Thomas Chaney, Zongbo Huang, David Sraer, and David Thesmar. 2022. “Quantifying Reduced-Form Evidence on Collateral Constraints.” *The Journal of Finance* 77 (4): 2143–2181.

Cejnek, Georg, Otto Randl, and Josef Zechner. 2021. “The COVID-19 Pandemic and Corporate Dividend Policy.” *Journal of Financial and Quantitative Analysis* 56 (7): 2389–2410.

Celik, S., G. Demirtaş, and M. Isaksson. 2020. *Corporate Bond Market Trends, Emerging Risks and Monetary Policy*. OECD Capital Market Series: OECD.

Chang, Neng-Chieh. 2020. “Double/debiased machine learning for difference-in-differences models.” *The Econometrics Journal* 23 (2): 177–191.

Chernozhukov, Victor, Denis Chetverikov, Mert Demirer, Esther Duflo, Christian Hansen, Whitney Newey, and James Robins. 2018. “Double/debiased machine learning for treatment and structural parameters.” *The Econometrics Journal* 21 (1): C1–C68.

Chernozhukov, Victor, Christian Hansen, Nathan Kallus, Martin Spindler, and Vasilis Syrgkanis. 2024. “Causal Inference with ML and AI.”

Chronopoulos, Ilias, Katerina Chrysikou, George Kapetanios, James Mitchell, and Aristeidis Raftopoulos. 2023. “Deep Neural Network Estimation in Panel Data Models.” arXiv:2305.19921 [econ].

Clarida, Richard H., Burcu Duygan-Bump, and Chiara Scotti. 2021. “The COVID-19 Crisis and the Federal Reserve’s Policy Response.” *Finance and Economics Discussion Series* 2021.0 (34): 1–23.

Crouzet, Nicolas, and Janice Eberly. 2020. “Rents and Intangibles: a Q+ Framework.”

Crouzet, Nicolas, and Fabrice Tourre. 2021. “Can the cure kill the patient? Corporate credit interventions and debt overhang.” *SSRN Electronic Journal*.

Darmouni, Olivier, and Kerry Y. Siani. 2024. “Bond market stimulus: Firm-level evidence.” *Journal of Monetary Economics*: 103728.

De Marco, Filippo, and Nicola Limodio. 2022. “The Financial Transmission of a Climate Shock: El Niño and US Banks.” *SSRN Electronic Journal*.

De Santis, Roberto A., and Andrea Zaghini. 2021. “Unconventional monetary policy and corporate bond issuance.” *European Economic Review* 135: 103727.

DeMarzo, Peter, Zhiguo He, and Fabrice Tourre. 2023. “Sovereign Debt Ratchets and Welfare Destruction.” *Journal of Political Economy* 131 (10): 2825–2892.

DeMarzo, Peter M. 2019. “Presidential Address: Collateral and Commitment.” *The Journal of Finance* 74 (4): 1587–1619.

DeMarzo, Peter M., and Zhiguo He. 2021. “Leverage Dynamics without Commitment.” *The Journal of Finance* 76 (3): 1195–1250.

Deng, Yongheng, Erik Devos, Shofiqur Rahman, and Desmond Tsang. 2016. “The Role of Debt Covenants in the Investment Grade Bond Market – The REIT Experiment.” *The Journal of Real Estate Finance and Economics* 2: 428–448.

Denis, David J., and Valeriy Sibilkov. 2010. “Financial Constraints, Investment, and the Value of Cash Holdings.” *Review of Financial Studies* 23 (1): 247–269.

Dick-Nielsen, Jens. 2014. “How to Clean Enhanced TRACE Data.” *SSRN Electronic Journal*.

Dutordoir, Marie, Joshua Shemesh, Chris Veld, and Qing Wang. 2024. “Can existing corporate finance theories explain security offerings during the COVID-19 pandemic?” *Journal of Empirical Finance* 79: 101558.

D’Amico, Stefania, Vamsidhar Kurakula, and Stephen Lee. 2020. “Impacts of the Fed Corporate Credit Facilities through the Lenses of ETFs and CDX.” Technical report, Federal Reserve Bank of Chicago.

Elgouacem, Assia, and Riccardo Zago. 2023. “Share Buybacks, Monetary Policy and the Cost of Debt.” *International Journal of Central Banking* 19 (2): 295–349.

Falato, Antonio, Dalida Kadyrzhanova, Jae Sim, and Roberto Steri. 2022. “Rising Intangible Capital, Shrinking Debt Capacity, and the U.S. Corporate Savings Glut.” *The Journal of Finance* 77 (5): 2799–2852.

Farre-Mensa, Joan, Roni Michaely, and Martin Schmalz. 2024. “Financing Payouts.” *Journal of Financial and Quantitative Analysis*: 1–39.

Farrell, Max H., Tengyuan Liang, and Sanjog Misra. 2021a. “Deep Neural Networks for Estimation and Inference.” *Econometrica* 89 (1): 181–213.

Farrell, Max H., Tengyuan Liang, and Sanjog Misra. 2021b. “Deep Learning for Individual Heterogeneity: An Automatic Inference Framework.” arXiv:2010.14694 [econ].

Faulkender, Michael, and Mitchell A Petersen. 2006. “Does the Source of Capital Affect Capital Structure?” *The Review of Financial Studies* 19 (1).

Feldhütter, Peter, and Stephen M. Schaefer. 2018. “The myth of the credit spread puzzle.” *The Review of Financial Studies* 31 (8): 2897–2942.

Feng, Guanhao, Stefano Giglio, and Dacheng Xiu. 2020. “Taming the Factor Zoo: A Test of New Factors.” *The Journal of Finance* 75 (3): 1327–1370.

Flanagan, Thomas, and Amiyatosh Purnanandam. 2020. “Corporate Bond Purchases After COVID-19: Who Did the Fed Buy and How Did the Markets Respond?”.

Gilchrist, Simon, Bin Wei, Vivian Z Yue, and Egon Zakrajšek. 2021. “The Fed takes on corporate credit risk: an analysis of the efficacy of the SMCCF.”

Gomez-Gonzalez, Jose E., Jorge M. Uribe, and Oscar Valencia. 2024. “Sovereign Risk and Economic Complexity.” Technical report, Inter-American Development Bank.

Gormsen, Niels Joachim, and Ralph S J Koijen. 2020. “Coronavirus: Impact on Stock Prices and Growth Expectations.” *The Review of Asset Pricing Studies* 10 (4): 574–597.

Greenwald, Daniel L., John Krainer, and Pascal Paul. 2023. “The Credit Line Channel.” *Federal Reserve Bank of San Francisco, Working Paper Series*: 1.000–96.000.

Grosse-Rueschkamp, Benjamin, Sascha Steffen, and Daniel Streitz. 2019. “A capital structure channel of monetary policy.” *Journal of Financial Economics* 133 (2): 357–378.

Gurkaynak, Refet S, Brian Sack, and Jonathan H. Wright. 2006. “The U.S. Treasury Yield Curve: 1961 to the Present.”

Haddad, Valentin, Alan Moreira, and Tyler Muir. 2021. “When Selling Becomes Viral: Disruptions in Debt Markets in the COVID-19 Crisis and the Fed’s Response.” *The Review of Financial Studies* 34 (11): 5309–5351.

Haddad, Valentin, Alan Moreira, and Tyler Muir. 2025. “Whatever It Takes? The Impact of Conditional Policy Promises.” *American Economic Review* 115 (1): 295–329.

Halling, Michael, Jin Yu, and Josef Zechner. 2020. "How Did COVID-19 Affect Firms' Access to Public Capital Markets?" *The Review of Corporate Finance Studies* 9 (3): 501–533.

Hansen, Jacob H., and Mathias V. Siggaard. 2024. "Double Machine Learning: Explaining the Post-Earnings Announcement Drift." *Journal of Financial and Quantitative Analysis* 59 (3): 1003–1030.

Haque, Sharjil M., and Richard Varghese. 2021. "The COVID-19 Impact on Corporate Leverage and Financial Fragility." *IMF Working Papers* 2021 (265): A001. ISBN: 9781589064126 Place: USA Publisher: International Monetary Fund.

Harford, Jarrad, and Vahap B. Uysal. 2014. "Bond market access and investment." *Journal of Financial Economics* 112 (2): 147–163.

Hassan, Tarek A, Stephan Hollander, Laurence Van Lent, Markus Schwedeler, and Ahmed Tahoun. 2023. "Firm-Level Exposure to Epidemic Diseases: COVID-19, SARS, and H1N1." *The Review of Financial Studies* 36 (12): 4919–4964.

Hayashi, Fumio. 1982. "Tobin's Marginal q and Average q: A Neoclassical Interpretation." *Econometrica* 50 (1): 213.

He, Zhiguo, Stefan Nagel, and Zhaogang Song. 2022. "Treasury inconvenience yields during the COVID-19 crisis." *Journal of Financial Economics* 143 (1): 57–79.

Hennessy, Christopher A., and Toni M. Whited. 2005. "Debt dynamics." *The Journal of Finance* 60 (3): 1129–1165.

Hotchkiss, Edith, Greg Nini, and David C Smith. 2022. "The Role of External Capital in Funding Cash Flow Shocks: Evidence From the COVID-19 Pandemic."

Hu, Yunzhi, Felipe Varas, and Chao Ying. 2024. "Debt Maturity Management."

Kargar, Mahyar, Benjamin Lester, David Lindsay, Shuo Liu, Pierre-Olivier Weill, and Diego Zúñiga. 2021. "Corporate Bond Liquidity during the COVID-19 Crisis." *The Review of Financial Studies* 34 (11): 5352–5401.

Kim, Alex G, and Valeri V Nikolaev. 2024a. "Contextualizing Profitability." *SSRN Electronic Journal*.

Kim, Alex G., and Valeri V. Nikolaev. 2024b. "Context-Based Interpretation of Financial Information." *Journal of Accounting Research*: 1475–679X.12593.

Kiyotaki, Nobuhiro, and John Moore. 1997. "Credit Cycles." *Journal of Political Economy* 105 (2): 211–248.

Krieger, Kevin, Nathan Mauck, and Stephen W. Pruitt. 2021. "The impact of the COVID-19 pandemic on dividends." *Finance Research Letters* 42: 101910.

Lee, Jongsub, Andy Naranjo, and Stace Sirmans. 2021. “CDS Momentum: Slow-Moving Credit Ratings and Cross-Market Spillovers.” *The Review of Asset Pricing Studies* 11 (2): 352–401.

Lee, Jongsub, Andy Naranjo, and Guner Velioglu. 2018. “When do CDS spreads lead? Rating events, private entities, and firm-specific information flows.” *Journal of Financial Economics* 130 (3): 556–578.

Leland, Hayne E. 1994. “Corporate Debt Value, Bond Covenants, and Optimal Capital Structure.” *The Journal of Finance* 49 (4): 1213–1252.

Li, Wenhao, and Ye Li. 2024. “Firm Quality Dynamics and the Slippery Slope of Credit Intervention.” *SSRN Electronic Journal*.

Ma, Yiming, Kairong Xiao, and Yao Zeng. 2022. “Mutual Fund Liquidity Transformation and Reverse Flight to Liquidity.” *The Review of Financial Studies* 35 (10): 4674–4711.

Ma, Yueran. 2019. “Nonfinancial Firms as Cross-Market Arbitrageurs.” *The Journal of Finance* 74 (6): 3041–3087.

Maasoumi, Esfandiar, Jianqiu Wang, Zhuo Wang, and Ke Wu. 2024. “Identifying factors via automatic debiased machine learning.” *Journal of Applied Econometrics* 39 (3): 438–461.

Miller, Douglas L. 2023. “An Introductory Guide to Event Study Models.” *Journal of Economic Perspectives* 37 (2): 203–230.

Momin, Rayhan. 2025a. “Central Bank Corporate Bond Purchase Programs: Commitment Matters.”

Momin, Rayhan. 2025b. “Heterogeneous Treatment Effects and Counterfactual Policy Targeting Using Deep Neural Networks: An Application to Central Bank Corporate Credit Facilities.”

Momin, Rayhan, and Jessica S. Li. 2025. “The Causal Effect of the Fed’s Corporate Credit Facilities on Eligible Issuer Bonds.” *SSRN Electronic Journal*.

Movaghari, Hadi, Serafeim Tsoukas, and Evangelos Vagenas-Nanos. 2024. “Corporate cash policy and double machine learning.” *International Journal of Finance & Economics*: ijfe.3039.

Nozawa, Yoshio, and Yancheng Qiu. 2021. “Corporate bond market reactions to quantitative easing during the COVID-19 pandemic.” *Journal of Banking & Finance* 133: 106153.

OECD. 2020. “OECD Tax Database.”

O'Hara, Maureen, and Xing (Alex) Zhou. 2021. "Anatomy of a liquidity crisis: Corporate bonds in the COVID-19 crisis." *Journal of Financial Economics* 142 (1): 46–68.

Pagano, Marco, and Josef Zechner. 2022. "COVID-19 and Corporate Finance." *The Review of Corporate Finance Studies* 11 (4): 849–879.

Pazarbasi, Altan. 2025. "Cash Heterogeneity and the Payout Channel of Monetary Policy."

Pegoraro, Stefano, and Mattia Montagna. 2025. "Demand-Driven Bond Financing in the Euro Area." *Journal of Financial and Quantitative Analysis*: 1–52.

Pettenuzzo, Davide, Riccardo Sabbatucci, and Allan Timmermann. 2023. "Payout suspensions during the Covid-19 pandemic." *Economics Letters* 224: 111024.

Rampini, Adriano A., and S. Viswanathan. 2010. "Collateral, Risk Management, and the Distribution of Debt Capacity." *The Journal of Finance* 65 (6): 2293–2322.

Sant'Anna, Pedro H.C., and Jun Zhao. 2020. "Doubly robust difference-in-differences estimators." *Journal of Econometrics* 219 (1): 101–122.

Saretto, Alessio, and Heather E. Tookes. 2013. "Corporate leverage, debt maturity, and credit supply: The role of credit default swaps." *The Review of Financial Studies* 26 (5): 1190–1247.

Simon, Frederik, Sebastian Weibels, and Tom Zimmermann. 2022. "Deep Parametric Portfolio Policies." *SSRN Electronic Journal*.

S&P. 2025. "Default, Transition, and Recovery: 2024 Annual Global Corporate Default And Rating Transition Study."

Todorov, Karamfil. 2020. "Quantify the quantitative easing: Impact on bonds and corporate debt issuance." *Journal of Financial Economics* 135 (2): 340–358.

Wasserbacher, Helmut, and Martin Spindler. 2024. "Credit Ratings: Heterogeneous Effect on Capital Structure." arXiv:2406.18936 [econ].

Whited, Toni M. 1992. "Debt, Liquidity Constraints, and Corporate Investment: Evidence from Panel Data." *The Journal of Finance* 47 (4): 1425–1460.

Yang, Jui-Chung, Hui-Ching Chuang, and Chung-Ming Kuan. 2020. "Double machine learning with gradient boosting and its application to the Big N audit quality effect." *Journal of Econometrics* 216 (1): 268–283.

Zaghini, Andrea. 2019. "The CSPP at work: Yield heterogeneity and the portfolio rebalancing channel." *Journal of Corporate Finance* 56: 282–297.